

2013

Stoichiometric and catalytic reactivity of tris(oxazoliny)phenylborato zinc and magnesium compounds

Debabrata Mukherjee
Iowa State University

Follow this and additional works at: <https://lib.dr.iastate.edu/etd>

 Part of the [Inorganic Chemistry Commons](#)

Recommended Citation

Mukherjee, Debabrata, "Stoichiometric and catalytic reactivity of tris(oxazoliny)phenylborato zinc and magnesium compounds" (2013). *Graduate Theses and Dissertations*. 13189.
<https://lib.dr.iastate.edu/etd/13189>

This Dissertation is brought to you for free and open access by the Iowa State University Capstones, Theses and Dissertations at Iowa State University Digital Repository. It has been accepted for inclusion in Graduate Theses and Dissertations by an authorized administrator of Iowa State University Digital Repository. For more information, please contact digirep@iastate.edu.

Stoichiometric and catalytic reactivity of tris(oxazoliny)phenylborato zinc and magnesium compounds

by

Debabrata Mukherjee

A dissertation submitted to the graduate faculty
in partial fulfillment of the requirements for the degree of
DOCTOR OF PHILOSOPHY

Major: Inorganic Chemistry

Program of Study Committee:

Aaron D. Sadow, Major Professor

Andreja Bakac

Gordon Miller

Malika Jeffries-El

Levi Stanley

Iowa State University

Ames, Iowa

2013

Copyright © Debabrata Mukherjee, 2013. All rights reserved.

To my wife, Payel Mukherjee, who has sacrificed the most for me.
And, also to both of our families and friends for their constant support.

Table of Contents

Acknowledgements	vii
Abstract	ix
Chapter 1 – Introduction.	1
General Introduction	1
References	6
Thesis Organization	8
Chapter 2 – Synthesis of New Mn and Re Tricarbonyl Complexes of Tris(oxazolinyl)phenyl borate Ligands: Comparison to Analogous Tris(pyrazolyl) borate Complexes.	12
Abstract	12
Introduction	13
Results and Discussion	14
Conclusions	24
References	24
Experimental	25
Chapter 3 – Conversion of a Zinc Disilazide to a Zinc Hydride Mediated by LiCl.	33
Abstract	33
Introduction	33
Results and Discussion	34

Conclusions	40
References	40
Experimental	41

Chapter 4 – Coordinatively Saturated Tris(oxazolinyl)borato

Zinc Hydride-Catalyzed Cross-Dehydrocoupling of Silanes and Alcohols. 57

Abstract	57
Introduction	57
Results and Discussion	59
Conclusions	71
References	71
Experimental	74

Chapter 5 – Remarkably robust monomeric alkylperoxyzinc compounds

from oxygen and tris(oxazolinyl)boratozinc alkyls. 92

Abstract	92
Introduction	93
Results and Discussion	95
Conclusions	110
References	111
Experimental	115

Chapter 6 – Divergent reaction pathways of tris(oxazoliny)borato zinc and magnesium silyl compounds.	153
Abstract	153
Introduction	154
Results and Discussion	154
Conclusions	162
References	163
Experimental	165
Chapter 7 – Coordinatively Saturated Tris(oxazoliny)borato Zinc Hydride-Catalyzed Carbonyl hydrosilylation and hydroboration.	180
Abstract	180
Introduction	180
Results and Discussion	182
Conclusions	196
References	196
Experimental	197
Chapter 8 – $\text{To}^{\text{M}}\text{MgMe}$ is a multifunctional pre-catalyst for reductive hydroboration of carbonyls and esters as well for Tishchenko reaction and reversible trans esterification.	205
Abstract	205
Introduction	205

Results and Discussion	206
Conclusions	225
References	225
Experimental	228
Chapter 9 – Conclusions.	239

Acknowledgements

Finally the moment has arrived! The journey started on 30th July, 2007, when I first landed in Des Moines, Iowa. It is the state, which is famously called as ‘the land of opportunity’! I always laughed at this tagline for Iowa until now, when I realize that it was truly a land of opportunity for me. By the way, that was my first time travelling outside the home country and first time riding an aircraft as well! I feel like the last five and half years of my life at Iowa State University have passed so quickly. I am getting emotional while writing this acknowledgement and so many thoughts, incidents, moments, and memories are crowding my mind right now. But before I get carried away, there are a number of people to whom I am really indebted and would like to thank them. First, I would like to thank my Ph.D. advisor Dr. Aaron D. Sadow, for giving me the opportunity to learn chemistry at its highest level and gather expertise in organometallic chemistry. You taught me to think like a chemist, communicate like a chemist and above all, act like a chemist. It is you from whom; I have learnt how much dedicated and passionate a scientist should be in his work. Thank you again for having faith on me despite watching a reaction, half way done, sitting on my bench and not being worked up for over six months. You always showed great excitement, enthusiasm and support at all the discoveries I made; no matter how tiny they are and never discouraged me to try new things. I have also learnt the right attitude needed to be a successful chemist and that is to look beyond the line and never get satisfied. Whenever I talked to you about an exciting result you always seemed to be not satisfied enough and started talking about what is the next thing to attempt or achieve. Your guidance, suggestions, and critiques have

motivated me each and every day and drove me to the right direction. In the lab, you took care of everything else so that I could only focus on doing reactions. I would also like to say ‘Thank you’ to all of my current and previous POS committee members – Dr. Andreja Bakac, Dr. Gordon Miller, Dr. Malika Jeffris-El, Dr. Javier Vela, Dr. Levi Stanley and also late professor Victor Lin – for their thoughtful insight, valuable comments and suggestion and exceedingly precious time. I am also grateful to the past and present of members of the Sadow research group for sharing their experiences and expertise’s whenever I needed. Thanks to Richard Thompson (Rick) for working with me as an undergraduate and bearing with my crazy work timing. I hope that I didn’t torture you too much! Thanks to my parents, in-laws, elder brother and other family members and friends for their constant support and encouragement. A special credit goes to my father for always asking me when I am going to graduate and inquiring about my publication. Lastly, I would like to express my gratitude and appreciation from the deepest layer of my heart to the person, without whom this whole journey would have been impossible. It is you, my beautiful wife Payel, who made all this possible and transformed the so-called most difficult five years of life into a delightful and memorable experience. Despite being the only child of your parents and having a fantastic university teaching job, you took the bravest decision to leave everything and everyone behind just to stay with me and help me in everyway possible. You didn’t hesitate despite knowing that your days will be lonely and mostly confined at home. You took care of everything you can so that I can only work in the lab. Thank you for spending the sleepless nights with me in the lab running crazy kinetics. Thanks for treating me with all the delicious dishes you made using your culinary research! Thanks for being with me all the time and sharing the ups and downs.

Abstract

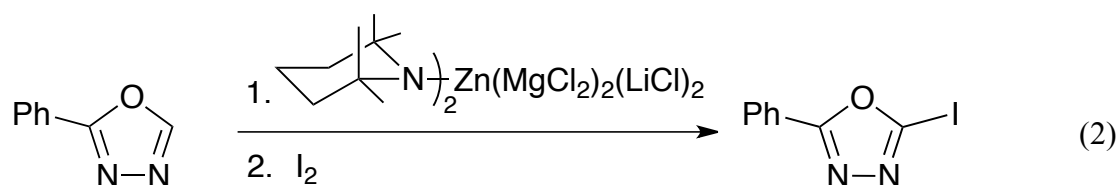
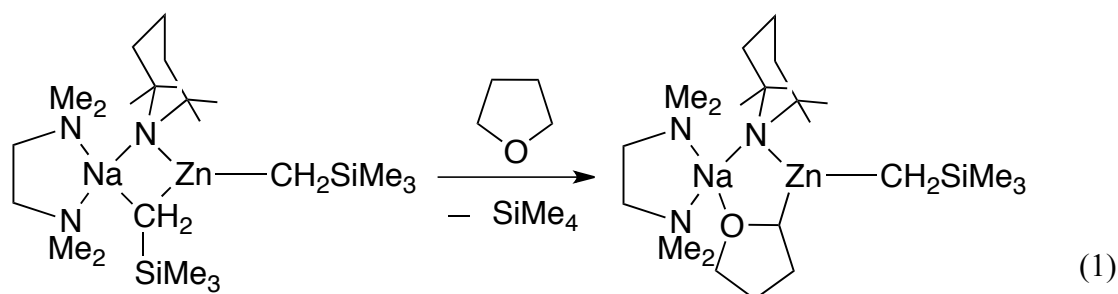
Recently, our research group has synthesized a new class of monoanionic tridentate ligands, To^R (To^M = tris(4,4-dimethyl-2-oxazolanyl)phenylborate and To^P = tris(4-S-isopropyl-2-oxazolanyl)phenylborate), and developed the corresponding stoichiometric and catalytic chemistry of zirconium, yttrium, rhodium, iridium, and magnesium complexes. This thesis begins with the comparison of this new class of scorpionate-type ligands (To^M and To^P) with more classical Tp (tris(pyrazolyl)borates) and Cp (cyclopentadienyl) analogues, both in terms of relative electron donating ability as well as steric bulk. Group 7 metal tricarbonyl complexes of To^M and To^P ($To^M M(CO)_3$ and $To^P M(CO)_3$; M = Re, Mn) were synthesized in this purpose and the corresponding ν_{CO} IR stretching frequency data were used for the electron donating ability comparison. Solid angles of these ancillary ligands were calculated using coordinates from crystal structures or molecular models with the program Solid-G to obtain a quantitative assessment of the relative steric properties. The thesis then mainly focuses on the chemistry of four-coordinate zinc complexes using To^M as the supportive ancillary ligand. The main interest lies on the synthesis of molecular terminal zinc hydride and its catalytic activity in Si–O bond formation reactions, as well as the isolation and reactivity study of alkylperoxy zinc compounds ($To^M ZnOOR$) obtained from the reactions of the corresponding zinc alkyls ($To^M ZnR$) with molecular O_2 . The later part of this thesis also discusses the chemistry of To^M -supported magnesium complexes and the comparison with analogous zinc complexes. It starts with the synthesis of To^M -supported zinc and magnesium bulky silyl complexes, both comprising with and without β -SiH moieties ($To^M M-SiR_3$; M =

Zn, Mg; R = SiHMe₂, SiMe₃). The study further extends to divergent reaction pathways of To^MMSi(SiHMe₂)₃ (M = Zn, Mg) towards CO₂. Finally, the thesis discusses the catalytic activity of To^MZnH and To^MMgMe in carbonyl reduction. To^MMgMe mediated catalytic Tischenko coupling of aldehydes, reversible trans-esterification, and reductive ester cleavage are also discussed in details.

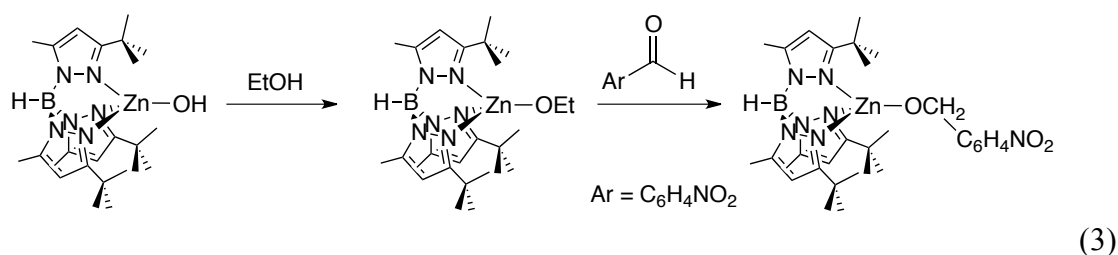
Chapter 1: Introduction

General introduction.

Zinc, as a metal, is blessed with several interesting features that include its flexible coordination geometry, fast ligand exchange, lewis acidity, intermediate polarizability (hard-soft character), cheap abundance, strong binding to suitable sites, and its lack of redox activity. It is the combination of these factors that makes zinc an attractive metal system in synthetic organometallic chemistry.¹ Organozinc complexes have a long-standing history of being extensively used in both organic and organometallic syntheses, especially as alkyl, aryl, silyl and hydride transfer agents that complement organolithium and organomagnesium reagents.² In particular, combination of zinc and alkali and/or alkaline earth metals often offer valuable alternatives to the corresponding magnesium and lithium reagents in terms of controlling both reactivity as well as selectivity as exemplified in eqn. 1 and 2.³

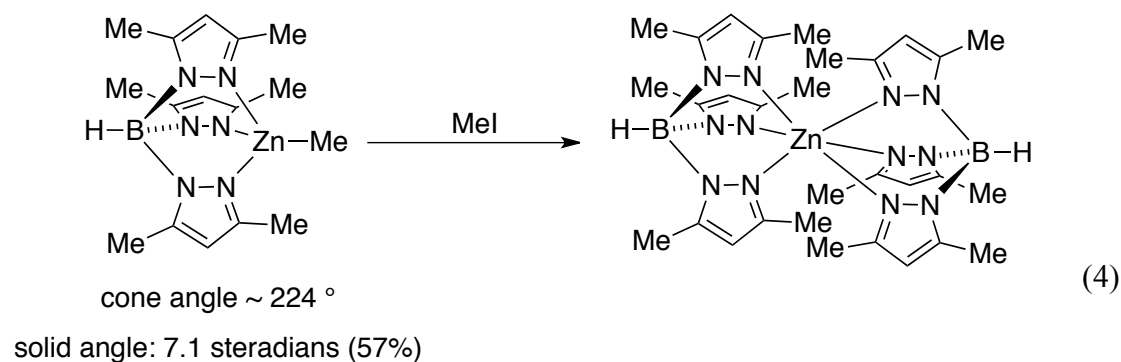


From biological standpoint, zinc is the second-most abundant metal in biology after iron and resides as the active sites of more than 300 enzymes, covering all six classes. Zinc binding sites in proteins are often distorted tetrahedral or trigonal bipyramidal, made up of sulphur or nitrogen or oxygen donor ligand environment. Therefore, mimicking the biologically active sites using synthetic molecular complexes containing *N,O,S*- donor ligands is often attempted to better understand the physiological processes. As for example, Parkin and coworkers modeled the catalytic activity of Liver Alcohol Dehydrogenase using tris(pyrazolyl)borato zinc alkoxides and hydroxides as shown in eqn. 3.⁴

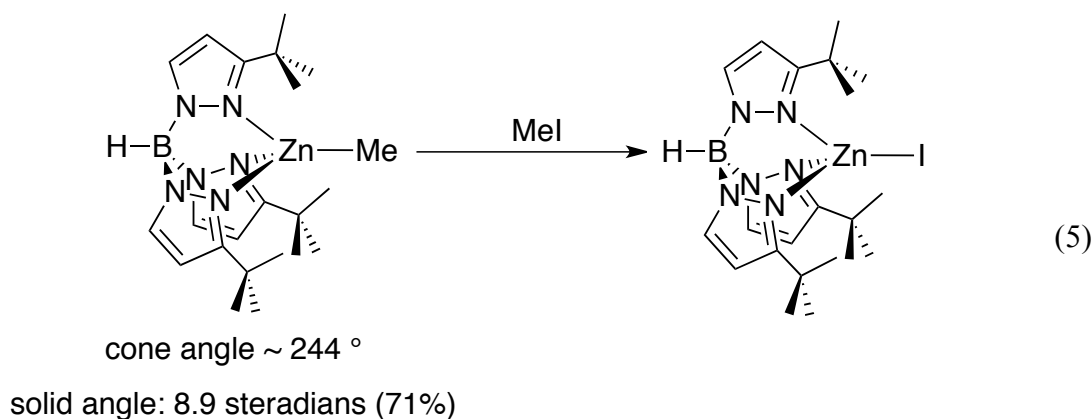


Our group has recently developed a new oxazoline-based monoanionic scorpionate ligands tris(4,4-dimethyl-2-oxazoliny)phenylborate [To^M] and developed the corresponding stoichiometric and catalytic chemistry of zirconium,⁵ yttrium,⁶ rhodium,⁷ iridium,⁸ aluminium,⁹ and magnesium¹⁰ complexes. The To^M ligand shares a close resemblance with the well known tris(3,5-dimethylpyrazolyl)borate [Tp^*] ligand in terms of appearance, electron donating ability as well as steric bulkiness. But the three-dimensional orientation of the To^M ligand in space is quite different (as revealed from solid angle calculation; chapter 2) from that of Tp^* . This interesting feature is advantageous in favor of To^M when it comes to the availability of free space on zinc and hence the reactivity. As for example, Parkin and coworkers reported that Tp^*ZnMe [Tp^* : cone angle 224° ; solid angle 7.1 steradians (57%)] reacts with methyl iodide to undergo unwanted ligand redistribution, providing $(\kappa^3-Tp^*)_2Zn$

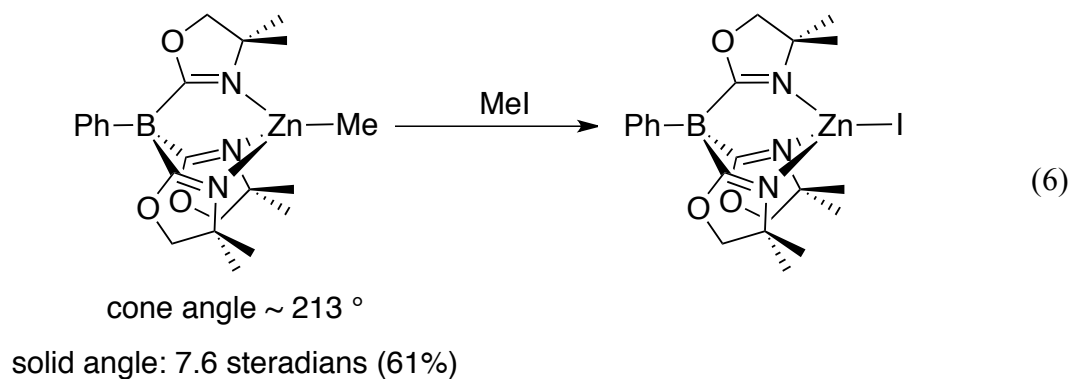
as shown in eqn. 4.^{11a}



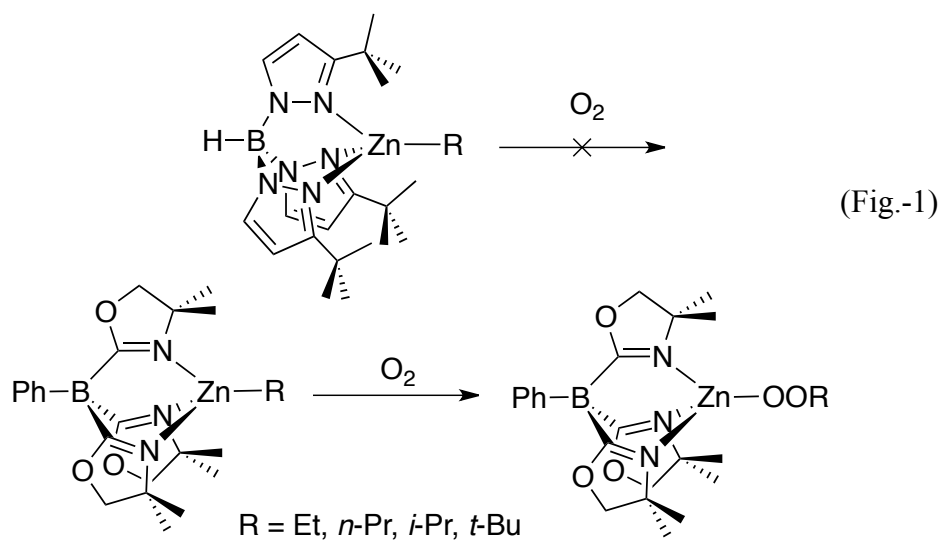
The bulkier TptBu, having a much higher cone angle (244°) and solid angle (8.9 steradians (71%)), can prevent ligand redistribution and provides the corresponding $\text{Tp}^{\text{tBu}}\text{ZnI}$ as shown in eqn. 5.^{11b} However, the bulky Tp^{tBu} leaves only a little free space around zinc, which makes it less reactive.



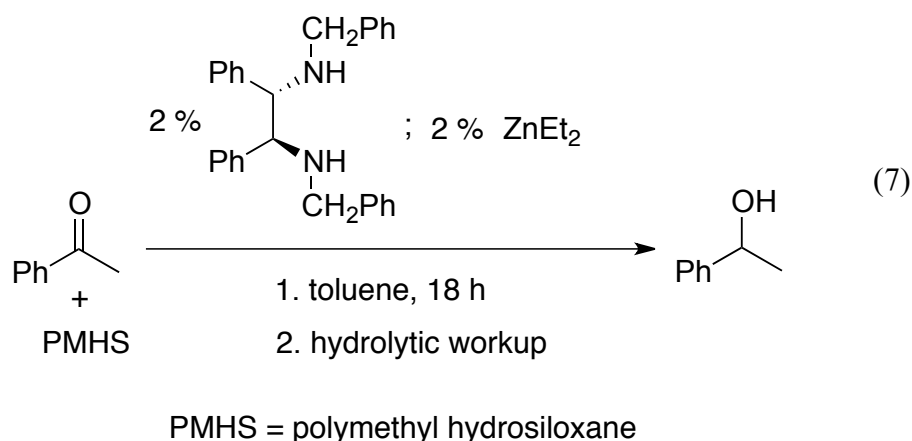
However, $\text{To}^{\text{M}}\text{ZnMe}$ (To^{M} : cone angle 213° ; solid angle 7.6 steradians (61%)), despite being similar to the Tp^* , does not undergo ligand redistribution but provides $\text{To}^{\text{M}}\text{ZnI}$ (eqn.6). $\text{To}^{\text{M}}\text{ZnI}$ has been fully characterized including X-ray structure (Fig.-S1).



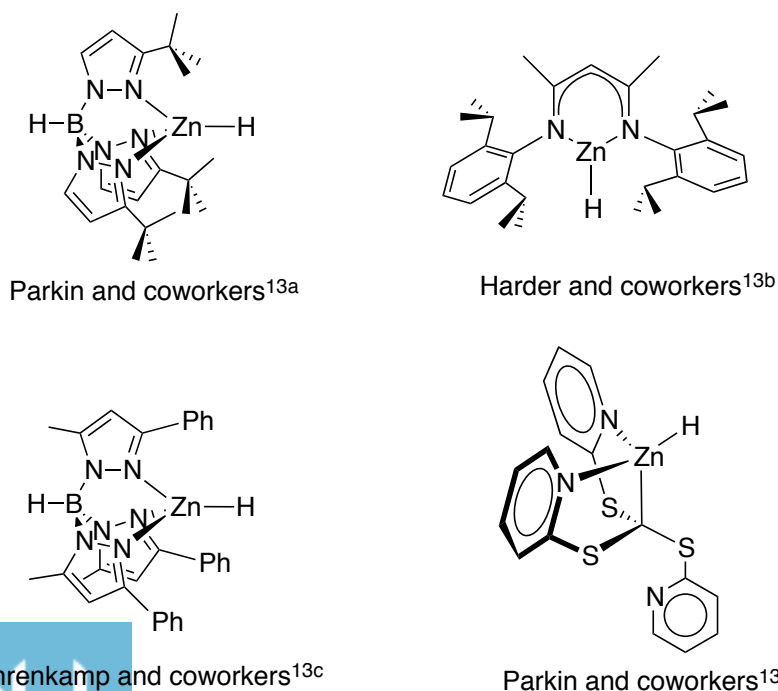
This indicates that the unique spatial orientation of To^M not only allows preventing ligand redistribution and provides stabilization the metal center but also keeps enough space to show reactivity like protonation, insertion, metathesis etc. (as discussed in the following chapters). The most striking example of this feature is discussed in chapter 5 where $To^M ZnR$ ($R = Et, n\text{-}Pr, i\text{-}Pr, t\text{-}Bu$) alkyls are found to react with O_2 providing isolable monomeric zinc alkyl peroxides, whereas, the corresponding $Tp^{tBu}ZnR$ complexes are inert to O_2 (Fig.-1).



Additionally, zinc hydrides are usually proposed as the catalytic active species or important intermediates in several zinc mediated group transfer reactions. As for example, zinc catalyzed hydrosilylation of carbonyls (eqn. 7) is proposed to involve zinc hydride as the reactive species.¹²



However, only a few isolable monomeric zinc hydrides are reported in the literature¹³ (Fig.-2) and their application in studying catalysis is little known.¹⁴



In this regard, To^M -coordinated zinc system has an enormous potential in studying catalysis, as individual stoichiometric steps could be probed and unique steric feature can facilitate isolation of reactive intermediates. The following chapters discuss our initial exploration of the stoichiometric and catalytic chemistry of To^M -ligand supported zinc complexes.

Similarly, our group has only recently started exploring the catalytic chemistry of To^M MgMe in intramolecular hydroamination/cyclization of aminoalkenes^{10a} and Si–N bond formation reactions via dehydrogenative coupling between amines and silanes.^{10b} This thesis also discusses the continuation of the research on other potential catalytic applications of To^M MgMe in several important organic transformations.

References.

- (1) Lipscomb, W. N.; Strater, N. *Chem. Rev.* **1996**, *96*, 2375–2434.
- (2) Knochel, P.; Perrone, S.; Grenouillat, N. In *Applications I: Main Group Compounds in Organic Synthesis*; Knochel, P., Ed.; Elsevier: Amsterdam, 2007; Vol. 9, pp 81-144.
- (3) (a) Kennedy, A. R.; Klett, J.; Mulvey, R. E.; Wright, D. S. *Science* **2009**, *326*, 706–708.
(b) Wunderlich, S. H.; Knochel, P. *Angew. Chem., Int. Ed.* **2007**, *46*, 7685–7688.
- (4) (a) Parkin, G. *Chem. Rev.* **2004**, *104*, 699–767. (b) Bergquist, C.; Storrie, H.; Koutcher, L.; Bridgewater, B. M.; Friesner, R. A.; Parkin, G. *J. Am. Chem. Soc.* **2000**, *122*, 12651–12658. (c) Bergquist, C.; Parkin, G. *Inorg. Chem.* **1999**, *38*, 422–423.
- (5) Dunne, J. F.; Su, J. C.; Ellern, A.; Sadow, A. D. *Organometallics* **2008**, *27*, 2399-2401.
- (6) Pawlikowski, A. V.; Ellern, A.; Sadow, A. D. *Inorg. Chem.* **2009**, *48*, 8020–8029.
- (7) Ho, H.; Dunne, J. F.; Ellern, A.; Sadow, A. D. *Organometallics* **2010**, *29*, 4104-4114.

- (8) (a) Baird, B.; Pawlikowski, A. V.; Su, J.; Wiench, J. W.; Pruski, M.; Sadow, A. D. *Inorg. Chem.* **2008**, *47*, 10208-10210. (b) Pawlikowski, A. V.; Gray, T. S.; Schoendorff, G.; Baird, B.; Ellern, A.; Windus, T. L.; Sadow, A. D. *Inorg. Chim. Acta* **2009**, *362*, 4517-4525.
- (9) Dunne, J. F.; Manna, K.; Wiench, J. W.; Ellern, A.; Pruski, M.; Sadow, A. D. *Dalton Trans.*, 2010, **39**, 641-653.
- (10) (a) Dunne, J. F.; Fulton, B.; Ellern, A.; Sadow, A. D. *J. Am. Chem. Soc.* **2010**, *132*, 17680-17683. (b) Dunne, J. F.; Neal, S. R.; Engelkeimer, J. Ellern, A.; Sadow, A. D. *J. Am. Chem. Soc.* **2011**, *133*, 16782-16785.
- (11) (a) Han, R.; Parkin, G. *Organometallics* **1991**, *10*, 1010-1020. (b) Looney, A.; Han, R.; Gorrell, I. B.; Cornebise, M.; Yoon, K.; Parkin, G. *Organometallics* **1995**, *14*, 274-288.
- (12) Mimoun, H.; Laumer, J. Y. S.; Giannini, L.; Scopelliti, R.; Floriani, C. *J. Am. Chem. Soc.* **1999**, *121*, 6158-6166.
- (13) (a) Han, R.; Gorrell, I. B.; Looney, A. G.; Parkin, G. *J. Chem. Soc., Chem. Commun.* **1991**, 717-719. (b) Spielmann, J.; Piesik, D.; Wittkamp, B.; Jansen, G.; Harder, S. *Chem. Commun.* **2009**, 3455-3456. (c) Rombach, M.; Brombacher, H.; Vahrenkamp, H. *Eur. J. Inorg. Chem.* **2002**, 153-159. (d) Sattler, W.; Parkin, G. *J. Am. Chem. Soc.* **2011**, *133*, 9708-9711.
- (14) Sattler, W.; Parkin, G. *J. Am. Chem. Soc.* **2012**, *134*, 17462-17465.

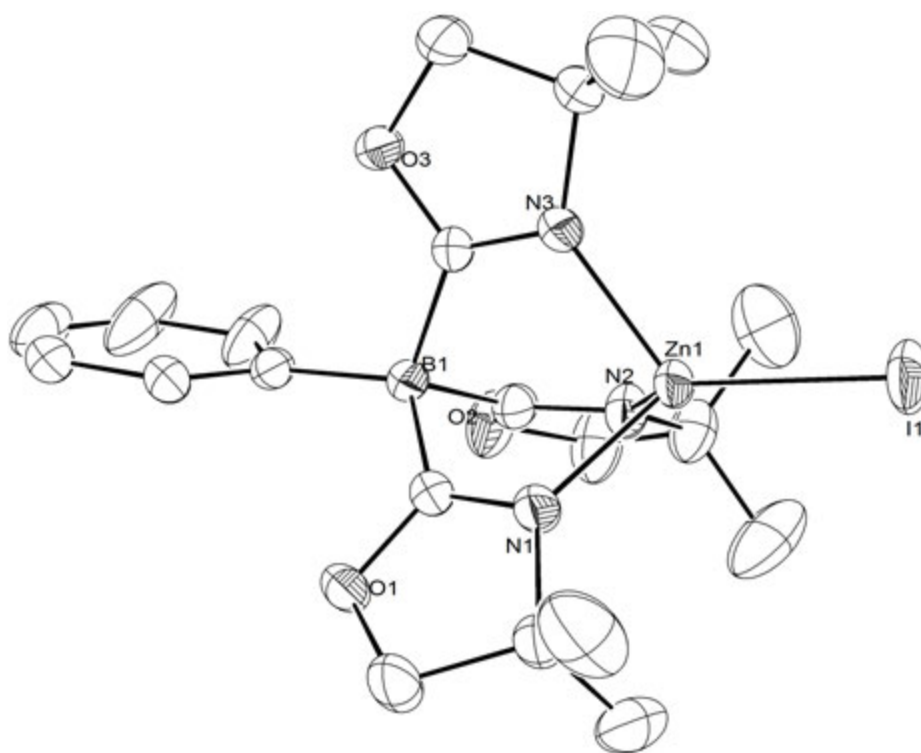


Figure S1. ORTEP diagram of $To^M ZnI$ with ellipsoids drawn at 50% probability. Hydrogen atoms are not included to enhance the clarity of heavy atom positions.

Thesis organization.

The thesis contains nine chapters. Chapter 1 gives a brief general introduction of the topic. Chapters 2 through 6 are published journal articles, which are slightly modified to have a coherent description. The chemistry discussed in chapter 7 and 8 are yet not published and the manuscripts for each are in progress. The thesis ends in Chapter 9 with a general conclusion.

Chapter 2 describes the synthesis of tris(oxazoliny)phenyl borato group 7 metal tricarbonyl complexes ($To^M M(CO)_3$ and $To^P M(CO)_3$; $M = Re$ and Mn). The ν_{CO} IR frequencies of these complexes were used to compare the relative donor strength of this new class of scorpionates with the classical hydridotris(pyrazolyl)borate (Tp) and

cyclopentadienyl (Cp) ligands. Solid angles of all these ancillary ligands (L) were also calculated from the X-ray crystal structures of the corresponding group 7 metal (Re and Mn) tricarbonyl complexes to obtain a relative trend in the steric bulk.

Chapter 3 discusses the synthesis of four-coordinated tris(4,4-ditheyly-2-oxazoliny)phenyl borato (To^{M}) zinc complexes with special importance on terminal hydride ($\text{To}^{\text{M}}\text{ZnH}$). An unusual β -elimination from a coordinatively saturated zinc center, mediated by LiCl, is highlighted in this chapter.

Chapter 4 demonstrates the catalytic activity of $\text{To}^{\text{M}}\text{ZnH}$ in Si–O bond formation reaction via dehydrogenative cross coupling between alcohols and hydrosilanes. A detailed mechanistic study was conducted to establish the empirical rate law for the reaction between 3,5- $\text{C}_6\text{H}_3\text{Me}_2\text{OH}$ and PhMeSiH_2 , which indicates that Si–O bond formation is turnover-limiting in the presence of excess phenol. Richard Thompson, a former undergraduate student of our group, had worked with me in this project and performed some of the NMR-scale reactions and assisted in kinetic plots.

Chapter 5 describes the synthesis of a series of zinc alkyl compounds of the type $\text{To}^{\text{M}}\text{ZnR}$ (To^{M} = tris(4,4-dimethyl-2-oxazoliny)phenylborate; R = Et, *n*- C_3H_7 , *i*- C_3H_7 , *t*-Bu, CH_2Ph , Ph) some of which react with O_2 at 25 °C to form isolable monomeric alkylperoxides $\text{To}^{\text{M}}\text{ZnOOR}$ (R = Et, *n*- C_3H_7 , *i*- C_3H_7 , *t*-Bu) in quantitative yield. However, $\text{To}^{\text{M}}\text{ZnMe}$ and $\text{To}^{\text{M}}\text{ZnH}$ are inert towards O_2 . Detailed mechanistic study using ^1H NMR spectroscopy for the O_2 insertion into the Zn–C bond of $\text{To}^{\text{M}}\text{ZnEt}$ provided the empirical rate law that is consistent with a radical chain mechanism, where the rate-limiting $\text{S}_{\text{H}2}$ step involves the interaction of $\cdot\text{OOEt}$ and $\text{To}^{\text{M}}\text{ZnEt}$. Monomeric $\text{To}^{\text{M}}\text{ZnOOR}$ compounds are thermally

resilient upto 120 °C. Yet, they show divergent reactivity towards phosphines (oxidation via O-atom transfer) and hydrosilanes (–OOR group transfer affording $To^M ZnH$ and alkylperoxosilanes).

Chapter 6 deals with the synthesis of To^M -ligand supported zinc and magnesium bulky silyl complexes, both comprising with and without β -SiH moieties ($To^M M-SiR_3$; $M = Zn, Mg$; $R = SiHMe_2, SiMe_3$). The reactivity difference between $To^M ZnSi(SiHMe_2)_3$ and $To^M MgSi(SiHMe_2)_3$ towards CO_2 was further probed in details. This piece of work was conducted in collaboration with Nicole L. Lampland from our group. The silyl ligand precursors, $KSi(SiHMe_2)_3$ and $KSi(SiMe_3)_3$, were first synthesized by Kaking Yan from our group, whereas James F. Dunne, a former graduate student, had first observed the formation of $To^M MgOMe$ species in NMR-scale reaction between $To^M MgMe$ and MeOH, mentioned in this chapter. Contributions from these authors were not removed to keep the cohesiveness of the discussion intact, rather mentioned in details at the beginning of the chapter.

Chapter 7 discusses the catalytic activity of $To^M ZnH$ in hydrosilylation and hydroboration of aldehydes and ketones. Carbonyl substrates with a wide range of functional groups were tested for the reduction with $BnMe_2SiH$ and HBpin (pinacolborane). Detailed kinetic study to probe the mechanism for the hydrosilylation of PhHCO with $BnMe_2SiH$ is currently underway and the primary results show an inhibition effect from PhCHO on the overall reaction rate, which is explained based on an observed adduct formation between zinc alkoxide ($To^M ZnOCH_2Ph$) and free PhHCO. Individual steps involved in the catalytic cycle are also being studied in details and important intermediates have been isolated.

Chapter 8 describes similar catalytic hydroboration reduction of aldehydes and ketones mediated by $To^M MgMe$ as the pre-catalyst and HBpin as the reductant. Similar functional group tolerance was envisaged as mentioned in chapter 7 for $To^M ZnH$ catalyzed hydroboration. Additionally, catalytic activity of $To^M MgMe$ in hydroboration mediated ester cleavage was also explored using HBpin again as the reductant. Furthermore, $To^M MgMe$ was also established as an active pre-catalyst for Tishchenko coupling of aldehydes as well reversible trans-esterification reactions. Detailed kinetic study to probe the mechanism for the ester cleavage is currently underway. Individual steps involved in the catalytic cycle are also being studied in details by approaching stoichiometric reactions and important intermediates have been isolated and characterized. A monomeric magnesium borohydride species, $To^M MgH_2 Bpin$, has been isolated and structurally characterized, which is a rare example of its kind. Chapter is general conclusion about the thesis.

Dr. Arkady Ellern, the crystallographer in the instrumentation services, had collected the X-ray data and solved the structures of all the compounds mentioned in this thesis.

Chapter 2: Synthesis of New Mn and Re Tricarbonyl Complexes of Tris(oxazoliny)phenyl borate Ligands: Comparison to Analogous Tris(pyrazoly) borate Complexes

Modified from a paper published in *New Journal of Chemistry*[†]

Kan Wu,^a Debabrata Mukherjee,^b Arkady Ellern,^b Aaron D. Sadow,^{*b,c} William E. Geiger^{*a,d}

Department of Chemistry, U.S. DOE Ames Laboratory, Iowa State University, Ames, IA

50011-3111

This paper was published in collaboration with Dr. Giger's group from University of Vermont, Burlington. This chapter mainly discusses the contribution from us.

Abstract

$M(\text{CO})_3$ ($M = \text{Mn, Re}$) complexes of two tris(oxazoliny)phenylborate ligands (To^{M} and To^{P}) have been prepared and characterized by spectroscopic and crystallographic methods. The steric bulk imparted by the sp^3 -hybridized carbons in the oxazoline ring give the tris(oxazoliny)borate ligands significant structural protection against dimerization while leaving the $M(\text{CO})_3$ face open for possible reactivity. Comparison of the ν_{CO} IR frequencies of these complexes gave a sequence of donor strength, $\text{Cp}^*, \text{To}^{\text{M}}, \text{To}^{\text{P}} > \text{Tp}^* > \text{Tp} > \text{Cp}$. Solid angles of these ancillary ligands (L) were also calculated from the X-ray crystal structures of $\text{LM}(\text{CO})_3$ ($M = \text{Re, Mn}$) complexes which provide the trend in steric bulk for the ancillary ligands as $\text{Cp} < \text{Cp}^* < \text{Tp} < \text{Tp}^* < \text{To}^{\text{P}} < \text{To}^{\text{M}}$.

Introduction.

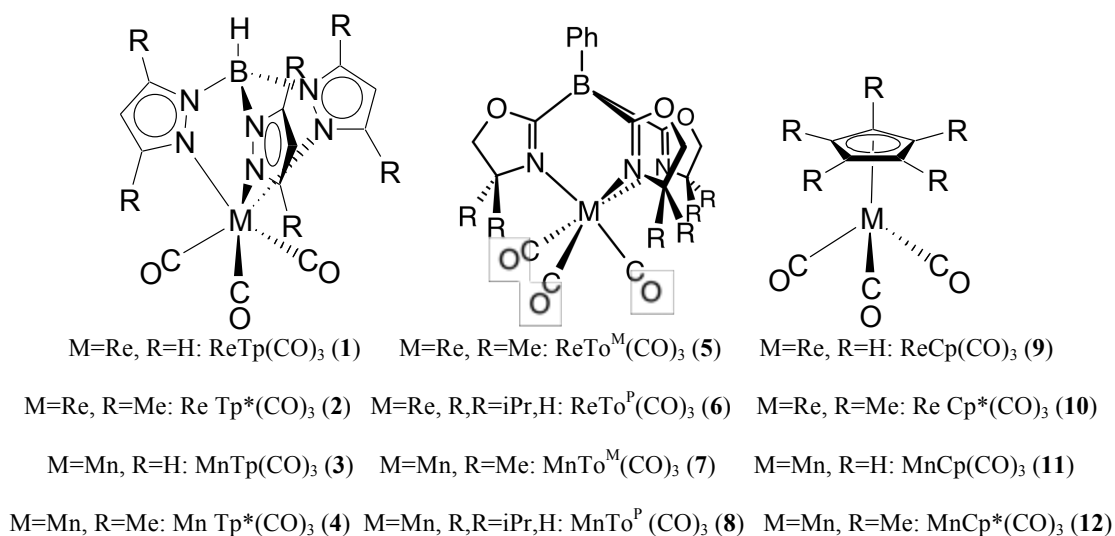
There has been a steady interest in developing mimics of the cyclopentadienyl (Cp) ligand as a monoanionic formal six- electron donor. Among the most broadly investigated analogues are the hydridotris(pyrazolyl)borate (Tp) ligands, which differ from the Cp ligand in terms of steric constraints and metal–ligand bonding.¹ A number of papers have compared the stoichiometric and catalytic reactivities of metal complexes derived from these two classes of ligands.² Quite recently, our group introduced a new type of scorpionate ligand, tris(oxazolanyl)phenyl borate, which contains three oxazoline donor groups in place of the pyrazolyl groups of the Tp ligand class.³ The oxazoline moiety provides access to chiral structures, and the substitution of B–C for B–N linkages limits the Lewis acid-mediated ligand epimerizations that complicate the chemistry of metal–Tp complexes.⁴

Owing to the fact that ligand electronic properties are important in determining the reactivity of metal complexes, effort has been made to characterize the relative donor properties of Cp- vs. scorpionate-type ligands. The most comprehensive of these studies is the compilation by Tellers et al. of the donor-related physical parameters published prior to 2000.⁵ Based largely on IR and electrochemical data, these authors discouraged generalizations about the relative donating abilities of the two types of ligands. Previous studies on the donor ability of oxazolines have focused on photoelectron spectroscopy and *ab initio* calculation of uncoordinated groups, and few comparisons to ligands such as cyclopentadienyl are available.^{6,7} We were interested in assessing the electron donating ability of our newly synthesized scorpionate [tris(oxazolanyl)phenyl borate] ligands in comparison with more classical cyclopentadienyl and hydridotris(pyrazolyl)borates using group VII $M(CO)_3$ complexes ($M = Mn, Re$). In this context ν_{CO} IR stretching bands of the new

tris(oxazolinyl)phenyl borato rhenium and manganese tricarbonyl complexes were measured under the identical conditions (both solid-state as well as CH_2Cl_2 solution) as reported for the $\text{CpM}(\text{CO})_3$, $\text{TpM}(\text{CO})_3$, and $\text{Tp}^*\text{M}(\text{CO})_3$ complexes ($\text{M} = \text{Re}, \text{Mn}$) in the literature.

The structures and numerical ordering of the compounds described in this paper are shown in Scheme 1. The acronym To^{M} is used for the tris(4,4-dimethyl-2-oxazolinyl)phenyl borate ligand and To^{P} is employed for the tris(4*S*-isopropyl-2-oxazolinyl)phenyl borate ligand.

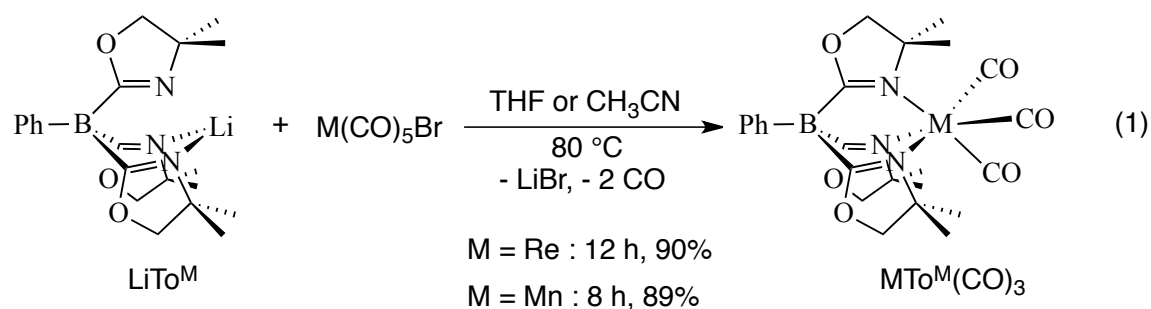
Scheme 1



Results and Discussion.

Synthesis and characterization of tris(oxazolinyl)borate compounds

Group 7 tris(oxazolinyl)borate compounds $\text{MTo}^{\text{M}}(\text{CO})_3$ [$\text{M} = \text{Re}$ (5), Mn (7)] were prepared by adaptation of the salt metathesis route that provides $\text{MTp}(\text{CO})_3$ ($\text{M} = \text{Mn}, \text{Re}$). Thus, $\text{Li}[\text{To}^{\text{M}}]$ and $\text{MBr}(\text{CO})_5$ ($\text{M} = \text{Mn}, \text{Re}$) were reacted in THF or acetonitrile at 80°C to afford $\text{MTo}^{\text{M}}(\text{CO})_3$ in good yield (Eq 1).



These compounds were fully characterized by spectroscopic, analytical, and single crystal X-ray diffraction methods. The spectroscopic data for all the new compounds reported in this chapter are summarized in Table 1.

Table 1. Summary of the characteristic data for tris(oxazolinyl)phenylboratorhenium and manganese tricarbonyl complexes.

Compound	ν_{CO} (KBr, cm^{-1})	ν_{CO} (solvent, cm^{-1})	ν_{CN} (KBr, cm^{-1})	^{15}N NMR (ppm)
$\text{ReTo}^{\text{M}}(\text{CO})_3$, 5	2012, 1892	2013, 1894 (THF) 2019, 1898 (CH_2Cl_2)	1582 cm^{-1}	-176.8
$\text{ReTo}^{\text{P}}(\text{CO})_3$, 6	2010, 1892	2012, 1896 (THF) 2014, 1897 (CH_2Cl_2)	1589 cm^{-1}	-195.6
$\text{MnTo}^{\text{M}}(\text{CO})_3$, 7	2018, 1899	2017, 1902 (THF) 2020, 1912 (CH_2Cl_2)	1592 cm^{-1}	-172.1
$\text{MnTo}^{\text{P}}(\text{CO})_3$, 8	2016, 1961	2017, 1908 (THF)	1601 cm^{-1}	not detected
$\text{H}[\text{To}^{\text{P}}]$	n.a.	n.a.	1601 cm^{-1}	-195.6

			(broad)	
K[To ^P]	n.a.	n.a.	1601 cm ⁻¹	-149.1

We briefly describe the general features of ReTo^M(CO)₃, as that compound and MnTo^M(CO)₃ are structurally and spectroscopically similar. The ¹H NMR spectrum of ReTo^M(CO)₃ (**5**) in benzene-*d*₆ contained singlet resonances for the methyl and methylene groups of the oxazoline moiety and three downfield multiplets corresponding to the phenyl group. The equivalence of the oxazoline rings indicates a κ³-*N,N,N*-coordination of the To^M ligand, consistent with a C_{3v}-symmetric structure. Likewise, the ¹³C spectrum of **5** contained a single set of oxazoline resonances and a single carbonyl resonance at 128.06 ppm. Crosspeaks between the oxazoline nitrogen and the ring methyl and methylene groups in a ¹H-¹⁵N HMBC experiment (performed at natural ¹⁵N abundance) provided a characteristic ¹⁵N NMR chemical shift of -176.8 ppm for **5**. This chemical shift is in the range of other late transition-metal complexes containing the To^M ligand and downfield from 2H-dimethyl-2-oxazoline (-127.9 ppm).

One ν_{CN} band at 1582 cm⁻¹ was observed in the solid-state infrared spectrum (KBr) of ReTo^M(CO)₃, which further supports the κ³-coordination. The solid-state IR spectrum of ReTo^M(CO)₃ also contains one sharp band and one broad absorption (2012 and 1892 cm⁻¹), corresponding to the symmetric and anti-symmetric carbonyl modes. These bands shift to slightly higher energy in the solution-phase spectrum acquired in THF (2013 and 1894 cm⁻¹) or dichloromethane (2019 and 1898 cm⁻¹).

X-ray quality single crystals of **5** and **7** were obtained from a concentrated toluene solution cooled to $-30\text{ }^{\circ}\text{C}$. The solution to the single crystal X-ray diffraction study confirms the identity of $\text{ReTo}^{\text{M}}(\text{CO})_3$ and reveals the tridentate *fac*- N,N,N - To^{M} coordination and also the presence of three carbonyl ligands (Figure 1). The relatively large rhenium(I) center and the steric and chelating properties of the To^{M} ligand result in small N-Re-N angles ($80.6(3)$ to $85.4(3)^{\circ}$). The carbonyl ligands are also slightly compressed, with C-Re-C angles less than 90° (from $86.1(5)$ to $87.2(5)^{\circ}$), away from the bulky To^{M} ligand. Compounds **5** and **7** form a fine isomorphous pair.

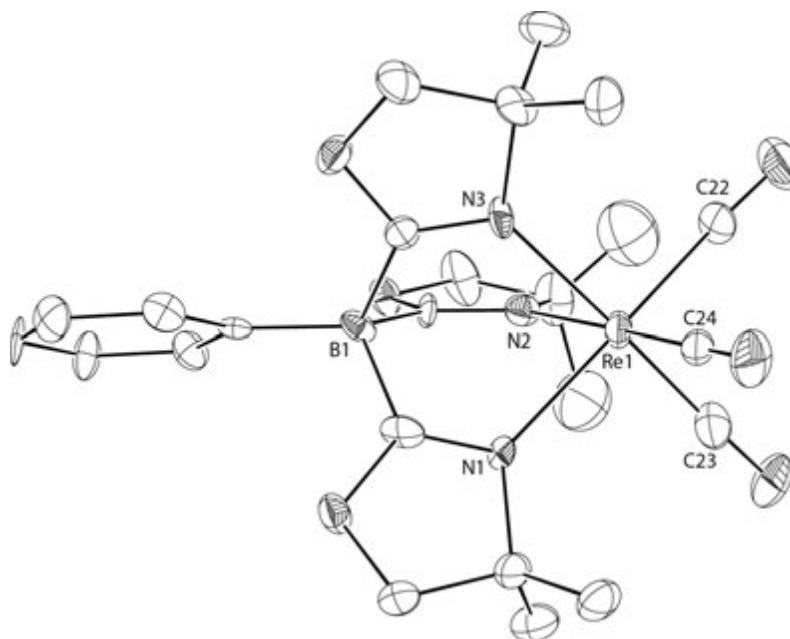
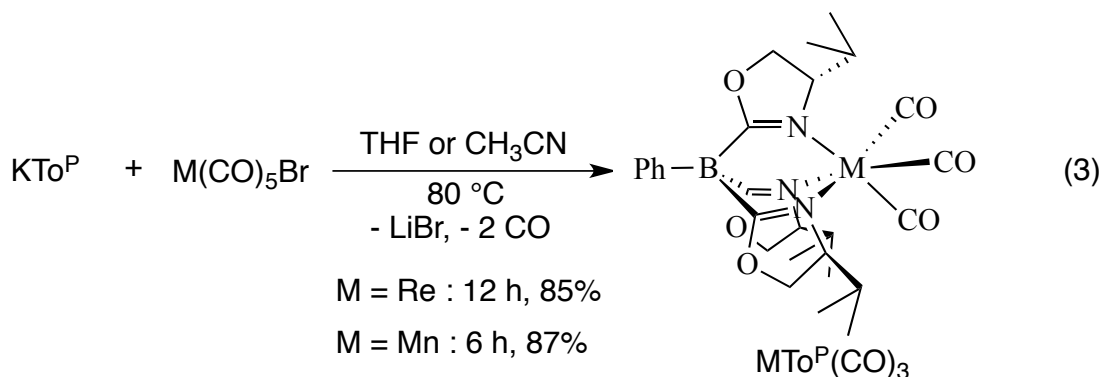


Fig.1 ORTEP diagram of **5**. Ellipsoids are drawn at 50% probability, and hydrogen and a disordered toluene (about an inversion center) are omitted for clarity. Compound **7** is isomorphous with **5**.

Reaction of optically active $\text{Li}[\text{To}^{\text{P}}]$ [To^{P} = tris(4*S*-isopropyl-2-oxazolinyl)phenyl borate] and $\text{MBr}(\text{CO})_5$ ($\text{M} = \text{Re}, \text{Mn}$) in THF at $80\text{ }^{\circ}\text{C}$ gave $\text{MTo}^{\text{P}}(\text{CO})_3$ which were contaminated with unidentified impurities. Unfortunately, recrystallization of the crude material in toluene at $-30\text{ }^{\circ}\text{C}$ was not effective for purification. We had previously found that the potassium salt

reactions of $\text{K}[\text{To}^{\text{P}}]$ with $\text{Re}(\text{CO})_5\text{Br}$ and $\text{Mn}(\text{CO})_5\text{Br}$ in THF at $80\text{ }^\circ\text{C}$ afforded $\text{ReTo}^{\text{P}}(\text{CO})_3$ (**6**) and $\text{MnTo}^{\text{P}}(\text{CO})_3$ (**8**), respectively, in 85% and 87% isolated yields (eqn (3)). As discussed for $\text{ReTo}^{\text{M}}(\text{CO})_3$, both **6** and **8** were characterized by crystallography and spectroscopy (Table 1).



X-Ray quality crystals were obtained for compounds **6** and **8**, and their structures reported here are the first containing the chiral To^{P} ligand. The X-ray crystal structures for these two compounds are isomorphous. The value of the Flack parameter, **6** = 0.010(6) and **8** = 0.005(9), establishes the absolute configuration of the structure as *S*, and this configuration is expected from our use of L-valine to prepare 4*S*-isopropyl-2-oxazoline. These structural studies provide valuable information about the steric properties of the chiral To^{P} ligand as well as the conformation favored in the solid state. The two $\text{MTo}^{\text{P}}(\text{CO})_3$ complexes have very similar structures, and the ORTEP diagram of **6** is shown in Fig. 2 (see ESIz for the X-ray structure of **8**). Significantly, in both **6** and **8**, the isopropyl groups are oriented so that the methine CH, rather than a methyl group, on each oxazoline is directed toward the $\text{Re}(\text{CO})_3$ moiety. This conformation appears to minimize unfavorable inter-ligand interactions.

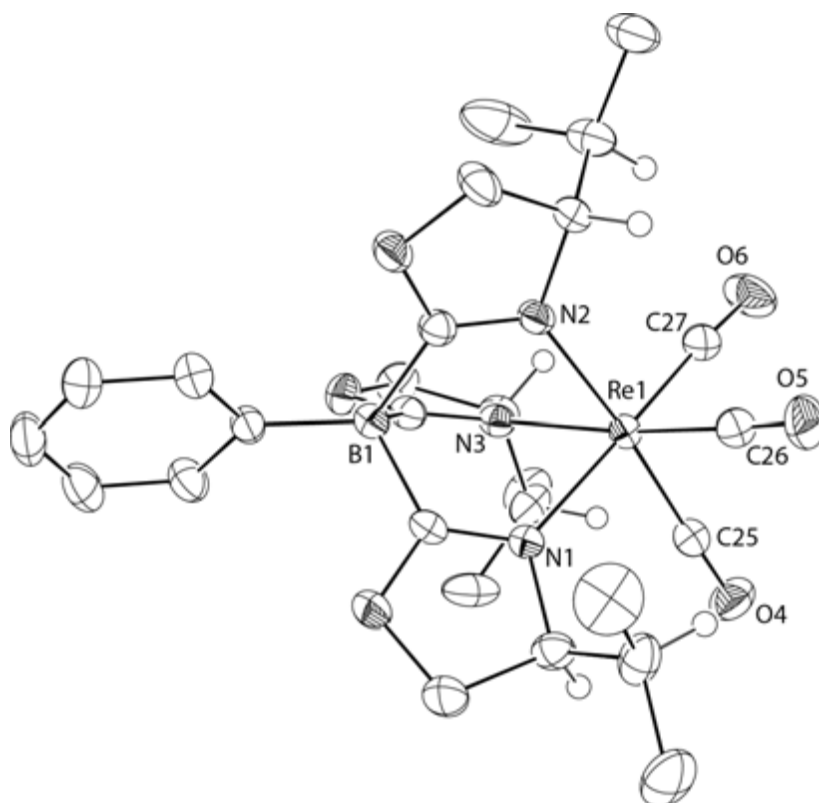


Figure 2. ORTEP diagram of $\text{ReTo}^{\text{P}}(\text{CO})_3$ (**6**). Hydrogen atoms on the methine carbons are shown to illustrate the *S* absolute configuration and isopropyl conformation for the oxazolines; all other hydrogen atoms and two co-crystallized toluene molecules are not included in the plot. A similar structure was observed for **8**.

Comparison of ligand donor strength of To^{M} , To^{P} , Tp , Tp^* , Cp and Cp^* ligands

In terms of the IR data, ligand (L) donor properties have traditionally been ranked by the ν_{CO} frequencies of $\text{ML}(\text{CO})$ complexes, with decreasing stretching frequencies being interpreted as increasing L donor strength.^{4, 8} Here we have compiled the ν_{CO} stretching frequency data (table 2) of the rhenium and manganese tricarbonyl complexes in CH_2Cl_2 to assess the relative donor ability of this new class of scorpionate compared to Cp and Tp-derivatives.

Table 2. ν_{CO} stretching frequency data of group 7 metal (Re, Mn) tricarbonyls.

Compounds	$\nu_{\text{CO,sym}}$ (cm^{-1})	$\nu_{\text{CO,asym}}$ (cm^{-1})	Avg $\nu_{\text{CO,sym}}$ (cm^{-1}) = $(\nu_{\text{CO,sym}} + 2 \nu_{\text{CO,asym}})/3$
ReTp(CO) ₃	2026	1912	1950
Re Tp*(CO) ₃	2018	1903	1941
ReCp(CO) ₃	2024	1926	1959
Re Cp*(CO) ₃	2005	1906	1939
ReTo ^M (CO) ₃	2019	1898	1938
ReTo ^P (CO) ₃	2014	1897	1936
MnTp(CO) ₃	2035	1932	1966
Mn Tp*(CO) ₃	2027	1922	1957
MnCp(CO) ₃	2022	1934	1963
Mn Cp*(CO) ₃	2004	1917	1946
MnTo ^M (CO) ₃	2020	1912	1948

Based on the ν_{CO} frequencies listed in Table 4, the scorpionate and Cp-like donor properties fall in the sequence Cp*, To^M, To^P > Tp* > Tp, Cp for the Mn complexes. In this ranking, we make no distinction between the averaged frequencies if they are the same within roughly the resolution of the IR measurement (4 cm^{-1}). For the Re complexes, the sequence is essentially the same: Cp*, To^M, To^P > Tp* > Tp > Cp. This analysis follows almost exactly the earlier trends summarized by Tellers *et al.*⁵ for Tp- and Cp-type complexes

and suggests that the tris (oxazolinyl)phenylborate ligands have an increased donor strength compared to Tp^* .

Comparison of steric properties of To^{M} , To^{P} , Tp , Tp^* , Cp and Cp^* ligands in $\text{Re}(\text{CO})_3$ complexes

A qualitative comparison of the steric properties of tris(oxazolinyl)borate and tris(pyrazolyl)borate ligands was obtained from Newman projections of the structures along their C_3 axis (Fig. 3). The steric bulk of the planar pyrazole groups in the Tp^* ligand is projected in the plane of the aromatic ring, leaving three large wedges of open space between the donor groups. In contrast, the non-planar oxazoline groups in To^{M} and To^{P} give a significantly different shape. The 4,4-dimethyl groups on To^{M} create a bowl-like hemi-sphere of steric bulk around the $-\text{Re}(\text{CO})_3$ moiety. In To^{P} , the steric bulk creates a windmill-like shape that blocks only one side of each carbonyl ligand.

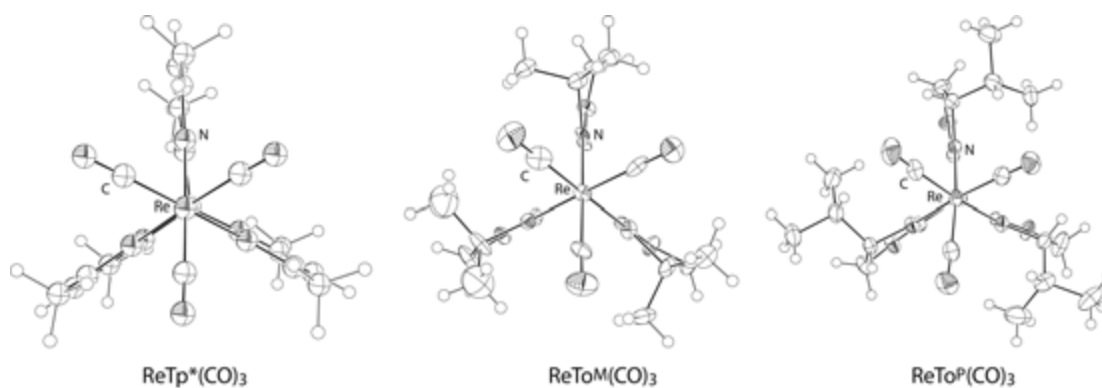


Figure 3. ORTEP diagrams of $\text{ReTp}^*(\text{CO})_3$,¹³ $\text{ReTo}^{\text{M}}(\text{CO})_3$, and $\text{ReTo}^{\text{P}}(\text{CO})_3$ molecules viewed along the C_3 -axis.

Solid angles provide a quantitative assessment of steric properties of a ligand,⁹ and may be calculated conveniently using coordinates from crystal structures or molecular models with

the program Solid-G.¹⁰ A solid angle is defined as the surface area of a projection of a ligand on a sphere surrounding a complex, and this approach for quantifying steric properties accounts for a ligand's shape.

Crystal structures have been reported for $\text{ReCp}(\text{CO})_3$,¹¹ $\text{ReCp}^*(\text{CO})_3$,¹² $\text{ReTp}(\text{CO})_3$, and $\text{ReTp}^*(\text{CO})_3$,¹³ as well as the corresponding manganese complexes. Those structures provided the coordinates to calculate solid angles for Cp, Cp*, Tp, and Tp* ligands (Table 3) in steradians. The crystal structures of To^{M} and To^{P} compounds reported here also were used to calculate solid angles. The second parameter given is the percent of a sphere's surface area that is taken up by the ligand's two-dimensional projection (maximized at 100% for a ligand that entirely surrounds a metal center).

Table 3. Solid angles for tris(oxazolinyl)phenyl borates, tris(pyrazolyl)borates, and cyclopentadienyls in rhenium tricarbonyl complexes.

Compound	Solid angle (steradians)	Percent of sphere occupied
$\text{ReTo}^{\text{M}}(\text{CO})_3$, 5	6.88	54.7
$\text{ReTo}^{\text{P}}(\text{CO})_3$, 6	6.61	52.6
$\text{Re Tp}^*(\text{CO})_3$, 2	6.49	51.6
$\text{ReTp}(\text{CO})_3$, 1	5.26	41.8
$\text{ReCp}^*(\text{CO})_3$, 10	4.72	37.6
$\text{ReCp}(\text{CO})_3$, 9	4.20	33.4

Comparison of the solid angles calculated for rhenium compounds provides the trend in steric bulk for the ancillary ligands: $\text{Cp} < \text{Cp}^* < \text{Tp} < \text{Tp}^* < \text{To}^{\text{P}} < \text{To}^{\text{M}}$, and the same trend is obtained for the manganese complexes. Notably, the tris(oxazolinyl)borate ligands occupy greater than a hemi-sphere around the rhenium center, and thus limit possible dimerization or ligand redistribution processes.

Conclusion.

This estimation of relative donor strength and three-dimensional orientation of this new class of scorpionate-type ligands around the group 7 metal centers (Re and Mn) will help us to assess and control the reactivity of To^M and To^P -metal complexes in future.

References.

- (1) (a) S. Trofimenko, *Scorpionates—The Coordination Chemistry of Polypyrazolylborate Ligands*, Imperial College Press, London, 1999; (b) S. Trofimenko, *Chem. Rev.*, 1993, **93**, 943; (c) J. Smith, *Comments Inorg. Chem.*, 2008, **29**, 189; (d) N. J. Beach, A. E. Williamson and G. J. Spivak, *J. Organomet. Chem.*, 2005, **690**, 4640.
- (2) (a) W. D. Jones and F. J. Feher, *J. Am. Chem. Soc.*, 1982, **104**, 4240; (b) D. M. Tellers and R. D. Bergman, *J. Am. Chem. Soc.*, 2001, **123**, 11508; (c) R. D. Bergman, T. R. Cundari, T. B. Gunnoe, W. D. Harman, T. R. Klinckman, M. D. Temple and M. D. White, *Organometallics*, 2003, **22**, 2331; (d) S. Milione, C. Cuomo and A. Grassi, *Top. Catal.*, 2006, **40**, 163.
- (3) (a) J. F. Dunne, J. Su, A. Ellern and A. D. Sadow, *Organometallics*, 2008, **27**, 2399; (b) H.-A. Ho, J. F. Dunne, A. Ellern and A. D. Sadow, *Organometallics*, 2010, **29**, 4105; (c) B. Baird, A. V. Pawlikowski, J. Su, J. W. Wiench, M. Pruski and A. D. Sadow, *Inorg. Chem.*, 2008, **47**, 10208.
- (4) D. D. LeCloux and W. B. Tolman, *J. Am. Chem. Soc.*, 1993, **115**, 1153.
- (5) D. M. Tellers, S. J. Skoog, R. G. Bergman, B. T. Gunnoe and D. W. Harman, *Organometallics*, 2000, **19**, 2428.
- (6) B. Kovac, L. Klasinc, Z. Raza and V. Sunjic, *J. Chem. Soc., Perkin Trans. 2*, 1999, 2455.
- (7) A. M. Tondreau, J. M. Darmon, B. M. Wile, S. K. Floyd, E. Lobkobsky and P. J. Chirik, *Organometallics*, 2009, **28**, 3928.
- (8) (a) D. R. Anton and R. H. Crabtree, *Organometallics*, 1983, **2**, 621; (b) C. A. Tolman, *J. Am. Chem. Soc.*, 1970, **92**, 2953.

- (9) D. White and N. J. Coville, *Adv. Organomet. Chem.*, Academic Press, New York, 1994, p. 95.
- (10) (a) I. A. Guzei and M. Wendt, *Dalton Trans.*, 2006, 3991; (b) I. A. Guzei and M. Wendt, Program Solid-G, UW-Madison, WI, USA, 2004.
- (11) P. J. Fitzpatrick, Y. Le Page and I. S. Butler, *Acta Crystallogr., Sect. B: Struct. Crystallogr. Cryst. Chem.*, 1981, **37**, 1052.
- (12) K. Raptis, E. Dornberger, B. Kanellakopulos, B. Nuber and M. L. Ziegler, *J. Organomet. Chem.*, 1991, **408**, 61.
- (13) J. E. Joachim, C. Apostolidis, B. Kanellakopulos, R. Maier, N. Marques, D. Meyer, J. Müller, A. Pires de Matos, B. Nuber, J. Rebizant and M. L. Ziegler, *J. Organomet. Chem.*, 1993, **448**, 119.

Experimental

General. All reactions were performed under a dry argon atmosphere using standard Schlenk techniques or under a nitrogen atmosphere in a glovebox, unless otherwise indicated. Water and oxygen were removed from benzene, toluene, pentane, acetonitrile, diethyl ether, and tetrahydrofuran solvents using an IT PureSolv system. Benzene- d_6 and tetrahydrofuran- d_8 were heated to reflux over Na/K alloy and vacuum-transferred. $\text{Re}(\text{CO})_5\text{Br}$ and $\text{Mn}(\text{CO})_5\text{Br}$ were prepared according to the literature procedure,¹ starting from $\text{Re}_2(\text{CO})_{10}$ and $\text{Mn}_2(\text{CO})_{10}$ respectively. $\text{Re}(\text{CO})_5\text{Br}$ was further purified by sublimation. $\text{Mn}(\text{CO})_5\text{Br}$ was used without further sublimation. $\text{Li}[\text{To}^{\text{M}}]_2$ and $\text{Li}[\text{To}^{\text{P}}]_3$ were prepared by literature procedures. ^{15}N chemical shifts were determined by ^1H - ^{15}N HMBC experiments on a Bruker Avance II 700 spectrometer with a Bruker Z-gradient inverse TXI $^1\text{H}/^{13}\text{C}/^{15}\text{N}$ 5 mm cryoprobe; ^{15}N chemical shifts were originally referenced to liquid NH_3 and recalculated to the CH_3NO_2 chemical shift scale by adding -381.9 ppm. ^{11}B NMR spectra were referenced to an external sample of $\text{BF}_3\text{Et}_2\text{O}$. Elemental analyses were performed using a Perkin-Elmer 2400 Series II

CHN/S by the Iowa State Chemical Instrumentation Facility. X-ray diffraction data was collected on a Bruker-AXS SMART or APEX II as described below.

ReTo^M(CO)₃ (5). A solution of LiTo^M (0.419 g, 1.08 mmol) in THF (20 mL) was added to Re(CO)₅Br (0.439 g, 1.08 mmol) suspended in THF (5 mL). The solution mixture was degassed with freeze-pump-thaw cycles (3×) and then heated to 80 °C for 8 h in a sealed flask. The volatile materials were removed under reduced pressure giving a yellowish solid, which was then extracted with benzene (12 mL). The benzene was evaporated to dryness providing an off-white solid that was washed with pentane (3 × 5 mL) and further dried under vacuum yielding 0.635 g of ReTo^M(CO)₃ (0.973 mmol, 90.0%) as a white powder. X-ray quality single crystals were grown from a concentrated toluene solution of ReTo^M(CO)₃ at -30 °C. ¹H NMR (400 MHz, methylene chloride-*d*₂): δ 1.08 (s, 18 H, CNCMe₂CH₂O), 3.36 (s, 6 H, CNCMe₂CH₂O), 7.36 (t, ³J_{HH} = 6.6 Hz 1 H, *para*-C₆H₅), 7.54 (t, ³J_{HH} = 7.6 Hz, 2 H, *meta*-C₆H₅), 8.28 (d, ³J_{HH} = 7.2 Hz, 2 H, *ortho*-C₆H₅). ¹³C{¹H} NMR (175 MHz, methylene chloride-*d*₂): δ 28.18 (CNCMe₂CH₂O), 70.47 (CNCMe₂CH₂O), 81.15 (CNCMe₂CH₂O), 126.16 (*para*-C₆H₅), 126.95 (*meta*-C₆H₅), 135.77 (*ortho*-C₆H₅), 145.71 (br, *ipso*-C₆H₅), 188.43 (br, CNCMe₂CH₂O), 197.90 (Re(CO)₃). ¹¹B NMR (128 MHz, methylene chloride-*d*₂): δ -17.4. ¹⁵N{¹H} NMR (71 MHz, methylene chloride-*d*₂): δ -176.8. IR (KBr, cm⁻¹): 2973 (w), 2934 (W), 2012 (s, ν_{CO, sym}), 1892 (s, ν_{CO, asym}), 1582 (s, ν_{C=N}), 1462 (m), 1390 (w), 1373 (w), 1354 (w), 1289 (m), 1254 (w), 1203 (m), 1179 (w), 1161 (w), 963 (w). Anal. Calcd. for C₂₄H₂₉BN₃O₆Re: C, 44.18; H, 4.48; N, 6.44. Found: C, 44.13; H, 4.61; N, 6.07. mp 236 °C (decomp.)

MnTo^M(CO)₃ (7). The preparation of MnTo^M(CO)₃ follows the method used for ReTo^M(CO)₃ given above. LiTo^M (0.380 g, 0.976 mmol) and Mn(CO)₅Br (0.269 g, 0.979

mmol) afforded 0.454 g of $\text{MnTo}^{\text{M}}(\text{CO})_3$ (0.871 mmol, 89.0%) as a crystalline yellow solid following that procedure. X-ray quality single crystals were grown from a concentrated toluene solution of $\text{MnTo}^{\text{M}}(\text{CO})_3$ at $-30\text{ }^\circ\text{C}$. ^1H NMR (400 MHz, benzene- d_6): δ 1.16 (s, 18 H, $\text{CNCMe}_2\text{CH}_2\text{O}$), 3.40 (s, 6 H, $\text{CNCMe}_2\text{CH}_2\text{O}$), 7.35 (br m, 1 H, *para*- C_6H_5), 7.53 (br m, 2 H, *meta*- C_6H_5), 8.30 (br m, 2 H, *ortho*- C_6H_5). $^{13}\text{C}\{^1\text{H}\}$ NMR (175 MHz, benzene- d_6): δ 27.53 ($\text{CNCMe}_2\text{CH}_2\text{O}$), 69.54 ($\text{CNCMe}_2\text{CH}_2\text{O}$), 80.96 ($\text{CNCMe}_2\text{CH}_2\text{O}$), 126.30 (*para*- C_6H_5), 127.29 (*meta*- C_6H_5), 222.74 ($\text{Mn}(\text{CO})_3$), 136.32 (*ortho*- C_6H_5), 142.80 (br, *ipso*- C_6H_5), 189.59 (br, $\text{CNCMe}_2\text{CH}_2\text{O}$). ^{11}B NMR (128 MHz, benzene- d_6): δ -17.1 . $^{15}\text{N}\{^1\text{H}\}$ NMR (71 MHz, benzene- d_6): δ -172.1 . IR (KBr, cm^{-1}): 2969 (w), 2930 (W), 2879 (w), 2018 (s, $\nu_{\text{CO, sym}}$), 1899 (s, $\nu_{\text{CO, asym}}$), 1592 (s, $\nu_{\text{C=N}}$), 1463 (m), 1390 (w), 1372 (w), 1352 (w), 1285 (m), 1200 (m), 1181 (w), 1158 (w), 993 (w), 969 (w). Anal. Calcd. for $\text{C}_{24}\text{H}_{29}\text{BN}_3\text{O}_6\text{Mn}$: C, 55.30; H, 5.61; N, 8.06. Found: C, 55.10; H, 5.75; N, 8.05. Mp: 210-212 $^\circ\text{C}$.

HTo^P. LiTo^{P} (6.150 g, 14.26 mmol) and $[\text{HNET}_3]\text{Cl}$ (2.159 g, 15.68 mmol) were dissolved in methylene chloride and were stirred for 8 h at room temperature. The solution was filtered through a plug of neutral alumina. The methylene chloride was evaporated under reduced pressure giving a yellow solid, which was extracted with benzene. The filtrate was evaporated to dryness, providing 3.245 g of HTo^{P} (7.63 mmol, 53.5 %) as a yellow gel. ^1H NMR (benzene- d_6 , 400 MHz): δ 0.68 (d, 9 H, $^3J_{\text{HH}} = 6.8$ Hz, $\text{CNC}(\text{CHMe}_2)\text{HCH}_2\text{O}$), 0.87 (d, 9 H, $^3J_{\text{HH}} = 6.4$ Hz, $\text{CNC}(\text{CHMe}_2)\text{HCH}_2\text{O}$), 1.43 (m, 3 H, $\text{CNC}(\text{CHMe}_2)\text{HCH}_2\text{O}$), 3.44 (m, 3 H, $\text{CNC}(\text{CHMe}_2)\text{HCH}_2\text{O}$), 3.61 (t, 3 H, $^3J_{\text{HH}} = 8.4$ Hz, $\text{CNC}(\text{CHMe}_2)\text{HCH}_2\text{O}$), 3.85 (m, 3 H, $\text{CNC}(\text{CHMe}_2)\text{HCH}_2\text{O}$), 7.26 (t, 1 H, $^3J_{\text{HH}} = 7.2$ Hz, *para*- C_6H_5), 7.46 (t, 2 H, $^3J_{\text{HH}} = 7.2$ Hz, *meta*- C_6H_5), 8.11 (br, 2 H, *ortho*- C_6H_5). $^{13}\text{C}\{^1\text{H}\}$ NMR (benzene- d_6 , 100 MHz): δ 19.00 ($\text{CNC}(\text{CHMe}_2)\text{HCH}_2\text{O}$), 19.01 ($\text{CNC}(\text{CHMe}_2)\text{HCH}_2\text{O}$), 33.20 ($\text{CNC}(\text{CHMe}_2)\text{HCH}_2\text{O}$), 69.56

(CNC(CHMe₂)HCH₂O), 71.06 (CNC(CHMe₂)HCH₂O), 126.40 (*para*-C₆H₅), 127.87 (*meta*-C₆H₅), 134.90 (*ortho*-C₆H₅), 146.20 (br, *ipso*-C₆H₅), 188.10 (br, CNCMe₂CH₂O). ¹¹B NMR (benzene-*d*₆, 128.4 MHz): δ -16.6. ¹⁵N NMR (benzene-*d*₆, 71 MHz): δ -195.6. IR (KBr, cm⁻¹): 2961 (w, br), 1601 (s, ν_{C=N}), 1468 (m), 1424 (w), 1385 (w), 1313 (w), 1262 (m), 1169 (w), 1105 (w), 1026 (w), 968 (m). MS (TOF EI) Exact mass calc. for C₂₄H₃₆BN₃O₃: m/e 425.2850 ([M]⁺), Found 425.2866.

KTo^P. Solid KH was slowly added in small portions to a solution of HTo^P (0.602 g, 1.415 mmol) in THF (15 mL) until gas evolution was no longer observed. The suspension was stirred at room temperature for 1 h and filtered. THF was evaporated affording a pale yellow gel, which was then triturated with pentane providing 0.616 g of KTo^P (1.33 mmol, 93.9%) as an off-white solid. ¹H NMR (acetonitrile-*d*₃, 400 MHz): δ 0.79 (d, 9 H, ³J_{HH} = 6.8 Hz, CNC(CHMe₂)HCH₂O), 0.90 (d, 9 H, ³J_{HH} = 6.8 Hz, CNC(CHMe₂)HCH₂O), 1.58 (m, 3 H, CNC(CHMe₂)HCH₂O), 3.54 (t, 3 H, ³J_{HH} = 7.6 Hz, CNC(CHMe₂)HCH₂O), 3.69 (m, 3 H, CNC(CHMe₂)HCH₂O), 3.79 (m, 3 H, CNC(CHMe₂)HCH₂O), 6.94 (t, 1 H, ³J_{HH} = 6.8 Hz, *para*-C₆H₅), 7.02 (t, 2 H, ³J_{HH} = 7.2 Hz, *meta*-C₆H₅), 7.56 (d, 2 H, ³J_{HH} = 6.4 Hz, *ortho*-C₆H₅). ¹³C{¹H} NMR (acetonitrile-*d*₃, 100 MHz): δ 18.35 (CNC(CHMe₂)HCH₂O), 19.88 (CNC(CHMe₂)HCH₂O), 33.67 (CNC(CHMe₂)HCH₂O), 67.29 (CNC(CHMe₂)HCH₂O), 73.72 (CNC(CHMe₂)HCH₂O), 124.80 (*para*-C₆H₅), 126.90 (*meta*-C₆H₅), 135.90 (*ortho*-C₆H₅), 152.74 (br, *ipso*-C₆H₅), 183.65 (br, CNCMe₂CH₂O). ¹¹B NMR (benzene-*d*₆, 128.4 MHz): δ -16.7. ¹⁵N NMR (benzene-*d*₆, 71 MHz): δ -149.1. IR (KBr, cm⁻¹): 2956 (w, br), 2882 (w), 1601 (s, ν_{C=N}), 1480 (m), 1467 (m), 1430 (m), 1385 (m), 1367 (m), 1263 (m), 1105 (w, br), 967 (m, br), 899 (m), 855 (m), 739 (w), 705 (m). Exact mass calc. for C₄₈H₇₀B₂KN₆O₆: m/e 887.5180 ([2M-K]⁺), Found 887.5279. Mp 95-97 °C.

ReTo^P(CO)₃ (6). The preparation of ReTo^P(CO)₃ follows the method used for ReTo^M(CO)₃ given above. KTo^P (0.314 g, 0.677 mmol) and Re(CO)₅Br (0.276 g, 0.677 mmol) afforded 0.400 g of ReTo^P(CO)₃ (0.576 mmol, 85.1%) as a pale yellow solid. X-ray quality colorless single crystals were grown from a concentrated toluene solution of ReTo^P(CO)₃ at – 30 °C. ¹H NMR (acetonitrile-*d*₃, 400 MHz): δ 0.64 (d, 9 H, ³J_{HH} = 4.0 Hz, CNC(CHMe₂)HCH₂O), 0.94 (d, 9 H, ³J_{HH} = 4.0 Hz, CNC(CHMe₂)HCH₂O), 2.46 (m, 3 H, CNC(CHMe₂)HCH₂O), 4.1 (m, 3 H, CNC(CHMe₂)HCH₂O), 4.26 (m, 6 H, CNC(CHMe₂)HCH₂O), 7.13 (t, 1 H, ³J_{HH} = 4.2 Hz, *para*-C₆H₅), 7.19 (t, 2 H, ³J_{HH} = 4.4 Hz, *meta*-C₆H₅), 7.63 (d, 2 H, ³J_{HH} = 4.0 Hz, *ortho*-C₆H₅). ¹³C{¹H} NMR (acetonitrile-*d*₃, 100 MHz): δ 13.89 (CNC(CHMe₂)HCH₂O), 18.90 (CNC(CHMe₂)HCH₂O), 30.19 (CNC(CHMe₂)HCH₂O), 70.63 (CNC(CHMe₂)HCH₂O), 73.83 (CNC(CHMe₂)HCH₂O), 126.54 (*para*-C₆H₅), 127.43 (*meta*-C₆H₅), 136.16 (*ortho*-C₆H₅), 142.62 (br, *ipso*-C₆H₅), 189.35 (br, CNCMe₂CH₂O), 198.31 (Re(CO)₃). ¹¹B NMR (acetonitrile-*d*₃, 128.4 MHz): δ –18.1. ¹⁵N NMR (acetonitrile-*d*₃, 71 MHz): δ –195.6. IR (KBr, cm⁻¹): 3045 (w), 2964 (m), 2873 (w), 2010 (s, ν_{CO, sym}), 1892 (s, br, ν_{CO, asym}), 1589 (s, ν_{C=N}), 1480 (m), 1463 (m), 1391 (m), 1373 (m), 1363 (m), 1352 (m), 1324 (w), 1277 (w), 1219 (s), 1143 (w), 1115 (m), 1046 (w), 1016 (w), 971 (m), 956 (m), 874 (m), 795 (w), 739 (w), 702 (m).). Anal. Calcd. for C₂₄₇H₃₅BN₃O₆Re: C, 46.69; H, 5.08; N, 6.05. Found: C, 45.94; H, 4.93; N, 5.82. Mp 205-207 °C (decomp.).

MnTo^P(CO)₃ (8). The preparation of MnTo^P(CO)₃ follows the method used for ReTo^M(CO)₃ given above. KTo^P (0.213 g, 0.460 mmol) and Mn(CO)₅Br (0.127 g, 0.462 mmol) yielded 0.227 g of MnTo^P(CO)₃ (0.402 mmol, 87%) as a yellow solid. X-ray quality single crystals were grown from a concentrated solution of MnTo^P(CO)₃ in a benzene-pentane mixture at ambient temperature. ¹H NMR (acetonitrile-*d*₃, 400 MHz): δ 0.64 (d, 9 H, ³J_{HH} = 4.0 Hz,

CNC(CHMe₂)HCH₂O), 0.94 (d, 9 H, ³J_{HH} = 4.0 Hz, CNC(CHMe₂)HCH₂O), 2.46 (m, 3 H, CNC(CHMe₂)HCH₂O), 4.1 (m, 3 H, CNC(CHMe₂)HCH₂O), 4.26 (m, 6 H, CNC(CHMe₂)HCH₂O), 7.13 (t, 1 H, ³J_{HH} = 4.2 Hz, *para*-C₆H₅), 7.19 (t, 2 H, ³J_{HH} = 4.4 Hz, *meta*-C₆H₅), 7.63 (d, 2 H, ³J_{HH} = 4.0 Hz, *ortho*-C₆H₅). ¹³C{¹H} NMR (benzene-*d*₆, 100 MHz): δ 13.96 (CNC(CHMe₂)HCH₂O), 19.17 (CNC(CHMe₂)HCH₂O), 29.90 (CNC(CHMe₂)HCH₂O), 69.90 (CNC(CHMe₂)HCH₂O), 72.95 (CNC(CHMe₂)HCH₂O), 126.17 (*para*-C₆H₅), 127.22 (*meta*-C₆H₅), 136.03 (*ortho*-C₆H₅), 142.80 (br, *ipso*-C₆H₅), 189.43 (br, CNCMe₂CH₂O), 222.85 (Mn(CO)₃). ¹¹B NMR (benzene-*d*₆, 128.4 MHz): δ -18.1. IR (KBr, cm⁻¹): 3045 (w), 2963 (m), 2873 (w), 2016 (s, ν_{CO, sym}), 1961 (s, br, ν_{CO, asym}), 1601 (s, ν_{C=N}), 1496 (w), 1481 (m), 1464 (m), 1432 (w), 1391 (m), 1372 (m), 1364 (m), 1350 (m), 1325 (w), 1278 (w), 1226 (s), 1116 (m), 1044 (m), 972 (m), 873 (m), 798 (m), 738 (w), 702 (m). Anal. Calcd. for C₂₇H₃₅BN₃O₆Mn: C, 57.57; H, 6.26; N, 7.46. Found: C, 57.20; H, 6.53; N, 7.36. mp 194-196 °C.

(1) S. P. Schmidt, W. C. Trogler and F. Basolo, *Inorg. Synth.*, 1985, **23**, 41.

(2) J. F. Dunne, J. Su, A. Ellern and A. D. Sadow, *Organometallics*, 2008, **27**, 2399.

(3) B. Baird, A. V. Pawlikowski, J. Su, J. W. Wiench, M. Pruski and A. D. Sadow, *Inorg. Chem.*, 2008, **47**, 10208.

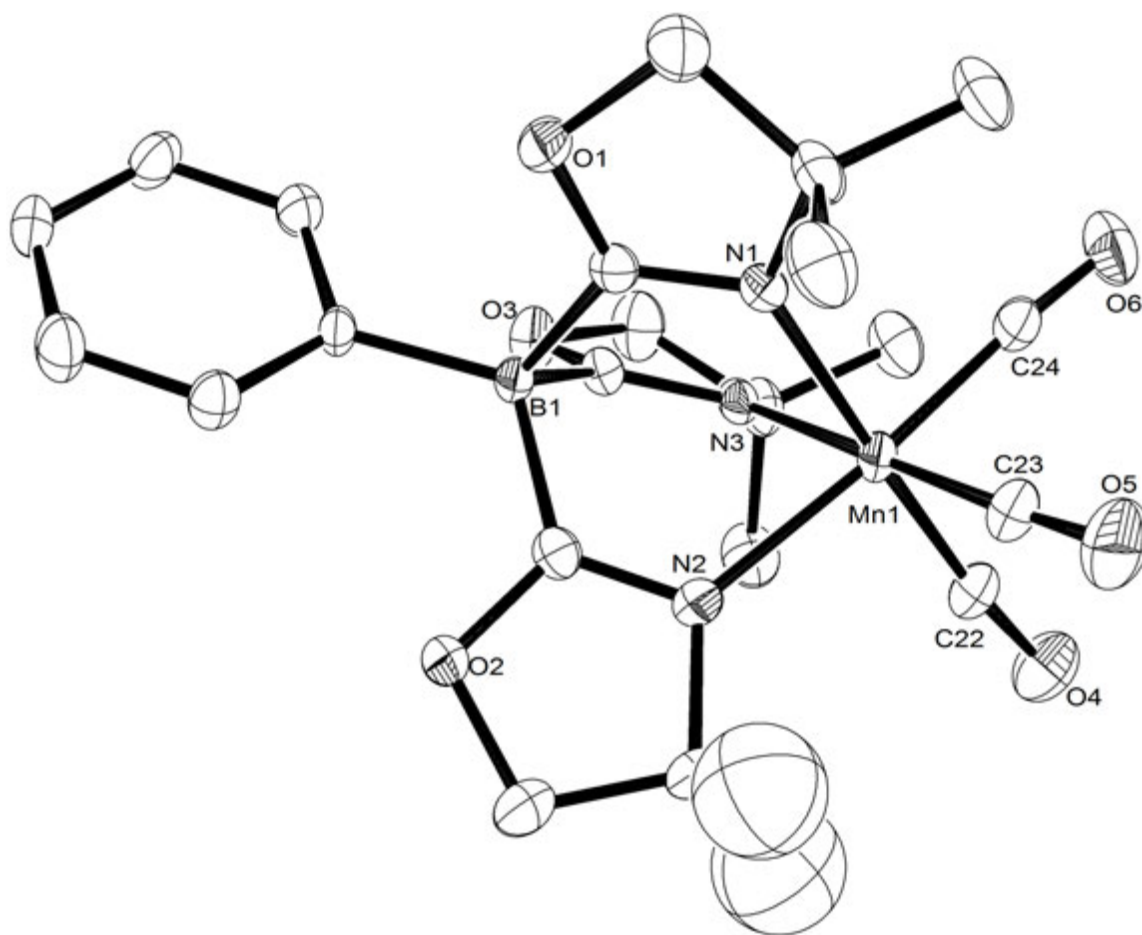


Fig. S-1 ORTEP diagram of $\text{MnTo}^{\text{M}}(\text{CO})_3$ (**7**). Ellipsoids are drawn at 50% probability, and hydrogen and a disordered toluene (about an inversion center) are omitted for clarity.

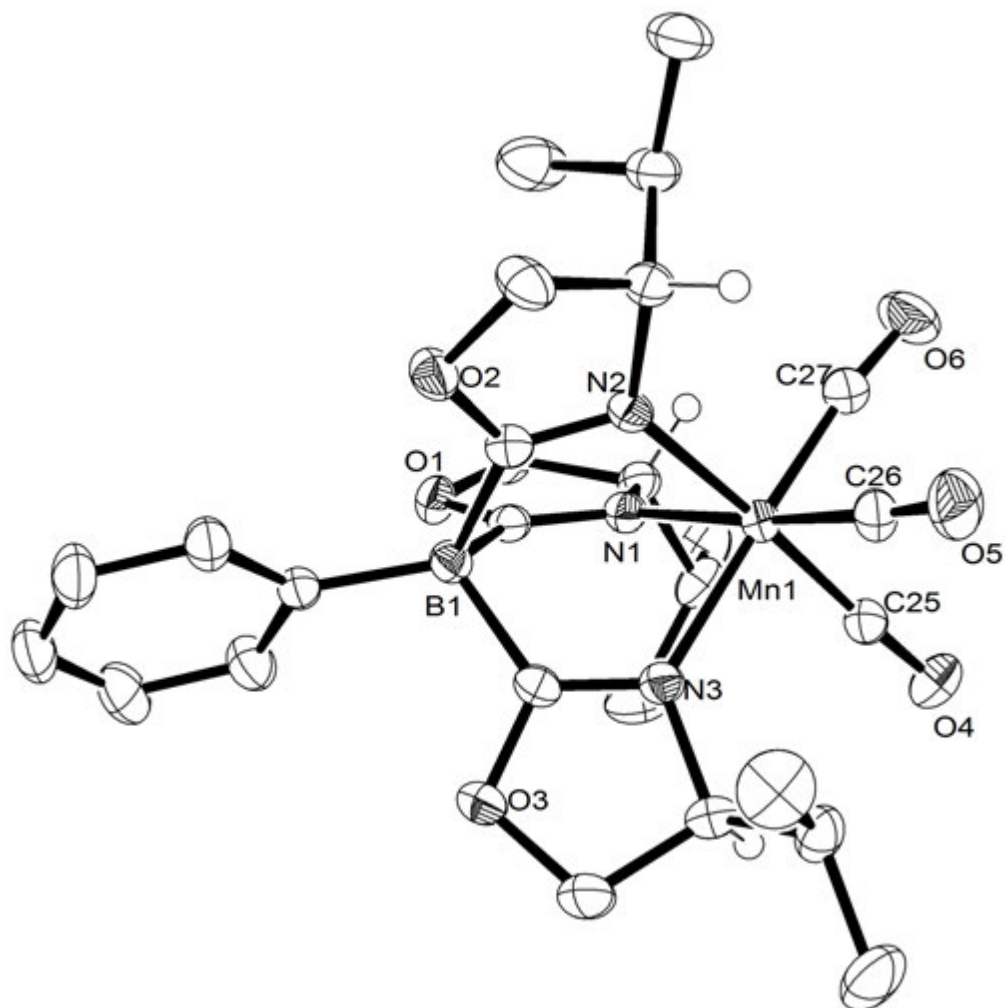


Fig. S-2 ORTEP diagram of $\text{MnTo}^{\text{P}}(\text{CO})_3$ (**8**). Hydrogen atoms on the methine carbons are shown to illustrate the *S* absolute configuration and isopropyl conformation for the oxazolines; all other hydrogen atoms and two co-crystallized benzene molecules are not included in the plot.

Chapter 3: Conversion of a Zinc Disilazide to a Zinc Hydride Mediated by LiCl

Modified from a paper published in *Journal of the American Chemical Society*[‡]

Debabrata Mukherjee, Arkady Ellern, and Aaron D. Sadow*

Department of Chemistry, U.S. DOE Ames Laboratory, Iowa State University, Ames, IA

50011-3111

Abstract.

An unusual β -elimination reaction involving Zn(II) and LiCl is reported. LiCl and a coordinatively saturated disilazido zinc compound form an adduct that contains activated SiH moieties. In THF/toluene mixtures, this adduct is transformed into a zinc hydride and 0.5 equiv. cyclodisilazane. The Li^+ and Cl^- ions apparently affect the reaction pathway of the disilazido zinc in a synergistic fashion. Thus the zinc hydride and cyclodisilazane products of formal β -elimination are not observed upon treatment of the zinc disilazide with Cl^- or Li^+ separately.

Introduction.

Organozinc compounds are valuable in synthetic chemistry as alkyl, aryl, silyl and hydride transfer agents that complement organolithium and organomagnesium reagents.¹ Importantly, alkali metal and alkaline earth metal salt adducts of zinc reagents give selective group transfer chemistry that is distinct from monometallic main group reagents, and related adducts facilitate selective arene, hydrocarbon, and alkylether metalations.² Zn(II) centers also mediate physiological processes involving group transfer as in liver alcohol dehydrogenase (LADH), where hydride transfer from a zinc alkoxide to NAD^+ is proposed.³

A connection between synthetic and physiological zinc chemistry is provided by molecular coordination complexes such as tris(pyrazolyl)borato zinc alkoxides and hydroxide that model LADH,⁴ carbonic anhydrase,⁵ and phosphatase.⁶ Likewise, hydrolase-like transesterifications are catalyzed by tris-1,1,1-(oxazoliny)ethane zinc dicarboxylato and ditriflato compounds for kinetic resolution of chiral esters.⁷

Given the importance of zinc-mediated group transfer chemistry, it is interesting that β -hydrogen elimination is not a common pathway for organozinc compounds. For example, ZnEt_2 undergoes β -elimination only upon IR laser pyrolysis at 600-650 °C, whereas thermal treatment results in Zn-C bond hemolysis.⁸ Few solution phase β -eliminations have been suggested, most notably in the thermolysis of $[\text{NaZnEt}_3]$ under reducing conditions.⁹ A three-coordinate diketiminato zinc hydride is prepared from the corresponding zinc chloride and $\text{KNH}i\text{-PrBH}_3$ via an unobserved amido- BH_3 intermediate.¹⁰ β -Elimination was also proposed as an initiation step in a zinc-catalyzed ketone hydrosilylation.¹¹ Identification of conditions that favor or disfavor β -H elimination in zinc(II) compounds may have important implications in group transfer reactions in synthetic and enzymatic chemistry. Here, we report a coordinatively saturated oxazolinyborato disilazidozinc(II) compound that undergoes a formal β -H elimination at room temperature facilitated by LiCl.

Results and Discussion.

Treatment of $\text{To}^{\text{M}}\text{ZnCl}$ (**1**) (To^{M} = tris(4,4-dimethyl-2-oxazoliny)phenylborate) with $\text{LiN}(\text{SiHMe}_2)_2$ in benzene readily provides $\text{To}^{\text{M}}\text{ZnN}(\text{SiHMe}_2)_2$ (**2**), and no other products are detected by ^1H NMR spectroscopy before or after workup. The spectroscopic features of the

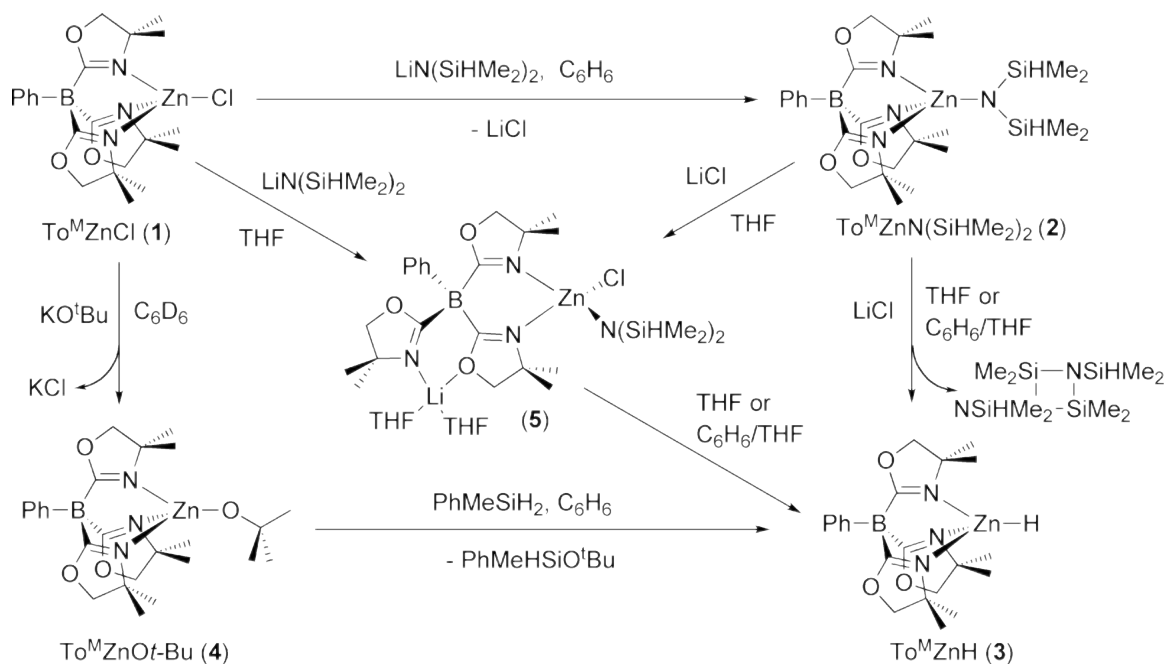
SiH, including its downfield chemical shift (5.26 ppm), high $^1J_{\text{SiH}}$ (185 Hz), and ν_{SiH} (2110 cm^{-1}), are consistent with a normal disilazido ligand. An X-ray crystal structure (see Supporting Information) contains Zn \cdots H and Zn \cdots Si distances (2.98 Å and 3.06 Å) that are longer than the sums of van der Waals radii.

Although **2** is formed quantitatively in benzene, in a benzene (10 mL) and THF (2 mL) mixture, the compounds **2**, **1**, and $\text{To}^{\text{M}}\text{ZnH}$ (**3**) (identified later) are present in a ratio of 20:1:8 upon workup after 24 h. Additionally, 1,3-diaza-2,4-disilacyclobutane ($\text{Me}_2\text{HSiN-SiMe}_2$)₂,¹² is observed. This cyclodisilazane is the head-to-tail dimer of silaimine $\text{Me}_2\text{HSiN=SiMe}_2$; its formation and the presence of zinc hydride **3** suggest a β -elimination reaction. Reactions of lithium hydrosilazides and group 14 electrophiles (e.g.,

Me_3SiCl) in hexane give cyclodisilazanes, and silaimines are suggested as intermediates in one of the two proposed mechanisms.¹² These literature transformations require nonpolar media, and THF solvent gives substitution rather than elimination. Our zinc system contrasts with that of Me_3SiCl , with nonpolar solvents giving substitution and THF favoring elimination. Neither $\text{HN}(\text{SiHMe}_2)_2$ and LiCl nor mixtures of **1**, $\text{HN}(\text{SiHMe}_2)_2$, and LiCl afford the cyclodisilazane.

The identity of zinc hydride **3** is provided by its independent preparation in a two-step sequence. Reaction of **1** and $\text{KO}t\text{-Bu}$ provides $\text{To}^{\text{M}}\text{ZnO}t\text{-Bu}$ (**4**). As shown in Scheme 1,

Scheme 1. LiCl Adduct Formation, β -Elimination and Independent Synthesis of $\text{To}^{\text{M}}\text{ZnH}$



PhMeSiH₂ and **4** react to give **3**. Notably, **2** and PhMeSiH₂ do not readily provide **3**, presumably due to the hindered, non-nucleophilic nature of the zinc disilazide. The IR spectrum of **3** contains a ν_{ZnH} (1745 cm⁻¹, KBr), and the ZnH resonance appears at 4.29 ppm in the ¹H NMR spectrum (cf. HB(3-*t*Bupz)₃ZnH, δ_{ZnH} 5.36; ν_{ZnH} 1770 cm⁻¹).¹³ A single crystal X-ray diffraction study reveals that **3** is monomeric and contains a terminal zinc hydride, of which there are relatively few crystallographically studied examples including the four-coordinate Tp^{*t*Bu}ZnH and Tp^{Ph,Me}ZnH (for which the ZnH are not located)¹³ and a three-coordinate diketiminate ZnH (Zn-H 1.46(2) Å).¹⁰ The four-coordinate ZnH in **3** (1.52(2) Å) is longer by 0.06 Å.

LiN(SiHMe₂)₂ and **1** react in THF-*d*₈ to provide possible intermediates in the apparent β -elimination process. Two C_s- symmetric compounds are detected after 10 min, rather than

C_{3v} - symmetric **1**, **2**, and **3**. After 12 h at room temperature, the minor species is partly converted into **3** and $(\text{Me}_2\text{HSiN}-\text{SiMe}_2)_2$. Attempts to isolate these intermediates from toluene/THF solvent mixtures (crystallization conditions) afford crystals of **3**.

We suspected that the intermediates formed from **1** and $\text{LiN}-(\text{SiHMe}_2)_2$ in THF were LiCl adducts. Therefore, LiCl and zinc disilazide **2** were allowed to interact. A crystallized sample of the 1:1 LiCl/**2** adduct (**5**) has the same ^1H NMR spectrum as 1:1 $\text{LiN}(\text{SiHMe}_2)_2/\mathbf{1}$ (major isomer). The ν_{SiH} of this material is lower (2061 cm^{-1}) than in the case of **2**, and the $^1J_{\text{SiH}}$ (102 Hz) is significantly lower. Compound **5** is fluxional, as it crystallizes at $-80\text{ }^\circ\text{C}$ from THF with a C_1 -symmetric structure (Figure 1). Although spectroscopic features suggest $[\text{M}]-\text{SiH}$ interactions, there are no close contacts between the SiH moieties and the Zn or Li centers in **5**. Additionally, this interesting structure contains an unusual $O\text{-Li-},N\text{-Zn}$ -coordinated bridging oxazoline group. The phenyl group on boron and the chloride on zinc are disposed *syn*, as are the *N*-lithiated oxazoline and $\text{N}(\text{SiHMe}_2)_2$ groups. Because Li^+ and Cl^- are separate in **5**, we investigated these ions independently to determine their role in the formal β -elimination.

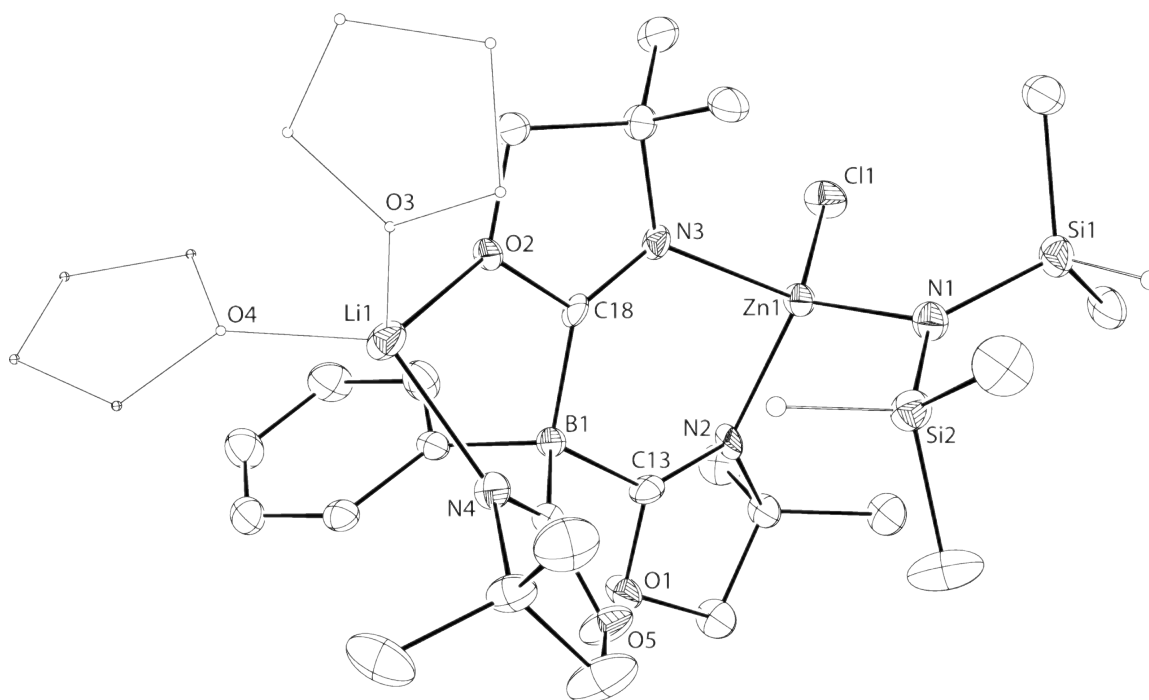
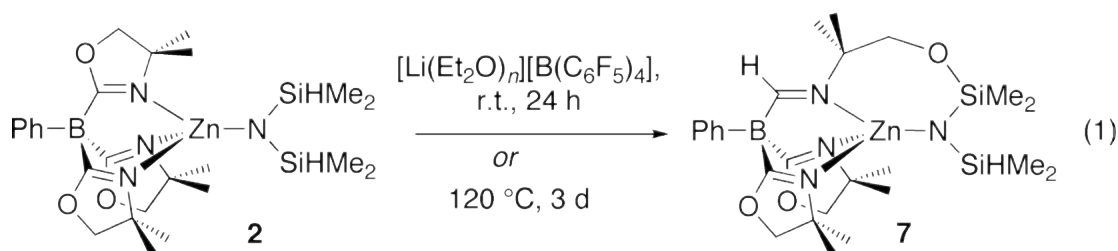


Figure 1. ORTEP diagram of **5** drawn at 35% probability.

Treatment of **2** with $[n\text{-Bu}_4\text{N}]\text{Cl}$ in a mixture of benzene- d_6 and THF- d_8 also gives two C_S -symmetric species. One of the isomers crystallizes and was structurally characterized as $[n\text{-Bu}_4\text{N}][(\kappa^2\text{-To}^M)\text{ZnClN}(\text{SiHMe}_2)_2]$ (**6**). The IR spectrum (KBr) of **6** shows a broad, intense ν_{SiH} at 2036 cm^{-1} , which is notably lower energy than in the case of **2** (2110 cm^{-1}) and **5** (2061 cm^{-1}). The 1J values in **6** (178 Hz) are slightly lower than in the case of **2** (185 Hz). After 1 week, neither **3** nor $(\text{Me}_2\text{HSiN-SiMe}_2)_2$ is observed, and no change is detected in the ^1H NMR spectrum. Thus, although addition of Cl^- affects the ν_{SiH} of the disilazide, it does not promote β -elimination from the Zn(II) amide.

Addition of $[\text{Li}(\text{Et}_2\text{O})_n][\text{B}(\text{C}_6\text{F}_5)_4]$ to **2** in benzene- d_6 /THF- d_8 mixtures results in oxazoline ring-opening giving O-Si bond formation and formal transfer of hydrogen from silicon to the (former) imidine carbon (eq 1).



A bimolecular transformation, in which a Zn-N bond of **5** reacts with a Si-H bond of a second molecule, might also explain the β -H elimination chemistry. However, THF- d_8 solutions of **5** and Et₃SiH (as a competitive tertiary SiH group) give To^MZnH and cyclodisilazane, while the Et₃SiH is unreacted. Also, only starting materials are observed upon treatment of **2** with Et₃SiH, ruling out an intermolecular dehydrocoupling-type mechanism.

Clearly, Li⁺ and Cl⁻ have a synergistic effect in this β -elimination reaction through the formation of the adduct **5**, and this requirement is surprising given the coordinative and electronic saturation in both **2** and **5**. It is tempting to suggest that Cl⁻ dissociation from **5** gives a three-coordinate zinc center that undergoes β -elimination. However, such a mechanism requires an unlikely 2 \times repetition of a Cl⁻ coordination and dissociation sequence since the final product, To^MZnH, does not form a detectable adduct with LiCl, and Cl⁻ appears to be necessary to inhibit oxazoline ring-opening. Cl⁻ also does not appear to bind to silicon, as H-transfer is not observed in the absence of Li⁺. Furthermore, addition of the Lewis acids BPh₃ or B(C₆F₅)₃ to **6** does not provide cyclodisilazane, suggesting that Li⁺ is not acting as a Lewis acid in **5** to mediate hydride transfer.

Conclusion.

Lithium chloride also affects the electronic properties of the disilazide ligand, as shown by the spectroscopy of the β -SiH moiety. This electronic effect may be more significant than a low coordination number for zinc because the dicoordinate $\text{Zn}(\text{N}(\text{SiHMe}_2)_2)_2$ is not reported to undergo β -elimination.¹⁴ Therefore, we favor a mechanism in which the zinc hydride is formed from the four-coordinate $[(\kappa^2\text{-To}^M)\text{ZnClN}(\text{SiHMe}_2)_2]^-$. Given the importance of Zn-mediated reactions in synthetic, catalytic, and enzymatic chemistry, we are currently investigating related zinc amido, alkyl, silyl, and alkoxide compounds in β -H and group transfer reactions.

References.

- (1) Knochel, P.; Perrone, S.; Grenouillat, N. In *Applications I: Main Group Compounds in Organic Synthesis*; Knochel, P., Ed.; Elsevier: Amsterdam, 2007; Vol. 9, pp 81-144.
- (2) (a) Kennedy, A. R.; Klett, J.; Mulvey, R. E.; Wright, D. S. *Science* **2009**, *326*, 706–708. (b) Wunderlich, S. H.; Knochel, P. *Angew. Chem., Int. Ed.* **2007**, *46*, 7685–7688.
- (3) Lipscomb, W. N.; Strater, N. *Chem. Rev.* **1996**, *96*, 2375–2434.
- (4) (a) Parkin, G. *Chem. Rev.* **2004**, *104*, 699–767. (b) Bergquist, C.; Storrie, H.; Koutcher, L.; Bridgewater, B. M.; Friesner, R. A.; Parkin, G. *J. Am. Chem. Soc.* **2000**, *122*, 12651–12658. (c) Bergquist, C.; Parkin, G. *Inorg. Chem.* **1999**, *38*, 422–423.
- (5) (a) Alsfasser, R.; Trofimenko, S.; Looney, A.; Parkin, G.; Vahrenkamp, H. *Inorg. Chem.* **1991**, *30*, 4098–100. (b) Alsfasser, R.; Powell, A. K.; Vahrenkamp, H. *Angew. Chem., Int. Ed. Engl.* **1990**, *29*, 898–899. (c) Walz, R.; Weis, K.; Ruf, M.; Vahrenkamp, H. *Chem. Ber./Recl.* **1997**, *130*, 975–980.
- (6) Hikichi, S.; Tanaka, M.; Moro-oka, Y.; Kitajima, N. *J. Chem. Soc., Chem. Commun.* **1992**,

814–815.

(7) Dro, C.; Bellemin-Lapponnaz, S.; Welter, R.; Gade, L. H. *Angew. Chem., Int. Ed.* **2004**, *43*, 4479–4482.

(8) (a) Kim, Y. S.; Won, Y. S.; Hagelin-Weaver, H.; Omenetto, N.; Anderson, T. *J. Phys. Chem. A* **2008**, *112*, 4246–4253. (b) Linney, R. E.; Russell, D. K. *J. Mater. Chem.* **1993**, *3*, 587–590.

(9) Lennartson, A.; Håkansson, M.; Jagner, S. *Angew. Chem., Int. Ed.* **2007**, *46*, 6678–6680.

(10) Spielmann, J.; Piesik, D.; Wittkamp, B.; Jansen, G.; Harder, S. *Chem. Commun.* **2009**, 3455–3456.

(11) Ge´rard, S.; Pressel, Y.; Riant, O. *Tetrahedron: Asymmetry* **2005**, *16*, 1889–1891.

(12) (a) Wiseman, G. H.; Wheeler, D. R.; Seyferth, D. *Organometallics* **1986**, *5*, 146–152. (b) Kosse, P.; Popowski, E. *Z. Anorg. Allg. Chem.* **1993**, *619*, 613–616.

(13) (a) Han, R.; Gorrell, I. B.; Looney, A. G.; Parkin, G. *J. Chem. Soc., Chem. Commun.* **1991**, 717–719. (b) Looney, A.; Han, R.; Gorrell, I. B.; Cornebise, M.; Yoon, K.; Parkin, G.; Rheingold, A. L. *Organometallics* **1995**, *14*, 274–288. (c) Rombach, M.; Brombacher, H.; Vahrenkamp, H. *Eur. J. Inorg. Chem.* **2002**, 153–159.

(14) Liang, Y.; Anwander, R. *Dalton Trans.* **2006**, 1909–1918.

Experimental.

General.

All reactions were performed under a dry argon atmosphere using standard Schlenk techniques or under a nitrogen atmosphere in a glovebox, unless otherwise indicated. Water and oxygen were removed from benzene, toluene, pentane, diethyl ether, and tetrahydrofuran solvents using an IT PureSolv system. Benzene-*d*₆ and tetrahydrofuran-*d*₈ were heated to

reflux over Na/K alloy and vacuum-transferred. Anhydrous ZnCl_2 was purchased from Aldrich and used as received. $\text{KO}t\text{-Bu}$ was purified by sublimation before use. PhMeSiH_2 was distilled and stored over 4 Å mol. sieves in the glovebox prior to use. $\text{Li}[\text{To}^{\text{M}}]$ and $\text{LiN}(\text{SiHMe}_2)_2$ were synthesized following the reported procedures.^{1,2} ^{15}N chemical shifts were determined by ^1H - ^{15}N HMBC experiments on a Bruker Avance II 700 spectrometer with a Bruker Z-gradient inverse TXI $^1\text{H}/^{13}\text{C}/^{15}\text{N}$ 5 mm cryoprobe; ^{15}N chemical shifts were originally referenced to liquid NH_3 and recalculated to the CH_3NO_2 chemical shift scale by adding -381.9 ppm. ^{11}B NMR spectra were referenced to an external sample of $\text{BF}_3\cdot\text{Et}_2\text{O}$. Elemental analyses were performed using a Perkin-Elmer 2400 Series II CHN/S by the Iowa State Chemical Instrumentation Facility. X-ray diffraction data was collected on a APEX II as described below.

$\text{To}^{\text{M}}\text{ZnCl}$ (1). A solution of $\text{Li}[\text{To}^{\text{M}}]$ (0.486 g, 1.25 mmol) in benzene (30 mL) was added to ZnCl_2 (0.174 g, 1.27 mmol) suspended in benzene (5 mL). This mixture was stirred at $50\text{ }^\circ\text{C}$ for 24 h in a teflon-valved storage flask and then filtered. The filtrate was evaporated to dryness providing an oil. Upon addition of pentane (15 mL), a white solid precipitated that was isolated by decanting the solvent. The solid was washed with pentane (3×5 mL) and dried under reduced pressure. Recrystallization was carried out from a concentrated toluene solution at $-30\text{ }^\circ\text{C}$ to obtain analytically pure $\text{To}^{\text{M}}\text{ZnCl}$ (0.471 g, 0.975 mmol, 78.1%).

Alternative synthesis of $\text{To}^{\text{M}}\text{ZnCl}$ via $\text{Tl}[\text{To}^{\text{M}}]$. A solution of $\text{Tl}[\text{To}^{\text{M}}]$ (1.054 g, 1.80 mmol) in benzene (15 mL) was added to ZnCl_2 (0.275 g, 2.02 mmol) suspended in benzene (5 mL). The solution instantaneously became turbid. This mixture was stirred for 24 h at room temperature and then filtered. The filtrate was evaporated to dryness providing a white solid

that was washed with pentane (3×5 mL) and further dried under vacuum yielding crystalline, analytically pure $\text{To}^{\text{M}}\text{ZnCl}$ (0.812 g, 1.68 mmol, 93.6%). X-ray quality single crystals were grown from a toluene solution of $\text{To}^{\text{M}}\text{ZnCl}$ at -30 °C. ^1H NMR (400 MHz, benzene- d_6): δ 1.09 (s, 18 H, $\text{CNCMe}_2\text{CH}_2\text{O}$), 3.43 (s, 6 H, $\text{CNCMe}_2\text{CH}_2\text{O}$), 7.35 (t, $^3J_{\text{HH}} = 7.2$ Hz, 1 H, *para*- C_6H_5), 7.53 (t, $^3J_{\text{HH}} = 7.2$ Hz, 2 H, *meta*- C_6H_5), 8.27 (d, $^3J_{\text{HH}} = 7.6$ Hz, 2 H, *ortho*- C_6H_5). $^{13}\text{C}\{^1\text{H}\}$ NMR (175 MHz, benzene- d_6): δ 28.11 ($\text{CNCMe}_2\text{CH}_2\text{O}$), 65.73 ($\text{CNCMe}_2\text{CH}_2\text{O}$), 81.35 ($\text{CNCMe}_2\text{CH}_2\text{O}$), 126.58 (*para*- C_6H_5), 127.38 (*meta*- C_6H_5), 136.26 (*ortho*- C_6H_5), 141.33 (br, *ipso*- C_6H_5), 190.58 (br, $\text{CNCMe}_2\text{CH}_2\text{O}$). ^{11}B NMR (128 MHz, benzene- d_6): δ -17.1. $^{15}\text{N}\{^1\text{H}\}$ NMR (71 MHz, benzene- d_6): δ -160.7. IR (KBr, cm^{-1}): 2969 (m), 1596 (s, ν_{CN}), 1461 (m), 1369 (m), 1352 (m), 1274 (m), 1195 (s), 1164 (m), 956 (s), 715 (m), 712 (s). Anal. Calcd. for $\text{C}_{21}\text{H}_{29}\text{BClN}_3\text{O}_3\text{Zn}$: C, 52.21; H, 6.05; N, 8.70. Found: C, 52.61; H, 6.11; N, 8.60. Mp 296-300 °C (dec).

$\text{To}^{\text{M}}\text{ZnN}(\text{SiHMe}_2)_2$ (2). A benzene solution of $\text{To}^{\text{M}}\text{ZnCl}$ (0.115 g, 0.238 mmol) was added to a benzene solution of $\text{LiN}(\text{SiHMe}_2)_2$ (0.033 g, 0.237 mmol). The resulting white mixture was stirred for 12 h at room temperature and then filtered. The filtrate was evaporated to obtain a white solid, which was washed with pentane (3×5 mL) and further dried under vacuum to obtain 0.092 g (0.159 mmol, 67.2%) of crystalline, analytically pure $\text{To}^{\text{M}}\text{ZnN}(\text{SiHMe}_2)_2$. X-ray quality single crystals were grown from a concentrated toluene solution of $\text{To}^{\text{M}}\text{ZnN}(\text{SiHMe}_2)_2$ at -30 °C. ^1H NMR (400 MHz, benzene- d_6): δ 0.54 (d, $^3J_{\text{HH}} = 3.2$ Hz, SiHMe_2), 1.19 (s, 18 H, $\text{CNCMe}_2\text{CH}_2\text{O}$), 3.43 (s, 6 H, $\text{CNCMe}_2\text{CH}_2\text{O}$), 5.26 (m, $^3J_{\text{HH}} = 3.2$ Hz, $^1J_{\text{SiH}} = 185$ Hz, SiHMe_2), 7.35 (t, $^3J_{\text{HH}} = 7.2$ Hz, 1 H, *para*- C_6H_5), 7.53 (t, $^3J_{\text{HH}} = 7.2$ Hz, 2 H, *meta*- C_6H_5), 8.29 (d, $^3J_{\text{HH}} = 7.6$ Hz, 2 H, *ortho*- C_6H_5). $^{13}\text{C}\{^1\text{H}\}$ NMR (175

MHz, benzene- d_6): δ 5.37 (SiHMe₂), 28.36 (CNCMe₂CH₂O), 66.50 (CNCMe₂CH₂O), 81.34 (CNCMe₂CH₂O), 126.29 (*para*-C₆H₅), 127.23 (*meta*-C₆H₅), 136.47 (*ortho*-C₆H₅), 142.63 (br, *ipso*-C₆H₅), 191.20 (br, CNCMe₂CH₂O). ¹¹B NMR (128 MHz, benzene- d_6): δ -17.1. ¹⁵N{¹H} NMR (71 MHz, benzene- d_6): -159.8 (CNCMe₂CH₂O), -170.2 (ZnN(SiHMe₂)₂). ²⁹Si{¹H} NMR (79.5 MHz, benzene- d_6): δ -13.9. IR (KBr, cm⁻¹): 2964 (m), 2110 (s, ν_{SiH}), 1594 (s, $\nu_{\text{C=N}}$), 1462 (m), 1353 (m), 1272 (m), 1244 (m), 1195 (m), 1040 (w), 959 (m), 922 (w), 886 (s), 810 (w). Anal. Calcd for C₂₅H₄₃BN₄O₃Si₂Zn: C, 51.77; H, 7.47; N, 9.66. Found: C, 51.31; H, 7.55; N, 9.46. Mp 232 – 234 °C (dec).

To^MZnH (3). PhMeSiH₂ (0.060 g, 0.491 mmol) and To^MZnOt-Bu (0.240 g, 0.461 mmol) were allowed to react at room temperature in benzene for 0.5 h. The volatile materials were removed under reduced pressure providing a white solid. This material was washed with pentane (3 × 5 mL) and dried under vacuum affording crystalline To^MZnH as an analytically pure white solid in good yield (0.182 g, 0.406 mmol, 88.0%). X-ray quality single crystals of To^MZnH were grown from a concentrated toluene solution at – 30 °C. ¹H NMR (400 MHz, benzene- d_6): δ 1.06 (s, 18 H, CNCMe₂CH₂O), 3.48 (s, 6 H, CNCMe₂CH₂O), 4.29 (s, 1 H, ZnH), 7.37 (t, ³J_{HH} = 7.2 Hz, 1 H, *para*-C₆H₅), 7.56 (t, ³J_{HH} = 7.6 Hz, 2 H, *meta*-C₆H₅), 8.37 (d, ³J_{HH} = 7.2 Hz, 2 H, *ortho*-C₆H₅). ¹³C{¹H} NMR (175 MHz, benzene- d_6): δ 28.30 (CNCMe₂CH₂O), 65.56 (CNCMe₂CH₂O), 80.99 (CNCMe₂CH₂O), 126.26 (*para*-C₆H₅), 127.26 (*meta*-C₆H₅), 136.42 (*ortho*-C₆H₅), 142.61 (br, *ipso*-C₆H₅), 190.28 (br, CNCMe₂CH₂O). ¹¹B NMR (128 MHz, benzene- d_6): δ -17.0. ¹⁵N{¹H} NMR (71 MHz, benzene- d_6): δ -156.0. IR (KBr, cm⁻¹): 2970 (s), 1745 (s, ν_{ZnH}), 1603 (s, $\nu_{\text{C=N}}$), 1461 (m), 1386 (m), 1367 (m), 1351 (m), 1272 (m), 1193 (m), 1161 (m), 953 (s), 895 (w), 842 (w), 818

(s), 749 (m), 709 (s), 673 (w), 658 (w). Anal. Calcd for $C_{21}H_{30}BN_3O_3Zn$: C, 56.22; H, 6.74; N, 9.37. Found: C, 55.89; H, 6.77; N, 9.20. Mp 272-276 °C (dec).

To^MZnOt-Bu (4). A benzene solution of To^MZnCl (0.405 g, 0.838 mmol, 10 mL) was added to KOt-Bu (0.094 g, 0.838 mmol) dissolved in benzene (5 mL). The reaction mixture was stirred for 12 h at room temperature. The KCl by-product was removed by filtration to provide a colorless solution. Evaporation of the benzene provided a white solid, which was washed with pentane (3 × 5 mL) and dried under vacuum affording crystalline, analytically pure To^MZnOt-Bu (0.390 g, 0.749 mmol, 89.4%). X-ray quality single crystals of To^MZnOt-Bu were obtained from a concentrated toluene solution at -30 °C. ¹H NMR (400 MHz, benzene-*d*₆): δ 1.16 (s, 18 H, CNCMe₂CH₂O), 1.65 (s, 9 H, ZnOCMe₃), 3.45 (s, 6 H, CNCMe₂CH₂O), 7.37 (t, ³J_{HH} = 7.2 Hz, 1 H, *para*-C₆H₅), 7.55 (t, ³J_{HH} = 7.6 Hz, 2 H, *meta*-C₆H₅), 8.31 (d, ³J_{HH} = 7.2 Hz, 2 H, *ortho*-C₆H₅). ¹³C{¹H} NMR (175 MHz, benzene-*d*₆): δ 28.27 (CNCMe₂CH₂O), 37.11 (ZnOCMe₃), 65.99 (CNCMe₂CH₂O), 68.59 (ZnOCMe₃), 81.16 (CNCMe₂CH₂O), 126.33 (*para*-C₆H₅), 127.27 (*meta*-C₆H₅), 136.40 (*ortho*-C₆H₅), 142.49 (br, *ipso*-C₆H₅), 190.35 (br, CNCMe₂CH₂O). ¹¹B NMR (128 MHz, benzene-*d*₆): δ -17.0. ¹⁵N{¹H} NMR (71 MHz, benzene-*d*₆): δ -158.8. IR (KBr, cm⁻¹): 2967 (s), 2931 (w), 1597 (s), 1578 (s), 1462 (m), 1368 (m), 1346 (m), 1274 (m), 1198 (s), 1163 (m), 990 (s), 967 (s), 940 (w), 899 (w), 845 (w), 818 (w), 745 (w), 733 (w), 704 (s), 675 (w). Anal. Calcd for $C_{25}H_{38}BN_3O_4Zn$: C, 57.66; H, 7.35; N, 8.07. Found: C, 57.18; H, 7.54; N, 8.00. Mp 260-262 °C (dec).

(THF)₂Li(μ-κ²-O,N-κ²-N,N-To^M)ZnClN(SiHMe₂)₂ (5). A THF solution of To^MZnN(SiHMe₂)₂ (0.856 g, 1.48 mmol) was added to a THF solution of LiCl (0.063 g, 1.49

mmol), and the resulting solution was cooled to $-80\text{ }^{\circ}\text{C}$. White crystalline material precipitated, which was then isolated and dried under vacuum to obtain $(\text{THF})_2\text{Li}(\mu\text{-}\kappa^2\text{-O,N-}\kappa^2\text{-N,N-To}^{\text{M}})\text{ZnClN}(\text{SiHMe}_2)_2$ (**5**) as a white solid in good yield (0.995 g, 1.30 mmol, 87.9%). X-ray quality single crystals were grown from a concentrated THF solution at $-80\text{ }^{\circ}\text{C}$. ^1H NMR (400 MHz, tetrahydrofuran- d_8): δ 0.09 (br d, 12 H, SiHMe_2), 1.34 (s, 6 H, $3.43\text{ CNCMe}_2\text{CH}_2\text{O}$), 1.45 (s, 6 H, $\text{CNCMe}_2\text{CH}_2\text{O}$), 1.50 (s, 6 H, $\text{CNCMe}_2\text{CH}_2\text{O}$), 1.78 (m, 8 H, $\alpha\text{-CH}_2$ THF), 3.62 (m, 8 H, $\beta\text{-CH}_2$ THF), 3.68 (d, $^2J_{\text{HH}} = 3.2$ Hz, 2 H, $\text{CN}(\text{Zn})\text{CMe}_2\text{CH}_2\text{O}$), 3.80 (d, $^2J_{\text{HH}} = 3.2$ Hz, 2 H, $\text{CN}(\text{Zn})\text{CMe}_2\text{CH}_2\text{O}$), 3.83 (s, 2 H, $\text{CN}(\text{Li})\text{CMe}_2\text{CH}_2\text{O}$), 4.61 (m, 2 H, $^1J_{\text{SiH}} = 102$ Hz, SiHMe_2), 6.97 (t, $^3J_{\text{HH}} = 4.0$ Hz, 1 H, *para*- C_6H_5), 7.05 (t, $^3J_{\text{HH}} = 4.0$ Hz, 2 H, *meta*- C_6H_5), 7.18 (d, $^3J_{\text{HH}} = 4.0$ Hz, 2 H, *ortho*- C_6H_5). $^{13}\text{C}\{^1\text{H}\}$ NMR (175 MHz, tetrahydrofuran- d_8): δ 4.15 (SiHMe_2), 26.52 (THF, $\beta\text{-CH}_2$), 28.36 ($\text{CNCMe}_2\text{CH}_2\text{O}$), 28.96 ($\text{CNCMe}_2\text{CH}_2\text{O}$), 68.20 ($\text{CNCMe}_2\text{CH}_2\text{O}$), 68.38 (THF, $\alpha\text{-CH}_2$), 78.72 ($\text{CNCMe}_2\text{CH}_2\text{O}$), 78.83 ($\text{CNCMe}_2\text{CH}_2\text{O}$), 125.73 (*para*- C_6H_5), 127.80 (*meta*- C_6H_5), 133.67 (*ortho*- C_6H_5), 149.79 (br, *ipso*- C_6H_5), 185.36 (br, $\text{CNCMe}_2\text{CH}_2\text{O}$). ^{11}B NMR (128 MHz, tetrahydrofuran- d_8): δ -17.1. $^{15}\text{N}\{^1\text{H}\}$ NMR: δ -161.0 ($\text{CN}(\text{Li})\text{CMe}_2\text{CH}_2\text{O}$), -161.6 ($\text{CN}(\text{Zn})\text{CMe}_2\text{CH}_2\text{O}$). $^{29}\text{Si}\{^1\text{H}\}$ NMR (79.5 MHz, tetrahydrofuran- d_8): δ -19.0. IR (KBr, cm^{-1}): 2965 (s), 2898 (m), 2061 (m, br, ν_{SiH}), 1613 (s, $\nu_{\text{C=N}}$), 1590 (s, $\nu_{\text{C=N}}$), 1463 (m), 1433 (m), 1370 (m), 1249 (m, br), 1197 (m), 998 (w), 971 (w), 930 (w), 895 (s), 738 (m). Anal. Calcd for $\text{C}_{33}\text{H}_{59}\text{BN}_4\text{O}_5\text{ClSi}_2\text{LiZn}$: C, 51.70; H, 7.76; N, 7.31. Found: C, 51.46; H, 7.75; N, 7.99. Mp $184\text{-}186\text{ }^{\circ}\text{C}$ (dec).

$[\text{nBu}_4\text{N}][(\kappa^2\text{-To}^{\text{M}})\text{Zn}(\text{Cl})\text{N}(\text{SiHMe}_2)_2]$ (**6**). A toluene solution of $\text{To}^{\text{M}}\text{ZnN}(\text{SiHMe}_2)_2$ (0.411 g, 0.709 mmol) was added to $[\text{nBu}_4\text{N}]\text{Cl}$ (0.197 g, 0.709 mmol) dissolved in THF (5 mL).

The reaction mixture was stirred for 1 h at room temperature inside the glove box. White crystalline solid precipitated upon partial evaporation of the solvent in vacuo. This mixture was cooled to $-30\text{ }^{\circ}\text{C}$ overnight to facilitate additional crystallization. The residual solvent was then decanted, and the crystalline solid was washed with cold toluene (5 mL) and pentane (5 mL) and finally dried under vacuum affording $[\text{nBu}_4\text{N}][(\kappa^2\text{-To}^{\text{M}})\text{Zn}(\text{Cl})\text{N}(\text{SiHMe}_2)_2]$ as analytically pure white solid in good yield (0.512 g, 0.594 mmol, 83.9%). $[\text{nBu}_4\text{N}][(\kappa^2\text{-To}^{\text{M}})\text{Zn}(\text{Cl})\text{N}(\text{SiHMe}_2)_2]$ is insoluble in pure benzene or toluene, so spectroscopic measurements were obtained in a 6:1 benzene- d_6 /tetrahydrofuran- d_8 mixture. Two isomers are present in a 3.6:1 ratio. X-ray quality single crystals were grown from a concentrated solution mixture containing toluene and tetrahydrofuran (20:1) at $-30\text{ }^{\circ}\text{C}$. ^1H NMR (400 MHz, benzene- d_6 :THF- d_8 = 6:1): δ 0.38 (d, $^3J_{\text{HH}} = 3.2$ Hz, SiHMe₂, minor isomer), 0.47 (d, $^3J_{\text{HH}} = 2.8$ Hz, SiHMe₂, major isomer), 0.87 (t, $^3J_{\text{HH}} = 7.2$ Hz, N(CH₂CH₂CH₂CH₃)₄), 1.17 (s, CNCMe₂CH₂O, minor isomer), 1.30-1.19 (m, N(CH₂CH₂CH₂CH₃)₄), 1.21 (s, CNCMe₂CH₂O, major isomer), 1.44 (s, CN(Zn)CMe₂CH₂O, major isomer), 1.50 (s, CN(Zn)CMe₂CH₂O, minor isomer), 1.55 (s, CN(Zn)CMe₂CH₂O, minor isomer), 1.57 (s, CN(Zn)CMe₂CH₂O, major isomer), 2.80 (t, br, $^3J_{\text{HH}} = 7.2$ Hz, N(CH₂CH₂CH₂CH₃)₄), 3.47 (d, $^2J_{\text{HH}} = 7.6$ Hz, CN(Zn)CMe₂CH₂O, major isomer), 3.49 (d, $^2J_{\text{HH}} = 7.6$ Hz, CN(Zn)CMe₂CH₂O, minor isomer), 3.52 (s, CNCMe₂CH₂O, minor isomer), 3.57 (s, CNCMe₂CH₂O, major isomer), 3.59 (d, $^2J_{\text{HH}} = 7.6$ Hz, CN(Zn)CMe₂CH₂O, major isomer), 3.65 (d, $^2J_{\text{HH}} = 7.6$ Hz, CN(Zn)CMe₂CH₂O, minor isomer), 5.01 (m, $^3J_{\text{HH}} = 3.2$ Hz, $^1J_{\text{SiH}} = 178$ Hz, SiHMe₂, minor isomer), 5.16 (m, $^3J_{\text{HH}} = 3.2$ Hz, $^1J_{\text{SiH}} = 178$ Hz, SiHMe₂, major isomer), 6.94-7.00 (m, *para*-C₆H₅, major and minor isomers), 7.08-7.12 (m, *meta*-C₆H₅, major and minor isomers), 7.84 (d, $^3J_{\text{HH}} = 7.6$ Hz, *ortho*-C₆H₅, minor isomer), 7.95 (d,

$^3J_{\text{HH}} = 6.8 \text{ Hz}$, *ortho*-C₆H₅, major isomer). $^{13}\text{C}\{^1\text{H}\}$ NMR (175 MHz, benzene-*d*₆:THF-*d*₈ = 6:1): δ 4.69 (N(SiHMe₂)₂, major isomer), 4.76 (N(SiHMe₂)₂, minor isomer), 14.18 (N(CH₂CH₂CH₂CH₃)₄), 20.36 (N(CH₂CH₂CH₂CH₃)₄), 24.50 (N(CH₂CH₂CH₂CH₃)₄), 28.14 (CN(Zn)CMe₂CH₂O, minor isomer), 28.28 (CN(Zn)CMe₂CH₂O, minor isomer), 28.35 (CN(Zn)CMe₂CH₂O, major isomer), 29.26 (CN(Zn)CMe₂CH₂O, major isomer), 29.38 (CN(Zn)CMe₂CH₂O, minor isomer), 29.52 (CN(Zn)CMe₂CH₂O, major isomer), 58.88 (N(CH₂CH₂CH₂CH₃)₄), 68.10 (CNCMe₂CH₂O, minor isomer), 68.27 (CNCMe₂CH₂O, major isomer), 76.86 (CNCMe₂CH₂O, minor isomer), 77.11 (CNCMe₂CH₂O, major isomer), 78.76 (CN(Zn)CMe₂CH₂O, minor isomer), 78.78 (CN(Zn)CMe₂CH₂O, major isomer), 124.61 (*para*-C₆H₅, major isomer), 124.77 (*para*-C₆H₅, minor isomer), 126.77 (*meta*-C₆H₅, minor isomer), 126.96 (*meta*-C₆H₅, major isomer), 135.48 (*ortho*-C₆H₅, major isomer), 136.30 (*ortho*-C₆H₅, minor isomer), 149.23 (br, *ipso*-C₆H₅, minor isomer), 150.36 (br, *ipso*-C₆H₅, major isomer), 177.63 (br, CNCMe₂CH₂O, major isomer), 180.25 (br, CNCMe₂CH₂O, minor isomer), 187.90 (br, CN(Zn)CMe₂CH₂O, minor isomer), 188.88 (br, CN(Zn)CMe₂CH₂O, major isomer). ^{11}B NMR (128 MHz, benzene-*d*₆): δ -16.9. $^{15}\text{N}\{^1\text{H}\}$ NMR (71 MHz, benzene-*d*₆): -168.1 (CN(Zn)CMe₂CH₂O, major isomer), -124.9 (CNCMe₂CH₂O, major isomer), -167.5 (CN(Zn)CMe₂CH₂O, minor isomer), -125.9 (CNCMe₂CH₂O, minor isomer), -163.4 (N(SiHMe₂)₂, major isomer), -162.6 (N(SiHMe₂)₂, minor isomer). $^{29}\text{Si}\{^1\text{H}\}$ NMR (benzene-*d*₆:THF-*d*₈ = 6:1, 79.5 MHz): δ -17.86 (major isomer), -18.68 (minor isomer). IR (KBr, cm⁻¹): 2964 s (br), 2878 s (br), 2045 (br s, ν_{SiH}), 1595 (s, $\nu_{\text{C=N}}$), 1463 (s), 1369 (m), 1272 (m), 1234 (s), 1197 (m), 1144 (m), 997 (s), 930 (m), 909 (s), 865 (m), 829 (w), 757 (m), 741 (m), 707 (s). Anal. Calcd for C₄₁H₇₉BN₅O₃Si₂ClZn : C, 57.40; H, 9.28; N, 8.16. Found: C, 57.57;

H, 9.02; N, 8.12. Mp 178-180 °C.

$\{\kappa^4\text{-}N,N,N,N\text{-PhB(Ox}^{\text{Me}_2})_2(\text{HCNCMe}_2\text{CH}_2\text{OSiMe}_2)\text{N(SiHMe}_2)\}\text{Zn}$ (7). A benzene solution of $\text{To}^{\text{M}}\text{ZnN(SiHMe}_2)_2$ (0.310 g, 0.585 mmol) was heated to 120 °C for 3 days in a sealable teflon-valved flask. The solvent was then evaporated to obtain a white solid, which was washed with pentane (3×5 mL) and dried under vacuum to obtain 0.210 g (0.396 mmol, 67.7%) of crystalline, analytically pure $\{\kappa^4\text{-}N,N,N,N\text{-PhB(Ox}^{\text{Me}_2})_2(\text{HCNCMe}_2\text{CH}_2\text{OSiMe}_2)\text{N(SiHMe}_2)\}\text{Zn}$. X-ray quality single crystals were grown from a concentrated toluene solution at -30 °C. ^1H NMR (400 MHz, benzene- d_6): δ 0.48 (s, 6 H, $\text{NSiMe}_2\text{O-}$), 0.53 (d, $^3J_{\text{HH}} = 3.2$ Hz, 6 H, NSiHMe_2), 0.84 (s, 6 H, $\text{HCNCMe}_2\text{CH}_2\text{OSiMe}_2$), 1.06 (s, 6 H, $\text{CNCMe}_2\text{CH}_2\text{O}$), 1.24 (s, 6 H, $\text{CNCMe}_2\text{CH}_2\text{O}$), 3.35 ($^3J_{\text{HH}} = 4.8$ Hz, 4 H, $\text{CNCMe}_2\text{CH}_2\text{O}$), 3.59 (s, 2 H, $\text{CNCMe}_2\text{CH}_2\text{O}$), 5.23 (m, 1 H, $^1J_{\text{SiH}} = 184$ Hz, NSiHMe_2), 7.40 (t, $^3J_{\text{HH}} = 7.2$ Hz, 1 H, *para*- C_6H_5), 7.57 (t, $^3J_{\text{HH}} = 7.6$ Hz, 2 H, *meta*- C_6H_5), 8.38 (d, $^3J_{\text{HH}} = 6.0$ Hz, 2 H, *ortho*- C_6H_5), 9.22 (s, 1 H, $\text{HCNCMe}_2\text{CH}_2\text{O}$). $^{15}\text{C}\{^1\text{H}\}$ NMR (175 MHz, benzene- d_6): δ 3.90 (SiMe_2), 4.69 (SiHMe_2), 25.47 ($\text{HCNCMe}_2\text{CH}_2\text{OSiMe}_2$), 28.18 ($\text{CNCMe}_2\text{CH}_2\text{O}$), 28.67 ($\text{CNCMe}_2\text{CH}_2\text{O}$), 62.73 ($\text{CNCMe}_2\text{CH}_2\text{O}$), 66.30 ($\text{CNCMe}_2\text{CH}_2\text{O}$), 71.02 ($\text{HCNCMe}_2\text{CH}_2\text{OSiMe}_2$), 80.59 ($\text{CNCMe}_2\text{CH}_2\text{O}$), 126.48 (*para*- C_6H_5), 127.90 (*meta*- C_6H_5), 135.40 (*ortho*- C_6H_5), 145.78 (br, *ipso*- C_6H_5), 190.13 (br, $\text{CNCMe}_2\text{CH}_2\text{O}$), 196.82 (br, $\text{HCN(Zn)CMe}_2\text{CH}_2\text{OSiMe}_2$). ^{11}B NMR (128 MHz, benzene- d_6): δ -16.8. $^{15}\text{N}\{^1\text{H}\}$ NMR (benzene- d_6 , 71 MHz): -263.6 ($\text{HCNCMe}_2\text{CH}_2\text{OSiMe}_2$), -166.1 ($\text{CNCMe}_2\text{CH}_2\text{O}$), -157.4 ($\text{ZnN(SiHMe}_2)(\text{SiMe}_2\text{O-})$). $^{29}\text{Si}\{^1\text{H}\}$ NMR (79.5 MHz, benzene- d_6): δ -67.63 (SiMe_2), -13.88 (SiHMe_2). IR (KBr, cm^{-1}): 2966 (s, br), 2891 (m, br), 2094 (s, ν_{SiH}), 1605 (m, $\nu_{\text{C=N}}$), 1557 (w), 1462 (m), 1368 (m),

1354 (m), 1274 (m), 1247 (s), 1195 (s), 1161 (m), 1109 (s), 1032 (s), 993 (w), 967 (w), 922 (m), 899 (m), 851 (m), 821 (w), 786 (w). Anal. Calcd for $C_{25}H_{43}BN_4O_3Si_2Zn$: C, 51.77; H, 7.47; N, 9.66. Found: C, 52.26; H, 7.46; N, 9.66. Mp 216-220 °C.

References

1. Dunne, J. F.; Su, J.; Ellern, A.; and Sadow, A. D. *Organometallics* **2008**, *27*, 2399–2401.
2. Eppinger, J.; Herdtweck, E.; Anwander, R. *Polyhedron* **1998**, *17*, 1195.

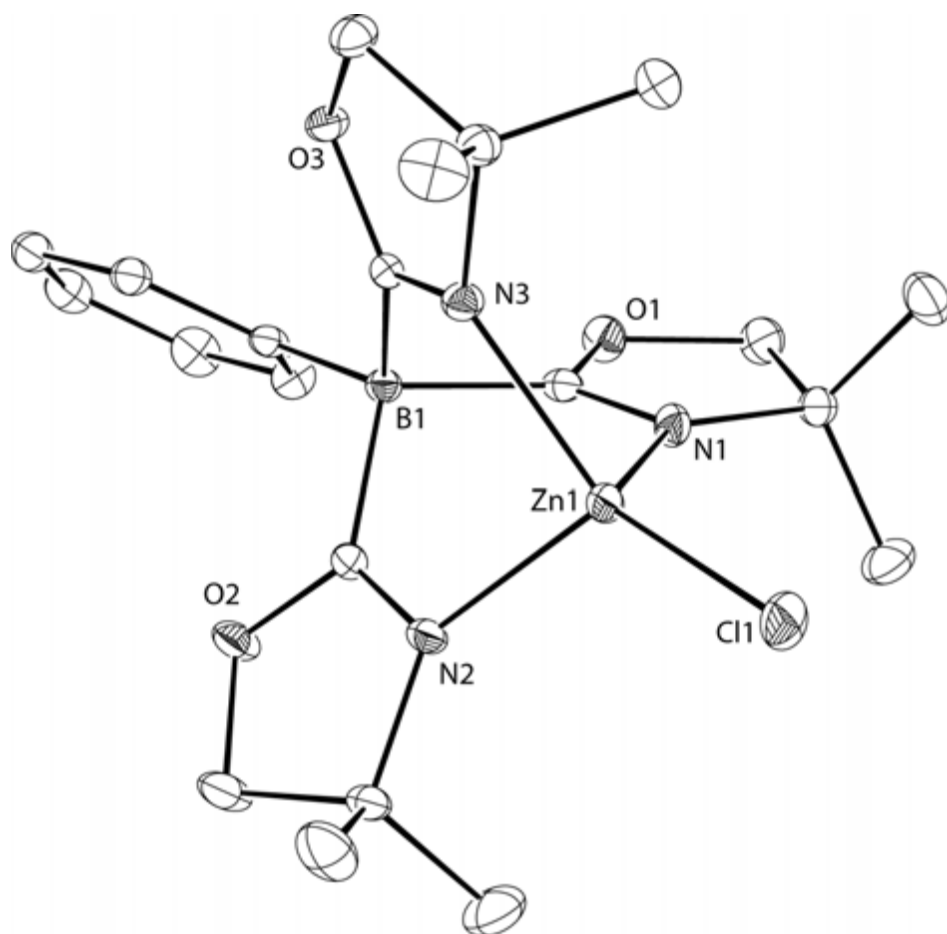


Figure S1. ORTEP diagram of $To^M ZnCl$ (**1**) with ellipsoids drawn at 50% probability. Hydrogen atoms are not included to enhance the clarity of heavy atom positions.

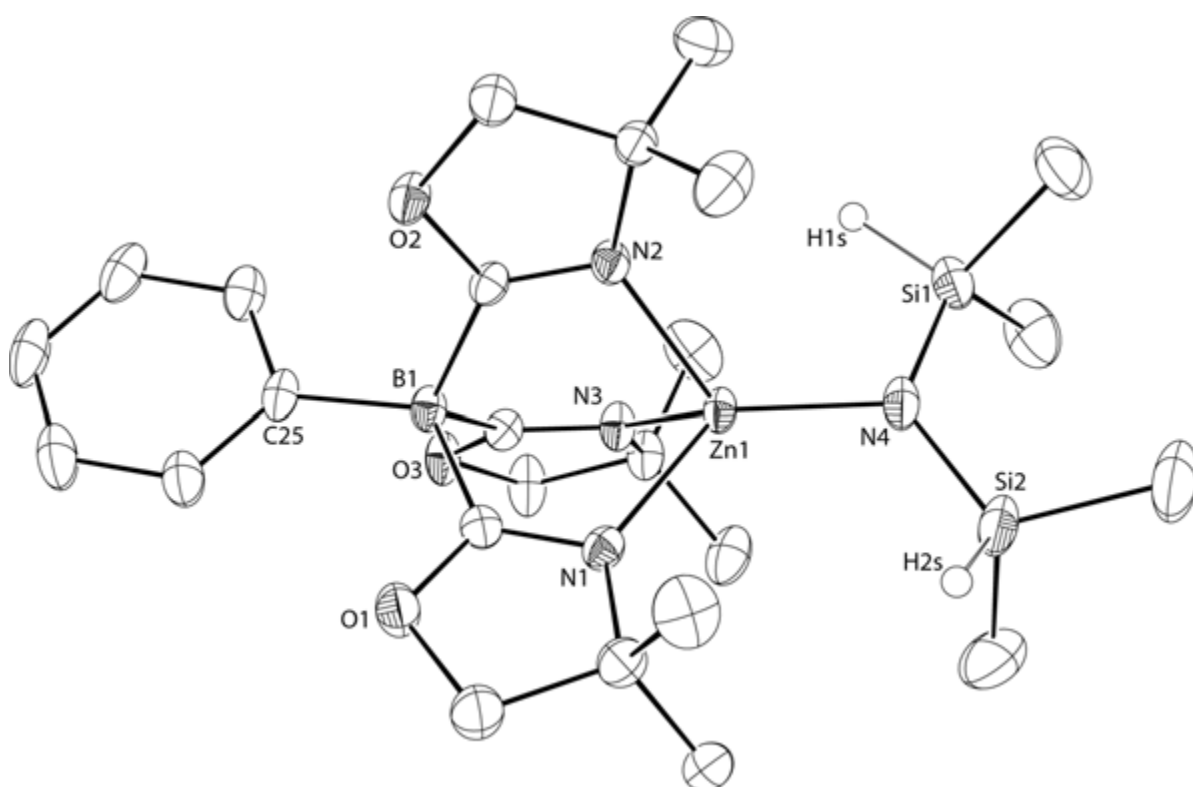


Figure S2. ORTEP diagram of $\text{To}^{\text{M}}\text{ZnN}(\text{SiHMe}_2)_2$ (**2**) with ellipsoids drawn at 50% probability. Hydrogen atoms, with the exception of those on Si, are not included to enhance the clarity of heavy atom positions.

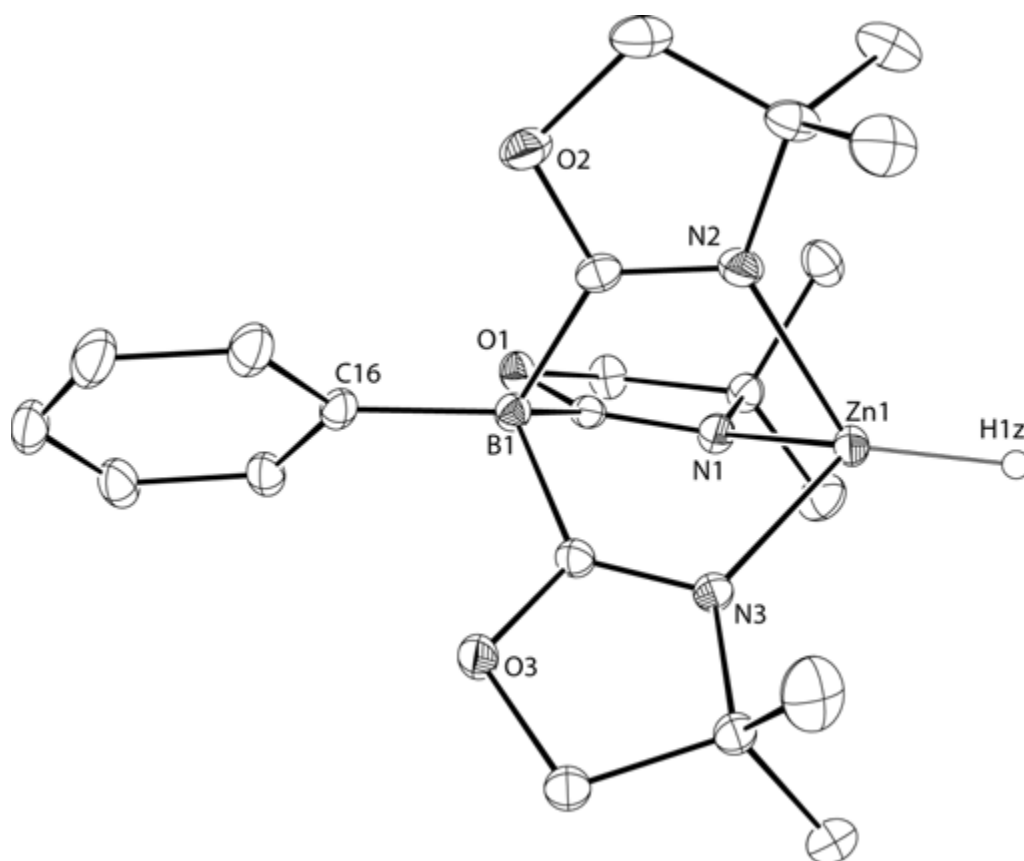


Figure S3. ORTEP diagram of $To^M ZnH$ (3) with ellipsoids drawn at 50% probability. Hydrogen atoms, with the exception of the one on Zn, are not included to enhance the clarity of heavy atom positions.

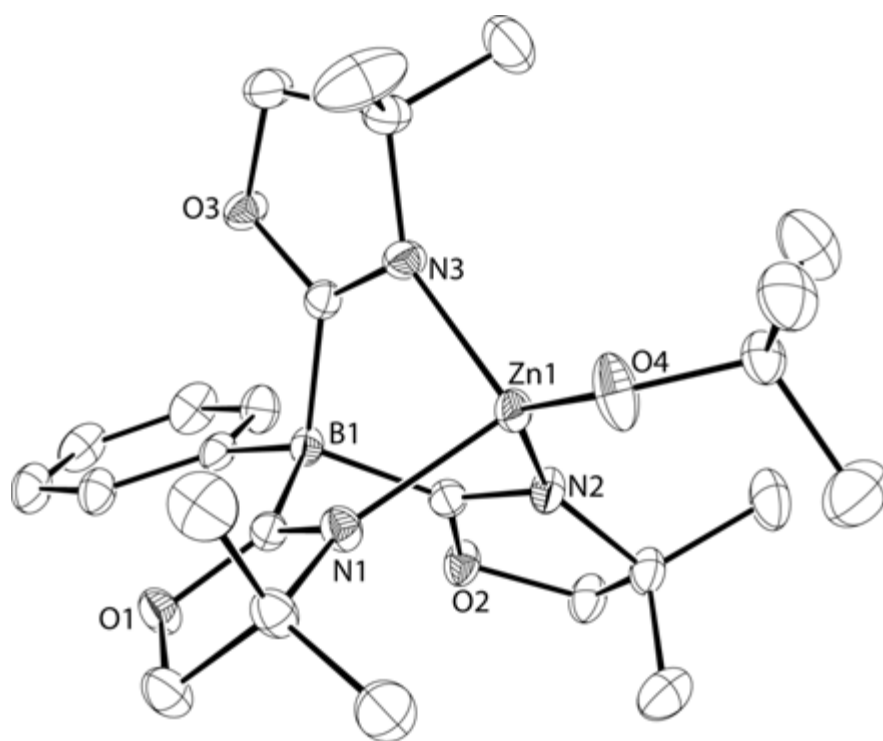


Figure S4. ORTEP diagram of $\text{To}^{\text{M}}\text{ZnOt-Bu}$ (**4**) with ellipsoids drawn at 50% probability. Hydrogen atoms are not included to enhance the clarity of heavy atom positions.

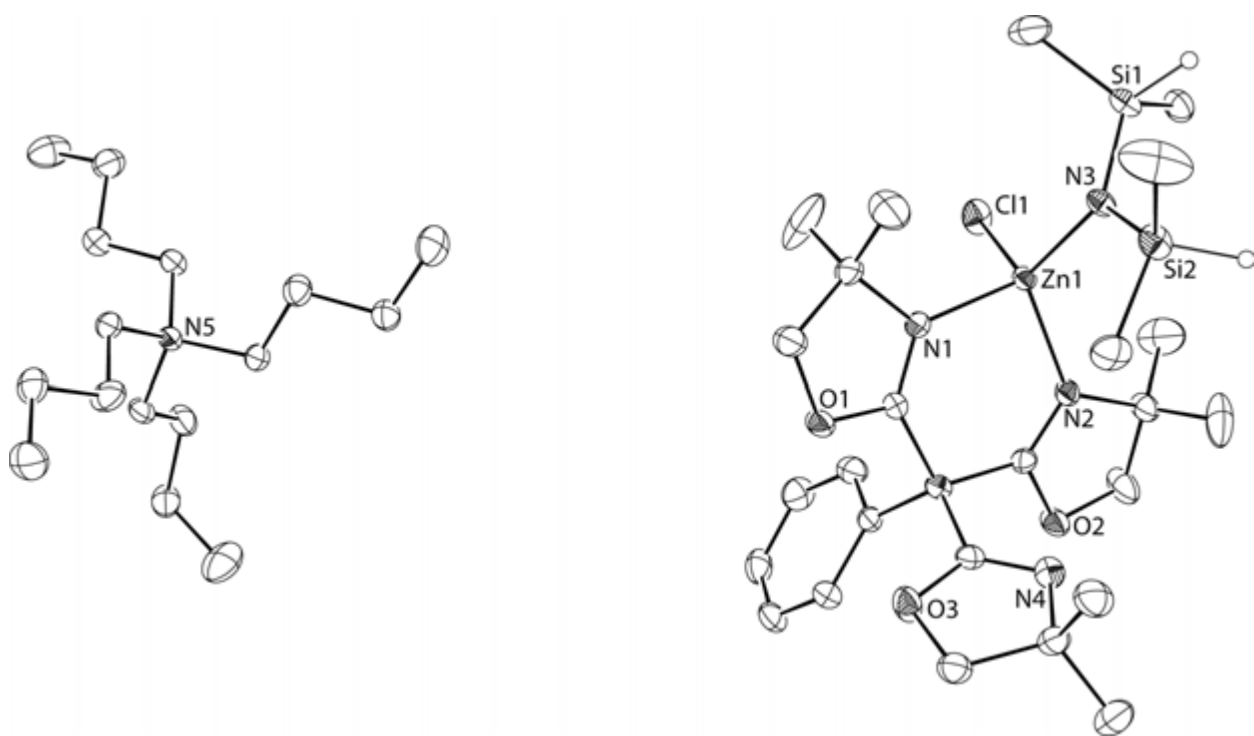


Figure S6. ORTEP diagram of $[n\text{Bu}_4\text{N}][\kappa^2\text{-To}^{\text{M}}]\text{Zn}(\text{Cl})\text{N}(\text{SiHMe}_2)_2$ (**6**) with ellipsoids drawn at 50% probability. Hydrogen atoms, with the exception of those bonded to Si, are not included to enhance the clarity of heavy atom positions.

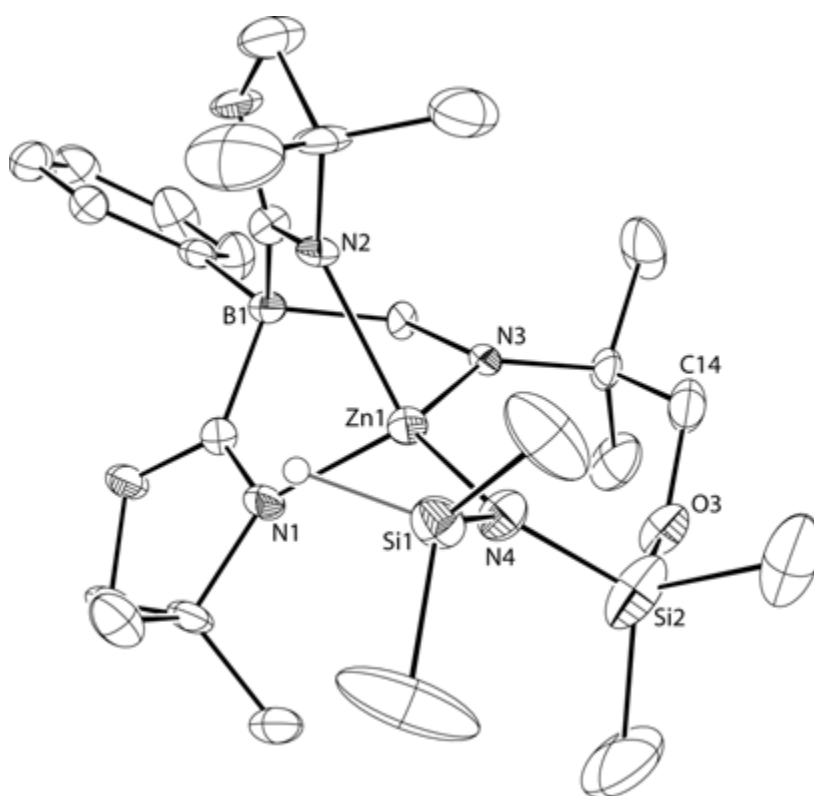


Figure S7. ORTEP diagram of $\{\kappa^4\text{-}N,N,N,N\text{-PhB(Ox}^{\text{Me}_2})_2(\text{CHNCMe}_2\text{CH}_2\text{OSiMe}_2)\text{N(SiHMe}_2)\}\text{Zn}$ (**7**) with ellipsoids drawn at 35% probability. Hydrogen atoms, with the exception of the one bonded to Si, are not included to enhance the clarity of heavy atom positions. Only one of the two superimposed molecules (resulting from disorder) is shown.

Chapter 4: Coordinatively Saturated Tris(oxazolinyl)borato Zinc Hydride-Catalyzed Cross-Dehydrocoupling of Silanes and Alcohols.

Modified from a paper published in *ACS Catalysis*[‡]

Debabrata Mukherjee, Richard R. Thompson, Arkady Ellern, and Aaron D. Sadow*

Department of Chemistry, U.S. DOE Ames Laboratory, Iowa State University, Ames, IA

50011-3111

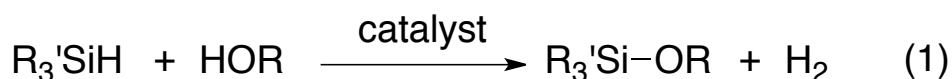
Abstract.

The four-coordinate zinc compound $\text{To}^{\text{M}}\text{ZnH}$ (**1**, To^{M} = tris(4,4-dimethyl-2-oxazolinyl)phenylborate) catalyzes selective alcoholysis of substituted hydrosilanes. The catalytic reaction of PhMeSiH_2 and aliphatic alcohols favors the monodehydrocoupled product PhMeHSi-OR . With the aryl alcohol 3,5- $\text{C}_6\text{H}_3\text{Me}_2\text{OH}$, the selectivity for mono(aryloxy)hydrosilane $\text{PhMeHSiOC}_6\text{H}_3\text{Me}_2$ and bis(aryloxy)silane $\text{PhMeSi}(\text{OC}_6\text{H}_3\text{Me}_2)_2$ is controlled by relative reagent concentrations. Reactions of secondary organosilanes and diols provide cyclic bis(oxo)silacycloalkanes in high yield. The empirical rate law for the $\text{To}^{\text{M}}\text{ZnH}$ -catalyzed reaction of 3,5-dimethylphenol and PhMeSiH_2 is $-\text{d}[\text{PhMeSiH}_2]/\text{dt} = k'_{\text{obs}}[\text{To}^{\text{M}}\text{ZnH}]^1[3,5\text{-C}_6\text{H}_3\text{Me}_2\text{OH}]^0[\text{PhMeSiH}_2]^1$ (determined at 96 °C) which indicates that Si–O bond formation is turnover-limiting in the presence of excess phenol.

Introduction.

Si–O bond formation is important in materials preparations and surface derivatizations. For example, alkoxy silanes are a central component in the preparation of functionalized mesoporous silica nanospheres (MSNs), either by co-condensation routes or grafting reactions

through hydrolytic Si–O bond formations.^{1,2} Our interest in the catalytic preparation of alkoxy silanes was inspired by our interactions with Prof. Victor Lin, as we sought to synthesize precursors for advanced silica-based functionalized nanomaterials for catalytic applications. Silyl ethers are also important building blocks in organosilicon chemistry and in synthetic organic chemistry as protecting groups.³ The reaction of chlorosilanes and alcohols provides a straightforward route to Si–O bonds. However, the HCl by-product of these reactions must be trapped with base, and this method is not useful for syntheses that require neutral conditions. The degree of condensation is difficult to control when more than one Si–Cl group is present in the silicon substrate. Furthermore, chlorosilanes are water sensitive and must be kept rigorously anhydrous prior to use. Catalytic Si–H bond alcoholysis (eq 1) can avoid these problems, giving H₂ as the byproduct and bypassing acid formation and/or basic conditions. Organosilanes are not hydrolytically sensitive (in the absence of a catalyst), and catalysts can control selectivity.

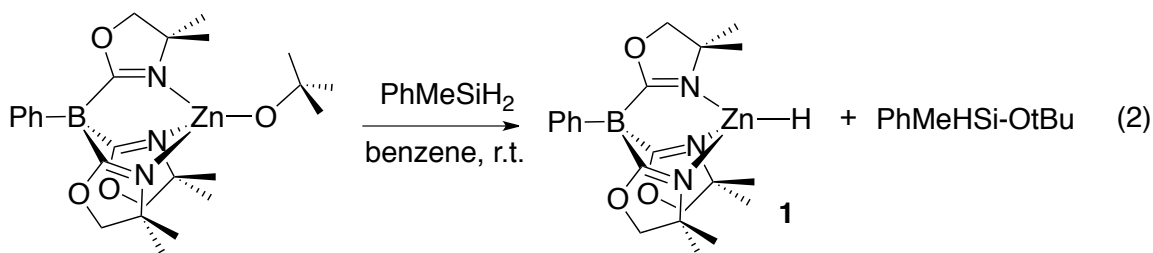


A range of homogeneous and heterogeneous catalytic systems have been developed for hydrosilane alcoholysis, including early, middle, and late transition metal complexes of titanium,^{4–6} manganese,⁷ rhenium,⁸ iron,⁹ ruthenium,^{10,11} rhodium,¹² iridium,¹³ nickel,^{14,15} copper,^{16–19} gold,²⁰ and platinum.²¹ Strong Lewis acids, such as B(C₆F₅)₃, are also catalysts.²² A number of reaction mechanisms have been proposed, including alcohol attack on η²-hydrosilane or silyl hydride transition-metal complexes formed via oxidative addition steps.^{7,13,14} In contrast, copper- and gold-catalyzed silane alcoholyses are proposed to involve

discrete metal hydride and metal-alkoxide intermediates (no M–Si bond).^{18,20} In situ generated zinc(II) catalysts are also proposed to follow this mechanism.²³ However, these zinc, copper, and gold catalysts are generated *in situ*, the catalytic speciation is unknown, and the turnover-limiting step has not been established.

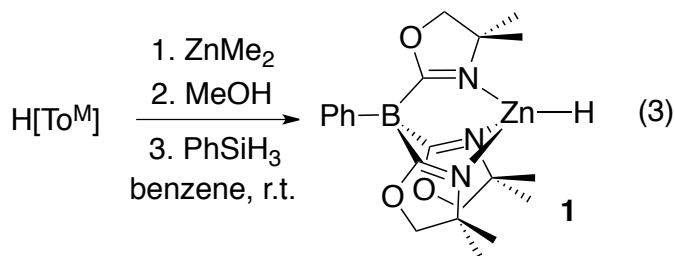
Results and Discussion.

Zinc(II) catalysts are particularly interesting, given the low cost, favorable biocompatibility, and high natural abundance of this main group metal. Although zinc hydrides are presumed intermediates in hydrosilane alcoholysis, the catalytic activity of the few isolable, monomeric, terminal zinc hydrides is not developed.^{24–28} We recently synthesized a monomeric zinc hydride $To^M ZnH$ (**1**; To^M = tris(4,4-dimethyl-2-oxazolanyl)phenylborate) by reaction of $To^M ZnOtBu$ (**2**) and $PhMeSiH_2$. The byproduct of this reaction is the silyl ether $PhMeHSi-OtBu$.



Incorporation of this step into a catalytic cycle for Si–O bond formation would provide an opportunity to use a well-defined set of alkoxide and hydride intermediates, as well as stoichiometric reactions, to study and develop zinc-catalyzed transformations. Furthermore, the zinc-catalyzed reactions are mechanistically distinct from transition-metal catalyzed silane alcoholyses in that oxidative addition pathways are unlikely in the main group system.

Here we present the reactivity and selectivity of **1** as a catalyst for silane alcoholysis and kinetic studies on a catalytic conversion. Although $\text{To}^{\text{M}}\text{ZnMe}$ (**3**), *tert*-butoxide **2**, and $\text{To}^{\text{M}}\text{ZnOAryl}$ (**4**; Aryl = $\text{C}_6\text{H}_3\text{Me}_2$) may be used as precatalysts,²⁹ these compounds have some limitations. For example, alkyl **3** reacts relatively slowly with some alcohols, and that step can impede efficient catalyst initiation. While *tert*-butoxide **2** is the catalyst precursor, 1 equiv of silane is wasted as $\text{R}_3\text{Si-OtBu}$. Therefore, compound **1** is the precatalyst of choice for these studies, and although it is moisture sensitive, **1** does not react with O_2 under ambient conditions. The monomeric zinc hydride **1** was previously prepared following a three-step synthesis where $\text{To}^{\text{M}}\text{ZnCl}$ and **2** intermediates were isolated from the TiCl_4 and KCl reaction byproducts.³⁰ An alternative and easy one pot preparation involves sequential treatment of $\text{H}[\text{To}^{\text{M}}]$ with ZnMe_2 , MeOH , and then PhMeSiH_2 in benzene or toluene (eq 3).



The byproducts of this synthesis are methane and PhMeHSi-OtBu , and evaporation of the volatile materials provides crystalline and spectroscopically pure **1**. The **3** intermediate is isolable and fully characterized, including an X-ray structure (Figure 1) that shows the pseudo- C_{3v} -symmetric four-coordinate zinc alkyl complex. The bowl-like steric properties of To^{M} prevent redistribution to $\{\kappa^3\text{-To}^{\text{M}}\}_2\text{Zn}$ yet allow sufficient space for reactivity.

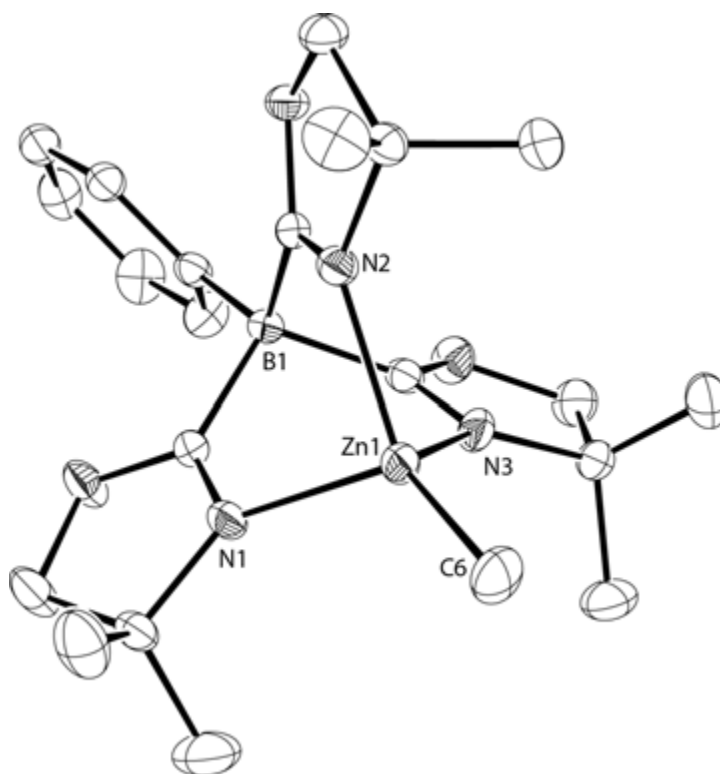


Figure 1. ORTEP diagram of $\text{To}^{\text{M}}\text{ZnMe}$ (**3**) drawn with ellipsoids at 50% probability. Hydrogen atoms are not shown. Selected bond distances (Å): Zn1–C6, 1.972(1); Zn1–N1, 2.0574(9); Zn1–N2, 2.0797(9); Zn1–N3, 2.0955(9). Selected bond angles (deg): C6–Zn1–N1, 122.25(5); C6–Zn1–N2, 130.25(5); C6–Zn1–N3, 122.93(5).

The constitution and pseudo C_{3v} -symmetry of **1** is maintained in solution. Thus, a 2D ^1H – ^{15}N NMR correlation experiment contained crosspeaks for the oxazoline nitrogen signal (–155.8 ppm), including one with the zinc methyl resonance that indicated both ligands are bonded in the same complex.

Compound **1** is a catalyst for reactions of aliphatic alcohols ROH (R = Me, Et, CH_2^tBu , ^iPr , ^tBu) and the secondary silane PhMeSiH_2 to give the monodehydrocoupled silyl ether PhMeHSi-OR as the major product with good selectivity (Table 1). At lower temperature, selectivity is further improved although the rate is sacrificed (e.g., MeOH and PhMeSiH_2

react to give 90% yield of PhMeHSi-OMe at 45 °C; PhMeHSi-OCH₂^tBu is formed with >99% selectivity at 85 °C). For comparison, the Cp₂TiCl₂/*n*-BuLi system converts all SiH groups of secondary and primary silanes to bis- and tris-alkoxy silanes, respectively.⁴ However, Wilkinson's catalyst and chiral phosphine/rhodium(I) catalysts provide alkoxy(hydro)silanes from secondary silanes and alcohols,¹² as does the chiral phosphine/copper system.¹⁷ The selectivity observed in these systems and the oxazolinylborato zinc system contrast the often observed relative reactivity of organosilanes versus alkoxy hydrosilanes, where the latter are more reactive (e.g., as in titanium-catalyzed hydrosilylations).³¹ Selectivity for the monoalkoxy silane product increases with increasing size of the alcohol, and sterically hindered alcohols require higher temperature and longer reaction times. Although sterics play a large role in this selectivity (in that PhMe(RO)SiH is more hindered than PhMeSiH₂), experiments with the tertiary organosilane BnMe₂SiH (Bn = CH₂C₆H₅) show that the effects are subtle.

Thus, compound **1** also catalyzes the dehydrocoupling of the tertiary silane BnMe₂SiH with primary, secondary, and tertiary alcohols. Unexpectedly, the Zn-catalyzed reactions of the tertiary organosilane BnMe₂SiH and alcohols are more rapid than the corresponding reactions with secondary silane PhMeSiH₂. All of these dehydrocoupling reactions are sensitive to the steric bulk of the alcohol. For example, PhMeSiH₂ reacts four times slower than BnMe₂SiH under equivalent conditions (catalyst loading, reagent concentrations, temperature). ^tBuOH is an exception to this trend likely because of high steric congestion (see Table 1). Despite the apparently greater rate of alcoholysis of tertiary organosilanes, the secondary organosilanes react with good selectivity for the monosilyl ether products. Notably,

To^MZnH is observed by ¹H NMR spectroscopy during the reactions, and apparently it is thermally stable and catalytically active to even 135 °C for 64h.

The thermal and kinetic stability of the To^MZnX-complexes suggested that lower catalyst loadings could be used in larger scale reactions for the convenient isolation of alkoxy silanes. In fact, catalyst loadings as low as 0.27 mol % provide product, albeit with increased reaction times. Additionally, these catalyses are efficient for gram-scale reactions of organosilanes, and the products PhMeHSiOMe, BnMe₂SiOMe, PhMeHSiOEt, PhMeHSiOⁱPr, and PhMeHSiO^tBu are readily obtained in our catalytic system.²⁹ Compound **1** also catalyzes the dehydrocoupling reaction of the substituted phenol 3,5-Me₂C₆H₃OH and PhMeSiH₂.

Table 1. Micromolar-Scale Reactions of PhMeSiH₂ and BnMe₂SiH with ROH

$\text{PhMeSiH}_2 + \text{HOR} \xrightarrow{10 \text{ mol\% To}^{\text{M}}\text{ZnH}} \text{PhMeHSi-OR} + \text{H}_2$				
Alcohol	Product ^a	Temperature	Time (h)	Selectivity (%) ^b
MeOH	PhMeHSiOMe	45 °C	10	89 : 11 ^c
MeOH	PhMeHSiOMe	60 °C	4.2	81 : 19 ^c
EtOH	PhMeHSiOEt	60 °C	20	89 : 11 ^c
^t BuCH ₂ OH	PhMeHSiOCH ₂ ^t Bu	135 °C	5	93 : 7
ⁱ PrOH	PhMeHSiO ⁱ Pr	85 °C	45	95:5 ^c
^t BuOH	PhMeHSiO ^t Bu	135 °C	13	>99

$\text{BnMe}_2\text{SiH} + \text{HOR} \xrightarrow{10 \text{ mol}\% \text{ To}^{\text{M}}\text{ZnH}} \text{BnMe}_2\text{Si-OR} + \text{H}_2$				
Alcohol	Product ^a	Temperature	Time (h)	Selectivity (%) ^b
MeOH	BnMe ₂ SiOMe	60 °C	1	n.a.
EtOH	BnMe ₂ SiOEt	60 °C	4	n.a.
ⁱ PrOH	BnMe ₂ SiO ⁱ Pr	60 °C	25	n.a.
^t BuOH	BnMe ₂ SiO ^t Bu	135 °C	64	n.a.

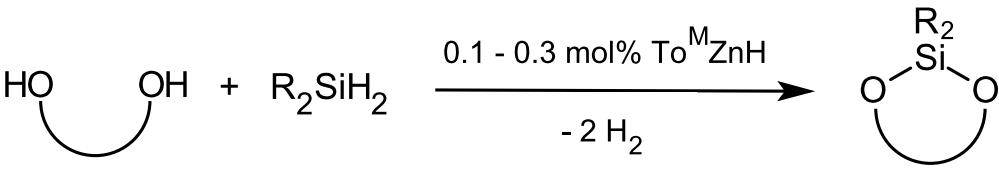
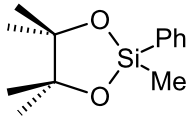
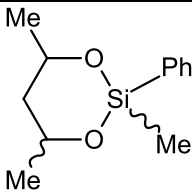
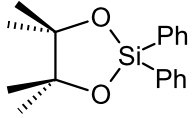
^a10 mol % catalyst loading for the reaction of equimolar ROH and PhMeSiH₂ to 100% conversion in benzene-*d*₆. ^b Products were identified and selectivity was determined by ¹H NMR spectroscopy and GC-MS, and by comparison with isolated materials. ^c The minor product is the dialkoxysilane PhMeSi(OR)₂.

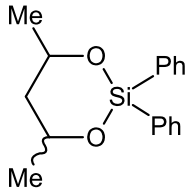
Equimolar PhMeSiH₂ and 3,5-Me₂C₆H₃OH affords 1:2:1 mixtures of PhMeSiH₂, PhMeHSiOC₆H₃Me₂ and PhMeSi(OC₆H₃Me₂)₂ under catalytic conditions, contrasting the higher selectivity found with aliphatic alcohols. However, relative ratios of starting materials can be used to control the product distribution, and both PhMeHSiOC₆H₃Me₂ and PhMeSi(OC₆H₃Me₂)₂ are isolable in pure form in high yield. For example, 5 equiv of PhMeSiH₂ with respect to 3,5-Me₂C₆H₃OH affords PhMeHSiOC₆H₃Me₂ (89.2%), whereas 3 equiv of 3,5-Me₂C₆H₃OH versus PhMeSiH₂ provides PhMeSi(OC₆H₃Me₂)₂ (90.8%). In both cases, the excess reagent is recovered in pure form during the distillation and is not wasted.

Diols are also challenging substrates for cross-dehydrocoupling because polymers, branched oligomers, and a range of cyclic species are possible products. Titanocene complexes are catalysts for cyclization to give five, six, and seven-member rings,⁴ and this provides a classic example for catalytic control over selectivity in Si–O bond forming reactions. The steric

control, efficient transformations, and high selectivities observed with the convenient $\text{To}^{\text{M}}\text{ZnH}$ system provide small cyclic dioxasilacycles in high yield and high purity using PhMeSiH_2 and Ph_2SiH_2 (Table 2).²⁹ Additionally, the PhMeSiH_2 /pinacol and Ph_2SiH_2 /2,4-pentanediol products are crystalline at room temperature, and their identities are confirmed by X-ray crystallography (see Supporting Information).

Table 2. Catalytic Cyclization of Secondary Silanes and Diols.

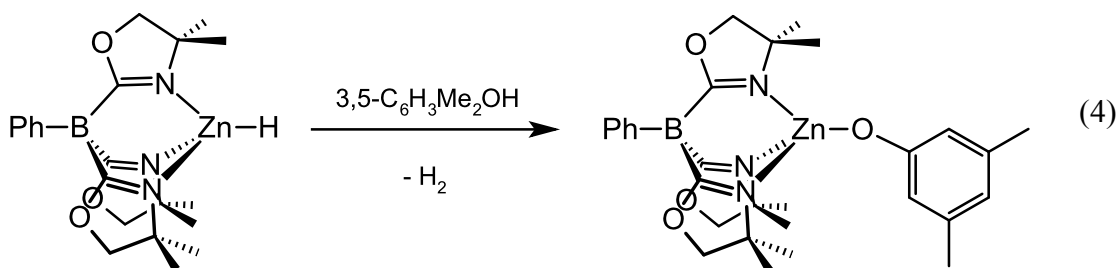
		
Product ^a	isolated yield ^b	selectivity
	92.2%	n.a.
	96.8%	1 : 2.11 : 2.27
	91.5%	n.a.

	93.0%	1 : 1.15
---	-------	----------

^aConditions for catalysis: 0.1–0.3 mol % $\text{To}^{\text{M}}\text{ZnH}$, 8 mmol diol, and 7 mmol organosilane were dissolved in benzene, degassed, and stirred at 60–90 °C.^b Products are isolated by distillation, and yield is calculated for five- or six-member ring product(s) after distillation.

Given the range of proposed mechanisms for metal-mediated dehydrogenative silylation of alcohols and the coordinative saturation of $\text{To}^{\text{M}}\text{ZnH}$, we have examined the $\text{To}^{\text{M}}\text{ZnH}$ -catalyzed dehydrocoupling reactions in greater detail. The phenolic alcohols had shown the greatest dependence of product identity on concentration of substrates, and therefore we chose 3,5- $\text{C}_6\text{H}_3\text{Me}_2\text{OH}$ and PhMeSiH_2 as the substrates to study the dehydrocoupling reaction mechanism to identify the factors that control relative rates of reactivity. Additionally, we have studied isolated **1**³⁰ and $\text{To}^{\text{M}}\text{ZnOC}_6\text{H}_3\text{Me}_2$ (**4**) as likely intermediates in the dehydrocoupling of 3,5- $\text{C}_6\text{H}_3\text{Me}_2\text{OH}$ and organosilanes to test their role in the catalytic cycle.

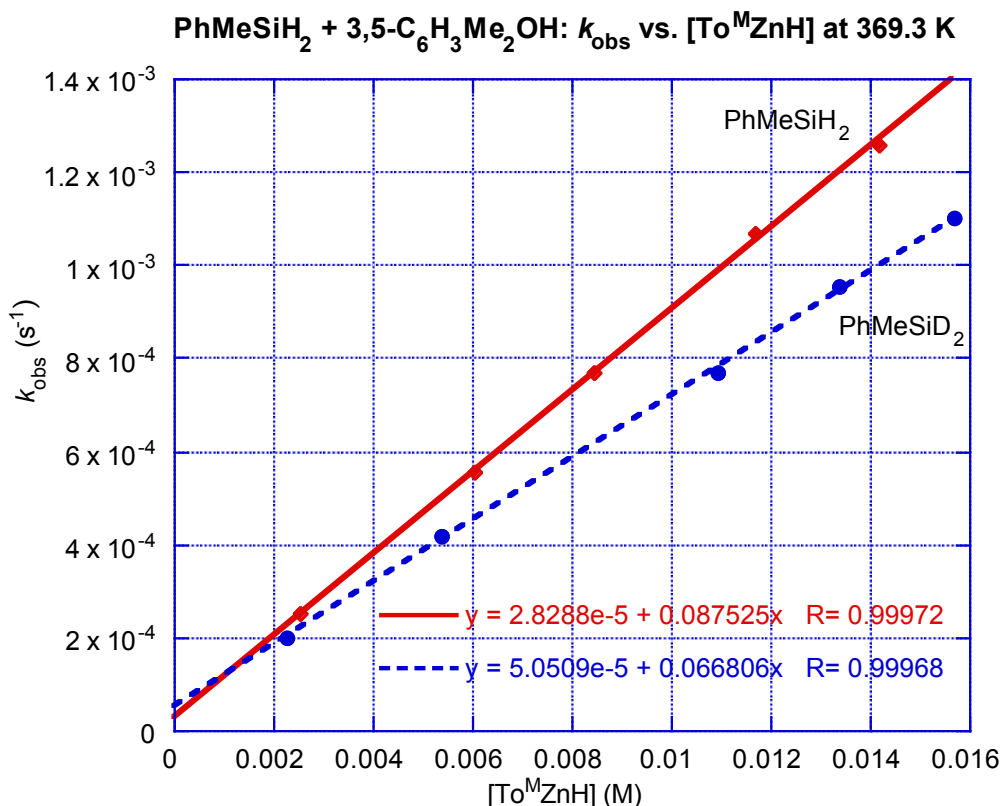
Reaction of $\text{To}^{\text{M}}\text{ZnH}$ and 3,5-dimethylphenol in benzene readily provides **4** (eq 4), which is isolated and fully characterized by spectroscopic, analytical and X-ray diffraction techniques (fig. S-7).



The reaction between $\text{To}^{\text{M}}\text{ZnOC}_6\text{H}_3\text{Me}_2$ and PhMeSiH_2 (benzene- d_6 , 60 °C) affords a mixture of $\text{PhMeHSi}(\text{OC}_6\text{H}_3\text{Me}_2)$ and $\text{PhMeSi}(\text{OC}_6\text{H}_3\text{Me}_2)_2$ in a 61:39 ratio. Additionally, the compounds **1** and **4** show the same activity under catalytic conditions for organosilane phenolysis. Thus, stoichiometric steps have been observed that support a two-step catalytic mechanism for dehydrocoupling of organosilanes and 3,5-dimethylphenol. Related steps have also been observed for the coupling of organosilanes and *tert*-butanol.

To provide further support for the proposed mechanism, the concentrations of species in the catalytic reactions were monitored by ^1H NMR spectroscopy over the reaction course. Under initial conditions of 200 mM $[\text{HOC}_6\text{H}_3\text{Me}_2]$, 130 mM $[\text{PhMeSiH}_2]$ with 1.5–12 mol % $\text{To}^{\text{M}}\text{ZnH}$ in toluene- d_8 at 96.3 °C (calibrated), plots of $[\text{HOC}_6\text{H}_3\text{Me}_2]$ versus time are linear, and curves of $[\text{PhMeSiH}_2]$ versus time follow an exponential decay over three half-lives (nonlinear least-squares analysis provides k_{obs} for a particular catalyst concentration). Several reactions were attempted with a range of concentrations of phenol with constant **1**; k_{obs} does not change with $[\text{HOC}_6\text{H}_3\text{Me}_2]$ ranging from 0.2–1.2 M. This lack of dependence on phenol concentration confirms its zero-order contribution to the rate law with PhMeSiH_2 as the limiting reagent. In contrast, a plot of k_{obs} versus $[\text{To}^{\text{M}}\text{ZnH}]$ shows a linear correlation (Figure 2) giving $k'_{\text{obs}}(\text{PhMeSiH}_2) = 8.8 \pm 0.3 \times 10^{-2} \text{ M}^{-1} \text{ s}^{-1}$.

Figure 2. Plot of k'_{obs} versus $[\text{To}^{\text{M}}\text{ZnH}]$ for the reaction of 3,5-dimethylphenol with PhMeSiH_2 and PhMeSiD_2 .

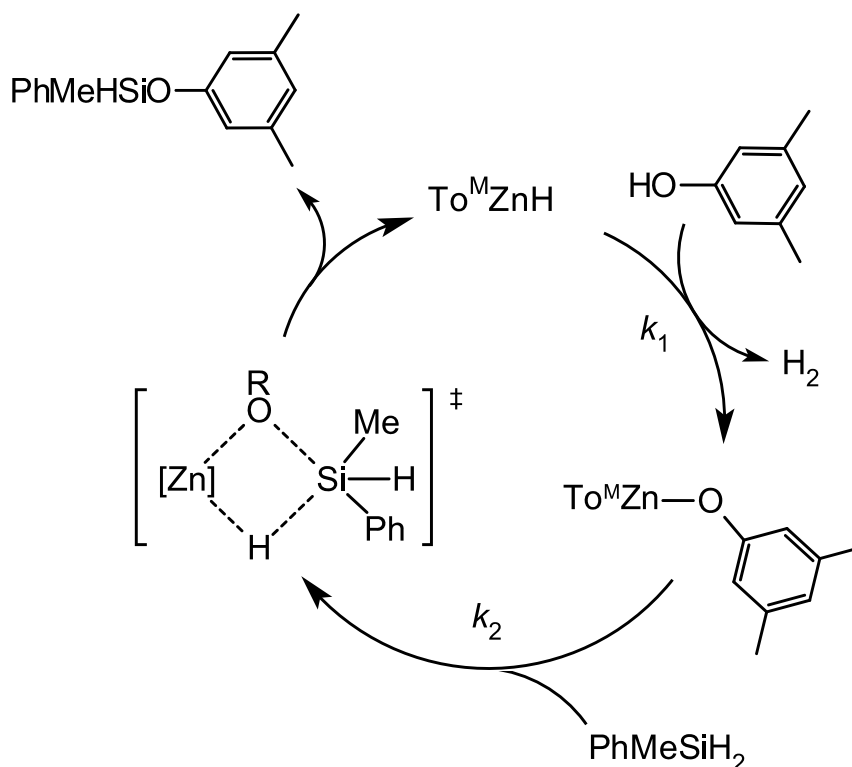


Under these conditions, an empirical rate law is:

$$-d[\text{PhMeSiH}_2]/dt = k'_{\text{obs}} (\text{PhMeSiH}_2) [\text{To}^{\text{M}}\text{ZnH}]^1 [\text{PhMeSiH}_2]^1 [\text{Phenol}]^0$$

This empirical rate law is consistent with the mechanism of Scheme 1, with the turnover-limiting step (k_2) involving interaction of PhMeSiH_2 and the catalyst. The experimentally determined k'_{obs} corresponds to the rate constant k_2 for the interaction of **4** and PhMeSiH_2 . The only $\text{To}^{\text{M}}\text{Zn}$ -species observed under these reaction conditions is **4**. This observation and the empirical rate law indicate that **4** is the resting state for the catalysis at 96 °C in the

presence of excess 3,5-dimethylphenol. Thus, the rate constant (k_1) for the hydrogen elimination reaction of **1** and $\text{HOC}_6\text{H}_3\text{Me}_2$ is greater than k_2 . Additionally, the kinetics reveals that under these conditions, neither step of the cycle is reversible.



Scheme 1. Proposed catalytic for $\text{To}^{\text{M}}\text{ZnH}$ -catalyzed dehydrocoupling of PhMeSiH_2 and 3,5-dimethylphenol.

To further probe the turnover-limiting step, we determined the empirical rate law and rate constant for the catalytic reaction of PhMeSiD_2 and $\text{HOC}_6\text{H}_3\text{Me}_2$. At 96.3 °C, $k'_{\text{obs}}(\text{PhMeSiD}_2)$ is $6.7 \pm 0.7 \times 10^{-2} \text{ M}^{-1}\text{s}^{-1}$. The ratio of $k'_{\text{obs}}(\text{PhMeSiH}_2)$ to $k'_{\text{obs}}(\text{PhMeSiD}_2)$, and hence the kinetic isotope effect ($k_{\text{H}}/k_{\text{D}}$) was calculated to be 1.3(1). This value suggests that the Si-H (or Si-D) bond is broken during the turnover-limiting step and is consistent with a four-centered transition state for Si-O bond formation where the $\angle\text{Zn}-\text{H}-\text{Si}$ is nonlinear.

However, this relatively small value could also be interpreted as resulting from a (large) secondary isotope effect.

Therefore, the nature of the proposed turnover-limiting step was further investigated by measurement of the rate law for the stoichiometric reaction of PhMeSiH₂ and **4**. Under pseudo-first order conditions (10–20 equiv of PhMeSiH₂ at 96 °C), the reaction is too fast to be easily monitored by ¹H NMR spectroscopy. Instead, we measured the (stoichiometric) second-order rate constants from 24 to 61 °C under pseudo-first order conditions and calculated the rate constant at 96 °C using the Eyring equation. This calculated value, 0.1 M⁻¹s⁻¹, is close to the value measured under catalytic conditions (0.088 (3) M⁻¹s⁻¹). Thus, the stoichiometric Si–O bond forming reaction of To^MZnOC₆H₃Me₂ and PhMeSiH₂ is chemically and kinetically competent for its proposed role in the catalytic cycle. The other step, namely, interaction of To^MZnH and HOC₆H₃Me₂, is rapid at room temperature (t_{1/2} < 5 min), and this step is also catalytically competent and consistent with the proposed mechanisms.

The activation parameter values obtained from the Eyring analysis, ΔH = 13 kcal mol⁻¹ and ΔS = - 27 cal mol⁻¹K⁻¹, further support a highly organized transition state for Si–O bond formation. Related four-center transition states that involve transfer of a hydrogen atom from silicon to a metal center have values for activation parameters with relatively low ΔH[‡] and highly negative ΔS[‡], as well as isotope effects that range from unity to about 3. For example, the reaction of CpCp*ClHfSiH₂Ph and PhSiH₃ or PhSiD₃ gives CpCp*ClHf–H (or [Hf]–D) with a k_H/k_D = 2.7(2) (at 70 °C) and activation parameters ΔH[‡] = 19 kcal mol⁻¹ and ΔS[‡] = - 33 e.u..³² The isotope effect for the related reaction of Cp*₂ScMe with Ph₂SiH₂ or Ph₂SiD₂

that gives Ph_2MeSiH or Ph_2MeSiD is 1.15(5), and the related value for the reaction of $[\text{DADMB}]\text{YMe}(\text{THF})$ and PhMeSiH_2 is 1.1(1) (at 298 K; $\text{DADMB} = 2,2'$ -bis(tert-butylidimethylsilylamido)-6,6'-dimethylbiphenyl).^{33,34} Related four-centered transition states are proposed in titanium-catalyzed hydrosilylation of ketones,³¹ in zinc-catalyzed hydrosilylations, and in gold and copper-catalyzed silane alcoholyses,^{18,20,35} although isotope effects for Si–O bond formation are not reported. Thus, the studies reported here for the $\text{To}^{\text{M}}\text{ZnH}$ -catalyzed reaction, including kinetics, isolable intermediates, stoichiometric reactions, and rate constants provide substantial support for the proposed two-step catalytic mechanism as well as concerted Si–H bond cleavage/Si–O bond formation previously suggested for *in situ* generated zinc, copper, and gold catalysts.

Conclusion.

We are currently working to identify relative rates of Si–O bond formation for reactions of isolated zinc alkoxides and zinc aryloxides with a range of organosilanes to better understand the selectivity of these reactions and to better characterize the bond cleavage and formation steps. Because the isolable $\text{To}^{\text{M}}\text{ZnH}$ can be reacted with aliphatic alcohols and phenols, the relative rate law(s) and rates of these reactions will also be used to probe the overall mechanism of catalytic silane alcoholysis and develop new bond-forming catalytic conversions.

References.

- (1) Huh, S.; Wiench, J. W.; Trewyn, B. G.; Song, S.; Pruski, M.; Lin, V. S.-Y. *Chem. Commun.* **2003**, 2364–2365.

- (2) Trewyn, B. G.; Slowing, I. I.; Giri, S.; Chen, H.-T.; Lin, V. S.-Y. *Acc. Chem. Res.* **2007**, *40*, 846–853.
- (3) Greene, T. W.; Wuts, P. G. *Protective Groups in Organic Synthesis*, 2nd ed.; Wiley: New York, 1991.
- (4) Bedard, T. C.; Corey, J. Y. *J. Organomet. Chem.* **1992**, *428*, 315–333.
- (5) Xin, S.; Harrod, J. F. *J. Organomet. Chem.* **1995**, *499*, 181–191.
- (6) Peterson, E.; Khalimon, A. Y.; Simionescu, R.; Kuzmina, L. G.; Howard, J. A. K.; Nikonov, G. I. *J. Am. Chem. Soc.* **2009**, *131*, 908–909.
- (7) Gregg, B. T.; Cutler, A. R. *Organometallics* **2002**, *13*, 1039–1043.
- (8) Corbin, R. A.; Ison, E. A.; Abu-Omar, M. M. *Dalton Trans.* **2009**, 2850–2855.
- (9) Chang, S.; Scharrer, E.; Brookhart, M. *J. Mol. Catal. A: Chem.* **1998**, *130*, 107–119.
- (10) Chung, M.; Ferguson, G.; Robertson, V.; Schalf, M. *Can. J. Chem.* **2001**, *79*, 949–957.
- (11) Maifield, S. V.; Miller, R. L.; Lee, D. *Tetrahedron Lett.* **2002**, *43*, 6363–6366.
- (12) Corriu, R. J. P.; Moreau, J. J. E. *J. Organomet. Chem.* **1976**, *120*, 337–346.
- (13) Luo, X.-L.; Crabtree, R. H. *J. Am. Chem. Soc.* **1989**, *111*, 2527–2535.
- (14) Barber, D. E.; Lu, Z.; Richardson, T.; Crabtree, R. H. *Inorg. Chem.* **2002**, *31*, 4709–4711.
- (15) Ohshita, J.; Taketsugu, R.; Nakahara, Y.; Kunai, A. *J. Organomet. Chem.* **2004**, *689*, 3258–3264.
- (16) Schubert, U.; Lorenz, C. *Inorg. Chem.* **1997**, *36*, 1258–1259.
- (17) Schmidt, D. R.; O'Malley, S. J.; Leighton, J. L. *J. Am. Chem. Soc.* **2003**, *125*, 1190–1191.

- (18) Ito, H.; Watanabe, A.; Sawamura, M. *Org. Lett.* **2005**, *7*, 1869–1871.
- (19) Rendler, S.; Auer, G.; Oestreich, M. *Angew. Chem., Int. Ed.* **2005**, *44*, 7620–7624.
- (20) Ito, H.; Takagi, K.; Miyahara, T.; Sawamura, M. *Org. Lett.* **2005**, *7*, 3001–3004.
- (21) Caseri, W.; Pregosin, P. S. *Organometallics* **1988**, *7*, 1373–1380.
- (22) Blackwell, J. M.; Foster, K. L.; Beck, V. H.; Piers, W. E. *J. Org. Chem.* **1999**, *64*, 4887–4892.
- (23) Mimoun, H. *J. Org. Chem.* **1999**, *64*, 2582–2589.
- (24) Han, R.; Gorrell, I. B.; Looney, A. G.; Parkin, G. *J. Chem. Soc., Chem. Commun.* **1991**, 717–719.
- (25) Looney, A.; Han, R.; Gorrell, I. B.; Cornebise, M.; Yoon, K.; Parkin, G.; Rheingold, A. L. *Organometallics* **1995**, *14*, 274–288.
- (26) Kläui, W.; Schilde, U.; Schmidt, M. *Inorg. Chem.* **1997**, *36*, 1598–1601.
- (27) Rombach, M.; Brombacher, H.; Vahrenkamp, H. *Eur. J. Inorg. Chem.* **2002**, 153–159.
- (28) Spielmann, J.; Piesik, D.; Wittkamp, B.; Jansen, G.; Harder, S. *Chem. Commun.* **2009**, 3455–3456.
- (29) See the Supporting Information for preparation and characterization of tris(oxazolanyl)borato zinc complexes and silyl ethers.
- (30) Mukherjee, D.; Ellern, A.; Sadow, A. D. *J. Am. Chem. Soc.* **2010**, *132*, 7582–7583.
- (31) Yun, J.; Buchwald, S. L. *J. Am. Chem. Soc.* **1999**, *121*, 5640–5644.
- (32) Woo, H.-G.; Walzer, J. F.; Tilley, T. D. *J. Am. Chem. Soc.* **1992**, *114*, 7047–7055.
- (33) Gountchev, T. I.; Tilley, T. D. *Organometallics* **1999**, *18*, 5661–5667.

(34) Sadow, A. D.; Tilley, T. D. *J. Am. Chem. Soc.* **2004**, *127*, 643–656.

(35) Mimoun, H.; de Saint Laumer, J. Y.; Giannini, L.; Scopelliti, R.; Floriani, C. *J. Am. Chem. Soc.* **1999**, *121*, 6158–6166.

Experimental.

General.

All reactions were performed under a dry argon atmosphere using standard Schlenk techniques or under a nitrogen atmosphere in a glovebox, unless otherwise indicated. Water and oxygen were removed from benzene, toluene, pentane, diethyl ether, and tetrahydrofuran solvents using an IT PureSolv system. Benzene- d_6 and toluene- d_8 were heated to reflux over Na/K alloy and vacuum-transferred. PhMeSiH₂ and Ph₂SiH₂ were synthesized by LiAlH₄ reduction of the corresponding chlorosilanes and purified by distillation and stored over 4 Å molecular sieves in the glovebox. PhMeSiD₂ was synthesized by LiAlD₄ reduction of PhMeSiCl₂. BnMe₂SiH was purchased from Gelest and stored over 4 Å molecular sieves in the glovebox. All the liquid alcohols (MeOH, EtOH, ⁱPrOH, ^tBuOH) were distilled from CaH₂ prior to use and stored over 4 Å molecular sieves in the glovebox. Pinacol and 2,4-pentanediol were purchased from Sigma-Aldrich and used as received. 3,5-Dimethylphenol was purchased from Sigma-Aldrich, purified by sublimation, and stored in the glovebox. Procedures for To^MZnH- catalyzed silyl ethers syntheses are given below with the appropriate literature citations for spectral data. ¹H, ¹³C{¹H}, and ¹¹B NMR spectra were collected on a Bruker DRX 400 spectrometer. ¹⁵N chemical shifts were determined by ¹H-¹⁵N HMBC experiments on a Bruker Avance II 700 spectrometer with a Bruker Z-gradient

inverse TXI $^1\text{H}/^{13}\text{C}/^{15}\text{N}$ 5mm cryoprobe; ^{15}N chemical shifts were originally referenced to an external liquid NH_3 standard and recalculated to the CH_3NO_2 chemical shift scale by adding -381.9 ppm. $^{29}\text{Si}\{^1\text{H}\}$ NMR were collected using a 400 MHz Varian NMR spectrometer. Elemental analyses were performed using a Perkin-Elmer 2400 Series II CHN/S by the Iowa State Chemical Instrumentation Facility. X-ray diffraction data was collected on a Bruker APEX II diffractometer.

To^MZnH (1) Single flask preparation. HTo^{M} (0.245 g, 0.639 mmol) and dimethylzinc (0.32 mL; 2 M in toluene) were mixed in benzene and stirred for 12 h at room temperature. Methanol (40 μL , 0.989 mmol) was added to the reaction, and the resulting solution was stirred for 24 h at room temperature. PhMeSiH_2 (0.20 mL, 1.456 mmol) was then added. The reaction was stirred for 1 h at room temperature and then filtered to remove minor impurities. As the filtrate was concentrated, white crystalline $\text{To}^{\text{M}}\text{ZnH}$ precipitated. Evaporation to dryness, followed by pentane washes (3×5 mL) and further drying yielded crystalline $\text{To}^{\text{M}}\text{ZnH}$ (0.260 g, 0.579 mmol, 90.6%). Spectroscopic data are identical to those of previously characterized $\text{To}^{\text{M}}\text{ZnH}$.¹

To^MZnMe (3). This compound was prepared in the same quantity as $\text{To}^{\text{M}}\text{ZnH}$ above. HTo^{M} (0.245 g, 0.639 mmol) and dimethylzinc (0.32 mL; 2 M in toluene) were mixed in benzene and stirred for 12 h at room temperature. Evaporation of the volatile components gave a white solid, which was then washed with pentane (3×5 mL) affording crystalline, analytically pure $\text{To}^{\text{M}}\text{ZnMe}$ as white solid. X-ray quality single crystals were grown from a concentrated toluene solution of 3 at -30 °C. ^1H NMR (400 MHz, benzene- d_6): δ 0.21 (s, 3 H, ZnMe), 1.02 (s, 18 H, $\text{CNCMe}_2\text{CH}_2\text{O}$), 3.49 (s, 6 H, $\text{CNCMe}_2\text{CH}_2\text{O}$), 7.33 (t, $^3J_{\text{HH}} = 4.0$

Hz, 1 H, *para*-C₆H₅), 7.51 (t, ³J_{HH} = 4.0 Hz, 2 H, *meta*-C₆H₅), 8.32 (d, ³J_{HH} = 4.0 Hz, 2 H, *ortho*-C₆H₅). ¹³C{¹H} NMR (175 MHz, benzene-*d*₆): δ -16.86 (ZnCH₃), 28.29 (CNCMe₂CH₂O), 65.68 (CNCMe₂CH₂O), 80.81 (CNCMe₂CH₂O), 126.18 (*para*-C₆H₅), 127.21 (*meta*-C₆H₅), 136.46 (*ortho*-C₆H₅), 142.98 (br, *ipso*-C₆H₅), 189.99 (br, CNCMe₂CH₂O). ¹¹B NMR (128 MHz, benzene-*d*₆): δ -17.2. ¹⁵N{¹H} NMR: δ -155.8. IR (KBr, cm⁻¹): 2967 (s), 2931 (m), 2897 (m), 1605 (s, ν_{CN}), 1460 (m), 1385 (m), 1366 (s), 1351 (m), 1270 (s), 1251 (m), 1193 (s), 1161 (s), 958 (s), 894 (w), 818 (w), 748 (m), 709 (s), 673 (m), 658 (m). Anal. Calcd. for C₂₂H₃₂BN₃O₃Zn: C, 57.11; H, 6.97; N, 9.08. Found: C, 57.20; H, 7.17; N, 9.17. mp 217-220 °C.

To^MZn(O-3,5-C₆H₃Me₂) (4). To^MZnH (0.128 g, 0.285 mmol) and 3,5-Me₂C₆H₃OH (0.035 g, 0.286 mmol) were dissolved in benzene (15 mL) and stirred for 1 h. Then, the volatiles materials were removed under reduced pressure. The resulting white solid was washed with pentane (3 × 5 mL) and dried under vacuum, affording analytically pure To^MZn(O-3,5-Me₂C₆H₃) (0.390 g, 0.749 mmol, 89.4%) as a white powdery solid. X-ray quality single crystals were grown by slow pentane diffusion into a concentrated toluene/THF solution of To^MZn(O-3,5-C₆H₃Me₂) at -30 °C. ¹H NMR (400 MHz, benzene-*d*₆): δ 1.07 (s, 18 H, CNCMe₂CH₂O), 2.36 (s, 6 H, C₆H₃Me₂), 3.43 (s, 6 H, CNCMe₂CH₂O), 6.51 (s, 1 H, *para*-C₆H₃Me₂), 6.87 (s, 2 H, *ortho*-C₆H₃Me₂), 7.36 (t, ³J_{HH} = 7.4 Hz, 1 H, *para*-C₆H₅), 7.54 (t, ³J_{HH} = 7.4 Hz, 2 H, *meta*-C₆H₅), 8.28 (d, ³J_{HH} = 7.2 Hz, 2 H, *ortho*-C₆H₅). ¹³C{¹H} NMR (100 MHz, benzene-*d*₆): δ 22.09 (C₆H₃Me₂), 28.16 (CNCMe₂CH₂O), 65.80 (CNCMe₂CH₂O), 81.25 (CNCMe₂CH₂O), 118.00 (*para*-C₆H₃Me₂), 118.49 (*ortho*-C₆H₃Me₂), 126.57 (*para*-C₆H₅), 127.40 (*meta*-C₆H₅), 136.28 (*ortho*-C₆H₅), 138.89 (*meta*-C₆H₃Me₂), 142.12 (br, *ipso*-

C_6H_5), 168.30 (*ipso*- $C_6H_3Me_2$), 191.12 (br, $CNCMe_2CH_2O$). ^{11}B NMR (128 MHz, benzene- d_6): δ - 18.2. $^{15}N\{^1H\}$ NMR (71 MHz, benzene- d_6): δ - 160.5. IR (KBr, cm^{-1}): 3083 (w), 3020 (w), 2971 (s), 2929 (w), 2869 (w), 1585 (s, $\nu_{C=N}$), 1494 (w), 1464 (s), 1432 (w), 1366 (m), 1355 (m), 1345 (m), 1336 (w), 1278 (s), 1198 (s), 1172 (s), 1037 (w), 990 (m), 959 (s), 896 (w), 858 (m), 843 (w), 819 (s), 747 (m), 708 (s), 694 (w), 666 (s). Anal. Calcd. for $C_{29}H_{38}BN_3O_4Zn$: C, 61.23; H, 6.73; N, 7.39. Found: C, 61.24; H, 6.47; N, 7.38. mp 259-262 °C.

PhMeHSiOMe. PhMeSiH₂ (0.691 g, 5.65 mmol) and methanol (0.091 g, 2.83 mmol) were added to $To^M ZnH$ (0.012 g, 0.027 mmol, 0.95 mol%) dissolved in benzene (18 mL). This solution was degassed with two freeze-pump-thaw cycles, sealed in a Teflon-valved flask, and heated at 45 °C for 10 h. The reaction mixture was cooled to room temperature and filtered through a short plug of celite. The celite plug was further washed with diethyl ether (3 × 10 mL), and the filtrate and washings were combined. The volatile solvents were removed to obtain a colorless liquid. Subsequent fractional distillation of the colorless liquid provided PhMeHSiOMe (0.39 g, 2.56 mmol, 90.7%) as the sole isolated product. 1H NMR (400 MHz, $CDCl_3$): δ 0.52 (d, $^3J_{HH} = 3.2$ Hz, 3 H, *SiMe*), 3.56 (s, 3 H, *OMe*), 5.06 (m, $^3J_{HH} = 2.8$ Hz, $^1J_{SiH} = 208$ Hz, 1 H, *SiH*), 7.45 (m, 3 H, *para* and *meta*- C_6H_5), 7.67 (m, 2 H, *ortho*- C_6H_5). $^{13}C\{^1H\}$ NMR (100 MHz, $CDCl_3$): -2.96 (*SiMe*), 52.17 (*OMe*), 128.21 (*meta*- C_6H_5), 130.38 (*para*- C_6H_5), 134.10 (*ortho*- C_6H_5), 135.55 (*ipso*- C_6H_5). $^{29}Si\{^1H\}$ NMR (79.5 MHz, $CDCl_3$): δ 0.79. EI-MS: $C_9H_{14}SiO$ m/e 152 (M⁺).

PhMeHSiOEt. A similar procedure as described for PhMeHSiOMe was used. PhMeSiH₂ (0.667 g, 5.46 mmol) and ethanol (0.210 g, 4.55 mmol) were added to $To^M ZnH$ (0.009 g,

0.020 mmol, 0.44 mol%) dissolved in benzene (18 mL). This solution was degassed with two freeze-pump-thaw cycles, sealed in a Teflon-valved flask, and heated to 60 °C for 24 h. Workup provided PhMeHSiOEt (0.71 g, 4.27 mmol, 93.7%) as the sole product. The product was characterized using ^1H , ^{13}C and ^{29}Si NMR spectroscopy and mass spectrometry; PhMeHSiOEt was previously reported, but spectral characterization was not given.² ^1H NMR (400 MHz, CDCl_3): δ 0.47 (d, $^3J_{\text{HH}} = 2.8$ Hz, 3 H, SiMe), 1.22 (t, $^3J_{\text{HH}} = 7.2$ Hz, 3 H, OCH_2CH_3), 3.75 (q, $^3J_{\text{HH}} = 7.2$ Hz, 2 H, OCH_2CH_3), 5.02 (m, $^3J_{\text{HH}} = 2.8$ Hz, $^1J_{\text{SiH}} = 208$ Hz, 1 H, SiH), 7.41 (m, 3 H, *para*, *meta*- C_6H_5), 7.62 (m, 2 H, *ortho*- C_6H_5). $^{13}\text{C}\{^1\text{H}\}$ NMR (100 MHz, CDCl_3): - 2.53 (SiMe), 18.30 (OCH_2CH_3), 60.23 (OCH_2CH_3), 128.12 (*meta*- C_6H_5), 130.22 (*para*- C_6H_5), 134.00 (*ortho*- C_6H_5), 136.06 (*ipso*- C_6H_5). $^{29}\text{Si}\{^1\text{H}\}$ NMR (79.5 MHz, CDCl_3): δ - 2.40. EI-MS: $\text{C}_9\text{H}_{14}\text{SiO}$ m/e 166 (M+).

PhMeHSiOiPr. A similar procedure as described for PhMeHSiOMe was used. PhMeSiH₂ (0.620 g, 5.07 mmol) and isopropanol (0.254 g, 4.23 mmol) were added to $\text{To}^{\text{M}}\text{ZnH}$ (0.010 g, 0.022 mmol, 0.52 mol%) dissolved in benzene (18 mL). This solution was degassed with two freeze-pump-thaw cycles, sealed in a Teflon-valved flask, and heated to 95 °C for 24 h. Workup provided PhMeHSiOiPr (0.69 g, 3.83 mmol; 90.5%) as the sole product. ^1H NMR (400 MHz, CDCl_3): δ 0.46 (d, $^3J_{\text{HH}} = 2.8$ Hz, 3 H, SiMe), 1.18 (d, $^3J_{\text{HH}} = 6.0$ Hz, 3 H, OCHMe_2), 1.21 (d, $^3J_{\text{HH}} = 6.0$ Hz, 3 H, OCHMe_2), 4.05 (m, 1 H, OCHMe_2), 5.05 (m, $^3J_{\text{HH}} = 2.8$ Hz, $^1J_{\text{SiH}} = 208$ Hz, 1 H, SiH), 7.41 (m, 3 H, *para*, *meta*- C_6H_5), 7.63 (m, 2 H, *ortho*- C_6H_5). $^{13}\text{C}\{^1\text{H}\}$ NMR (100 MHz, CDCl_3): - 1.92 (SiMe), 25.43 (OCHMe_2), 25.57 (OCHMe_2), 67.06 (OCHMe_2), 128.13 (*meta*- C_6H_5), 130.18 (*para*- C_6H_5), 134.07 (*ortho*- C_6H_5), 136.65 (*ipso*- C_6H_5). $^{29}\text{Si}\{^1\text{H}\}$ NMR (79.5 MHz, CDCl_3): δ - 5.41. EI-MS: $\text{C}_{10}\text{H}_{16}\text{SiO}$ m/e 180 (M+).

PhMeHSiOtBu. A similar procedure as described for the synthesis of PhMeHSiOMe was used. PhMeSiH₂ (0.625 g, 5.11 mmol) and *tert*-butanol (0.316 g, 4.26 mmol) were successively added to To^MZnH (0.014 g, 0.031 mmol, 0.73 mol%) dissolved in benzene (18 mL). This mixture was degassed with two freeze-pump-thaw cycles, sealed in a Teflon-valved flask, and heated to 95 °C for 36 h. Workup provided methylphenylsilyl-*tert*-butoxide (0.76 g, 91.6%) as the sole product. ³ ¹H NMR (400 MHz, CDCl₃): δ 0.43 (d, ³J_{HH} = 3.2 Hz, 3 H, SiMe), 1.31 (s, 9 H, OCMe₃), 5.16 (m, ³J_{HH} = 2.8 Hz, ¹J_{SiH} = 208 Hz, 1 H, SiH), 7.39 (m, 3 H, *para*, *meta*-C₆H₅), 7.63 (m, 2 H, *ortho*-C₆H₅). ¹³C{¹H} NMR (100 MHz, CDCl₃): -0.15 (SiMe), 31.68 (OCMe₃), 73.29 (OCMe₃), 128.02 (*meta*-C₆H₅), 129.82 (*para*-C₆H₅), 133.92 (*ortho*-C₆H₅), 138.22 (*ipso*-C₆H₅). ²⁹Si{¹H}NMR (79.5 MHz, CDCl₃): δ - 14.88. EI-MS: C₁₁H₁₈SiO m/e 194 (M+).

BnMe₂SiOMe. A similar procedure as described for the preparation of PhMeHSiOMe was used. BnMe₂SiH (0.861 g, 5.73 mmol) and methanol (0.153 g, 4.78 mmol) were added to To^MZnH (0.006 g, 0.013 mmol, 0.27 mol %) dissolved in benzene (18 mL). This solution was degassed with two freeze-pump-thaw cycles, sealed in a Teflon-valved flask, and heated to 60 °C for 10 h, which provided BnMe₂Si-OMe (0.84 g, 97.7%) as the sole product. ¹H NMR (400 MHz, CDCl₃): δ 0.01 (s, 6 H, SiMe₂), 2.11 (s, 2 H, PhCH₂), 3.33 (s, 3 H, OMe), 6.99 (m, 3 H, *para*, *meta*-C₆H₅), 7.13 (m, 2 H, *ortho*-C₆H₅). ¹³C{¹H} NMR (100 MHz, CDCl₃): -2.76 (SiMe₂), 26.39 (OMe), 50.75 (PhCH₂), 124.40 (*para*-C₆H₅), 128.47 (*meta*-C₆H₅), 128.49 (*ortho*-C₆H₅), 139.16 (*ipso*-C₆H₅). ²⁹Si{¹H} NMR (79.5 MHz, CDCl₃): δ 16.70. EI-MS: C₁₀H₁₆SiO m/e 180 (M+).

PhMeHSi(O-3,5-C₆H₃Me₂). A similar procedure as described for PhMeHSiOMe was used.

PhMeSiH₂ (1.308 g, 10.70 mmol) and 3,5-Me₂C₆H₃OH (0.261 g, 2.14 mmol) were added to To^MZnH (0.007 g, 0.016 mmol, 0.75 mol %) dissolved in benzene (18 mL). This reaction mixture was degassed with two freeze-pump-thaw cycles, sealed in a Teflon-valved flask, and heated to 50 °C for 10 h. Workup provided PhMeHSi(O-3,5-C₆H₃Me₂) (0.463 g, 89.2%) as the sole product. ¹H NMR (400 MHz, CDCl₃): δ 0.66 (d, ³J_{HH} = 2.8 Hz, 3 H, SiMe), 2.32 (s, 6 H, C₆H₃Me₂), 5.43 (m, 3J_{HH} = 2.8 Hz, ¹J_{SiH} = 208 Hz, 1 H, SiH), 6.64 (s, 2 H, *ortho*-C₆H₃Me₂), 6.70 (s, 1 H, *para*-C₆H₃Me₂) 7.49 (m, 3 H, *meta*, *para*-C₆H₅), 7.74 (m, 2 H, *ortho*-C₆H₅). ¹³C{¹H} NMR (100 MHz, CDCl₃): -2.76 (SiMe₂), 26.39 (SiOCH₃), 50.75 (PhCH₂), 117.19 (*ortho*-C₆H₃Me₂), 123.73 (*para*-C₆H₃Me₂), 128.26 (*meta*-C₆H₅), 130.56 (*para*-C₆H₅), 134.06 (*ortho*-C₆H₅), 137.27 (*ipso*-C₆H₅), 139.43 (*meta*-C₆H₃Me₂), 155.44 (*ipso*-C₆H₃Me₂). ²⁹Si{¹H} NMR (79.5 MHz, CDCl₃): δ -11.19. EI-MS: C₁₅H₁₈SiO m/e 242 (M⁺).

PhMeSi(O-3,5-C₆H₃Me₂)₂. A similar procedure as described for PhMeHSiOMe was used. PhMeSiH₂ (0.583 g, 4.77 mmol) and 3,5-Me₂C₆H₃OH (1.748 g, 14.31 mmol) were added to To^MZnH (0.015 g, 0.033 mmol, 0.69 mol %) dissolved in benzene (18 mL). This solution was degassed with two freeze-pump-thaw cycles, sealed in a Teflon-valved flask, and heated to 95 °C for 24 h. Workup provided PhMeSi(O-C₆H₃Me₂)₂ (1.57 g, 90.8%) as the sole product. ¹H NMR (400 MHz, CDCl₃): δ 0.67 (s, 3 H, SiMe), 2.33 (s, 12 H, C₆H₃Me₂), 6.73 (s, 6 H, C₆H₃Me₂), 7.51 (m, 3 H, *meta*, *para*-C₆H₅), 7.13 (m, 2 H, *ortho*-C₆H₅). ¹³C{¹H} NMR (100 MHz, CDCl₃): -3.15 (SiMe), 21.46 (C₆H₃Me₂), 117.82 (*ortho*-C₆H₃Me₂), 124.02 (*para*-C₆H₃Me₂), 128.17 (*meta*-C₆H₅), 130.73 (*para*-C₆H₅), 133.62 (*ipso*-C₆H₅), 134.29 (*ortho*-C₆H₅), 139.34 (*meta*-C₆H₃Me₂), 154.21 (*ipso*-C₆H₃Me₂). ²⁹Si{¹H} NMR (79.5 MHz, CDCl₃): δ -21.59. EI-MS: C₂₃H₃₆SiO₂ m/e 362 (M⁺).

2,4,6-trimethyl-2-phenyl-1,3-dioxo-2-silacyclohexane. A similar procedure as described for PhMeHSiOMe was used. PhMeSiH₂ (0.864 g, 7.07 mmol) and 2,4-pentanediol (0.870 g, 8.35 mmol) were added to To^MZnH (0.004 g, 0.009 mmol, 0.13 mol %) dissolved in benzene (18 mL). This reaction mixture was degassed with two freeze-pump-thaw cycles, sealed in a Teflon-valved flask, and heated to 80 °C for 6 h. Workup provided 2,4,6-trimethyl-2-phenyl-1,3-dioxo-2-silacyclohexane (three diastereomers in a 1: 2.27: 2.11 ratio) (1.53 g, 96.8%).⁴ ¹H NMR (400 MHz, CDCl₃): 0.39-0.45 (m, 3 H), 1.21-1.37 (m, 6 H), 1.54-1.90 (m, 2 H), 4.06-4.53 (m, 2 H), 7.40 (m, 3 H, *meta, para*-C₆H₅), 7.65 (m, 2 H, *ortho*-C₆H₅). ¹³C{¹H} NMR (100 MHz, CDCl₃): - 3.35, - 1.28, - 0.32, 23.58, 23.68, 23.74, 24.37, 24.56, 24.71, 42.85, 45.93, 65.49, 66.63, 67.22, 69.78, 69.92, 127.97, 128.14, 130.11, 130.14, 130.44, 133.58, 133.83, 133.96, 135.59, 135.80, 137.22. ²⁹Si{¹H} NMR (79.5 MHz, CDCl₃): - 15.31, - 13.81, - 12.97. EI-MS: C₁₂H₁₈SiO₂ m/e 222 (M⁺).

2,4,4,5,5-pentamethyl-2-phenyl-1,3-dioxo-2-silacyclopentane. PhMeSiH₂ (0.857 g, 7.01 mmol) and pinacol (0.994 g, 8.41 mmol) were added to To^MZnH (0.004 g, 0.009 mmol, 0.13 mol %) dissolved in benzene (18 mL). This solution was degassed with two freeze-pump-thaw cycles, sealed in a Teflon-valved flask, and heated to 95 °C for 60 h. Workup provided 2,4,4,5,5-pentamethyl-2-phenyl-1,3-dioxo-2-silacyclopentane (1.53 g, 92.2%) as the sole product.⁴ ¹H NMR (400 MHz, CDCl₃): δ 0.51 (s, SiMe), 1.26 (s, 6 H, CMe₂), 1.34 (s, 6 H, CMe₂), 7.39 (m, 3 H, *meta, para*-C₆H₅), 7.67 (m, 2 H, *ortho*-C₆H₅). ¹³C{¹H} NMR (100 MHz, CDCl₃): δ - 0.43 (SiMe), 25.91 (CMe₂), 25.95 (CMe₂), 81.99 (CMe₂), 128.03 (*meta*-C₆H₅), 130.41 (*para*-C₆H₅), 133.74 (*ortho*-C₆H₅), 135.62 (*ipso*-C₆H₅). ²⁹Si{¹H} NMR (79.5 MHz, CDCl₃): δ 3.87. EI-MS: C₁₃H₂₀SiO₂ m/e 236 (M⁺).

4,6-dimethyl-2,2-diphenyl-1,3-dioxane-2-silacyclohexane. Ph_2SiH_2 (0.917 g, 4.98 mmol) and 2,4-pentanediol (0.613 g, 5.89 mmol) were added to $\text{To}^{\text{M}}\text{ZnH}$ (0.004 g, 0.009 mmol, 0.18 mol %) dissolved in benzene (18 mL). The resulting solution was degassed with two freeze-pump-thaw cycles, sealed in a Teflon-valved flask, and heated to 60 °C for 6 h. Workup provided 4,6-dimethyl-2,2-diphenyl-1,3-dioxane-2-silacyclohexane as two diastereomers in 1:1.15 ratio (1.32 g, 4.64 mmol, 93.0%) as the sole products.⁴ ^1H NMR (400 MHz, CDCl_3): δ 1.16 (d, $^3J_{\text{HH}} = 6.4$ Hz, 6 H, *minor diastereomer* $\text{MeCHCH}_2\text{CHMe}$), 1.19 (d, $^3J_{\text{HH}} = 6.4$ Hz, 6 H, *major diastereomer* $\text{MeCHCH}_2\text{CHMe}$), 1.49 (m, 2 H, *minor diastereomer* $\text{MeCHCH}_2\text{CHMe}$), 1.69 (m, 2 H, *major diastereomer* $\text{MeCHCH}_2\text{CHMe}$), 4.12 (m, 2 H, *minor diastereomer* $\text{MeCHCH}_2\text{CHMe}$), 4.39 (m, 2 H, *major diastereomer* $\text{MeCHCH}_2\text{CHMe}$), 7.22 (m, 12 H, C_6H_5), 7.54 (m, 8 H, C_6H_5). $^{13}\text{C}\{^1\text{H}\}$ NMR (100 MHz, CDCl_3): δ 23.79 (*MeCHCH}_2\text{CHMe}*), 24.75 (*MeCHCH}_2\text{CHMe}*), 43.10 (*MeCHCH}_2\text{CHMe}*), 46.17 (*MeCHCH}_2\text{CHMe}*), 67.50 (*MeCHCH}_2\text{CHMe}*), 70.41 (*MeCHCH}_2\text{CHMe}*), 127.98 (*meta-C}_6\text{H}_5*), 128.19 (*meta-C}_6\text{H}_5*), 130.51 (*para-C}_6\text{H}_5*), 130.82 (*para-C}_6\text{H}_5*), 133.49 (*ipso-C}_6\text{H}_5*), 133.64 (*ipso-C}_6\text{H}_5*), 134.73 (*ortho-C}_6\text{H}_5*), 135 (*ortho-C}_6\text{H}_5*). $^{29}\text{Si}\{^1\text{H}\}$ NMR (79.5 MHz, CDCl_3): δ -29.79 (*major diastereomer*), -27.74 (*minor diastereomer*). EI-MS: $\text{C}_{17}\text{H}_{20}\text{SiO}_2$ m/e 284 (M⁺).

4,4,5,5-tetramethyl-2,2-diphenyl-1,3-dioxane-2-silacyclopentane. Ph_2SiH_2 (0.595 g, 3.23 mmol) and pinacol (0.462 g, 3.91 mmol) were added to $\text{To}^{\text{M}}\text{ZnH}$ (0.004 g, 0.009 mmol, 0.28 mol %) dissolved in benzene (18 mL). This solution was degassed with two freeze-pump-thaw cycles, sealed in a Teflon-valved flask, and heated to 95 °C for 60 h. Workup provided 4,4,5,5-tetramethyl-2,2-diphenyl-1,3-dioxane-2-silacyclopentane (0.882 g, 2.96 mmol, 91.5%)

as the sole product.⁴ ¹H NMR (400 MHz, CDCl₃): δ 1.39 (s, 12 H, CMe₂), 7.40 (t, ³J_{HH} = 7.2 Hz, 4 H, *meta*-C₆H₅), 7.47 (t, ³J_{HH} = 7.2 Hz, 2 H, *para*-C₆H₅), 7.73 (d, ³J_{HH} = 7.6 Hz, 4 H, *ortho*-C₆H₅). ¹³C{¹H} NMR (100 MHz, CDCl₃): δ 26.12 (CMe₂), 82.43 (CMe₂), 127.93 (*meta*-C₆H₅), 130.73 (*para*-C₆H₅), 133.51 (*ipso*-C₆H₅), 135.10 (*ortho*-C₆H₅). ²⁹Si{¹H} NMR (79.5 MHz, CDCl₃): δ - 10.61. EI-MS: C₁₈H₂₂SiO₂ m/e 298 (M⁺).

General procedure for NMR-scale catalytic dehydrocoupling. In a typical experiment, To^MZnH catalyst (0.009 mmol), alcohol (0.18 mmol), and organosilane (0.18 mmol) were dissolved in 0.7 mL benzene-*d*₆ and placed in a NMR tube with a resealable Teflon valve. The tube was sealed, and placed in an oil bath that was preheated to the necessary temperature (45 – 150 °C). The reaction was monitored at regular intervals by ¹H NMR spectroscopy.

General description of ¹H NMR kinetic experiments. All kinetics measurements were conducted by monitoring the reactions with ¹H NMR spectroscopy using a Bruker DRX-400 spectrometer. Prior to the experiments, a toluene-*d*₈ solution containing known concentrations of cyclooctane (16.04 mM, as an internal standard), 3,5-dimethylphenol (0.990 M) and phenylmethylsilane (0.646 M) was prepared. The samples were prepared by adding a measured volume (0.6 mL) of this solution To^MZnH (**1**) giving catalyst concentrations ranging from 2.44 mM to 14.18 mM. The NMR probe was pre-heated to 369.3 K, and the temperature was calibrated using an 80% ethylene glycol sample in 20% DMSO-*d*₆. Single scan spectra were acquired automatically at preset time intervals. The concentrations of the catalyst, substrates and products were determined by comparison of corresponding integrated resonances to the known concentration of cyclooctane. The peaks

were integrated relative to cyclooctane as an internal standard. Pseudo-first order rate constants (k_{obs}) were obtained by a nonweighted linear least-squares fit of the data to the pseudo-first order rate law, $\ln[\text{PhMeSiH}_2] = \ln[\text{PhMeSiH}_2]_0 + k_{\text{obs}}t$ (Figure S1). The second order rate constant k'_{obs} was determined by measuring k_{obs} for several catalyst concentrations. Nonweighted linear least-square fit of the data to the equation $k_{\text{obs}} = C + k'_{\text{obs}}[\text{To}^{\text{M}}\text{ZnH}]$ provided the desired second order rate constant (Figure S2).

Figure S1. Plots of $\ln[\text{PhMeSiH}_2]$ versus time for the $\text{To}^{\text{M}}\text{ZnH}$ (1)-catalyzed reaction of 3,5-dimethylphenol and PhMeSiH_2 at $96.3\text{ }^\circ\text{C}$ in toluene- d_8 (1.53 equiv. of 3,5-dimethylphenol is present with respect to PhMeSiH_2). The catalyst concentration was varied from 2.4 mM to 11.7 mM.

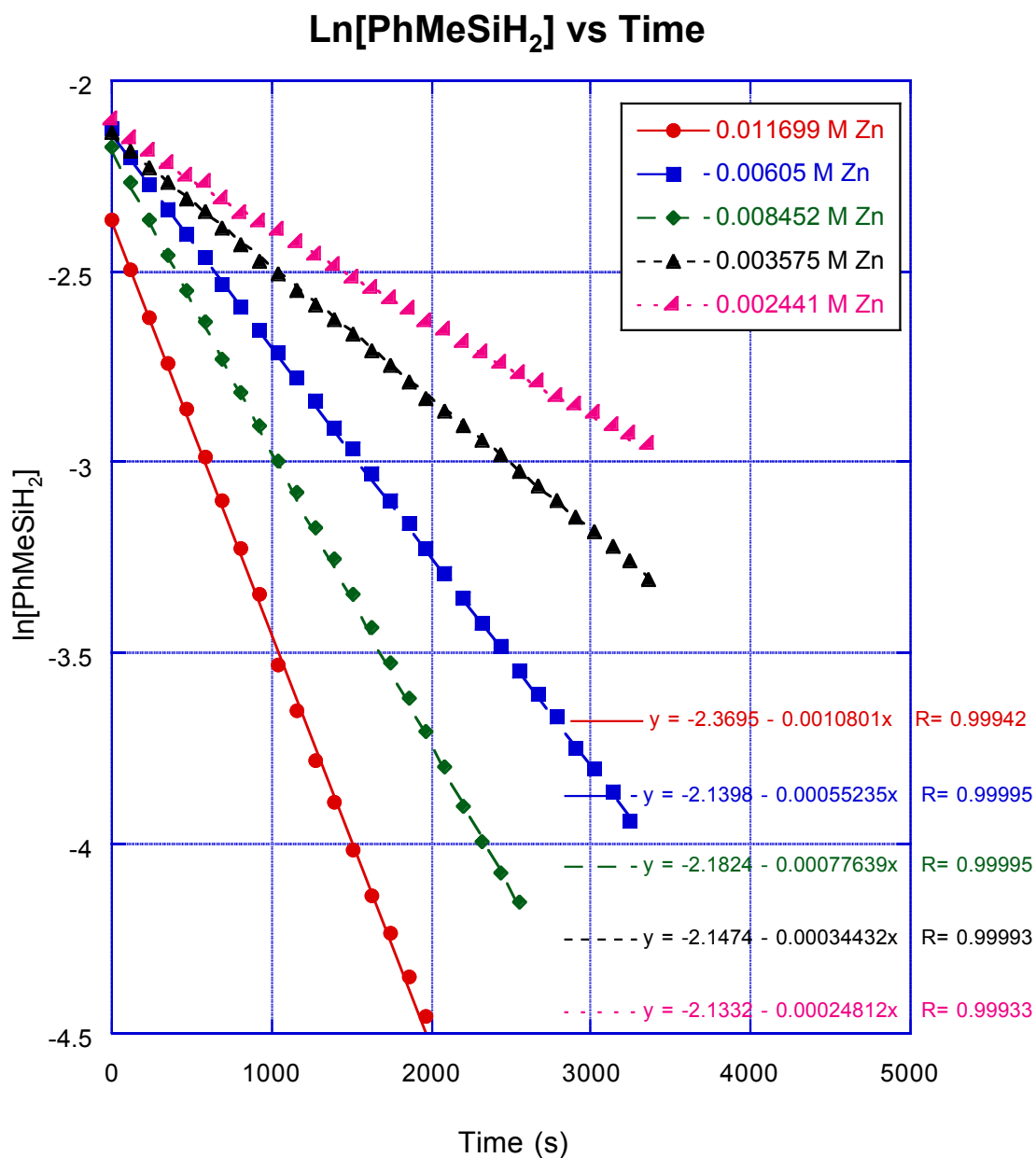


Figure S2. Plots of $\ln[\text{PhMeSiD}_2]$ versus time for the $\text{To}^{\text{M}}\text{ZnH}$ (1)-catalyzed reaction of 3,5-dimethylphenol (0.974 M) and PhMeSiD_2 (0.636 M) at 96.3 °C in toluene- d_8 (1.53 equiv. of 3,5-dimethylphenol is present with respect to PhMeSiD_2). The catalyst concentration was varied from 2.26 mM to 15.69 mM.

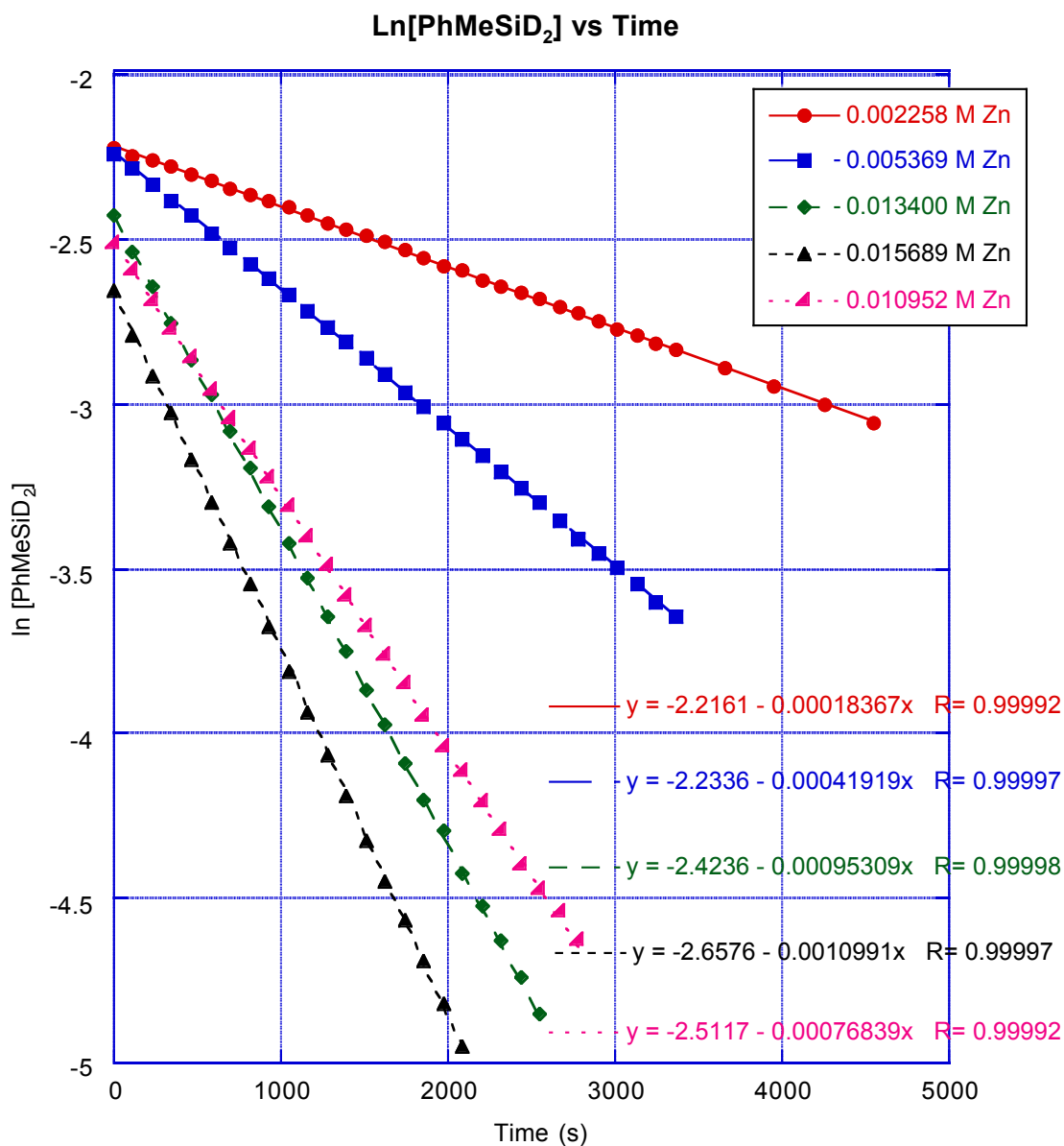


Figure S3. Plot of k_{obs} versus $[\text{To}^{\text{M}}\text{ZnH}]$ concentration showing first-order dependence on catalyst concentration. Each $k_{\text{obs}}[\text{PhMeSiH}_2]$ or $k_{\text{obs}}[\text{PhMeSiD}_2]$ is determined from the linear least squares regression analysis in Figures S1 and S2. From the slope of the curves shown below, $k'_{\text{obs}}^{\text{H}}/k'_{\text{obs}}^{\text{D}} = 1.3(1)$.

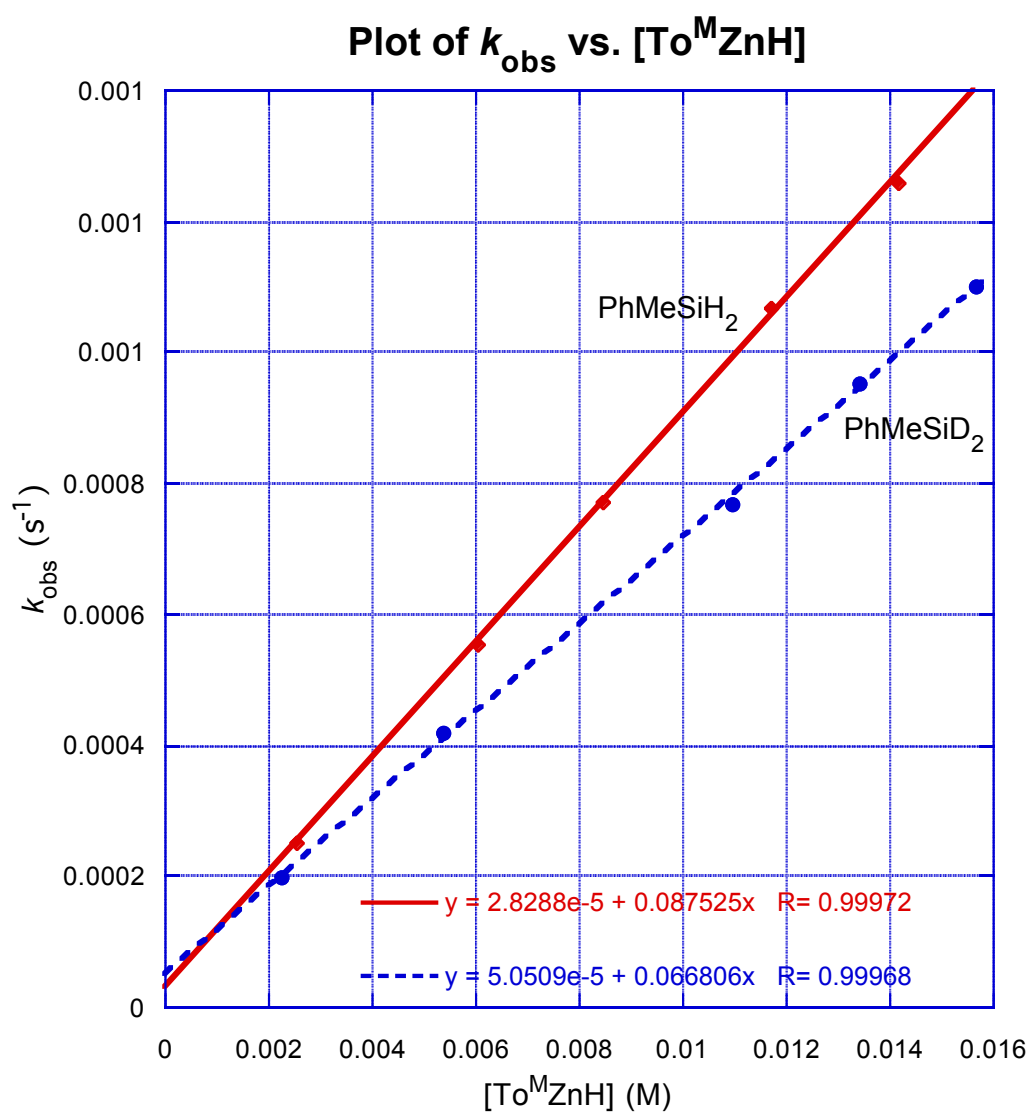


Figure S4. Pseudo-first order plot of $\ln[\text{To}^{\text{M}}\text{ZnOC}_6\text{H}_3\text{Me}]$ vs. time for five $[\text{PhMeSiH}_2]$ at 61 °C. The curves are linear-least squares best fits of the equations below to the data.

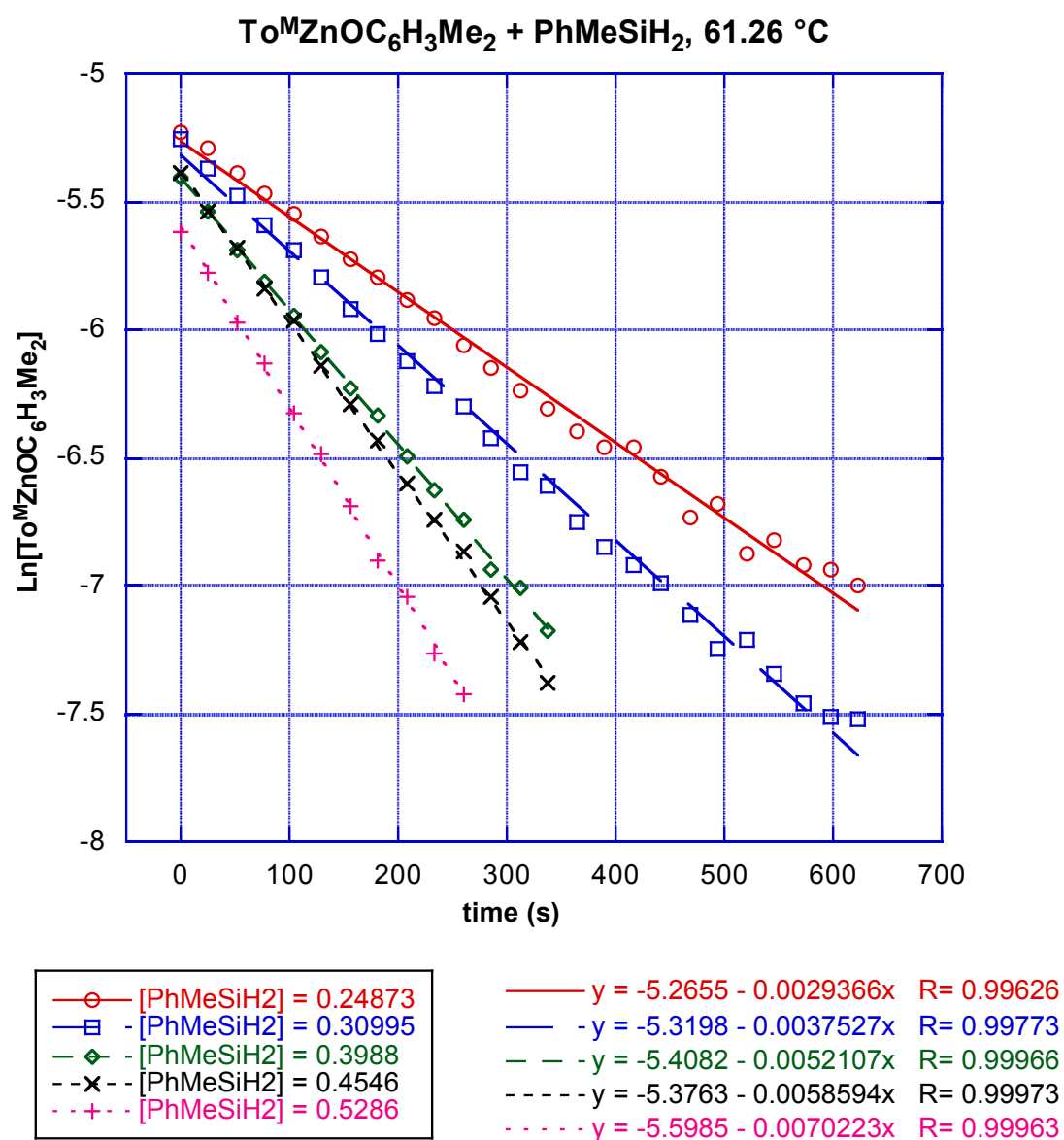


Figure S5. Plot of k_{obs} vs $[\text{PhMeSiH}_2]$ from the plot in Figure S4 for determining the second-order rate constant for the interaction of $\text{To}^{\text{M}}\text{ZnOC}_6\text{H}_3\text{Me}_2$ and PhMeSiH_2 at 61 °C. This plot is representative of data acquired at 24, 36, 47, and 54 °C used in the Eyring plot of Figure S6.

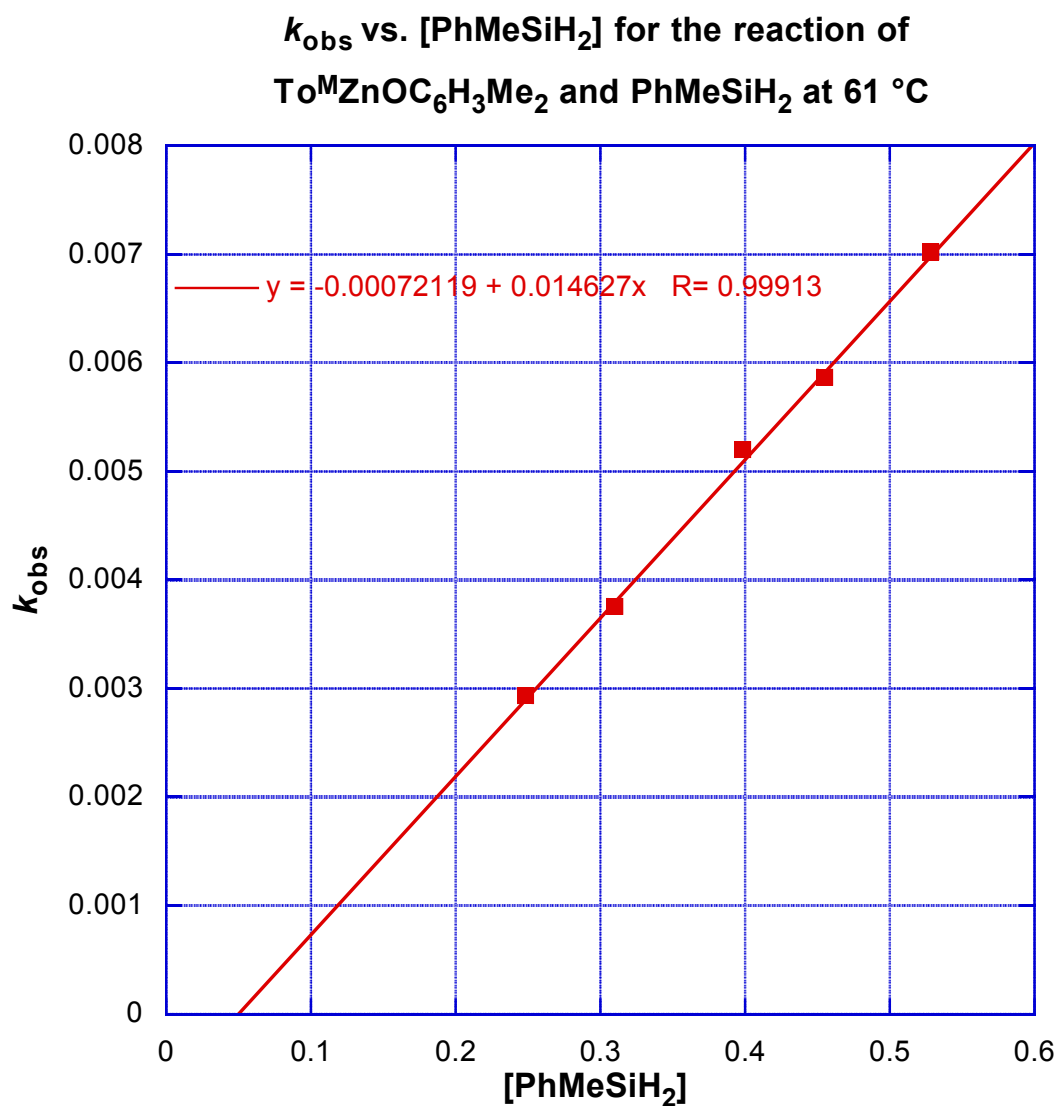
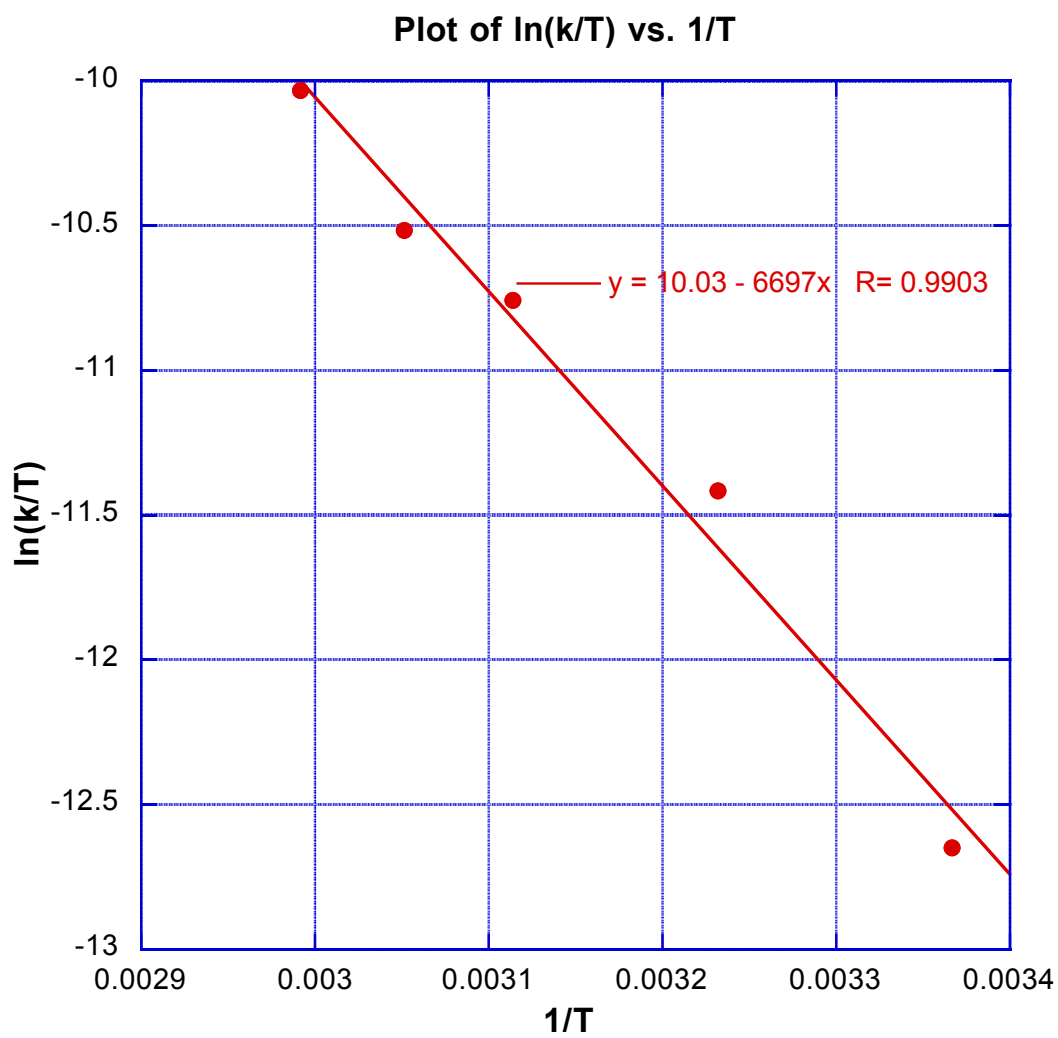


Figure S6. Plot of $\ln(k/T)$ vs. $1/T$ used to calculate activation parameters and the stoichiometric second-order rate constant for the reaction of $\text{To}^{\text{M}}\text{ZnOC}_6\text{H}_3\text{Me}_2$ and PhMeSiH_2 at 96 °C.



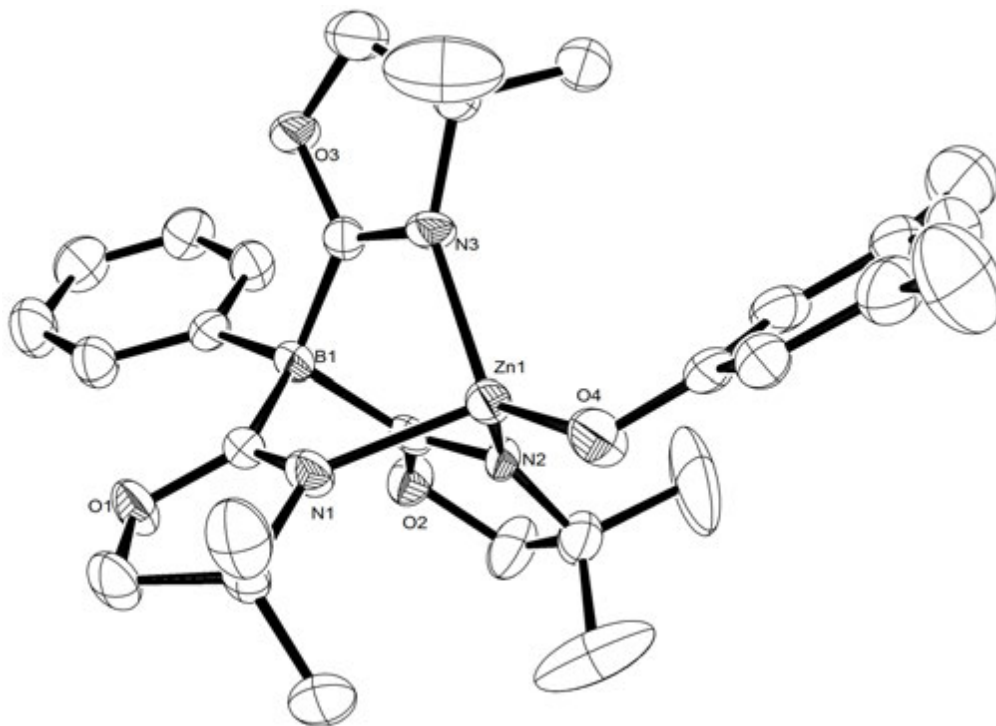


Figure S-7. ORTEP diagram of $\text{To}^{\text{M}}\text{ZnOC}_6\text{H}_3\text{Me}_2$ (**4**) drawn with ellipsoids at 50% probability. Hydrogen atoms are not shown for clarity.

References

- (1) Mukherjee, D.; Ellern, A.; Sadow, A. D. *J. Am. Chem. Soc.* **2010**, *132*, 7582-7583.
- (2) Khankhodzhaeva, D. A. *Zhurnal Obshchei Khimii* **1978**, *48*, 2046.
- (3) Ojima, I.; Nihonyanagi, M.; Kogure, T.; Kumagi, M.; Horiuchi, S.; Nakatsugawa, K.; Nagai, Y. *J. Organomet. Chem.* **1975**, *94*, 449.
- (4) (a) Bedard, T. C.; Corey, J. Y. *J. Organomet. Chem.* **1992**, *428*, 315-333. (b) Cragg, R.H. and Lane, R.D. *Main Group Met. Chem.*, **1987**, *5*, 315. (c) Cragg, R.H. and Lane, R.D. *J. Organomet. Chem.*, **1984**, *267*, 1.

Chapter 5: Remarkably robust monomeric alkylperoxyzinc compounds from oxygen and tris(oxazolinyl)boratozinc alkyls

Modified from a paper published in *Journal of the American Chemical Society*[‡]

Debabrata Mukherjee, Arkady Ellern, and Aaron D. Sadow*

Department of Chemistry, U.S. DOE Ames Laboratory, Iowa State University, Ames, IA

50011-3111

Abstract.

Metal alkylperoxides are remarkable, highly effective, yet often thermally unstable, oxidants that may react through a number of possible pathways including O–O homolytic cleavage, M–O homolytic cleavage, nucleophilic O-atom transfer, and electrophilic O-atom transfer. Here we describe a series of zinc alkyl compounds of the type $To^M ZnR$ (To^M = tris(4,4-dimethyl-2-oxazolinyl)phenylborate; R = Et, *n*-C₃H₇, *i*-C₃H₇, *t*-Bu) that react with O₂ at 25 °C to form isolable monomeric alkylperoxides $To^M ZnOOR$ in quantitative yield. The series of zinc alkylperoxides is crystallographically characterized, and the structures show systematic variations in the Zn–O–O angle and O–O distances. The observed rate law for the reaction of $To^M ZnEt$ (**2**) and O₂ is consistent with a radical chain mechanism, where the rate-limiting S_{H2} step involves the interaction of $\cdot OOR$ and $To^M ZnR$. In contrast, $To^M ZnH$ and $To^M ZnMe$ are unchanged even to 120 °C under 100 psi of O₂ and in the presence of active radical chains (e.g., $\cdot OOEt$). This class of zinc alkylperoxides is unusually thermally robust, in that the compounds are unchanged after heating at 120 °C in solution for several days. Yet, these compounds are reactive as oxidants with phosphines. Additionally, an unusual alkylperoxy group transfer to organosilanes affords $To^M ZnH$ and $ROOSiR_3'$.

Introduction.

Reactions of alkylzinc reagents and O_2 provide environmentally and economically appealing approaches for useful oxidations, including epoxidations,¹ hydroxylations,² and peroxidations.³ In addition, alkylzinc compounds and their reactions with oxygen are fundamentally interesting because zinc occupies a unique position as a non-transition-element and non-redox active divalent metal center whose chemistry nonetheless bears resemblance to the 3d metals. Reactions of (non-metallic) alkylboranes and O_2 provide a close well-studied main group system and are proposed to follow a radical chain based on compelling evidence from kinetic studies, inhibition by radical traps such as galvinoxyl, stereochemical studies, and spectroscopic radical trapping experiments. Galvinoxyl similarly inhibits the reactions of ZnR_2 and O_2 ,⁴ and additional evidence for open-shell alkyl, alkoxy, and alkylperoxy intermediates is provided by EPR spectroscopy of trapped species.⁵ Oxygen initiates carbozincations, which is taken as evidence for a radical chain pathway.^{6,7} However, direct kinetic support for a radical chain reaction is limited,⁴ and a rate law for the reaction of alkylzinc compounds and O_2 has not even been reported.

Furthermore, detailed mechanistic investigations of reactions between organotransition-metal compounds and O_2 have provided a number of mechanisms, including the radical chain, O_2 coordination/protonation, and direct insertion.⁸ Likewise, several pathways have been proposed for oxidations and metal alkylperoxide formations involving main group organometallic systems including zinc.^{4,5,9} At one extreme, $\cdot R$ or $\cdot OOR$, formed through a radical chain, could directly oxidize an organic substrate. A radical chain could also give discrete $[Zn]OOR$ intermediates, or alternatively such alkylperoxyzinc species could form

via electron transfer steps that excludes the chain reaction. Low temperature reactions of L_2ZnR_2 ($L = 4\text{-methylpyridine, 1,4-diazabutadiene, 2,2'-(1'-pyrrolinyl)pyrrole}$) and O_2 that yield isolable and crystallographically-characterized alkylperoxyzinc species provide support for the latter mechanism.^{9c,10,11} However, the products of these reactions invariably contain multimetallic bridging alkoxides and/or alkylperoxides that can obscure the reaction mechanism.

Highly reactive, monomeric alkylperoxy main-group compounds $[M]OOR$ ($M = Mg$,¹² Zn ,^{9c,10,13} Ga ¹⁴, In ¹⁵) have been prepared from organometallics and O_2 , although these systems are not amenable to quantitative kinetic investigations. For example, Parkin's seminal $Tp^{t-Bu}MgOOR$ compounds ($Tp^{t-Bu} = HB(N_2C_3H_2t-Bu)_3$; $R = Me, Et, i-C_3H_7, t-Bu$) are proposed to form through a radical chain pathway based on galvinoxyl inhibition, and the relative rates follow the expected stability of $\cdot R$.¹² Interestingly, the analogous $Tp^{t-Bu}ZnR$ compounds and O_2 do not provide detectable quantities of $Tp^{t-Bu}ZnOOR$.¹⁶ The diketinimate ligand supports a monomeric aluminum *tert*-butylperoxide formed from alkane elimination with $HOOt-Bu$,¹⁷ but bridging alkylperoxy-magnesium and zinc species are formed from (diketinimate)MR and O_2 [$M = Mg, R = CH_2Ph$,^{12c} $M = Zn, R = Et$].¹³ Monomeric structures may have enhanced kinetic stability because $[M]R$ and $[M]OOR$ can comproportionate to metal alkoxides.² Still, monomeric, divalent, tetrahedral 3d transition-metal alkylperoxides, stabilized by bulky tris(pyrazolyl)borate ligands, decompose rapidly by homolysis at room temperature.¹⁸

Kinetic investigations of reactions of $[Zn]R$ and O_2 , then, may be simplified by monomeric alkylperoxyzinc products. The tridentate monoanionic tris(4,4-dimethyl-2-oxazolinyl)phenylborate ligand $[To^M]$ supports monomeric zinc hydride, alkyls, amides, and

alkoxides,¹⁹ and therefore this ancillary ligand might also stabilize zinc alkylperoxides. Here, we report the synthesis and characterization of a series of remarkably robust, monomeric, terminal $\text{To}^{\text{M}}\text{ZnOOR}$ compounds, kinetic studies of their formation from reactions of O_2 and $\text{To}^{\text{M}}\text{ZnR}$, as well as their slow decomposition and mild atom- and group transfer reactivity.

Results and Discussion.

Synthesis and characterization of $\text{To}^{\text{M}}\text{ZnOOR}$ ($\text{R} = \text{Et}$, $n\text{-C}_3\text{H}_7$, $i\text{-C}_3\text{H}_7$, $t\text{-Bu}$, CMe_2Ph).

A series of zinc alkyl compounds $\text{To}^{\text{M}}\text{ZnR}$ [$\text{R} = \text{Me}$ (**1**),^{19b} Et (**2**), $n\text{-C}_3\text{H}_7$ (**3**), $i\text{-C}_3\text{H}_7$ (**4**), $t\text{-Bu}$ (**5**), Ph (**6**), CH_2Ph (Bn ; **7**)] are synthesized by metathesis from $\text{Tl}[\text{To}^{\text{M}}]$ and ZnR_2 , protonolysis of ZnR_2 with HTo^{M} , or salt elimination reaction of $\text{To}^{\text{M}}\text{ZnCl}$ and RLi .²⁰ Some of these compounds are precursors to the targeted $\text{To}^{\text{M}}\text{ZnOOR}$ species. Compounds **1-7** are characterized by spectroscopic and analytical methods, as well as single crystal diffraction for all compounds except **4**. Compounds **1-7** are all pseudo- C_{3v} symmetric, as indicated by equivalent oxazoline groups in ^1H and ^{13}C NMR spectra. This spectroscopy is consistent with tridentate coordination of the tris(oxazoliny)borate ligand to a single zinc center. Additionally, the ^1H NMR spectra contained diagnostic upfield resonances assigned to the $\alpha\text{-CH}$ of Zn-R moiety. These spectral data are consistent with the monomeric structures and four-coordinate zinc centers confirmed by single crystal X-ray diffraction studies (see Figure 1 for **2** and Figures S-13 – S-16 in the Supporting Information (SI) for **3** and **5-7**).

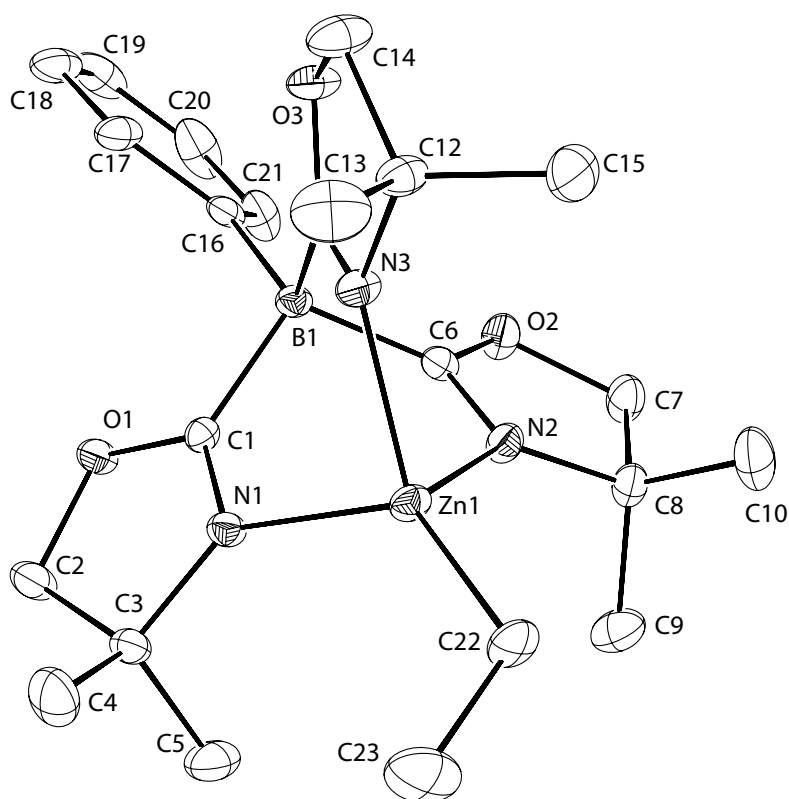
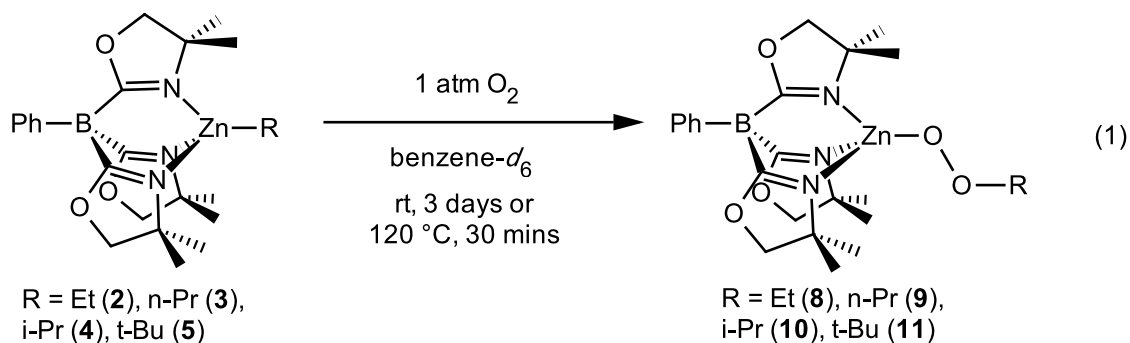


Figure 1. ORTEP diagram of $\text{To}^{\text{M}}\text{ZnEt}$ (**2**). Significant interatomic distances (\AA): Zn1-C22, 1.994(2); Zn1-N1, 2.058(1); Zn1-N2, 2.084(1); Zn1-N3, 2.075(1). Significant interatomic angles ($^{\circ}$): Zn1-C22-C23, 118.7(1); N1-Zn1-C22, 128.83(6); N2-Zn1-C22, 120.53(7); N3-Zn1-C22, 126.35(7).

Compounds **1-7** are resistant to thermal decomposition; for example, compound **2** was recovered quantitatively after thermolysis at $170\text{ }^{\circ}\text{C}$ for 24 h in a sealed NMR tube. Thus, initiation of the radical chain mechanism, proposed for reactions with O_2 (vide infra), is unlikely to involve spontaneous Zn-C bond homolysis in this system.^{10a}

Compounds **2-5** react with O_2 (1 atm) in benzene- d_6 over 3 days at room temperature, 6-8 h at $60\text{ }^{\circ}\text{C}$, or 30 min. at $120\text{ }^{\circ}\text{C}$ to form $\text{To}^{\text{M}}\text{ZnOOR}$ [$\text{R} = \text{Et}$ (**8**), $n\text{-C}_3\text{H}_7$ (**9**), $i\text{-C}_3\text{H}_7$ (**10**), $t\text{-Bu}$ (**11**)] as the only species detected (eq. 1). These synthetic conditions highlight the remarkable thermal stability of **8-11** and strongly contrast the low temperature preparation and kinetic lability typically associated with 3d transition-metal and many main-group alkylperoxides.



Compounds **8-11** form quantitatively, and evaporation of the reaction mixtures provide analytically pure products. The room temperature ^1H NMR spectra of **8-11** contain resonances assigned to equivalent oxazoline groups that suggest pseudo- C_{3v} symmetry for the To^M ligand. Downfield $[\text{Zn}]O\text{OCH}$ resonances of **8-10** replace the upfield $[\text{Zn}]CH$ signals of **2-4**. However, *tert*-butyl **5** and *tert*-butylperoxy **11** are distinguished only by the $^{13}\text{C}\{^1\text{H}\}$ NMR resonance for the CMe_3 that shifts from 35.82 to 77.60 ppm.

Oxygen NMR spectra were obtained from samples of ^{17}O enriched **8-11** that were synthesized by reaction of compounds **2-5** and $^{17}\text{O}_2$ in benzene- d_6 . The data is listed in Table 1. Interestingly, the chemical shifts for the two resonances in **8- $^{17}\text{O}_2$** are similar to the shifts for **9- $^{17}\text{O}_2$** . The chemical shift differences for the two resonances from **10** ($\Delta(\delta\text{O}) = \delta\text{O}_a - \delta\text{O}_b = 111$ ppm) are smaller than the differences in **8** and **9** ($\Delta(\delta\text{O}) = 150$ and 155 ppm, respectively). The *tert*-butyl compound **11** give even smaller differences in ^{17}O chemical shifts ($\Delta(\delta\text{O}) = 80$ ppm). A similar observation was reported for $\text{Tp}^{\text{tBu}}\text{MgOOR}$ compounds, and by comparison we assign the downfield signal as $[\text{Zn}]O\text{OR}$, whereas the upfield resonance is attributed to $[\text{Zn}]O\text{OR}$. Interestingly, the ZnOOR signals are upfield relative to $\text{Tp}^{\text{tBu}}\text{MgOOR}$ chemical shifts, and the $[\text{Zn}]O\text{OR}$ are downfield with respect to the

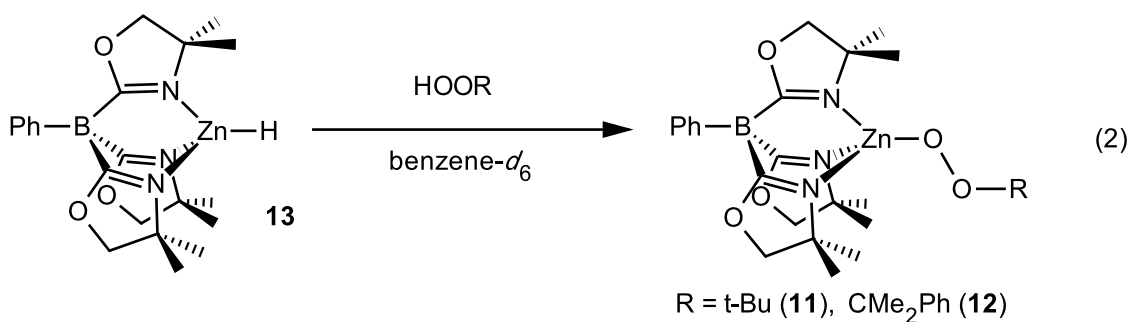
corresponding magnesium alkylperoxide. Perhaps the smaller peak separation for $\text{To}^{\text{M}}\text{ZnOOR}$ vs. $\text{Tp}^{\text{tBu}}\text{MgOOR}$ reflect the smaller electronegativity difference between Zn and O versus Mg and O.

Table 1. ^{17}O NMR chemical shifts of $\text{To}^{\text{M}}\text{ZnOOR}$ and $\text{Tp}^{\text{tBu}}\text{MgOOR}$ (vs. H_2O).

	$\delta([\text{M}]\text{OOR})$	$\delta([\text{M}]\text{OOR})$
$\text{To}^{\text{M}}\text{ZnOOEt}$ (8)	319	169
$\text{Tp}^{\text{tBu}}\text{MgOO}(\text{Et})^a$	407	130
$\text{To}^{\text{M}}\text{ZnOO}(\text{n-Pr})$ (9)	322	167
$\text{To}^{\text{M}}\text{ZnOO}(\text{i-Pr})$ (10)	304	193
$\text{Tp}^{\text{tBu}}\text{MgOO}(\text{i-Pr})^a$	373	159
$\text{To}^{\text{M}}\text{ZnOO}(\text{t-Bu})$ (11)	284	204
$\text{Tp}^{\text{tBu}}\text{MgOO}(\text{t-Bu})^a$	323	183

^aData from reference 12b.

Additionally, compounds **11** and $\text{To}^{\text{M}}\text{ZnOOCMe}_2\text{Ph}$ (**12**) are readily prepared by reaction of $\text{To}^{\text{M}}\text{ZnH}$ (**13**) with HOOt-Bu and HOOCMe_2Ph , respectively (eq. 2).



As noted in the Introduction, the related $\text{Tp}^{t\text{-Bu}}\text{ZnEt}$ is not oxidized by O_2 even at $100\text{ }^\circ\text{C}$.²¹ Surprisingly, only starting materials are evident after treatment of $\text{To}^{\text{M}}\text{ZnMe}$ (**1**) and $\text{To}^{\text{M}}\text{ZnH}$ (**13**) with O_2 from room temperature to $120\text{ }^\circ\text{C}$ and from 1 atm to 100 psi for 12 h. Addition of O_2 to mixtures of **2** and **1** or **13** convert **2** to **8** while **1** or **13** remain unreacted. Alternatively, $\text{To}^{\text{M}}\text{ZnPh}$ (**6**) and $\text{To}^{\text{M}}\text{ZnBn}$ (**7**) react under O_2 at $120\text{ }^\circ\text{C}$ to form $(\text{k}^2\text{-To}^{\text{M}})_2\text{Zn}$ (**14**) in benzene over 48 h (see Figure S-22). Compound **14** is prepared independently from $\text{Ti}[\text{To}^{\text{M}}]$ and **13**. Neither light nor the radical initiator AIBN facilitates reactions of **1**, **6**, **7**, and **13** with O_2 to provide isolable organoperoxide species. Reactions of oxygen and alkylzinc compounds are known to often yield alkoxides rather than peroxides, and the synthesis of alkylperoxyzinc compounds typically requires carefully controlled conditions to avoid formation of alkoxides.^{3,9,10} $\text{To}^{\text{M}}\text{ZnOR}$ are not formed in these reactions based on the combustion analyses of **8-12**, their X-ray structures (see below), the poorer benzene solubility of $\text{To}^{\text{M}}\text{ZnOR}$ (R = Et, *n*-C₃H₇, *i*-C₃H₇) in comparison to **8-10**, and the non-equivalence of the ¹H NMR spectra of **8-11** to spectra obtained from treatment of $\text{To}^{\text{M}}\text{ZnH}$ and ROH (R = Et, *n*-C₃H₇, *i*-C₃H₇, *t*-Bu). Interestingly, these reactions of alcohols give broad ¹H NMR resonances in benzene; upon evaporation of volatile materials, benzene-insoluble white solids are obtained that suggest oligomeric structures. (The bulkier $\text{To}^{\text{M}}\text{ZnO}t\text{-Bu}$ is

monomeric and soluble in benzene, and it is also spectroscopically distinct from **11**).^{19a} The monomeric structures of **8-12** are verified by X-ray crystallography (see Figure 2 for **8** and Figures S-18 – S-21 for **9-12**). The alkylperoxy group of **9** is disordered over two positions and will not be discussed.

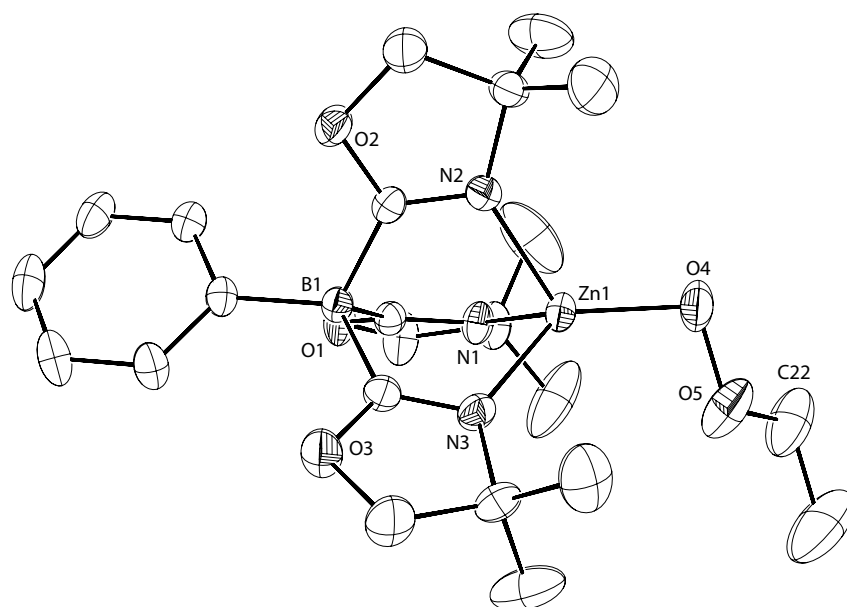


Figure 2. ORTEP diagram of $\text{To}^{\text{M}}\text{ZnOOEt}$ (**8**); ellipsoids are plotted at 35% probability, and hydrogen atoms and a toluene solvent molecule are not plotted. Significant interatomic distances (Å): Zn1-O4, 1.877(1); Zn1-O5, 2.630(2); Zn1-N1, 2.027(1); Zn1-N2, 2.045(1); Zn1-N3, 2.033(1); O4-O5, 1.466(2). Significant interatomic angles (°): Zn1-O4-O5, 103.1(1); N1-Zn1-O4, 121.34(6); N2-Zn1-O4, 119.87(6); N3-Zn1-O4, 128.53(6).

The Zn-O_a distances in **8** and **10-12** are similar (from 1.873(2) Å in **10** to 1.877(1) Å in **8**).

Bridging [diketiminatoZn(μ^2 -OOEt)]₂ contains longer Zn-O distances [1.971(1) and 2.044(1) Å],¹³ and triply-bridging Zn₃(μ^3 -OOMe) Zn-O distances are much longer (2.132 Å average)

in the tetrameric cube [(MeZn)₄(μ^3 -OOMe)₂(μ^3 -OZnMeL)₂] (L = diazabutadiene).¹⁰

However, the related alkoxide $\text{To}^{\text{M}}\text{ZnOt-Bu}$ contains a shorter Zn-O distance of 1.835(1)

Å.^{19a} Additionally, the general structural features of **8-12** are roughly similar to those of crystallographically characterized monomeric tris(pyrazolyl)borato transition-metal alkylperoxides.¹⁸ These 3d transition metal alkylperoxides are typically synthesized from hydroperoxides which limits the diversity of readily accessible alkyl groups. The preparation of **8-11** from O₂, as well as the availability of cumylperoxy **12**, provides a range of alkylperoxy zinc compounds for structural comparison.

Interestingly, the compound with the longest O-O distance contains the smallest Zn-O-O angle and shortest Zn-O_b distance (Table 2).

Table 2. Comparison of interatomic O-O and Zn-O (Å) distances and Zn-O-O angles (°) for compounds **8** and **10-12**.

Compound	O-O	∠Zn-O-O	Zn-O _b
To ^M ZnOOEt (8)	1.466(2)	103.1(1)	2.630(2)
To ^M ZnOO(<i>i</i> -C ₃ H ₇) (10)	1.441(3)	105.1(1)	2.644(2)
To ^M ZnOO <i>t</i> -Bu (11)	1.490(2)	97.11(9)	2.534(2)
To ^M ZnOOCMe ₂ Ph (12)	1.477(3)	103.4(2)	2.637(2)

Thus, the O-O distances follow the trend **10** < **8** < **12** < **11** that inversely tracks the Zn-O_a-O_b angles and the Zn-O_b distances **11** < **8** ~ **12** < **10**. All of the Zn-O_b distances in **8** and **10-12** are within the sum of Zn and O van der Waals radii (2.91 Å), but well outside the sum of covalent radii for Zn and oxygen (1.88 Å).²² The nature of that interaction may be considered

in the context of the systematically monomeric structures for **8-12** that contrast dimeric or oligomeric $[\text{To}^{\text{M}}\text{ZnOR}]_n$ ($\text{R} = \text{Et}, n\text{-C}_3\text{H}_7, i\text{-C}_3\text{H}_7$) compounds. As noted above, the spectroscopic and physical properties of $\text{To}^{\text{M}}\text{ZnOR}$ are more consistent with oligomeric structures. Thus, the Zn-O_b interaction likely perturbs the atomic distances to a small but important degree to stabilize compounds **8-12** as the first structurally characterized monomeric zinc alkylperoxides.

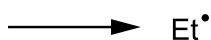
Mechanistic investigations and kinetics of $\text{To}^{\text{M}}\text{ZnR}$ and O_2 .

General observations for the reactions of $\text{To}^{\text{M}}\text{ZnR}$ and O_2 allow comparison to alkylzinc/ O_2 systems that are less amenable to rate law determinations. Reactions of $\text{To}^{\text{M}}\text{ZnEt}$ (**2**) and O_2 (50 psi) performed under ambient lighting and in the dark give equivalent conversion of **2** and yield (93%) of **8** after 32 h. Galvinoxyl inhibits the conversion. The $\text{To}^{\text{M}}\text{ZnOOR}$ compounds are the only detectable products from reactions of **2**, **3**, **4**, or **5** with O_2 in the presence or absence of azobis(isobutyronitrile) (AIBN). Species such as C_4H_{10} , C_2H_6 , $\text{To}^{\text{M}}\text{ZnCMe}_2\text{CN}$, $\text{To}^{\text{M}}\text{ZnOOCMe}_2\text{CN}$ (or related products from **3**, **4**, and **5**) that might be expected from radical initiation or termination processes are not observed for reactions of oxygen and $\text{To}^{\text{M}}\text{ZnEt}$.

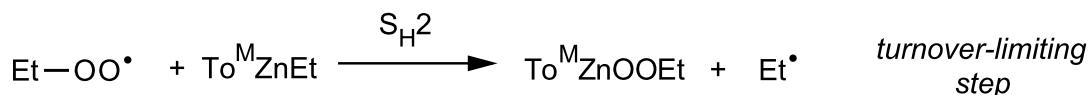
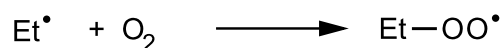
Rate law measurements for the reaction of **2** and O_2 from 45 – 96 °C and 30 – 100 psi O_2 were thwarted by variable induction periods and inconsistent concentration dependencies for both O_2 and $\text{To}^{\text{M}}\text{ZnEt}$. However, in the presence of AIBN (0.2 – 1.3 equiv), plots of **[2]** vs. time follow an exponential decay providing the pseudo-first-order rate constant k_{obs} . Notably, k_{obs} values are equivalent within error at O_2 pressures of 30, 50, 70, 80 and 100 psi, showing zero-order oxygen dependence (Figure S-3). A linear correlation of $[\text{AIBN}]^{1/2}$ vs. k_{obs} passes

through the origin ($[2]_{\text{ini}} = 25 \text{ mM}$, $[\text{AIBN}]_{\text{ini}} = 5.4 - 33.9 \text{ mM}$, $54 \text{ }^\circ\text{C}$), giving the rate law - $d[2]/dt = k'[2]^1[\text{O}_2]^0[\text{AIBN}]^{1/2}$ ($k' = 3.0 \pm 0.1 \times 10^{-3} \text{ M}^{-1/2} \text{ s}^{-1}$) which appears valid over at least three half-lives of the reaction time-course. This rate law is consistent with a radical chain mechanism (Scheme 1) and is similar to empirical rate laws for autoxidation of organic compounds, organoboranes,² and a few O_2 insertions into transition-metal alkyls. Thus, our studies provide the first rate law-based support for a radical chain process for the interaction of alkylzinc species and O_2 .

Initiation



Propagation



Scheme 1. Proposed radical chain mechanism for $\text{To}^{\text{M}}\text{ZnOOEt}$ formation from $\text{To}^{\text{M}}\text{ZnEt}$ and O_2 .

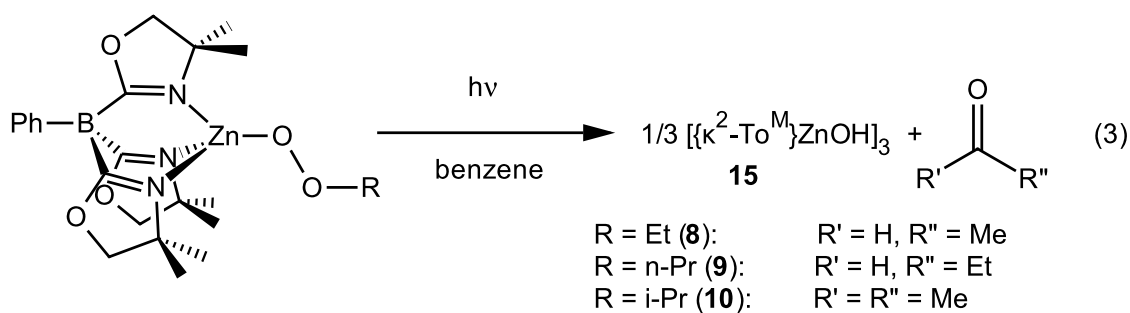
The postulated radical chain mechanism includes a bimolecular homolytic substitution process ($\text{S}_{\text{H}2}$) at zinc that likely involves an electron transfer from the HOMO (the Zn-C bond) to OOEt^\bullet to form a Zn-O bond and Et^\bullet . The inert nature of $\text{To}^{\text{M}}\text{ZnMe}$ (**1**) and $\text{To}^{\text{M}}\text{ZnH}$ (**13**) with O_2 under these conditions suggests that OOR^\bullet ($\text{R} = \text{H}, \text{Me}$) is not able to oxidize the Zn-H and Zn-Me bonds even in the presence of AIBN and an initiated radical chains (i.e., OOEt^\bullet).

Previously, the weaker EtZn-Et bond vs. MeZn-Me provided a rationalization for the slower reaction of oxygen and ZnMe_2 in comparison to ZnEt_2 .⁵ Although the bond dissociation

energies (BDE's) for $\text{To}^{\text{M}}\text{Zn-R}$ have not yet been determined, the values are expected to follow the trends of RZn-R , which have been determined from statistical unimolecular reaction calculations (RRKM theory): $\text{EtZn-Et} < \text{MeZn-Me}$ ($\text{EtZn-CH}_2\text{CH}_3 = 219 \pm 8 \text{ kJ/mol}$ ($52.4 \pm 2.0 \text{ kcal/mol}$); $\text{MeZn-CH}_3 = 266.5 \pm 6.3 \text{ kJ/mol}$ ($63.7 \pm 1.5 \text{ kcal/mol}$).²³ However, the experimental intrinsic BDE (determined from the ion beam method) for $[\text{Zn-H}]^+$ is much *smaller* than $[\text{Zn-CH}_3]^+$ BDE: $[\text{Zn-H}]^+ = 231 \pm 13 \text{ kJ/mol}$ ($55.2 \pm 3.1 \text{ kcal/mol}$); $[\text{Zn-CH}_3]^+ = 295 \pm 13 \text{ kJ/mol}$ ($70.6 \pm 3.2 \text{ kcal/mol}$).²⁴ The intrinsic BDE's also provide the BDE for MeZn-CH_3 as $290 \pm 13 \text{ kJ/mol}$ ($69.3 \pm 3.2 \text{ kcal/mol}$) for comparison between the two sets of values. Regardless, the inert nature of $\text{To}^{\text{M}}\text{ZnH}$ toward O_2 is not readily rationalized by known BDE's.

Oxidation reactivity of $\text{To}^{\text{M}}\text{ZnOOR}$.

The concentration of $\text{To}^{\text{M}}\text{ZnOOEt}$ in benzene- d_6 is unchanged after 24 h at 120 °C in a sealed NMR tube. After 3 days at 140 °C, 63% of $\text{To}^{\text{M}}\text{ZnOOEt}$ is converted to $(\text{k}^2\text{-To}^{\text{M}})_2\text{Zn}$ (**14**). *Tert*-butylperoxide **11** is even slower to form **14** (30% after 3 d at 135 °C), and cumylperoxy **12** is unchanged after 1 d at 165 °C. Photolysis of the alkylperoxy zinc compounds **8-12** (350 nm, benzene, room temperature) provides a trimeric zinc hydroxide species $[(\text{k}^2\text{-To}^{\text{M}})\text{Zn}(\text{m-OH})]_3$ (**15**) that deposits as white crystals over 24 h (eq. 3). The organic carbonyl products are MeCHO , Me_2CO , and EtCHO from **8**, **9**, and **10**, respectively. Compound **11** forms Me_2CO , while the cumylperoxyzinc **12** forms acetophenone, methane, and the epoxide 2-methyl-2-phenyloxirane.

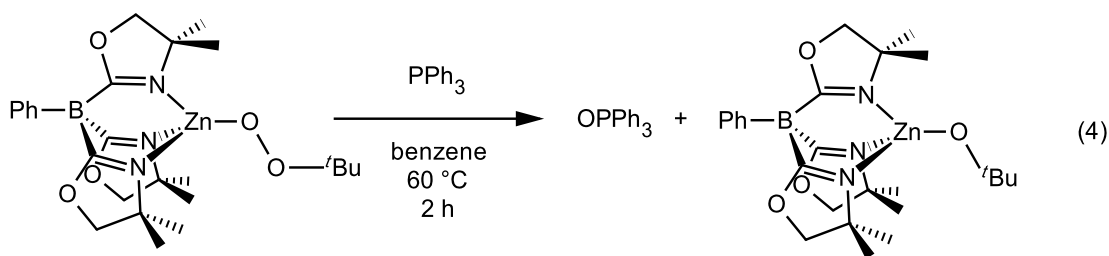


X-ray crystallography of disordered **15** establishes its connectivity as a trimeric $[\text{Zn}(\mu\text{-OH})_3]$ structure. Compound **15** is soluble in methylene chloride but insoluble in benzene, toluene, and tetrahydrofuran. The room temperature ^1H NMR spectrum of **15** in methylene chloride- d_2 was broad. The spectrum was resolved at $-53\text{ }^\circ\text{C}$ indicated local C_s -symmetry with equivalent zinc centers that are related by a rotation axis that is assumed to be C_3 based on the solid-state structure. Bidentate coordination of To^{M} to Zn in **15** is further supported by two oxazoline ν_{CN} bands in the IR spectrum at 1577 (coordinated) and 1623 cm^{-1} (non-coordinated) in an approximately 2:1 ratio.

The formation of zinc hydroxide and an oxidized organic species is consistent with O–O homolysis; for example, thermal decomposition of $\text{Cp}^*_2\text{Hf}(\text{Ph})\text{OOR}$ gives $\text{Cp}^*_2\text{Hf}(\text{Ph})\text{OH}^{25}$ and photolysis of dialkylperoxides are well known to provide 2 $\cdot\text{OR}$ that decompose to similar products.²⁶ Compound **15** is a likely intermediate in the thermolysis of alkylperoxides **8-12**. That process also likely involves homolytic O–O bond cleavage because thermal treatment of **15** (in benzene- d_6) gives **14** (8 h, 120 $^\circ\text{C}$). Conversion of **15** to **14** is faster than the overall rate of alkylperoxide decomposition, making that step kinetically competent for the overall conversion. Thus, the rate-determining step of conversion of **8-12** to **14** is O–O bond homolysis.

The thermal stability of the [Zn]OOR moieties is remarkable in comparison to related main group and transition-metal species, and this may be at least partly related to the monomeric nature of compounds **8-12**. We therefore further investigated their reactivity for comparison with zinc alkylperoxides known to have multimetallic or unknown structures. For example, rapid disproportionation of alkylzinc and alkylperoxyzinc compounds to alkoxyzinc species starkly contrasts the present system. ^1H NMR spectra of mixtures of alkylperoxyzincs **8-11** with the corresponding tris(oxazolinyl)boratozinc alkyl (**2**, **3**, **4**, or **5**) or hydride **13** only contained signals assigned to starting materials, even after the mixtures were heated at 80 °C for 12 h.

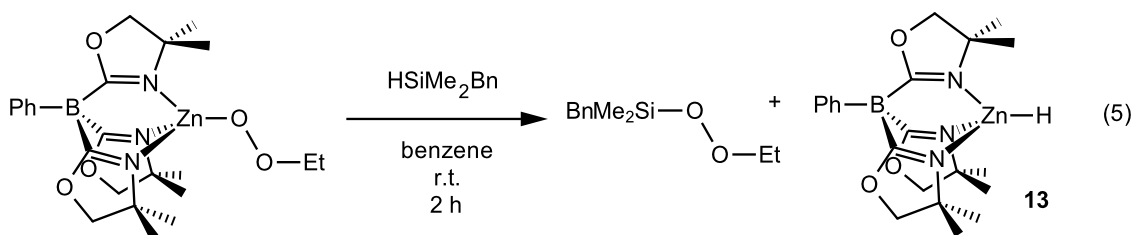
Despite their thermal stability, **8-12** are reactive in oxidation processes and group transfer chemistry. Compounds **8-12** readily react with phosphines such as PH_2Ph , PPh_3 , $\text{P}(p\text{-C}_6\text{H}_4\text{Me})_3$, and PMe_3 to form the corresponding phosphine oxides via stoichiometric O-atom transfer (eq. 4). Kinetic studies of stoichiometric phosphine oxidations, particularly on a series of isolable monomeric alkylperoxymetal compounds, are surprisingly rare even though a range of mechanisms are conceivable (and proposed in related metal-alkylperoxide systems), including radical chains via O–O bond homolysis to give alkoxyradical intermediates,²⁷ nucleophilic attack of the phosphine on an η^2 -peroxyzinc, and coordination of phosphine to zinc followed by nucleophilic attack by the alkylperoxide.^{28, 29}



Reaction rates for $\text{To}^{\text{M}}\text{ZnOO}t\text{-Bu}$ and PR_3 follow the trend $\text{PPh}_3 < \text{P}(p\text{-C}_6\text{H}_4\text{Me})_3 < \text{PMe}_3 < \text{PH}_2\text{Ph}$; PPh_3 reacts in less than 2 h at 60 °C, whereas PMe_3 reacts in less than 5 minutes at ambient temperature. The second-order rate law $-d[\text{To}^{\text{M}}\text{ZnOOR}]/dt = k[\text{To}^{\text{M}}\text{ZnOOR}][\text{P}(p\text{-C}_6\text{H}_4\text{Me})_3]$ emphasizes the mononuclear nature of alkylperoxyzinc species and the bimolecular nature of the reaction. The rate constants follow the trend: **8** > **9** > **10** >> **11** ($k_{259\text{K}}^{(8)} = 8.8 \pm 0.3 \times 10^{-2} \text{ M}^{-1}\text{s}^{-1}$, $k_{259\text{K}}^{(9)} = 7.5 \pm 0.2 \times 10^{-2} \text{ M}^{-1}\text{s}^{-1}$, $k_{259\text{K}}^{(10)} = 6.3 \pm 0.2 \times 10^{-3} \text{ M}^{-1}\text{s}^{-1}$, $k_{294\text{K}}^{(11)} = 1.22 \pm 0.04 \times 10^{-3} \text{ M}^{-1}\text{s}^{-1}$; $[\text{P}(p\text{-C}_6\text{H}_4\text{Me})_3] = 30 \text{ mM}$) showing steric effects in the reactivity of the alkylperoxyzinc reagents. Eyring analysis of the reaction between **8** and $\text{P}(p\text{-C}_6\text{H}_4\text{Me})_3$ provides $\Delta H^\ddagger = 9.5 \pm 0.3 \text{ kcal}\cdot\text{mol}^{-1}$ and $\Delta S^\ddagger = -27 \pm 1 \text{ cal}\cdot\text{mol}^{-1}\cdot\text{K}^{-1}$.³⁰ The second-order rate law, activation parameters, and reaction conditions rule out a mechanism for phosphine oxidation by $\text{To}^{\text{M}}\text{ZnOOR}$ involving oxygen-oxygen bond homolysis.²⁷ The rate of $\text{P}(p\text{-C}_6\text{H}_4\text{Me})_3$ oxidation by **8-11** follows the size of the peroxyalkyl group ($t\text{-Bu} < i\text{-C}_3\text{H}_7 < n\text{-C}_3\text{H}_7 < \text{Et}$), but no relationship with Zn–O–O angles or O–O distances (obtained from the X-ray data) could be identified. Faster reaction rates with smaller alkyl groups suggest the mechanism involving nucleophilic attack of phosphine on an electrophilic alkylperoxide.

Alkylperoxy group transfer reactivity with hydrosilanes.

In addition to the phosphine oxidation via O-atom transfer, metal peroxides are also known to oxidize C-H and Si-H bonds to give alcohol and silanol (SiOH) groups, respectively.^{19b,29,31} In contrast, the $\text{To}^{\text{M}}\text{ZnOOR}$ compounds **8-12** react with organosilanes (HSiR'_3) by peroxy-group transfer to silicon. For example, **8** and HSiMe_2Bn react according to eq. 5.



This alkylperoxy- group transfer reactivity resembles previously observed alkoxy-group transfer to silicon from zinc alkoxides,^{19b} and that reaction is likely important in zinc-catalyzed dehydrocoupling of alcohols and silanes as well as hydrosilylation of carbonyls.³² Related Si-O bond formations may be involved in transition-metal, rare earth, and main-group metal catalyzed hydrosilylations.³³ While zinc alkylperoxides may be hydrolyzed to alkyl hydroperoxides,^{3,34} the hydrolysis product is [Zn]OH. In the reactions here with organosilanes, $\text{To}^{\text{M}}\text{ZnH}$ is the product, and that gives a possibility for (future) catalysis (e.g., zinc-catalyzed hydrosilylation of O_2).

The empirical rate law for the reaction of **8** and BnMe_2SiH of $-d[\text{To}^{\text{M}}\text{ZnOOEt}]/dt = k[\text{To}^{\text{M}}\text{ZnOOEt}][\text{BnMe}_2\text{SiH}]$ ($k^{309\text{K}} = 1.64 \pm 0.09 \times 10^{-2} \text{ M}^{-1}\text{s}^{-1}$) was measured from 288 K to 320 K. The steric effects in this reactivity of the zinc alkyl peroxides also follow the similar trend as observed in phosphine oxidation: **8** > **9** > **10** ($k_{309\text{K}}^{(8)} = 1.64 \pm 0.09 \times 10^{-2} \text{ M}^{-1}\text{s}^{-1}$, $k_{309\text{K}}^{(9)} = 1.17 \pm 0.02 \times 10^{-2} \text{ M}^{-1}\text{s}^{-1}$, $k_{309\text{K}}^{(10)} = 1.9 \pm 0.02 \times 10^{-3} \text{ M}^{-1}\text{s}^{-1}$). The activation parameters for the reaction of **8** and BnMe_2SiH , $\Delta H^\ddagger = 12.6 \pm 0.7 \text{ kcal}\cdot\text{mol}^{-1}$ and $\Delta S^\ddagger = -26 \pm 2 \text{ cal}\cdot\text{mol}^{-1}\text{K}^{-1}$, are consistent with an ordered transition-state associated with a second-order process.³⁰ Primary isotope effects for the reactions of $\text{To}^{\text{M}}\text{ZnOOR}$ and BnMe_2SiH or BnMe_2SiD are unity [$k_{\text{H}}/k_{\text{D}}^{(8)} = 1.10(7)$, $k_{\text{H}}/k_{\text{D}}^{(10)} = 1.11(9)$].

For comparison, the second-order Si-O bond forming reaction of the aryloxyzinc $\text{To}^{\text{M}}\text{ZnOC}_6\text{H}_3\text{Me}_2$ and PhMeSiH_2 occurs with similar activation parameter values ($\Delta H^\ddagger = 13$

$\text{kcal}\cdot\text{mol}^{-1}$; $\Delta S^\ddagger = -27 \text{ cal}\cdot\text{mol}^{-1}\text{K}^{-1}$) and an isotope effect of 1.3(1).^{19b} The isotope effect for the σ -bond metathesis reaction of $\text{CpCp}^*\text{ClHf-SiH}_2\text{Ph}$ and PhSiH_3 or PhSiD_3 is 2.7(2), with $\Delta H^\ddagger = 19 \text{ kcal}\cdot\text{mol}^{-1}$ and $\Delta S^\ddagger = -33 \text{ cal}\cdot\text{mol}^{-1}\text{K}^{-1}$.³⁵ Rare earth mediated Si-C bond formations provide isotope effects closer to unity.³⁶ For example, Cp^*_2ScMe and Ph_2SiH_2 or Ph_2SiD_2 react with an isotope effect of 1.15(5) and activation parameters of $\Delta H^\ddagger = 6.6 \text{ kcal}\cdot\text{mol}^{-1}$ and $\Delta S^\ddagger = -43 \text{ cal}\cdot\text{mol}^{-1}\text{K}^{-1}$. Additionally, the reaction of $\text{To}^{\text{M}}\text{MgNH}t\text{-Bu}$ and PhMeSiH_2 involving Si-N bond formation occurs with an isotope effect of 1.0(2), $\Delta H^\ddagger = 5.7(2) \text{ kcal}\cdot\text{mol}^{-1}$, and $\Delta S^\ddagger = -46.1(8) \text{ cal}\cdot\text{mol}^{-1}\text{K}^{-1}$.³⁷ Although a number of variables are not constant between these experiments (including variations in organosilane and metal center, as well as various Si-E bond formations including Si-O, Si-N, and Si-C bonds), a rough empirical trend of isotope effect and activation parameters may be noted from the kinetic parameters associated with these reactions. In particular, metathesis reactions involving isovalent metal-mediated group transfer to silicon in which Si-H or Si-D bonds are broken have isotope effects closer to unity in highly ordered transition states ($\Delta S^\ddagger \ll 0$) and small enthalpic activation barriers. While these parameters are not correlated,³⁸ a second-order elementary step in which the barrier is highly dependent on the activation entropy and has a small primary isotope effect may indicate an early transition state in which little bond-cleavage has occurred. However, more experiments, as well as theoretical treatments that probe isotope effects and activation parameters of concerted Si-H bond cleavages/Si-E bond formations are still needed before significant conclusions may be drawn from these observations.

This metathetical pathway is apparently accessible because Zn-O and O-O bond homolysis

pathways, which are common for transition-metal alkylperoxides, are not fast in this monomeric zinc system at moderate temperatures. Comproportionation reactions of peroxyzinc and alkylzinc compounds also are inhibited by tris(oxazolanyl)borate ligand. Once these decomposition pathways are blocked, the reaction chemistry of peroxyzinc compounds provides several intriguing reactions and observations including a non-oxidative peroxy group transfer.

Conclusion.

Aspects of the chemistry of $To^M ZnOOR$ **8-12** are distinct from transition-metal alkyl peroxides. A particularly interesting comparison is with monomeric $d^0 Cp_2ClTiOOt-Bu$, in which Cp_2ClTiO^{\bullet} is easily formed.²⁷ Neither Ti(IV) nor Zn(II) can be further oxidized, yet the apparent homolysis of the O–O bond in the two compounds occur at very different rates. The origin of this effect may be thermodynamic (O–O bond strength versus oxyl radical stability), but it also may result from transition-state effects. With $3d^n$ transition-elements, metal-centered oxidation may further contribute to the destabilization of alkylperoxides. The tris(pyrazolyl)borato transition-metal alkylperoxides clearly show these effects, and the resulting compounds can oxidize CH bonds. A second interesting comparison is with the autocatalytic chain reactions of Tp^*PtHMe_2 and O_2 , where $Tp^*Me_2PtOO^{\bullet}$ reacts with the thermodynamically stronger Pt–H bond rather than the Pt–Me moiety.³⁹ H-atom abstraction, however, is more plausible than $^{\bullet}CH_3$ abstraction, and in this sense the Tp^*PtHMe_2 oxidation is similar autocatalytic oxidation of organic compounds (where weaker C–C bonds are less reactive than C–H bonds). While the zinc-carbon BDE's in **1-5** are expected to follow the trend $1 > 2 > 3 > 4 > 5$ and the reaction rates with O_2 follow $5 > 4 \sim 3 \sim 2$ (with **1** not reacting), the unreactive Zn–H bond in **13** is expected to be weaker than the Zn–C bonds.

The trend of reaction rate for Zn–Me, Zn–Et, and Zn–CMe₃ follows the expected trend from the BDE's, while Zn–H does not. Thus, unlike the selectivity (i.e., relative rates) of radical chains in autoxidation of hydrocarbyl species that are thought to be governed by C–H BDE's (tertiary > secondary > primary), the radical chains of these reactions are not entirely dominated by cleavage of the weakest Zn–E bond.

References.

- (1) Porter, M. J.; Skidmore, J. *Chem. Commun.* **2000**, 1215–1225.
- (2) Davies, A. G. *J. Chem. Res.* **2008**, 361–375.
- (3) Klement, I.; Lütjens, H.; Knochel, P. *Tetrahedron* **1997**, *53*, 9135–9144.
- (4) Davies, A. G.; Roberts, B. P. *J. Chem. Soc. B* **1968**, 1074–1078.
- (5) Maury, J.; Feray, L.; Bazin, S.; Clément, J. -L.; Marque, S. R. A.; Siri, D. Bertrand, M. P. *Chem.–Eur. J.* **2011**, *17*, 1586–1595.
- (6) Cohen, T.; Gibney, H.; Ivanov, R.; Yeh, E. A. -H.; Marek, I.; Curran, D. P. *J. Am. Chem. Soc.* **2007**, *129*, 15405–15409.
- (7) Akindele, T.; Yamada, K. -I.; Tomioka, K. *Acc. Chem. Res.* **2009**, *42*, 345–355.
- (8) (a) Denney, M. C.; Smythe, N. A.; Cetto, K. L.; Kemp, R. A.; Goldberg, K. I. *J. Am. Chem. Soc.* **2006**, *128*, 2508–2509. (b) Konnick, M. M.; Stahl, S. S. *J. Am. Chem. Soc.* **2008**, *130*, 5753–5762. (c) Boisvert, L.; Denney, M. C.; Hanson, S. K.; Goldberg, K. I. *J. Am. Chem. Soc.* **2009**, *131*, 15802–15814. (d) Szajna-Fuller, E.; Bakac, A. *Inorg. Chem.* **2010**, *49*, 781–785. (e) Decharin, N.; Popp, B. V.; Stahl, S. S. *J. Am. Chem. Soc.* **2011**, *133*, 13268–13271.
- (9) (a) Lewiński, J.; Zachara, J.; Gos, P.; Grabska, E.; Kopec, T.; Madura, I.; Marciniak, W.; Prowotorow, I. *Chem.–Eur. J.* **2000**, *6*, 3215–3227. (b) Lewiński, J.; Marciniak, W.;

Lipkowski, J.; Justyniak, I. *J. Am. Chem. Soc.* **2003**, *125*, 12698–12699. (c) Lewiński, J.; Śliwiński, W.; Dranka, M.; Justyniak, I.; Lipkowski, J. *Angew. Chem., Int. Ed.* **2006**, *45*, 4826–4829.

(10) (a) Lewiński, J.; Suwala, K.; Kubisiak, M.; Ochal, Z.; Justyniak, I.; Lipkowski, J. *Angew. Chem., Int. Ed.* **2008**, *47*, 7888–7891. (b) Lewiński, J.; Suwala, K.; Kaczorowski, T.; Galezowski, M.; Gryko, D. T.; Justyniak, I.; Lipkowski, J. *Chem. Commun.* **2009**, 215–217.

(11) Hollingsworth, N.; Johnson, A. L.; Kingsley, A.; Kociok-Köhn, G.; Molloy, K. C. *Organometallics* **2010**, *29*, 3318–3326.

(12) (a) Han, R.; Parkin, G. *J. Am. Chem. Soc.* **1990**, *112*, 3662–3663. (b) Han, R.; Parkin, G. *J. Am. Chem. Soc.* **1992**, *114*, 748–757. (c) Bailey, P. J.; Coxall, R. A.; Dick, C. M.; Fabre, S.; Henderson, L. C.; Herber, C.; Liddle, S. T.; Loroño-González, D.; Parkin, A.; Parsons, S. *Chem.–Eur. J.* **2003**, *9*, 4820–4828.

(13) Lewiński, J.; Ochal, Z.; Bojarski, E.; Tratkiewicz, E.; Justyniak, I.; Lipkowski, J. *Angew. Chem., Int. Ed.* **2003**, *42*, 4643–4646.

(14) Barron, A. R. *Chem. Soc. Rev.* **1993**, *22*, 93–99.

(15) Cleaver, W. M.; Barron, A. R. *J. Am. Chem. Soc.* **1989**, *111*, 8967–8969.

(16) Gorrell, I. B.; Looney, A.; Parkin, G. *J. Chem. Soc., Chem. Commun.* **1990**, 220–222.

(17) Uhl, W.; Jana, B. *Chem.–Eur. J.* **2008**, *14*, 3067–3071.

(18) (a) Kitajima, N.; Katayama, T.; Fujisawa, K.; Iwata, Y.; Moro-oka, Y. *J. Am. Chem. Soc.* **1993**, *115*, 7872–7873. (b) Hikichi, S.; Komatsuzaki, H.; Akita, M.; Moro-oka, Y. *J. Am. Chem. Soc.* **1998**, *120*, 4699–4710. (c) Komatsuzaki, H.; Sakamoto, N.; Satoh, M.; Hikichi, S.; Akita, M.; Moro-oka, Y. *Inorg. Chem.* **1998**, *37*, 6554–6555. (d) Hikichi, S.; Okuda, H.; Ohzu, Y.; Akita, M. *Angew. Chem., Int. Ed.* **2009**, *48*, 188–191. (e) Hikichi, S.; Kobayashi, C.; Yoshizawa, M.; Akita, M. *Chem. Asian J.* **2010**, *5*, 2086–2092.

- (19) (a) Mukherjee, D.; Ellern, A.; Sadow, A. D. *J. Am. Chem. Soc.* **2010**, *132*, 7582–7583. (b) Mukherjee, D.; Thompson, R. R.; Ellern, A.; Sadow, A. D. *ACS Catal.* **2011**, *1*, 698–702.
- (20) (a) Ho, H.-A.; Dunne, J. F.; Ellern, A.; Sadow, A. D. *Organometallics* **2010**, *29*, 4105–4114. (b) Dunne, J. F.; Su, J.; Ellern, A.; Sadow, A. D. *Organometallics* **2008**, *27*, 2399–2401.
- (21) Looney, A.; Han, R.; Gorrell, I. B.; Cornebise, M.; Yoon, K.; Parkin, G.; Rheingold, A. L. *Organometallics* **1995**, *14*, 274–288.
- (22) Cordero, B.; Gómez, V.; Platero-Prats, A. E.; Revés, M.; Echeverría, J.; Cremades, E.; Barragán, F.; Alvarez, S. *Dalton Trans* **2008**, 2832–2838.
- (23) Jackson, R. L. *Chem. Phys. Lett.* **1989**, *163*, 315–322.
- (24) (a) Armentrout, P. B.; Beauchamp, J. L. *Acc. Chem. Res.* **1989**, *22*, 315–321. (b) Georgiadis, R.; Armentrout, P. B. *J. Am. Chem. Soc.* **1986**, *108*, 2119–2126.
- (25) van Asselt, A.; Santarsiero, B. D.; Bercaw, J. E. *J. Am. Chem. Soc.* **1986**, *108*, 8291–8293.
- (26) Davies, A. G. *Tetrahedron* **2007**, *63*, 10385–10405.
- (27) (a) DiPasquale, A. G.; Kaminsky, W.; Mayer, J. M. *J. Am. Chem. Soc.* **2002**, *124*, 14534–14535. (b) DiPasquale, A. G.; Hrovat, D. A.; Mayer, J. M. *Organometallics* **2006**, *25*, 915–924.
- (28) Suzuki, H.; Matsuura, S.; Moro-oka, Y.; Ikawa, T. *J. Organomet. Chem.* **1985**, *286*, 247–258.
- (29) Conte, V.; Bortolini, O. In *The Chemistry of Peroxides*; Wiley: Chichester, U.K., 2006; pp 1053–1128.
- (30) (a) Espenson, J. H. *Chemical kinetics and reaction mechanisms*; 2nd ed.; McGraw-Hill: New York, 1995. (b) Taylor, J. R. *An introduction to error analysis: the study of*

uncertainties in physical measurements; 2nd ed.; University Science Books: Sausalito, CA, 1997. (c) Morse, P. M.; Spencer, M. D.; Wilson, S. R.; Girolami, G. S. *Organometallics* **1994**, *13*, 1646–1655.

(31) (a) Tan, H.; Yoshikawa, A.; Gordon, M. S.; Espenson, J. H. *Organometallics* **1999**, *18*, 4753–4757. (b) Adam, W.; Mitchell, C. M.; Saha-Müller, C. R.; Weichold, O. *J. Am. Chem. Soc.* **1999**, *121*, 2097–2103.

(32) (a) Mimoun, H.; de Saint Laumer, J. Y.; Giannini, L.; Scopelliti, R.; Floriani, C. *J. Am. Chem. Soc.* **1999**, *121*, 6158–6166. (b) Mimoun, H. *J. Org. Chem.* **1999**, *64*, 2582–2589.

(33) Marciniec, B. *Hydrosilylation: a comprehensive review on recent advances*; Springer: Berlin, Germany, 2009.

(34) Klement, I.; Knochel, P. *Synlett* **1995**, 1113–1114.

(35) Woo, H.-G.; Heyn, R. H.; Tilley, T. D. *J. Am. Chem. Soc.* **1992**, *114*, 5698–5707.

(36) (a) Gountchev, T. I.; Tilley, T. D. *Organometallics* **1999**, *18*, 5661–5667. (b) Sadow, A. D.; Tilley, T. D. *J. Am. Chem. Soc.* **2005**, *127*, 643–656.

(37) Dunne, J. F.; Neal, S. R.; Engelkemier, J.; Ellern, A.; Sadow, A. D. *J. Am. Chem. Soc.* **2011**, *133*, 16782–16785.

(38) A reviewer pointed out that reactions with small activation enthalpies can have small or large isotope effects.

(39) Look, J. L.; Wick, D. D.; Mayer, J. M.; Goldberg, K. I. *Inorg. Chem.* **2009**, *48*, 1356–1369.

(40) Côté, A.; Charette, A. B. *J. Am. Chem. Soc.* **2008**, *130*, 2771–2773.

Experimental and other supporting informations.

General Procedures.

All reactions were performed under a dry argon atmosphere using standard Schlenk techniques or under a nitrogen atmosphere in a glovebox, unless otherwise indicated. Benzene, toluene, pentane, diethyl ether, and tetrahydrofuran were dried and deoxygenated using an IT PureSolv system. Benzene-*d*₆ and toluene-*d*₈ were heated to reflux over Na/K alloy and vacuum-transferred. Dichloromethane-*d*₂ was vacuum transferred from CaH₂. To^MZnMe (**1**),^{19b} To^MZnH (**13**),^{19a} H[To^M],^{20b} Tl[To^M],^{20a} and dialkylzincs were synthesized according to literature procedures.⁴⁰ Grignard reagents were purchased from Sigma-Aldrich and transferred to flasks equipped with re-sealable Teflon valves for storage. *t*-BuOOH (5.5 M in decane), PhMe₂COOH (80% technical grade), and AIBN were purchased from Sigma-Aldrich and stored inside glove box freezer at – 30 °C. Benzyldimethylsilane was purchased from Gelest. Benzyldimethylsilane-*d*₁ was synthesized by reduction of benzyldimethylchlorosilane with LiAlD₄.

¹H, ¹³C{¹H}, ¹¹B, and ¹⁷O NMR spectra were collected on a Bruker DRX400 spectrometer or an Avance II 600 spectrometer. ¹⁵N chemical shifts were determined by ¹H-¹⁵N HMBC experiments on a Bruker Avance II 700 spectrometer with a Bruker Z-gradient inverse TXI ¹H/¹³C/¹⁵N 5mm cryoprobe; ¹⁵N chemical shifts were originally referenced to an external liquid NH₃ standard and recalculated to the CH₃NO₂ chemical shift scale by adding – 381.9 ppm. Elemental analyses were performed using a Perkin-Elmer 2400 Series II CHN/S in the Iowa State Chemical Instrumentation Facility.

Caution! High-pressure glass apparatuses, reactions of oxygen and reduced compounds, and

peroxide-containing materials must be handled with care. Isolated alkylperoxide compounds **8-12** were tested for possible explosive properties, and they did not ignite with attempted initiation under thermal, physical, or electrical stress. Regardless, only small quantities of alkylperoxides were prepared at a single instance. Thick-walled NMR tubes equipped with J. Young-style re-sealable Teflon valves (pressured to 100 psi with O₂) were obtained from Wilmad-Labglass and attached to a high-pressure steel manifold through commercial Swagelock fittings.^{8c} The tubes were handled in protective jackets for safety concerns. Due to the potentially pyrophoric and explosive nature of silylalkylperoxides,²⁶ the BnMe₂SiOOR (R = Et, n-C₃H₇, i-C₃H₇ and t-Bu) species were not isolated; these compounds were characterized in solution and compared with the corresponding BnMe₂SiOR using ¹H, ¹³C{¹H} and ²⁹Si NMR spectroscopy.

Synthetic Methods.

To^MZnEt (2). Diethylzinc (73.2 mL, 0.0882 g, 0.714 mmol) was added to a solution of HTo^M (0.274 g, 0.714 mmol) in 10 mL of benzene in a dropwise fashion. The solution was stirred for 12 h at room temperature, and then the volatiles were evaporated under reduced pressure. The resulting white solid was washed with pentane to provide analytically pure To^MZnEt (2) as a crystalline white solid (0.304 g, 0.638 mmol, 89.3%). X-ray quality crystals were obtained from a concentrated toluene solution that was allowed to stand at -30 °C. ¹H NMR (400 MHz, benzene-*d*₆): δ 0.68 (q, 2 H, ZnCH₂CH₃), 1.02 (s, 18 H, CNCMe₂CH₂O), 1.81 (t, 3 H, ZnCH₂CH₃), 3.48 (s, 6 H, CNCMe₂CH₂O), 7.35 (t, ³J_{HH} = 4.0 Hz, 1 H, *para*-C₆H₅), 7.53 (t, ³J_{HH} = 4.0 Hz, 2 H, *meta*-C₆H₅), 8.34 (d, ³J_{HH} = 4.0 Hz, 2 H, *ortho*-C₆H₅). ¹³C{¹H} NMR (175 MHz, benzene-*d*₆): δ -2.08 (ZnCH₂CH₃), 15.36 (ZnCH₂CH₃), 28.33

(CNCMe₂CH₂O), 65.61 (CNCMe₂CH₂O), 80.78 (CNCMe₂CH₂O), 126.19 (*para*-C₆H₅), 127.21 (*meta*-C₆H₅), 136.48 (*ortho*-C₆H₅), 142.92 (br, *ipso*-C₆H₅), 190.02 (br, CNCMe₂CH₂O). ¹¹B NMR (128 MHz, benzene-*d*₆): δ -17.3. ¹⁵N{¹H} NMR: d -155.5. IR (KBr, cm⁻¹): 2969 (s), 2929 (m), 2896 (m), 1603 (s, ν_{CN}), 1461 (m), 1385 (m), 1366 (m), 1350 (m), 1268 (s), 1193 (s), 1159 (s), 953 (s), 892 (w), 741 (m), 706 (s). Anal. Calcd. for C₂₃H₃₄BN₃O₃Zn: C, 57.95; H, 7.19; N, 8.81. Found: C, 57.77; H, 7.10; N, 8.82. mp 167-170 °C (dec).

To^MZn(*n*-C₃H₇) (3). A suspension of Zn(OMe)₂ (0.174 g, 1.36 mmol) in Et₂O (20 mL) was cooled to 0 °C. *n*-C₃H₇MgBr (1.4 mL, 2 M in Et₂O) was added, and the resulting mixture was allowed to warm to room temperature and stirred for 1 h. The mixture was filtered to remove the insoluble magnesium salts from (*n*-C₃H₇)₂Zn, and the solution was added to Tl[To^M] (0.200 g, 0.341 mmol). Immediately, a black mixture formed. This mixture was stirred for 20 min., the volatile materials were evaporated under reduced pressure, and the residue was extracted with benzene (10 mL). Evaporation of the colorless extracts provided a white solid that was washed with pentane (3 × 5 mL) and dried under vacuum. Analytically pure To^MZn(*n*-C₃H₇) (0.143 g, 0.291 mmol, 85.3%) was obtained as a white crystalline solid. X-ray quality crystals were grown by slow diffusion of pentane into a concentrated toluene solution standing at -30 °C. ¹H NMR (400 MHz, benzene-*d*₆): δ 0.70 (m, 2 H, ZnCH₂CH₂CH₃), 1.02 (s, 18 H, CNCMe₂CH₂O), 1.46 (t, ³J_{HH} = 7.2 Hz, 3 H, ZnCH₂CH₂CH₃), 2.08 (m, 2 H, ZnCH₂CH₂CH₃), 3.47 (s, 6 H, CNCMe₂CH₂O), 7.37 (t, ³J_{HH} = 6.8 Hz, 1 H, *para*-C₆H₅), 7.56 (t, ³J_{HH} = 7.6 Hz, 2 H, *meta*-C₆H₅), 8.36 (d, ³J_{HH} = 7.2 Hz, 2 H, *ortho*-C₆H₅). ¹³C{¹H} NMR (175 MHz, benzene-*d*₆): δ 10.92 (ZnCH₂CH₂CH₃), 23.29 (ZnCH₂CH₂CH₃),

24.93 (ZnCH₂CH₂CH₃), 28.33 (CNCMe₂CH₂O), 65.67 (CNCMe₂CH₂O), 80.78 (CNCMe₂CH₂O), 126.22 (*para*-C₆H₅), 127.24 (*meta*-C₆H₅), 136.49 (*ortho*-C₆H₅), 146.10 (br, *ipso*-C₆H₅), 190.32 (br, CNCMe₂CH₂O). ¹¹B NMR (128 MHz, benzene-*d*₆): δ -17.3. ¹⁵N{¹H} NMR (71 MHz, benzene-*d*₆): δ -155.8. IR (KBr, cm⁻¹): 3074 (w), 3045 (w), 2966 (s), 2935 (s), 2825 (m), 1601 (s, ν_{CN}), 1495 (w), 1462 (s), 1432 (w), 1384 (m), 1365 (m), 1354 (m), 1272 (s), 1251 (w), 1195 (s), 1161 (s), 957 (s), 896 (w), 867 (w), 841 (w), 816 (m), 746 (s), 703 (s), 668 (s). Anal. Calcd. for C₂₄H₃₆BN₃O₃Zn: C, 58.74; H, 7.39; N, 8.56. Found: C, 58.98; H, 7.59; N, 8.43. Mp 180-184 °C (dec).

To^MZn(*i*-C₃H₇) (4). A solution of (*i*-C₃H₇)₂Zn was prepared following the procedure for (*n*-C₃H₇)₂Zn above with Zn(OMe)₂ (0.850 g, 6.67 mmol) and *i*-C₃H₇MgBr (3.2 mL, 2 M in Et₂O). The (*i*-C₃H₇)₂Zn was added to Tl[To^M] (1.215 g, 2.071 mmol) in benzene (10 mL) to give a black mixture that was allowed to stir for 20 min. To^MZn(*i*-C₃H₇) (4; 0.895 g, 1.82 mmol, 88.1%) was isolated as described for 2. ¹H NMR (400 MHz, benzene-*d*₆): δ 1.02 (s, 18 H, CNCMe₂CH₂O), 1.04 (m, ³J_{HH} = 7.7 Hz, 1 H, ZnCHMe₂), 1.83 (d, ³J_{HH} = 7.6 Hz, 6 H, ZnCHMe₂), 3.45 (s, 6 H, CNCMe₂CH₂O), 7.37 (t, ³J_{HH} = 4.2 Hz, 1 H, *para*-C₆H₅), 7.56 (t, ³J_{HH} = 7.4 Hz, 2 H, *meta*-C₆H₅), 8.35 (d, ³J_{HH} = 7.5 Hz, 2 H, *ortho*-C₆H₅). ¹³C{¹H} NMR (175 MHz, benzene-*d*₆): δ 10.08 (ZnCHMe₂), 26.74 (ZnCHMe₂), 28.31 (CNCMe₂CH₂O), 65.68 (CNCMe₂CH₂O), 80.22 (CNCMe₂CH₂O), 126.21 (*para*-C₆H₅), 127.21 (*meta*-C₆H₅), 136.52 (*ortho*-C₆H₅), 143.16 (br, *ipso*-C₆H₅), 190.54 (br, CNCMe₂CH₂O). ¹¹B NMR (128 MHz, benzene-*d*₆): δ -17.3. ¹⁵N{¹H} NMR (71 MHz, benzene-*d*₆): δ -156.0. IR (KBr, cm⁻¹): 3077 (m), 3047 (m), 2965 (s), 2896 (s), 2796 (w), 1602 (s, ν_{CN}), 1495 (w), 1462 (s), 1432 (w), 1384 (m), 1366 (m), 1352 (m), 1308 (w), 1271 (s), 1250 (w), 1195 (s), 1161 (s), 1049 (m),

1019 (m), 954 (s), 897 (w), 841 (w), 817 (m), 744 (s), 704 (s), 666 (s). Anal. Calcd. for $C_{24}H_{36}BN_3O_3Zn$: C, 58.74; H, 7.39; N, 8.56. Found: C, 59.00; H, 7.26; N, 8.53. Mp: 165-170 °C (dec).

To^MZn(*t*-Bu) (5). A solution of (*t*-Bu)₂Zn was prepared following the procedure for (*n*-C₃H₇)₂Zn above with Zn(OMe)₂ (0.661 g, 5.186 mmol) and *t*-BuMgBr (5.1 mL, 2 M in Et₂O). The (*t*-Bu)₂Zn was added to TI[To^M] (0.950 g, 1.62 mmol) in benzene (10 mL) to give a black mixture that was allowed to stir for 20 min. To^MZn(*t*-Bu) (**5**; 0.763 g, 1.51 mmol, 93.3%) was isolated as described for **2**. X-ray quality crystals were grown from slow pentane diffusion into a concentrated toluene solution of **5** at -30 °C. ¹H NMR (400 MHz, benzene-*d*₆): δ 1.04 (s, 18 H, CNCMe₂CH₂O), 1.59 (s, 9 H, ZnCMe₃), 3.43 (s, 6 H, CNCMe₂CH₂O), 7.37 (t, ³J_{HH} = 7.6 Hz, 1 H, *para*-C₆H₅), 7.56 (t, ³J_{HH} = 7.0 Hz, 2 H, *meta*-C₆H₅), 8.36 (d, ³J_{HH} = 7.2 Hz, 2 H, *ortho*-C₆H₅). ¹³C{¹H} NMR (175 MHz, benzene-*d*₆): δ 17.25 (ZnCMe₃), 28.26 (CNCMe₂CH₂O), 35.82 (ZnCMe₃), 65.92 (CNCMe₂CH₂O), 80.80 (CNCMe₂CH₂O), 126.13 (*para*-C₆H₅), 127.13 (*meta*-C₆H₅), 136.58 (*ortho*-C₆H₅), 143.32 (br, *ipso*-C₆H₅), 190.49 (br, CNCMe₂CH₂O). ¹¹B NMR (128 MHz, benzene-*d*₆): δ -18.6. ¹⁵N{¹H} NMR (71 MHz, benzene-*d*₆): δ -155.7. IR (KBr, cm⁻¹): 3078 (w), 3039 (w), 2968 (s), 2937 (s), 2805 (s), 2746 (w), 2685 (w), 1589 (s, ν_{CN}), 1495 (w), 1461 (s), 1388 (s), 1353 (s), 1274 (s), 1200 (s), 1180 (s), 1158 (s), 1022 (w), 960 (s), 893 (m), 840 (m), 811 (s), 750 (s), 707 (s), 665 (s). Anal. Calcd. for C₂₅H₃₈BN₃O₃Zn: C, 59.48; H, 7.59; N, 8.32. Found: C, 59.56; H, 7.43; N, 8.32. Mp 127-130 °C (dec).

To^MZnPh (6). To^MZnCl (0.206 g, 0.426 mmol) and PhLi (0.036 g, 0.430 mmol) were dissolved in THF (12 mL) and stirred for 8 h at ambient temperature. A white solid was

obtained by evaporation of the volatile materials, and the residue was extracted with 12 mL of benzene. Evaporation of the benzene, followed by pentane washes (3 × 5 mL) and drying under vacuum provided crystalline, analytically pure $\text{To}^{\text{M}}\text{ZnPh}$ (0.207 g, 0.394 mmol, 94.5%). X-ray quality single crystals were grown from a concentrated toluene solution of $\text{To}^{\text{M}}\text{ZnPh}$ at $-30\text{ }^{\circ}\text{C}$. ^1H NMR (400 MHz, benzene- d_6): δ 1.03 (s, 18 H, $\text{CNCMe}_2\text{CH}_2\text{O}$), 3.46 (s, 6 H, $\text{CNCMe}_2\text{CH}_2\text{O}$), 7.38 (m, 1 H, *para*- C_6H_5), 7.38 (m, 1 H, *para*- ZnC_6H_5), 7.51 (t, $^3J_{\text{HH}} = 7.2\text{ Hz}$, 2 H, *meta*- C_6H_5), 7.58 (dt, $^3J_{\text{HH}} = 3.2\text{ Hz}$, $^3J_{\text{HH}} = 7.2\text{ Hz}$, 2 H, *meta*- C_6H_5), 8.09 (dd, $^3J_{\text{HH}} = 7.6\text{ Hz}$, $^3J_{\text{HH}} = 4.0\text{ Hz}$, 2 H, *ortho*- ZnC_6H_5), 8.38 (d, $^3J_{\text{HH}} = 4.0\text{ Hz}$, 2 H, *ortho*- C_6H_5). $^{13}\text{C}\{^1\text{H}\}$ NMR (175 MHz, benzene- d_6): δ 28.40 ($\text{CNCMe}_2\text{CH}_2\text{O}$), 65.86 ($\text{CNCMe}_2\text{CH}_2\text{O}$), 81.06 ($\text{CNCMe}_2\text{CH}_2\text{O}$), 126.32 (*para*- C_6H_5), 126.66 (*para*- C_6H_5), 127.28 (*meta*- C_6H_5), 127.95 (*meta*- ZnC_6H_5), 136.49 (*ortho*- C_6H_5), 140.41 (*ortho*- ZnC_6H_5), 142.52 (br, *ipso*- C_6H_5), 154.40 (*ipso*- ZnC_6H_5), 190.52 (br, $\text{CNCMe}_2\text{CH}_2\text{O}$). ^{11}B NMR (128 MHz, benzene- d_6): δ -18.1. $^{15}\text{N}\{^1\text{H}\}$ NMR: δ -157.4. IR (KBr, cm^{-1}): 3048 (w), 2966 (m), 2928 (w), 2891 (w), 1594 (s, ν_{CN}), 1460 (m), 1389 (m), 1369 (m), 1352 (m), 1275 (s), 1196(s), 1158 (m), 1071 (w), 948 (m), 895 (w), 842 (w), 817 (m), 758 (s), 746 (m), 727 (s), 704 (s). $\text{C}_{28}\text{H}_{36}\text{BN}_3\text{O}_3\text{Zn}$: C, 61.80; H, 6.53; N, 8.01. Found: C, 61.25; H, 6.30; N, 8.01. Mp: 197-200 $^{\circ}\text{C}$ (dec).

$\text{To}^{\text{M}}\text{ZnBn}$ (7). A solution of Bn_2Zn was prepared following the procedure for $(n\text{-C}_3\text{H}_7)_2\text{Zn}$ above with $\text{Zn}(\text{OMe})_2$ (0.623 g, 4.89 mmol) and BnMgBr (4.8 mL, 2 M in Et_2O). The Bn_2Zn was added to $\text{Ti}[\text{To}^{\text{M}}]$ (1.530 g, 2.608 mmol) in benzene (10 mL) to give a black mixture that was allowed to stir for 20 min. $\text{To}^{\text{M}}\text{ZnBn}$ (7; 1.305 g, 2.422 mmol, 92.9%) was isolated as described for **2**. X-ray quality crystals were grown from slow pentane diffusion into a

concentrated toluene solution of **7** at $-30\text{ }^{\circ}\text{C}$. ^1H NMR (400 MHz, benzene- d_6): δ 0.93 (s, 18 H, $\text{CNCMe}_2\text{CH}_2\text{O}$), 2.32 (s, 2 H, $\text{ZnCH}_2\text{C}_6\text{H}_5$) 3.43 (s, 6 H, $\text{CNCMe}_2\text{CH}_2\text{O}$), 6.95 (t, $^3J_{\text{HH}} = 7.6$ Hz, 1 H, *para*- $\text{ZnCH}_2\text{C}_6\text{H}_5$), 7.26 (t, $^3J_{\text{HH}} = 7.6$ Hz, 2 H, *meta*- $\text{ZnCH}_2\text{C}_6\text{H}_5$), 7.36 (m, 2 H, *ortho*- $\text{ZnCH}_2\text{C}_6\text{H}_5$), 7.36 (m, 1 H, *para*- C_6H_5), 7.54 (t, $^3J_{\text{HH}} = 7.6$ Hz, 2 H, *meta*- C_6H_5), 8.31 (d, $^3J_{\text{HH}} = 7.6$ Hz, 2 H, *ortho*- C_6H_5). $^{13}\text{C}\{^1\text{H}\}$ NMR (175 MHz, benzene- d_6): δ 19.11 (ZnCH_2Ph), 28.20 ($\text{CNCMe}_2\text{CH}_2\text{O}$), 65.67 ($\text{CNCMe}_2\text{CH}_2\text{O}$), 80.94 ($\text{CNCMe}_2\text{CH}_2\text{O}$), 121.03 (*para*- $\text{ZnCH}_2\text{C}_6\text{H}_5$) 126.30 (*para*- C_6H_5), 126.91 (*meta*- $\text{ZnCH}_2\text{C}_6\text{H}_5$), 127.25 (*meta*- C_6H_5), 128.94 (*ortho*- $\text{ZnCH}_2\text{C}_6\text{H}_5$), 136.44 (*ortho*- C_6H_5), 142.76 (br, *ipso*- C_6H_5), 152.90 (*ipso*- $\text{ZnCH}_2\text{C}_6\text{H}_5$), 190.33 (br, $\text{CNCMe}_2\text{CH}_2\text{O}$). ^{11}B NMR (128 MHz, benzene- d_6): δ -17.3. $^{15}\text{N}\{^1\text{H}\}$ NMR (71 MHz, benzene- d_6): δ -157.3. IR (KBr, cm^{-1}): 3071 (w), 3013 (w), 2966 (m), 2927 (w), 2889 (w), 1594 (s, ν_{CN}), 1487 (s), 1461 (s), 1435 (w), 1385 (m), 1366 (m), 1353 (m), 1273 (s), 1196 (s), 1163 (s), 1051 (s), 996 (w), 956 (s), 896 (w), 841 (w), 817 (m), 800 (m), 748 (s), 709 (s). Anal. Calcd. for $\text{C}_{28}\text{H}_{36}\text{BN}_3\text{O}_3\text{Zn}$: C, 62.42; H, 6.73; N, 7.80. Found: C, 62.09; H, 6.74; N, 7.77. Mp: 194-197 $^{\circ}\text{C}$.

To^MZnOOEt (8). A 100 mL re-sealable Teflon-valved flask was charged with a benzene solution (20 mL) of $\text{To}^{\text{M}}\text{ZnEt}$ (0.450 g, 0.944 mmol). The solution was degased with freeze-pump-thaw cycles, placed under an atmosphere of O_2 , and then sealed. The solution was heated at $60\text{ }^{\circ}\text{C}$ for 12 h and then allowed to cool to room temperature. The volatile materials were removed under reduced pressure. The resulting white residue was washed with pentane (3×5 mL) and dried under vacuum yielding analytically pure $\text{To}^{\text{M}}\text{ZnOOEt}$ (**8**; 0.436 g, 0.857 mmol, 90.8%). X-ray quality crystals were grown by allowing pentane to slowly diffuse into a saturated toluene solution of **8** cooled to $-30\text{ }^{\circ}\text{C}$. ^1H NMR (400 MHz, benzene- d_6): δ 1.14 (s, 18 H, $\text{CNCMe}_2\text{CH}_2\text{O}$), 1.40 (t, $^3J_{\text{HH}} = 6.8$ Hz, 3 H, $\text{ZnOOCH}_2\text{CH}_3$), 3.48 (s, 6

H, CNCMe₂CH₂O), 4.34 (q, ³J_{HH} = 6.8 Hz, 2 H, ZnOOCH₂CH₃), 7.37 (t, ³J_{HH} = 7.2 Hz, 1 H, *para*-C₆H₅), 7.55 (t, ³J_{HH} = 7.6 Hz, 2 H, *meta*-C₆H₅), 8.32 (d, ³J_{HH} = 7.2 Hz, 2 H, *ortho*-C₆H₅). ¹³C{¹H} NMR (175 HMz, benzene-*d*₆): δ 14.85 (ZnOOCH₂CH₃), 28.15 (CNCMe₂CH₂O), 65.67 (CNCMe₂CH₂O), 71.94 (ZnOOCH₂CH₃), 81.19 (CNCMe₂CH₂O), 126.47 (*para*-C₆H₅), 127.35 (*meta*-C₆H₅), 136.36 (*ortho*-C₆H₅), 142.03 (br, *ipso*-C₆H₅), 190.66 (br, CNCMe₂CH₂O). ¹¹B NMR (128 MHz, benzene-*d*₆): δ -17.1. ¹⁵N{¹H} NMR (71 MHz, benzene-*d*₆): δ -159.2. ¹⁷O NMR (81 MHz, benzene-*d*₆): δ 319 (ZnOO(CH₂CH₃)], 169 (ZnOO(CH₂CH₃)). IR (KBr, cm⁻¹): 3083 (w), 3042 (w), 2969 (m), 2929 (w), 2885 (w), 1592 (s, ν_{CN}), 1495 (w), 1462 (s), 1435 (w), 1387 (m), 1368 (m), 1351 (m), 127 (s), 1198 (s), 1198 (s), 1164 (s), 963 (s), 898 (w), 819 (w), 744(w). Anal. Calcd. for C₂₃H₃₄BN₃O₅Zn: C, 54.30; H, 6.73; N, 8.26. Found: C, 54.52; H, 6.74; N, 8.12. Mp: 208-211 °C.

To^MZnOO(*n*-C₃H₇) (9). A 25 mL re-sealable Teflon-valved flask was charged with To^MZn(*n*-C₃H₇) (3; 0.250 g, 0.509 mmol) dissolved benzene (12 mL). The solution was degassed with freeze-pump-thaw cycles. O₂ (1 atm) was added, the solution was stirred for 12 h at 60 °C, and then the reaction mixture was allowed to cool to room temperature. The volatile material were evaporated under reduced pressure, and the resulting white residue was washed with pentane (3 × 5 mL) and dried under vacuum, yielding analytically pure To^MZnOO(*n*-C₃H₇) (9; 0.230 g, 0.440 mmol, 86.4%) as a white crystalline solid. X-ray quality single crystals were grown by vapor diffusion of pentane into a concentrated toluene solution of 9 standing at -30 °C. ¹H NMR (400 MHz, benzene-*d*₆): δ 1.04 (t, ³J_{HH} = 7.2 Hz, 3 H, ZnOOCH₂CH₂CH₃), 1.15 (s, 18 H, CNCMe₂CH₂O), 1.91 (m, 2 H, ZnOOCH₂CH₂CH₃), 3.48 (s, 6 H, CNCMe₂CH₂O), 4.28 (t, ³J_{HH} = 6.4 Hz, 2 H, ZnOOCH₂CH₂CH₃), 7.36 (t, ³J_{HH} =

7.6 Hz, 1 H, *para*-C₆H₅), 7.55 (t, ³J_{HH} = 7.6 Hz, 2 H, *meta*-C₆H₅), 8.32 (d, ³J_{HH} = 7.6 Hz, 2 H, *ortho*-C₆H₅). ¹³C{¹H} NMR (175 HMz, benzene-*d*₆): δ 11.72 (ZnOOCH₂CH₂CH₃), 21.76 (ZnOOCH₂CH₂CH₃), 28.16 (CNCMe₂CH₂O), 65.67 (CNCMe₂CH₂O), 78.67 (ZnOOCH₂CH₂CH₃), 81.19 (CNCMe₂CH₂O), 126.47 (*para*-C₆H₅), 127.36 (*meta*-C₆H₅), 136.35 (*ortho*-C₆H₅), 142.07 (br, *ipso*-C₆H₅), 190.56 (br, CNCMe₂CH₂O). ¹¹B NMR (128 MHz, benzene-*d*₆): δ -17.1. ¹⁵N{¹H} NMR (71 MHz, benzene-*d*₆): δ -160. ¹⁷O NMR (81 MHz, benzene-*d*₆): δ 322 (ZnOOCH₂CH₂CH₃), 167 (ZnOOCH₂CH₂CH₃). IR (KBr, cm⁻¹): 3069 (w), 2965 (m), 2923 (w), 2878 (w), 1578 (s, n_{CN}), 1492 (w), 1463 (s), 1432 (w), 1385 (m), 1369 (m), 1279 (m), 1262 (m), 1198 (m), 1198 (m), 1161 (m), 1000 (m), 970 (m). Anal. Calcd. for C₂₄H₃₆BN₃O₅Zn: C, 55.14; H, 6.94; N, 8.04. Found: C, 54.91; H, 6.78; N, 8.12. Mp: 158-160 °C.

To^MZnOO(*i*-C₃H₇) (10). The procedure described above for To^MZnOO(*n*-C₃H₇) was used, starting from To^MZn(*i*-C₃H₇) (**4**; 0.310 g, 0.632 mmol) to afford **10** (0.291 g, 0.557 mmol, 88.1%). ¹H NMR (300 MHz, benzene-*d*₆): δ 1.15 (s, 18 H, CNCMe₂CH₂O), 1.47 (d, ³J_{HH} = 6.3 Hz, 6 H, ZnOOCHMe₂), 3.47 (s, 6 H, CNCMe₂CH₂O), 4.49 (m, ³J_{HH} = 6 Hz, 1 H, ZnOOCHMe₂), 7.36 (t, ³J_{HH} = 7.5 Hz, 1 H, *para*-C₆H₅), 7.55 (t, ³J_{HH} = 7.5 Hz, 2 H, *meta*-C₆H₅), 8.32 (d, ³J_{HH} = 7.5 Hz, 2 H, *ortho*-C₆H₅). ¹³C{¹H} NMR (175 HMz, benzene-*d*₆): δ 21.95 (ZnOOCHMe₂), 28.16 (CNCMe₂CH₂O), 65.69 (CNCMe₂CH₂O), 76.32 (ZnOOCHMe₂), 81.20 (CNCMe₂CH₂O), 126.46 (*para*-C₆H₅), 127.35 (*meta*-C₆H₅), 136.36 (*ortho*-C₆H₅), 144.41 (br, *ipso*-C₆H₅), 190.59 (br, CNCMe₂CH₂O). ¹¹B NMR (128 MHz, benzene-*d*₆): δ -17.3. ¹⁵N{¹H} NMR (71 MHz, benzene-*d*₆): δ -159.2. ¹⁷O NMR (81 MHz, benzene-*d*₆): δ 304 (ZnOOCHMe₂), 193 (ZnOOCHMe₂). IR (KBr, cm⁻¹): 3069 (w), 3044 (w),

2968 (s), 2929 (w), 2896 (w), 2870 (w), 1579 (s, ν_{CN}), 1490 (w), 1462 (s), 1433 (m), 1388 (w), 1368 (m), 1279 (s), 1255 (m), 1197 (s), 1160 (s), 1117 (w), 1001 (s), 970 (s), 943 (m), 898 (w), 877 (w), 847 (w), 817 (w), 733 (m), 708 (m). Anal. Calcd. for $\text{C}_{24}\text{H}_{36}\text{BN}_3\text{O}_5\text{Zn}$: C, 55.14; H, 6.94; N, 8.04. Found: C, 54.83; H, 6.71; N, 8.02. Mp: 165-167 °C.

To^MZnOO(*t*-Bu) (11). A solution of To^MZnH (0.550 g, 1.226 mmol) in 12 mL of benzene was treated with *t*-BuOOH (0.23 mL, 5.5 M in decane). The mixture was allowed to stir at room temperature for 1 h. The solvent was then evaporated to obtain a white residue that was washed with pentane (3 × 5 mL) and dried under vacuum affording crystalline, analytically pure 11 (0.549 g, 1.023 mmol, 83.4% yield) as a white solid. X-ray quality single crystals were grown from a concentrated toluene solution of To^MZnOO(*t*-Bu) at -30 °C. ¹H NMR (400 MHz, benzene-*d*₆): δ 1.15 (s, 18 H, CNCMe₂CH₂O), 1.59 (s, 9 H, ZnOOCMe₃), 3.48 (s, 6 H, CNCMe₂CH₂O), 7.37 (t, ³J_{HH} = 7.4 Hz, 1 H, *para*-C₆H₅), 7.55 (t, ³J_{HH} = 7.6 Hz, 2 H, *meta*-C₆H₅), 8.32 (d, ³J_{HH} = 7.6 Hz, 2 H, *ortho*-C₆H₅). ¹³C{¹H} NMR (175 MHz, benzene-*d*₆): δ 27.57 (ZnOOCMe₃), 28.16 (CNCMe₂CH₂O), 65.69 (CNCMe₂CH₂O), 77.60 (ZnOOCMe₃), 81.20 (CNCMe₂CH₂O), 126.44 (*para*-C₆H₅), 127.34 (*meta*-C₆H₅), 136.37 (*ortho*-C₆H₅), 142.12 (br, *ipso*-C₆H₅), 190.49 (br, CNCMe₂CH₂O). ¹¹B NMR (128 MHz, benzene-*d*₆): δ -17.1. ¹⁵N{¹H} NMR (71 MHz, benzene-*d*₆): δ -158.8. ¹⁷O NMR (81 MHz, benzene-*d*₆, obtained from To^MZnCM₃ and ¹⁷O₂): δ 284 (ZnOOCMe₃), 204 (ZnOOCMe₃). IR (KBr, cm⁻¹): 3078 (w), 3048 (w), 2967 (m), 2927 (w), 2897 (w), 2870 (w), 1598 (s, ν_{CN}), 1496 (w), 1464 (s), 1433 (w), 1367 (m), 1353 (s), 1278 (s), 1198 (s), 1164 (s), 963 (s), 898 (w), 819 (w), 744 (w). Anal. Calcd. for $\text{C}_{25}\text{H}_{38}\text{BN}_3\text{O}_5\text{Zn}$: C, 55.94; H, 7.14; N, 7.83. Found: C, 55.85; H, 7.38; N, 7.83. Mp: 193-195 °C.

To^MZnOOCMe₂Ph (12). The procedure described above for To^MZnOO(*t*-Bu) was used, starting from To^MZnH (**4**; 0.625 g, 1.393 mmol) and PhMe₂COOH (0.28 mL, 80 % technical grade), affording To^MZnOOCMe₂Ph (**12**; 0.764 g, 1.276 mmol, 91.6 %). X-ray quality single crystals were grown from a concentrated toluene solution of To^MZnOOCMe₂Ph at -30 °C. ¹H NMR (400 MHz, benzene-*d*₆): δ 1.14 (s, 18 H, CNCMe₂CH₂O), 1.86 (s, 6 H, ZnOOCMe₂Ph), 3.48 (s, 6 H, CNCMe₂CH₂O), 7.18 (t, ³J_{HH} = 7.2 Hz, 1 H, *para*-CMe₂C₆H₅), 7.35 (t, ³J_{HH} = 7.6 Hz, 1 H, *meta*-CMe₂C₆H₅), 7.38 (t, ³J_{HH} = 8.0 Hz, 1 H, *para*-BC₆H₅), 7.54 (t, ³J_{HH} = 7.6 Hz, 2 H, *meta*-BC₆H₅), 7.85 (d, ³J_{HH} = 7.6 Hz, 2 H, *ortho*-CMe₂C₆H₅), 8.31 (d, ³J_{HH} = 7.2 Hz, 2 H, *ortho*-BC₆H₅). ¹³C{¹H} NMR (175 MHz, benzene-*d*₆): δ 28.19 (CNCMe₂CH₂O), 28.22 (ZnOOCMe₂Ph), 65.68 (CNCMe₂CH₂O), 81.22 (CNCMe₂CH₂O), 81.78 (ZnOOCMe₂Ph), 126.62 (*para*-BC₆H₅), 126.65 (*para*-CMe₂C₆H₅), 127.01 (*ortho*-CMe₂C₆H₅), 127.35 (*meta*-BC₆H₅), 127.92 (*meta*-CMe₂C₆H₅), 136.36 (*ortho*-C₆H₅), 140.94 (br, *ipso*-C₆H₅), 149.80 (*ipso*-CMe₂C₆H₅), 190.58 (br, CNCMe₂CH₂O). ¹¹B NMR (128 MHz, benzene-*d*₆): δ -17.2. ¹⁵N{¹H} NMR (71 MHz, benzene-*d*₆): δ -158.1. IR (KBr, cm⁻¹): 3080 (w), 3047 (w), 2968 (m), 2929 (w), 2901 (w), 2870 (w), 1595 (s, ν_{CN}), 1494 (w), 1462 (m), 1446 (w), 1432 (w), 1386 (w), 1367 (m), 1351 (m), 1275 (s), 1197 (s), 1165 (s), 1104 (w), 1073 (w), 1029 (w), 956 (s), 902 (w), 843 (w), 818 (w), 762 (w), 746 (w), 699 (w), 662 (w), 639 (m), 629 (m), 552 (m), 480 (m). Anal. Calcd. for C₃₀H₄₀BN₃O₅Zn: C, 60.17; H, 6.73; N, 7.02. Found: C, 59.98; H, 6.48; N, 7.02. Mp: 168-170 °C.

(k²-To^M)₂Zn (14). To^MZnH (0.250 g, 0.557 mmol) and TI[To^M] (0.327 g, 0.557 mmol) were dissolved in benzene (15 mL) and heated to 85 °C for 48 h. A shiny metallic black precipitate appeared during the course of the reaction. A colorless solution was obtained upon filtration.

Removal of the volatiles materials from the filtrate gave a white solid that was washed with

pentane (3 × 5 mL) and dried under vacuum, affording analytically pure bis(k^2 -To^M)Zn (0.417 g, 0.502 mmol, 90.1%) as a white powdery solid. X-ray quality single crystals were grown from a slow pentane diffusion into a concentrated toluene solution of 14 at -30 °C. ¹H NMR (benzene-*d*₆, 400 MHz): δ 0.94 (s, 6 H, CNCMe₂CH₂O), 1.12 (s, 6 H, CNCMe₂CH₂O), 1.23 (s, 6 H, CNCMe₂CH₂O), 1.31 (s, 18 H, CNCMe₂CH₂O), 3.29-3.38 (m, 6 H, ZnNCMe₂CH₂O), 3.51 (d, ³J_{HH} = 8.4 Hz, 2 H, ZnNCMe₂CH₂O), 3.69 (s, 4 H, CNCMe₂CH₂O), 7.25 (t, ³J_{HH} = 7.2 Hz, 2 H, *para*-C₆H₅), 7.44 (t, ³J_{HH} = 7.2 Hz, 4 H, *meta*-C₆H₅), 8.05 (d, ³J_{HH} = 7.2 Hz, 4 H, *ortho*-C₆H₅). ¹³C{¹H} NMR (benzene-*d*₆, 100 MHz): δ 25.80 (ZnNCMe₂CH₂O), 27.84 (ZnNCMe₂CH₂O), 28.64 (ZnNCMe₂CH₂O), 28.66 (ZnNCMe₂CH₂O), 29.57 (CNCMe₂CH₂O), 66.44 (ZnNCMe₂CH₂O), 67.30 (ZnNCMe₂CH₂O), 68.32 (CNCMe₂CH₂O), 77.35 (CNCMe₂CH₂O), 78.67 (ZnNCMe₂CH₂O), 79.18 (ZnNCMe₂CH₂O), 126.15 (*para*-C₆H₅), 127.74 (*meta*-C₆H₅), 134.56 (*ortho*-C₆H₅), 147.40 (*ipso*-C₆H₅), 194 (br, CNCMe₂CH₂O). ¹¹B NMR (benzene-*d*₆, 128 MHz): δ 17.0. ¹⁵N{¹H} NMR (benzene-*d*₆, 71 MHz): δ -120.6 (CNCMe₂CH₂O), -178.9 (CN(Zn)CMe₂CH₂O). IR (KBr, cm⁻¹): 2966 (s), 2928 (w), 2878 (w), 1604 (m, ν_{CN}), 1560 (s, ν_{CN}), 1490 (w), 1464 (m), 1432 (w), 1369 (m), 1359 (m), 1278 (m), 1250 (m), 1199 (m), 1152 (m), 1002 (s), 969 (s), 892 (w), 848 (w). Anal. Calcd. for C₄₂H₅₈B₂N₆O₆Zn: C, 60.78; H, 7.04; N, 10.13. Found: C, 60.91; H, 7.38; N, 9.95. Mp 190-195 °C (dec).

(To^MZnOH)₃ (**15**). A benzene solution of To^MZnOOEt (0.210 g, 0.413 mmol) was photolyzed in a Rayonet chamber at 350 nm for 24 h at ambient temperature. Colorless, X-ray quality crystals were formed during the photolysis. The crystals were isolated by decantation of the supernatant solution. Further grinding and washing with pentane (3 × 5

mL) followed by drying under reduced pressure provided analytically pure $\text{To}^{\text{M}}\text{ZnOH}$ (0.123 g, 0.265 mmol, 64.1%) as a trimeric species. ^1H NMR (400 MHz, methylene chloride- d_2 , 25 °C): δ 1.26 (s, br, 18 H, $\text{CNCMe}_2\text{CH}_2\text{O}$), 3.88 (s, br, 6 H, $\text{CNCMe}_2\text{CH}_2\text{O}$), 7.13 (m, 3 H, *para* and *meta*- C_6H_5), 7.24 (d, $^3J_{\text{HH}} = 6.4$ Hz, 2 H, *ortho*- C_6H_5). $^{13}\text{C}\{^1\text{H}\}$ NMR (175 MHz, methylene chloride- d_2 , 25 °C): δ 29.59 ($\text{CNCMe}_2\text{CH}_2\text{O}$), 66.78 ($\text{CNCMe}_2\text{CH}_2\text{O}$), 79.19 ($\text{CNCMe}_2\text{CH}_2\text{O}$), 125.92 (*para*- C_6H_5), 127.88 (*meta*- C_6H_5), 133.57 (*ortho*- C_6H_5), 149.42 (br, *ipso*- C_6H_5), 191.09 (br, $\text{CNCMe}_2\text{CH}_2\text{O}$). ^{11}B NMR (128 MHz, methylene chloride- d_2): δ -18.2. $^{15}\text{N}\{^1\text{H}\}$ NMR (71 MHz, methylene chloride- d_2 , 25 °C): δ -160.7. IR (KBr, cm^{-1}): 3069 (w), 2969 (m), 2930 (w), 1623 (m, ν_{CN}), 1577 (s, ν_{CN}), 1492 (w), 1462 (m), 1433 (w), 1383 (w), 1367 (m), 1280 (m), 1197 (m), 1160 (m), 1121 (w), 999 (s), 970 (s), 944 (m), 879 (w), 846 (w), 732 (m), 706 (m), 651 (w). Anal. Calcd. for $\text{C}_{63}\text{H}_{90}\text{B}_3\text{N}_9\text{O}_9\text{Zn}_3$: C, 54.28; H, 6.51; N, 9.04. Found: C, 54.22; H, 6.30; N, 8.69. Mp 260-263 °C.

General synthesis of $\text{BnMe}_2\text{SiOOR}$ (R=Et, *i*- C_3H_7 , *t*-Bu). BnMe_2SiH (0.012 g, 0.08 mmol) and $\text{To}^{\text{M}}\text{ZnOOR}$ (0.02 mmol) were allowed to react in benzene- d_6 (0.6 mL). Upon completion of the reaction (R = Et, 2 h; R = *i*- C_3H_7 , 6 h; R = *t*-Bu, 12 h at 80 °C), the products were identified and characterized by ^1H , $^{13}\text{C}\{^1\text{H}\}$ and ^{29}Si NMR spectroscopy. Equimolar $\text{To}^{\text{M}}\text{ZnH}$ and $\text{BnMe}_2\text{SiOOR}$ were formed in each reaction. Additionally, the products' spectra were not equivalent with spectra of BnMe_2SiH starting material and BnMe_2SiOR (synthesized below).

General synthesis of BnMe_2SiOR (R=Et, *i*- C_3H_7 , *t*-Bu). BnMe_2SiH (0.014 g, 0.09 mmol) and ROH (equimolar with respect to BnMe_2SiH) were added to $\text{To}^{\text{M}}\text{ZnH}$ (5 mg, 0.01 mmol) dissolved in benzene- d_6 (0.6 mL). The resulting solution was heated in a Teflon-valved NMR

tube (R = Et, 60 °C, 4 h; R = *i*-C₃H₇, 80 °C, 10 h; R = *t*-Bu, 135 °C, 65 h). Upon completion of the reaction, the products were identified and characterized based on their ¹H, ¹³C{¹H} and ²⁹Si NMR spectra.

BnMe₂SiOOEt. ¹H NMR (600 MHz, C₆D₆): δ 0.14 (s, 6 H, SiMe₂), 1.04 (t, 3 H, ³J_{HH} = 7.2 Hz, OCH₂CH₃), 2.26 (s, 2 H, PhCH₂), 3.91 (q, 2 H, ³J_{HH} = 7.2 Hz, OCH₂CH₃), 7.06 (m, 3 H, *para*- and *meta*-C₆H₅), 7.15 (m, 2 H, *ortho*-C₆H₅). ¹³C{¹H} NMR (150 MHz, C₆D₆): δ -2.93 (SiMe₂), 13.70 (SiOCH₂CH₃), 25.70 (PhCH₂), 72.76 (SiOCH₂CH₃), 125.14 (*para*-C₆H₅), 129.01 (*meta*-C₆H₅), 129.22 (*ortho*-C₆H₅), 139.12 (*ipso*-C₆H₅). ²⁹Si NMR (120 MHz, C₆D₆): δ 21.63.

BnMe₂SiOEt. ¹H NMR (600 MHz, C₆D₆): δ 0.01 (s, 6 H, SiMe₂), 1.05 (t, 3 H, ³J_{HH} = 7.2 Hz, OCH₂CH₃), 2.06 (s, 2 H, PhCH₂), 3.44 (q, 2 H, ³J_{HH} = 7.2 Hz, OCH₂CH₃), 7.0 (m, 3 H, *para*- and *meta*-C₆H₅), 7.13 (m, 2 H, *ortho*-C₆H₅). ¹³C{¹H} NMR (150 MHz, C₆D₆): δ -1.96 (SiMe₂), 19.09 (SiOCH₂CH₃), 27.34 (PhCH₂), 58.85 (SiOCH₂CH₃), 124.92 (*para*-C₆H₅), 128.94 (*meta*-C₆H₅), 129.08 (*ortho*-C₆H₅), 139.91 (*ipso*-C₆H₅). ²⁹Si NMR (120 MHz, C₆D₆): δ 12.50.

BnMe₂SiOO(*i*-C₃H₇). ¹H NMR (600 MHz, C₆D₆): δ 0.15 (s, 6 H, SiMe₂), 1.11 (d, 6 H, ³J_{HH} = 6.0 Hz, OCHMe₂), 2.27 (s, 2 H, PhCH₂), 4.13 (sept, 1 H, ³J_{HH} = 6.0 Hz, OCHMe₂), 7.05 (m, 3 H, *para*- and *meta*-C₆H₅), 7.14 (m, 2 H, *ortho*-C₆H₅). ¹³C{¹H} NMR (150 MHz, C₆D₆): δ -2.79 (SiMe₂), 20.70 (OCHMe₂), 25.80 (PhCH₂), 78.19 (SiOCHMe₂), 125.11 (*para*-C₆H₅), 128.99 (*meta*-C₆H₅), 129.24 (*ortho*-C₆H₅), 139.23 (*ipso*-C₆H₅). ²⁹Si NMR (120 MHz, C₆D₆): δ 21.26.

BnMe₂SiO(*i*-C₃H₇). ¹H NMR (600 MHz, C₆D₆): δ 0.05 (s, 6 H, SiMe₂), 1.07 (d, 6 H, ³J_{HH} = 6.0 Hz, OCHMe₂), 2.11 (s, 2 H, PhCH₂), 3.80 (sept, 1 H, ³J_{HH} = 6.0 Hz, OCHMe₂), 7.03 (m, 3 H, *para*- and *meta*-C₆H₅), 7.16 (m, 2 H, *ortho*-C₆H₅). ¹³C{¹H} NMR (150 MHz, C₆D₆): δ -1.32 (SiMe₂), 26.37 (OCHMe₂), 27.84 (PhCH₂), 65.56 (SiOCHMe₂), 124.90 (*para*-C₆H₅), 128.89 (*meta*-C₆H₅), 129.12 (*ortho*-C₆H₅), 140.01 (*ipso*-C₆H₅). ²⁹Si NMR (120 MHz, C₆D₆): δ 10.38.

BnMe₂SiOO(*t*-Bu). ¹H NMR (600 MHz, C₆D₆): δ 0.16 (s, 6 H, SiMe₂), 1.21 (s, 9 H, OMe₃), 2.28 (s, 2 H, PhCH₂), 7.07 (m, 3 H, *para*- and *meta*-C₆H₅), 7.14 (m, 2 H, *ortho*-C₆H₅). ¹³C{¹H} NMR (150 MHz, C₆D₆): δ -2.55 (SiMe₂), 25.80 (PhCH₂), 26.55 (SiOCMe₃), 81.41 (SiOCMe₃), 125.08 (*para*-C₆H₅), 128.80 (*meta*-C₆H₅), 129.19 (*ortho*-C₆H₅), 139.48 (*ipso*-C₆H₅). ²⁹Si NMR (120 MHz, C₆D₆): δ 20.45.

BnMe₂SiO(*t*-Bu). ¹H NMR (600 MHz, C₆D₆): δ 0.10 (s, 6 H, SiMe₂), 1.16 (s, 9 H, OMe₃), 2.14 (s, 2 H, PhCH₂), 7.04 (m, 3 H, *para*- and *meta*-C₆H₅), 7.17 (m, 2 H, *ortho*-C₆H₅). ¹³C{¹H} NMR (150 MHz, C₆D₆): δ 1.09 (SiMe₂), 29.49 (PhCH₂), 32.47 (SiOCMe₃), 65.56 (SiOCMe₃), 125.02 (*para*-C₆H₅), 128.80 (*meta*-C₆H₅), 129.19 (*ortho*-C₆H₅), 140.42 (*ipso*-C₆H₅). ²⁹Si NMR (120 MHz, C₆D₆): δ 4.35.

Kinetic experiments of To^MZnEt + O₂. Reactions were monitored with ¹H NMR spectroscopy using a Bruker DRX-400 spectrometer. The concentrations of NMR-active reactants, initiators and products were determined by comparison of corresponding integrated resonances to the known concentration of the internal standards. The experiments were performed under pseudo-first order conditions with excess O₂, and the [To^MZnEt] was monitored for at least three half lives.

Determination of rate dependence on [AIBN]. A benzene- d_6 stock solution was prepared to contain known concentrations of cyclooctane (5.2 mM) as an internal standard and $\text{To}^{\text{M}}\text{ZnEt}$ (25 mM). An experiment was initiated by adding a known quantity of AIBN to a measured volume (0.6 mL) of the stock solution; the [AIBN] was then verified by comparison with the internal standard in the integrated ^1H NMR spectrum. The resulting solution was pressurized with O_2 (50 psi) in a high-pressure NMR tube using a high-pressure manifold. The mixture was shaken vigorously and then inserted into a NMR probe that was pre-heated to 54 °C. The [AIBN] was varied from 5.4 mM to 31.5 mM. The integrated intensities of $\text{To}^{\text{M}}\text{ZnEt}$ were measured over the reaction time-course. For each experiment, the $-\text{d}[\text{To}^{\text{M}}\text{ZnEt}]/\text{dt}$ followed an exponential decay (Figure S-1) to give k_{obs} . The half-order dependence on [AIBN] was obtained by a non-weighted linear least squares fit of the k_{obs} values against $[\text{AIBN}]^{1/2}$. (Figure S-2).

Figure S-1. Exponential decay plot of $[\text{To}^{\text{M}}\text{ZnEt}]$ (2) vs. time in its reaction with O_2 (50 psi) in the presence of AIBN.

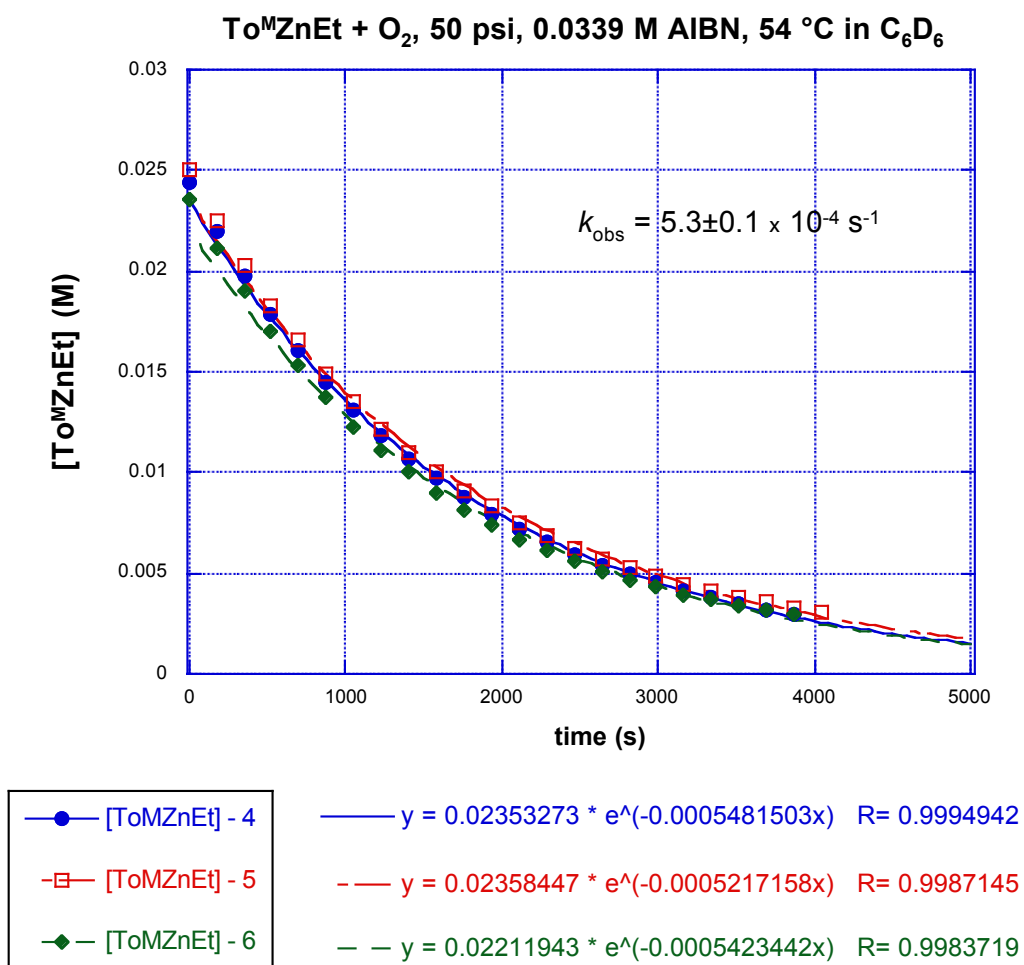
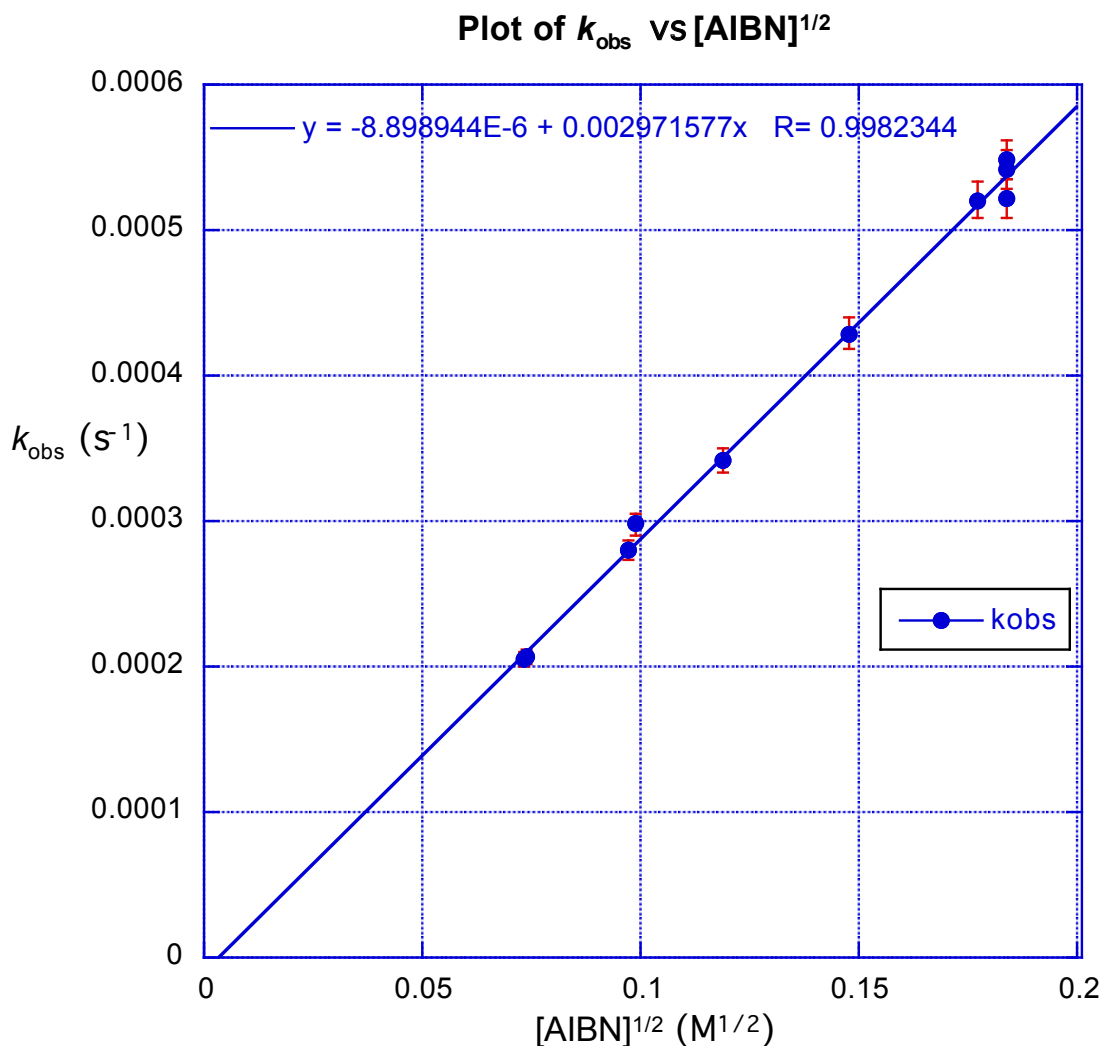


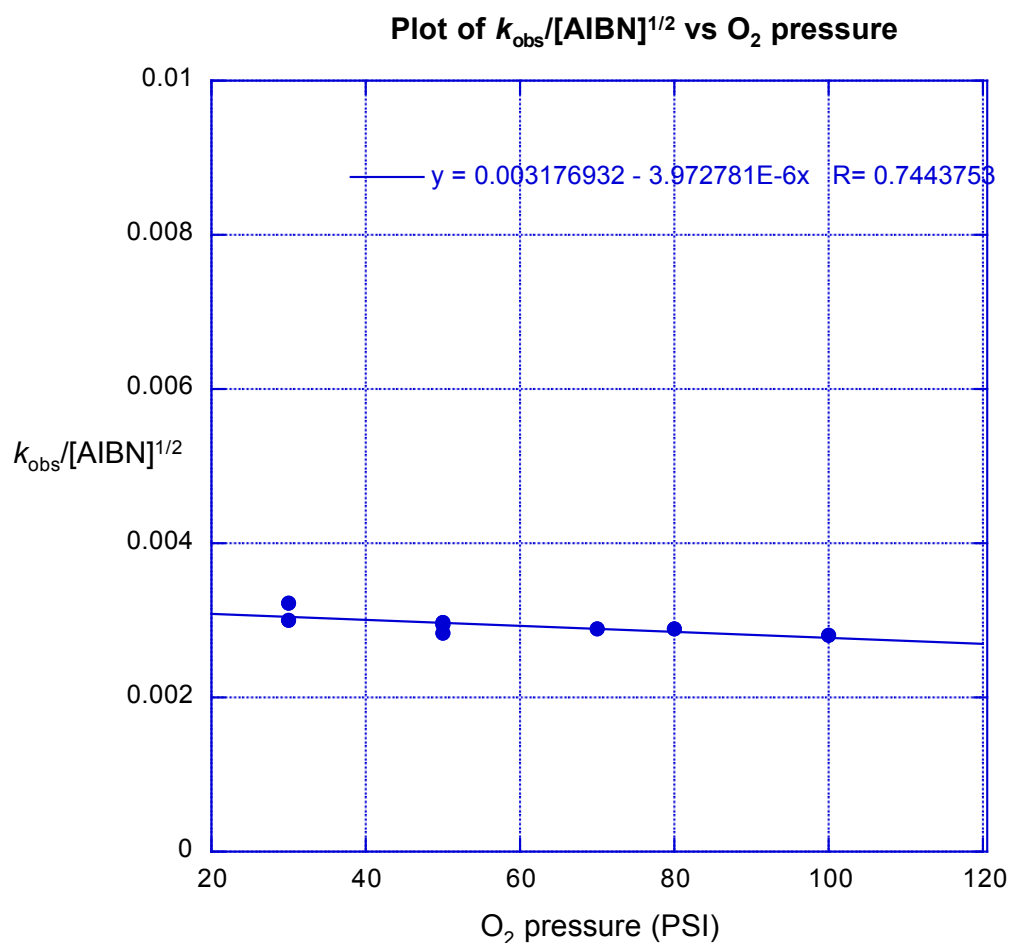
Figure S-2. A plot of $[\text{AIBN}]^{1/2}$ vs. k_{obs} for the reaction of $\text{To}^{\text{M}}\text{ZnEt}$ and O_2 .



Determination of rate dependence on P_{O_2} . A benzene- d_6 stock solution containing cyclooctane (9.6 mM), $\text{To}^{\text{M}}\text{ZnEt}$ (33 mM) and AIBN (14.1 mM) was prepared. A known volume of this solution (0.6 mL) was added to a thick-walled J. Young NMR tube. The tube was charged with a measured pressure of O_2 (30 psi – 100 psi) using a high-pressure manifold. The tube was shaken vigorously and then placed in a pre-heated NMR spectrometer probe (54 °C). The integrated intensities of $\text{To}^{\text{M}}\text{ZnEt}$ were measured over the

reaction time-course. The observed pseudo-first-order rate constants k_{obs} , determined from non-linear least square analysis, were identical within error for each O_2 pressure (Figure S-3).

Figure S-3. A plot of $k_{\text{obs}}/[\text{AIBN}]^{1/2}$ vs. O_2 pressure (psi). The reactions were performed at $54\text{ }^\circ\text{C}$ in benzene- d_6 ; each experiment was performed under pseudo-first order conditions (50 psi O_2) and each point showed pseudo-first order dependence on $[\text{To}^{\text{M}}\text{ZnEt}]$ for three half-lives.



General description of ^1H NMR kinetic experiments for the reactions between $\text{To}^{\text{M}}\text{ZnOOR}$ and $\text{P}(p\text{-C}_6\text{H}_4\text{Me})_3$. A toluene- d_8 stock solution containing known concentrations of cyclooctane (9.9 mM) and $\text{To}^{\text{M}}\text{ZnOOR}$ (20 mM) was prepared. A measured quantity of this stock solution (0.6 mL) was placed in a septa-capped NMR tube, and the tube was cooled to $-78\text{ }^\circ\text{C}$. Tris(*para*-tolyl)phosphine was dissolved in a minimal amount (50 μL)

of toluene- d_8 , and this solution was added through the septa using a microliter syringe, and the hole was sealed with silicone grease. The sample was placed in a pre-cooled NMR spectrometer probe. Single scan spectra were acquired automatically at preset time intervals. The concentrations of $To^M ZnOOR$, $P(p-C_6H_4Me)_3$, and $OP(p-C_6H_4Me)_3$ were determined by comparison of corresponding integrated resonances to the known concentration of the internal standard. The second order rate constants (k_{obs}) were obtained by a non-weighted linear least-squares fit of the data to the second-order rate law:

$$\ln \frac{[P(p-C_6H_4Me)_3]}{[To^M ZnOOR]} = \ln \frac{[P(p-C_6H_4Me)_3]_o}{[To^M ZnOOR]_o} + k_{obs} \Delta_o t \quad (6)$$

(Figures S-4 to S-8).

Figure S-4. A second-order plot of $\ln\{[\text{P}(p\text{-tolyl})_3]/[\text{To}^{\text{M}}\text{ZnOOEt}]\}/\Delta_0$ vs. time for the reaction of $\text{To}^{\text{M}}\text{ZnOO}(\text{Et})$ and tris(*para*-tolyl)phosphine at 259 K. The slope of curve obtained from the linear least squares fit of the data equals k_{obs} ($8.8 \pm 0.3 \times 10^{-2} \text{ M}^{-1}\text{s}^{-1}$).

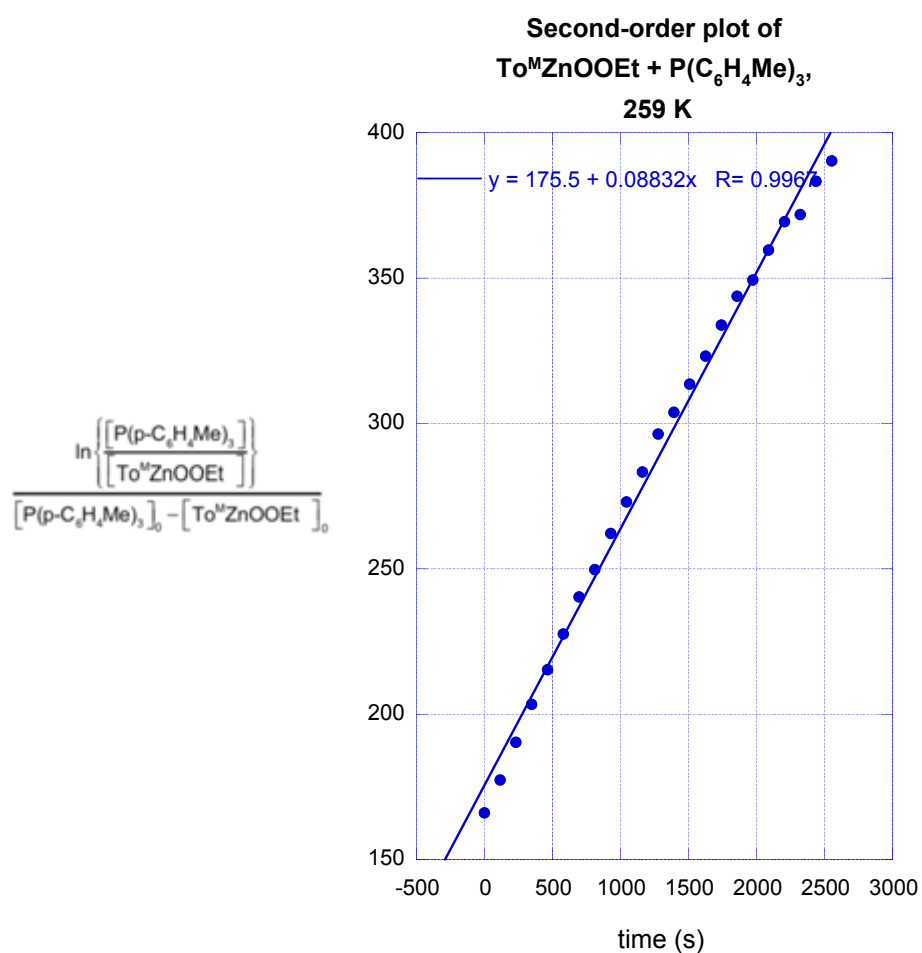


Figure S-5. A second-order plot of $\ln\{[P(p\text{-tolyl})_3]/[To^M ZnOO(i-C_3H_7)]\}/\Delta_0$ vs. time for the reaction of $To^M ZnOO(i-C_3H_7)$ and tris(*para*-tolyl)phosphine at 259 K. The slope of curve obtained from the linear least squares fit of the data equals k_{obs} ($6.3 \pm 0.2 \times 10^{-3} M^{-1}s^{-1}$).

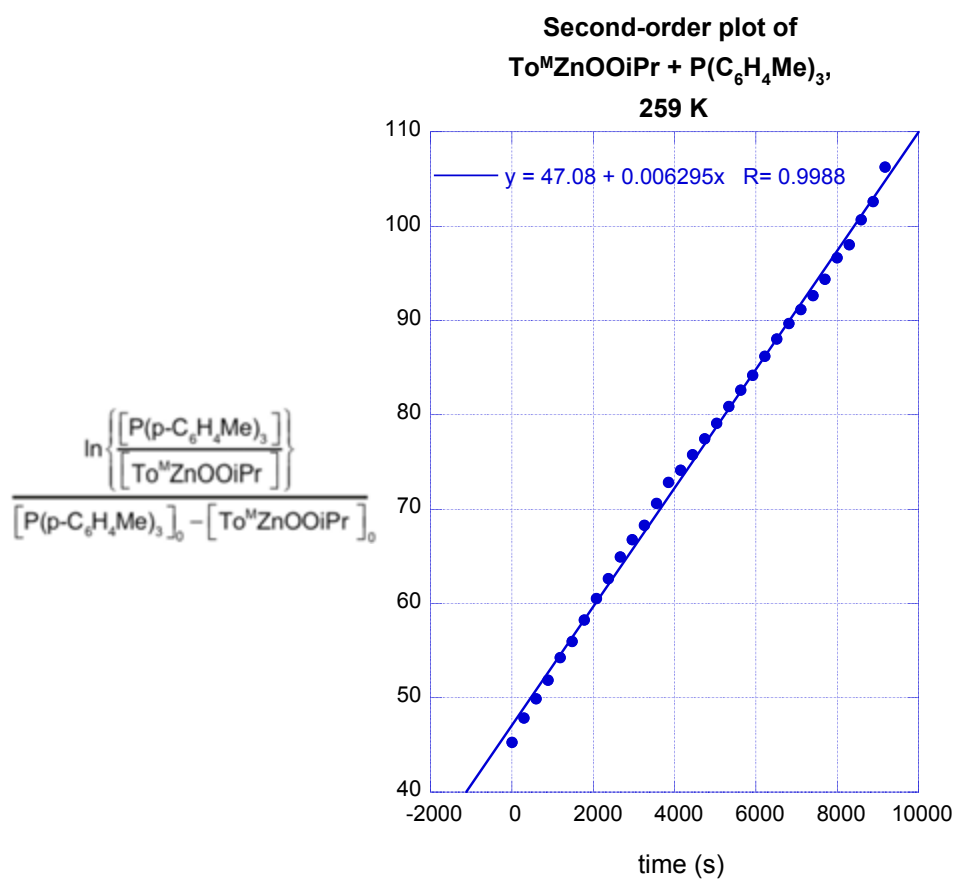


Figure S-6. A second-order plot of $\ln\{[P(p\text{-tolyl})_3]/[To^M ZnOO(n\text{-}C_3H_7)]\}/\Delta_0$ vs. time for the reaction of $To^M ZnOO(n\text{-}C_3H_7)$ and tris(*para*-tolyl)phosphine at 259 K. The slope of curve obtained from the linear least squares fit of the data equals k_{obs} ($7.5 \pm 0.2 \times 10^{-2} M^{-1}s^{-1}$).

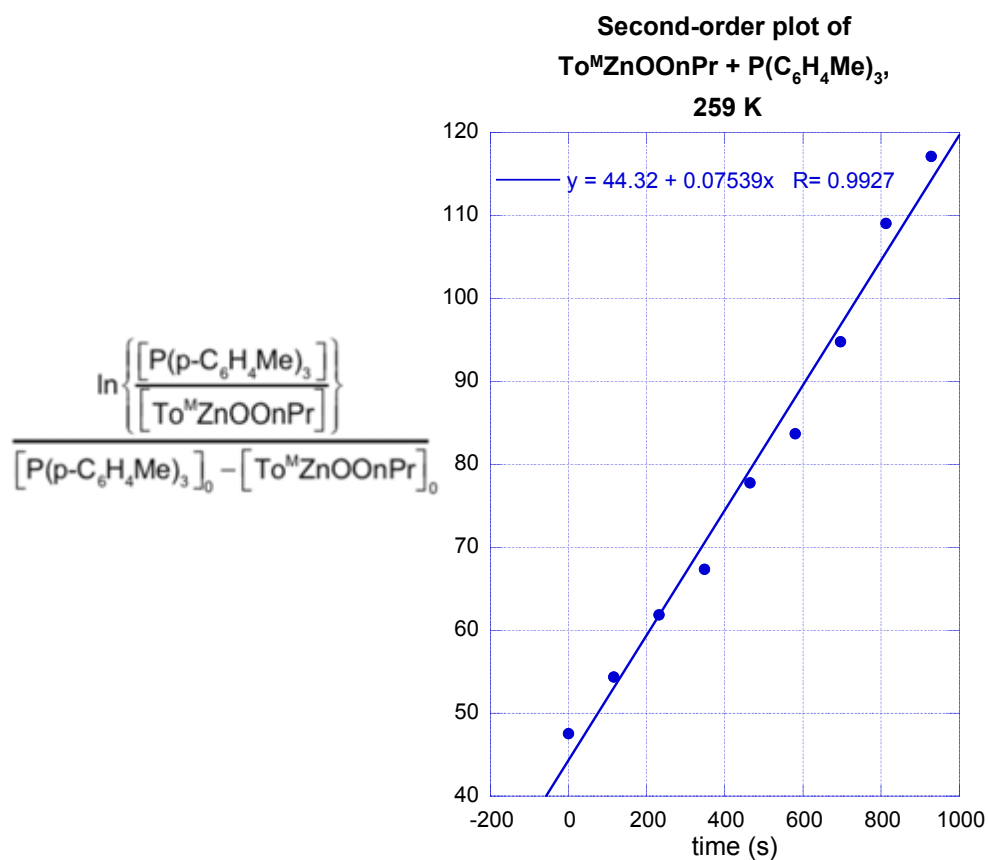


Figure S-7. A second-order plot of $\ln\{[P(p\text{-tolyl})_3]/[To^M ZnOO(t\text{-Bu})]\}/\Delta_0$ vs. time for the reaction of $To^M ZnOO(t\text{-Bu})$ and tris(*para*-tolyl)phosphine at 294 K. The slope of curve obtained from the linear least squares fit of the data equals k_{obs} ($1.22 \pm 0.04 \times 10^{-3} \text{ M}^{-1}\text{s}^{-1}$).

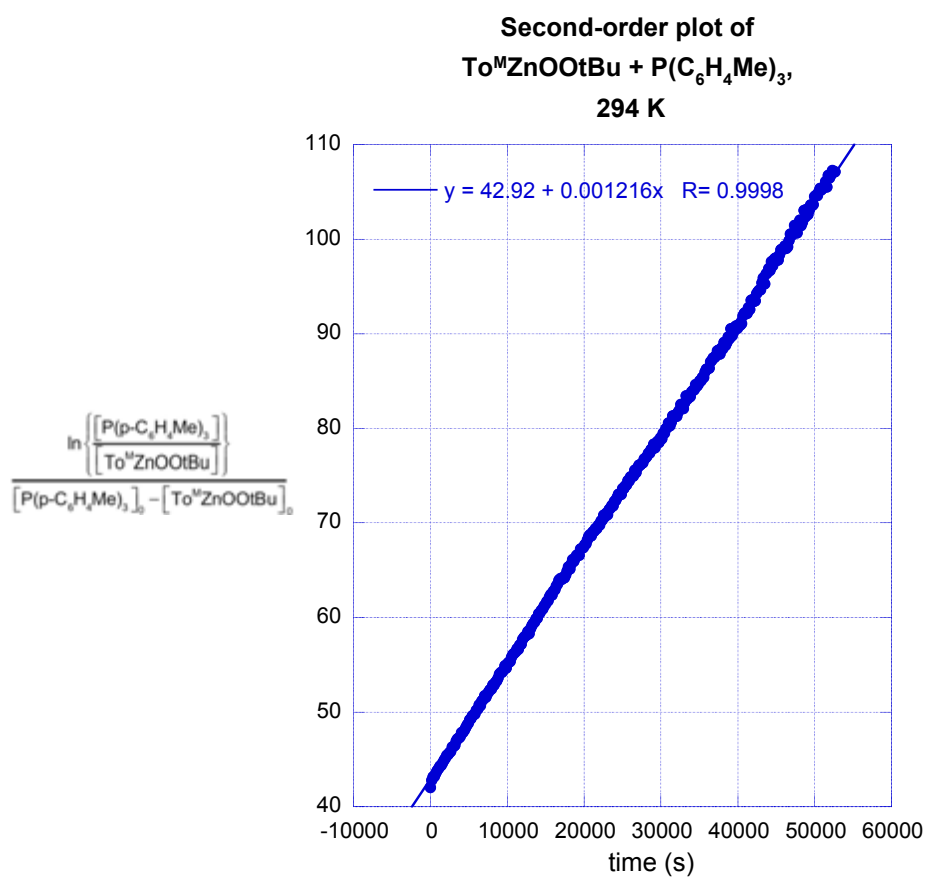


Figure S-8. Representative second-order plots for the reaction of $\text{To}^{\text{M}}\text{ZnOOEt}$ and tris(*para*-tolyl)phosphine at 232.5, 249.2, 259.3, 267.9 and 275.4 K. The slope of the linear-least squares best fit curves corresponds to observed rate constants: $k_{\text{obs}}^{232.5\text{K}} = 9.6 \pm 0.3 \times 10^{-3} \text{ M}^{-1}\text{s}^{-1}$; $k_{\text{obs}}^{249.2\text{K}} = 3.0 \pm 0.1 \times 10^{-2} \text{ M}^{-1}\text{s}^{-1}$; $k_{\text{obs}}^{259.3\text{K}} = 8.8 \pm 0.3 \times 10^{-2} \text{ M}^{-1}\text{s}^{-1}$; $k_{\text{obs}}^{267.9\text{K}} = 1.65 \pm 0.05 \times 10^{-1} \text{ M}^{-1}\text{s}^{-1}$; $k_{\text{obs}}^{275.4\text{K}} = 2.27 \pm 0.07 \times 10^{-1} \text{ M}^{-1}\text{s}^{-1}$.

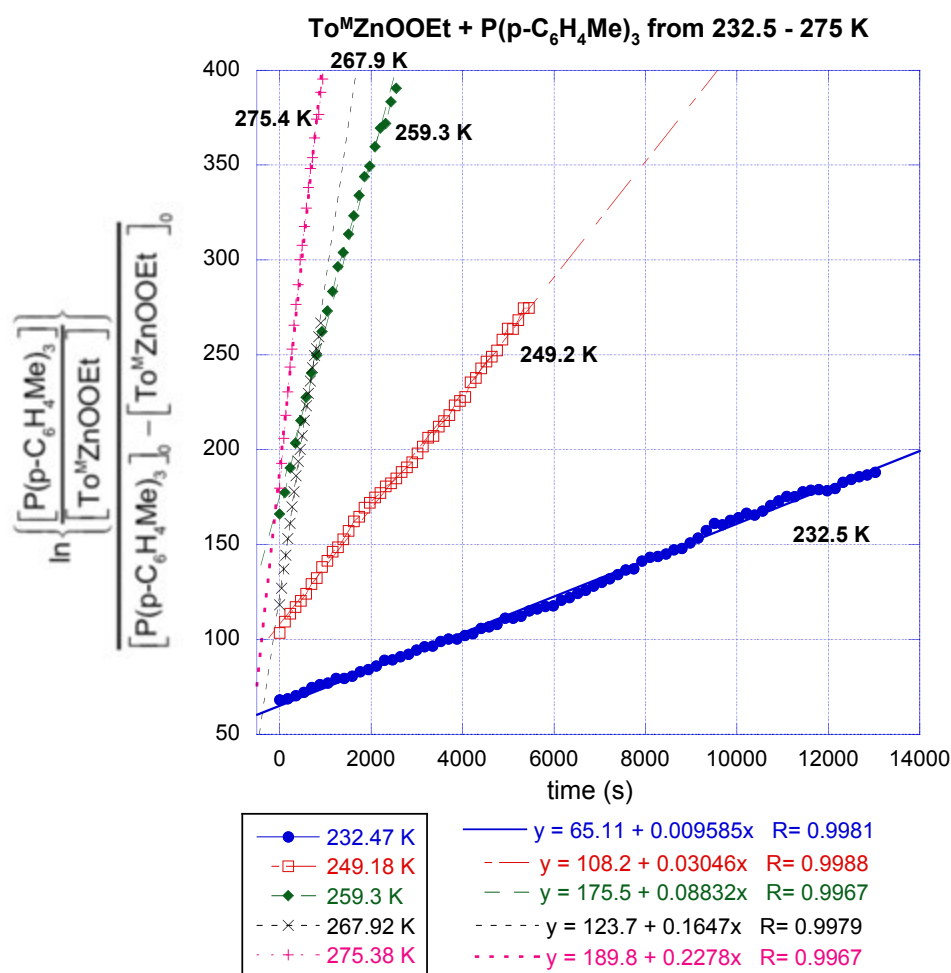
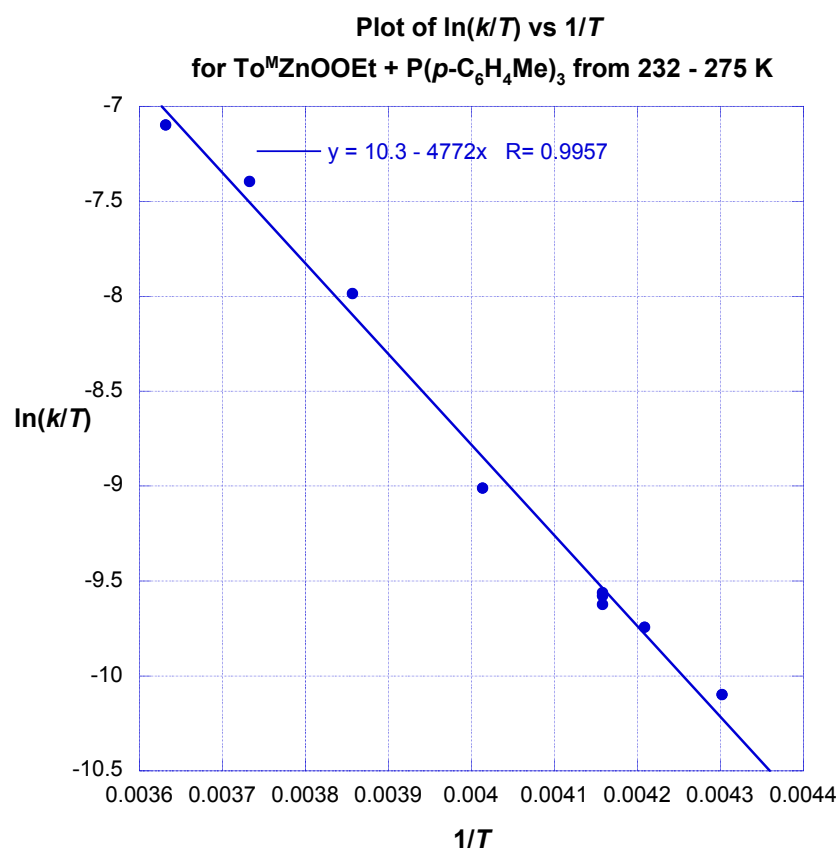


Figure S-9. An Eyring plot showing temperature dependence of tris(*para*-tolyl)phosphine oxidation by $\text{To}^{\text{M}}\text{ZnOOEt}$. From the slope and intercept of the plot, $\Delta H^{\ddagger} = 9.5 \pm 0.3 \text{ kcal}\cdot\text{mol}^{-1}$ and $\Delta S^{\ddagger} = -27 \pm 1 \text{ cal}\cdot\text{mol}^{-1}\cdot\text{K}^{-1}$.



General description of ^1H NMR kinetic experiments for the reactions between $\text{To}^{\text{M}}\text{ZnOOR}$ and BnMe_2SiH . A toluene- d_8 stock solution containing known concentrations of cyclooctane (15.7 mM) and $\text{To}^{\text{M}}\text{ZnOOEt}$ (20.7 mM) was prepared. A measured quantity of this stock solution (0.6 mL) was placed in a septa-capped NMR tube, and the tube was cooled to $-78\text{ }^\circ\text{C}$. BnMe_2SiH (100 mM) was added through the septa using a microliter syringe, and the hole was sealed with silicone grease. The sample was placed in a pre-cooled NMR spectrometer probe. Single scan spectra were acquired automatically at preset time intervals. The concentrations of $\text{To}^{\text{M}}\text{ZnOOEt}$, BnMe_2SiH , $\text{To}^{\text{M}}\text{ZnH}$, and $\text{BnMe}_2\text{SiOOEt}$ were determined by comparison of the corresponding integrated resonances to the known concentration of the internal standard. The second order rate constants (k_{obs}) were obtained by a non-weighted linear least-squares fit of the data to the second-order rate law:

$$\ln \frac{[\text{BnMe}_2\text{SiH}]}{[\text{To}^{\text{M}}\text{ZnOOEt}]} = \ln \frac{[\text{BnMe}_2\text{SiH}]_0}{[\text{To}^{\text{M}}\text{ZnOOEt}]_0} + k_{\text{obs}} \Delta_o t \quad (7)$$

Figure S-10. Representative second-order plots for the reaction of $\text{To}^{\text{M}}\text{ZnOOEt}$ and BnMe_2SiH to give $\text{BnMe}_2\text{SiOOEt}$ and $\text{To}^{\text{M}}\text{ZnH}$ (**13**). $k_{\text{obs}}^{288.8\text{K}} = 3.9 \pm 0.2 \times 10^{-3} \text{ M}^{-1}\text{s}^{-1}$; $k_{\text{obs}}^{295.7\text{K}} = 5.6 \pm 0.3 \times 10^{-3} \text{ M}^{-1}\text{s}^{-1}$; $k_{\text{obs}}^{301.5\text{K}} = 8.1 \pm 0.4 \times 10^{-3} \text{ M}^{-1}\text{s}^{-1}$; $k_{\text{obs}}^{309.9\text{K-MEAN}} = 1.6 \pm 0.5 \times 10^{-2} \text{ M}^{-1}\text{s}^{-1}$; $k_{\text{obs}}^{320.3\text{K}} = 3.7 \pm 0.2 \times 10^{-2} \text{ M}^{-1}\text{s}^{-1}$.

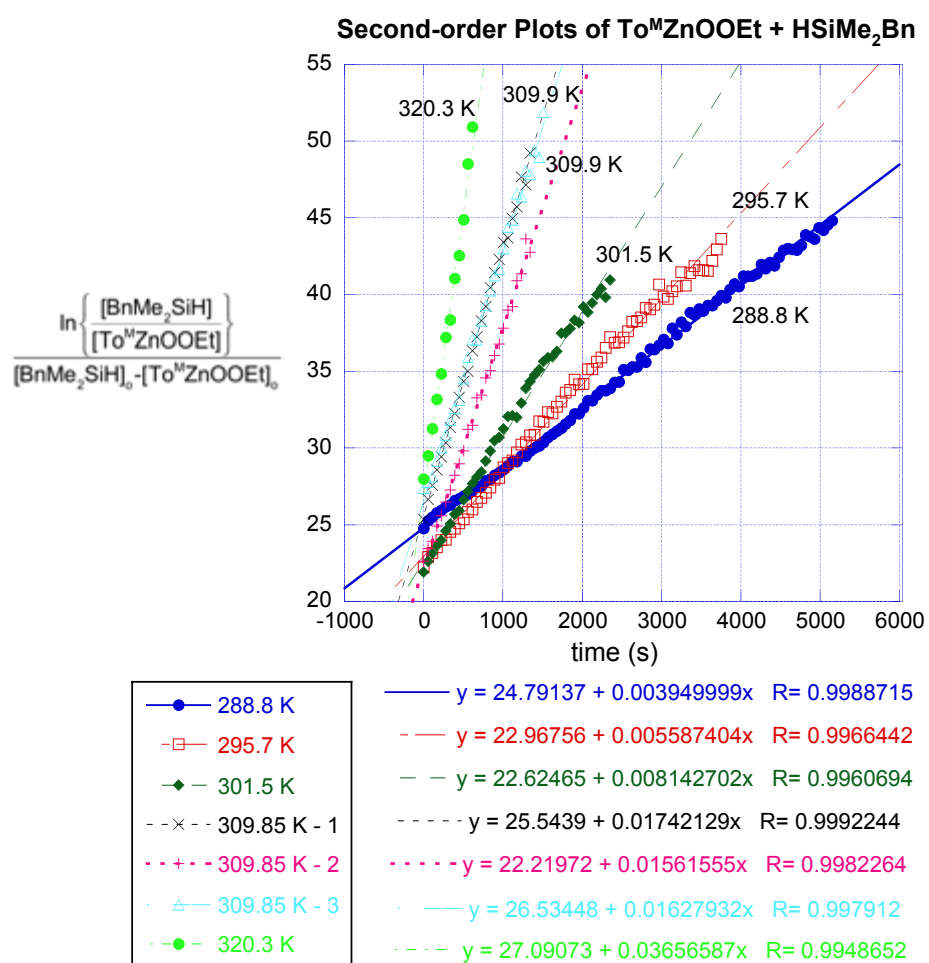
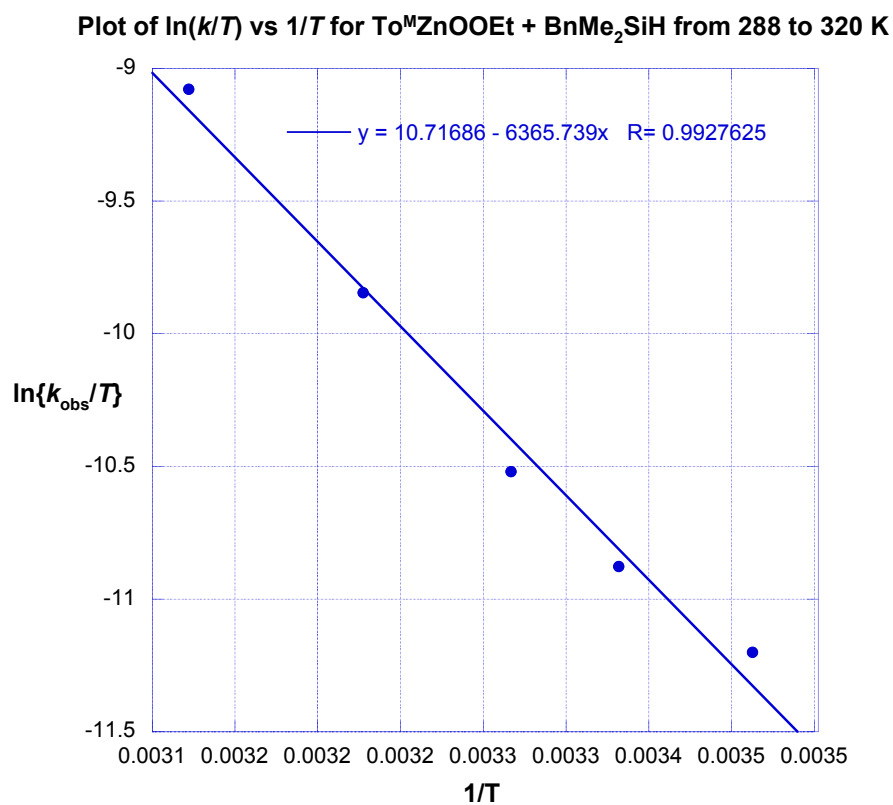


Figure S-11. Eyring plot showing temperature dependence of the reaction of $\text{To}^{\text{M}}\text{ZnOOEt}$ and BnMe_2SiH to give $\text{To}^{\text{M}}\text{ZnH}$ and $\text{BnMe}_2\text{SiOOEt}$. $\Delta H^\ddagger = 12.6 \pm .7 \text{ kcal}\cdot\text{mol}^{-1}$; $\Delta S^\ddagger = -26 \pm 2 \text{ cal}\cdot\text{mol}^{-1}\text{K}^{-1}$.



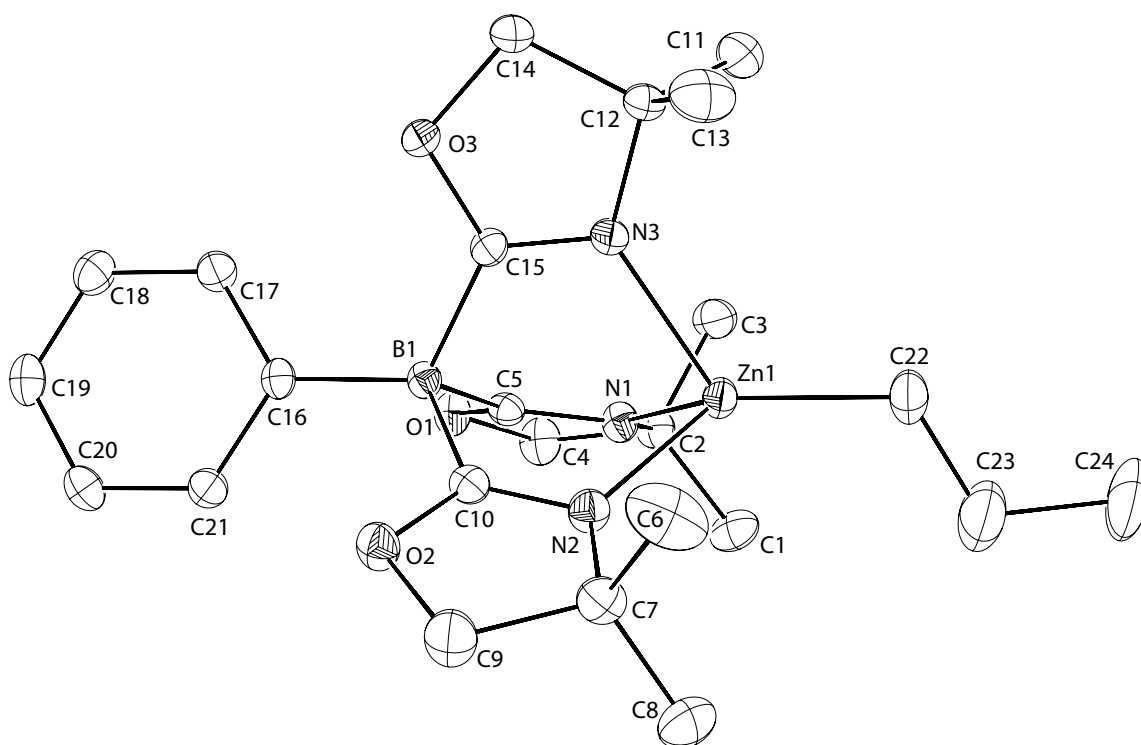


Figure S-13. ORTEP diagram of $\text{To}^{\text{M}}\text{Zn}(n\text{-C}_3\text{H}_7)$ (**3**). Ellipsoids are drawn at 35% probability. Hydrogen atoms and disordered toluene solvent are not shown for clarity.

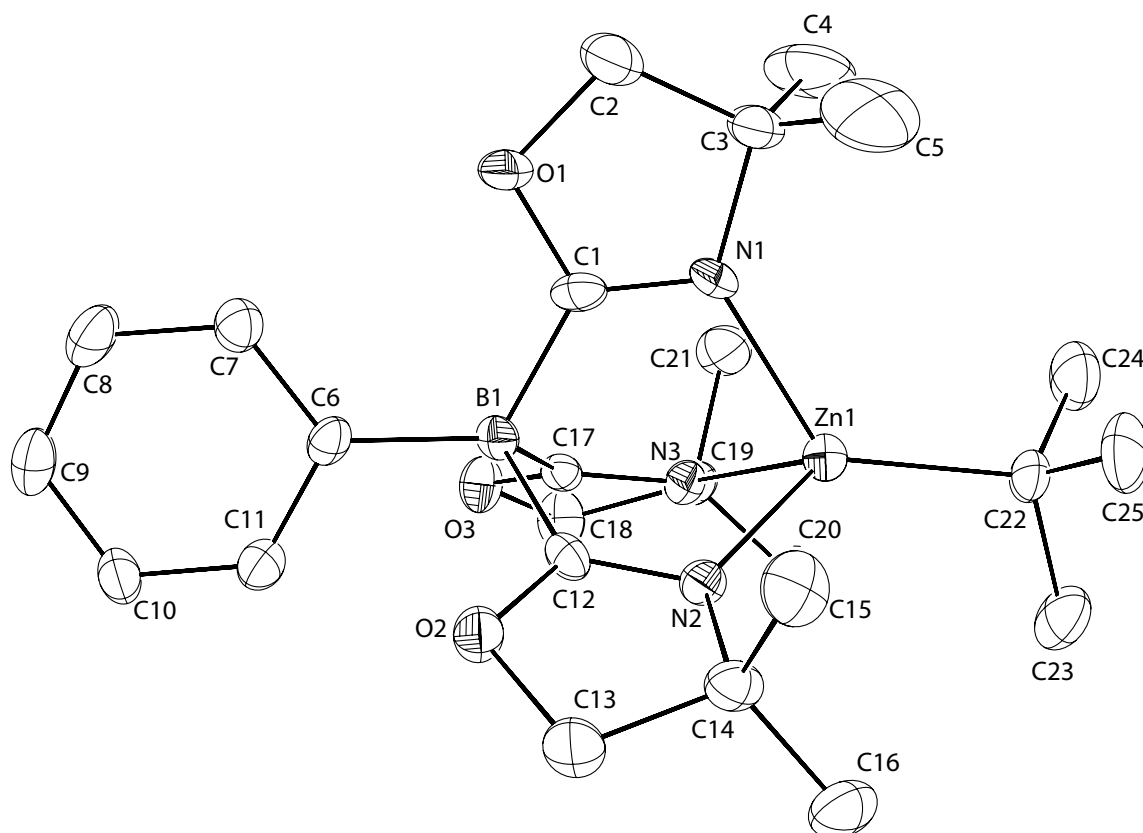


Figure S-14. ORTEP diagram of $\text{To}^{\text{M}}\text{Zn}(t\text{-Bu})$ (**5**). Ellipsoids are drawn at 35% probability. Hydrogen atoms are not shown for clarity.

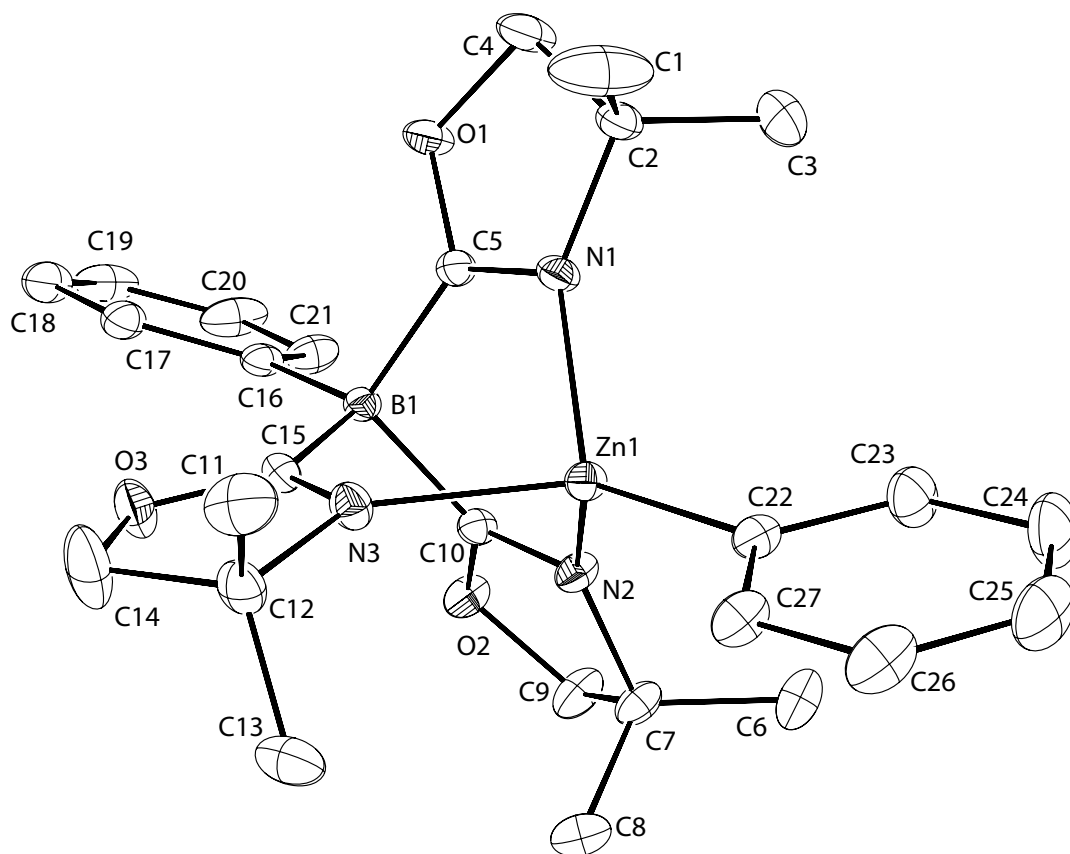


Figure S-15. ORTEP diagram of $To^M ZnPh$ (**6**). Ellipsoids are drawn at 35% probability. Hydrogen atoms and a tetrahydrofuran solvent molecule are not shown for clarity.

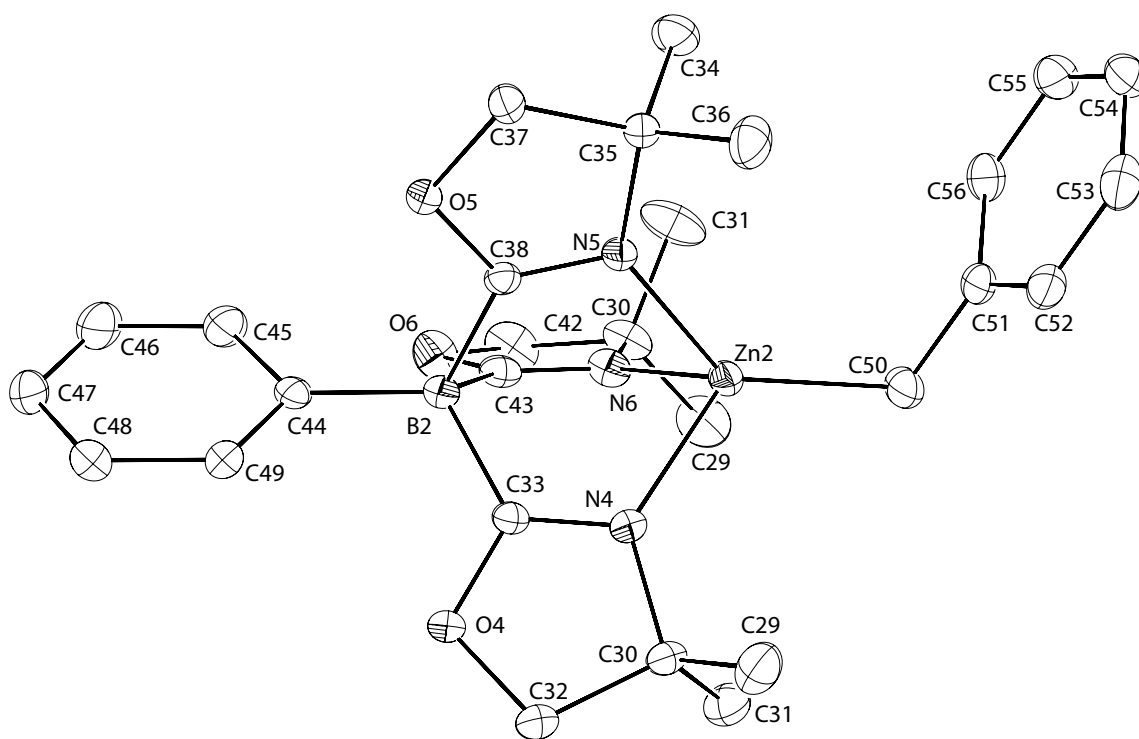


Figure S-16. ORTEP diagram of $\text{To}^{\text{M}}\text{ZnCH}_2\text{Ph}$ (**7**). Ellipsoids are drawn at 35% probability. The unit cell contains two independent molecules of $\text{To}^{\text{M}}\text{ZnCH}_2\text{Ph}$ and a co-crystallized toluene molecule. One of the independent $\text{To}^{\text{M}}\text{ZnCH}_2\text{Ph}$ is illustrated. Hydrogen atoms and a toluene solvent molecule are not shown for clarity.

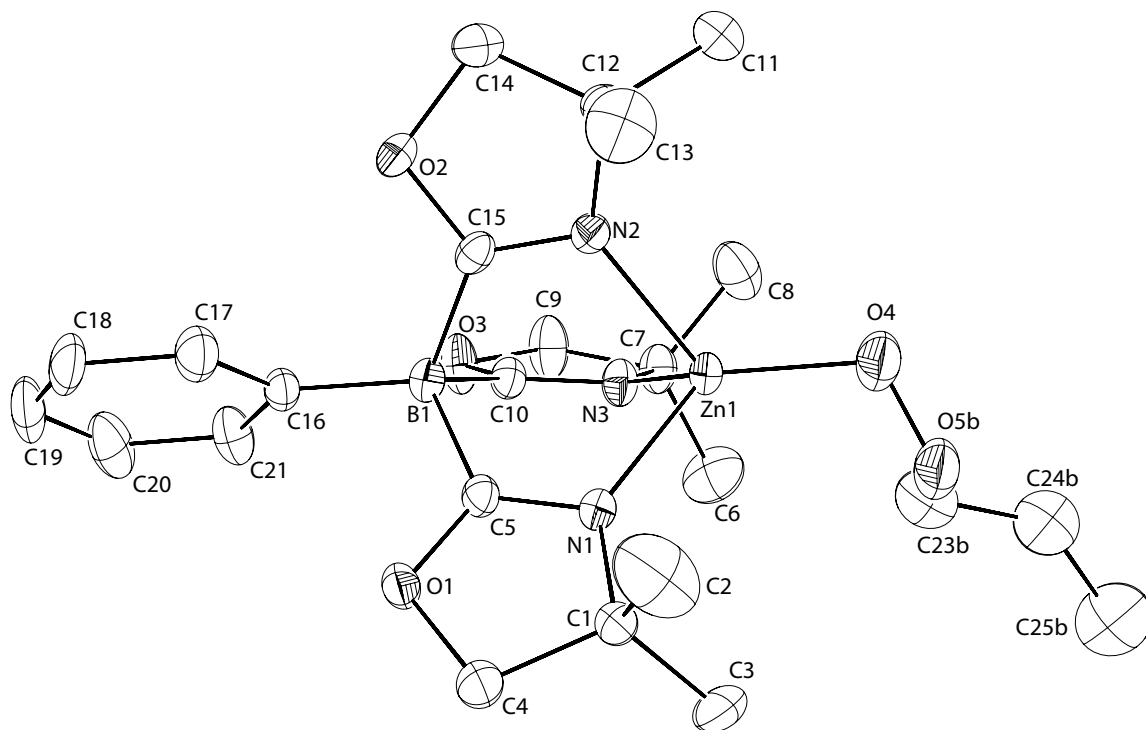


Figure S-18. ORTEP diagram of $\text{To}^{\text{M}}\text{ZnOO}(n\text{-C}_3\text{H}_7)$ (**9**). Ellipsoids are drawn at 35% probability. The *n*-propylperoxide group, beginning at the O5. The disorder was modeled over two positions to give two chemically reasonable $\text{OCH}_2\text{CH}_2\text{CH}_3$ chains, labeled A and B. For clarity, hydrogen atoms and the A chain (O5a, C23a, C24a, and C25a) are not shown for clarity.

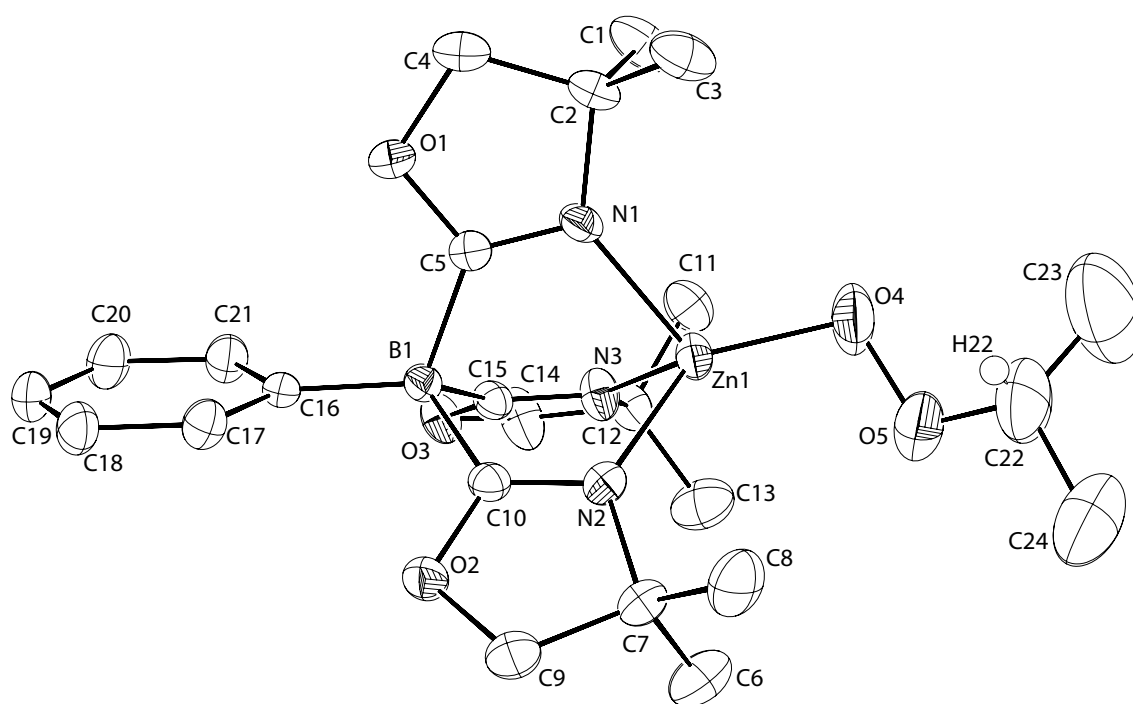


Figure S-19. ORTEP diagram of $\text{To}^{\text{M}}\text{ZnOO}(i\text{-C}_3\text{H}_7)$ (**10**). Ellipsoids are drawn at 35% probability. Only the hydrogen atoms bonded to the isopropyl methine carbon is illustrated for clarity.

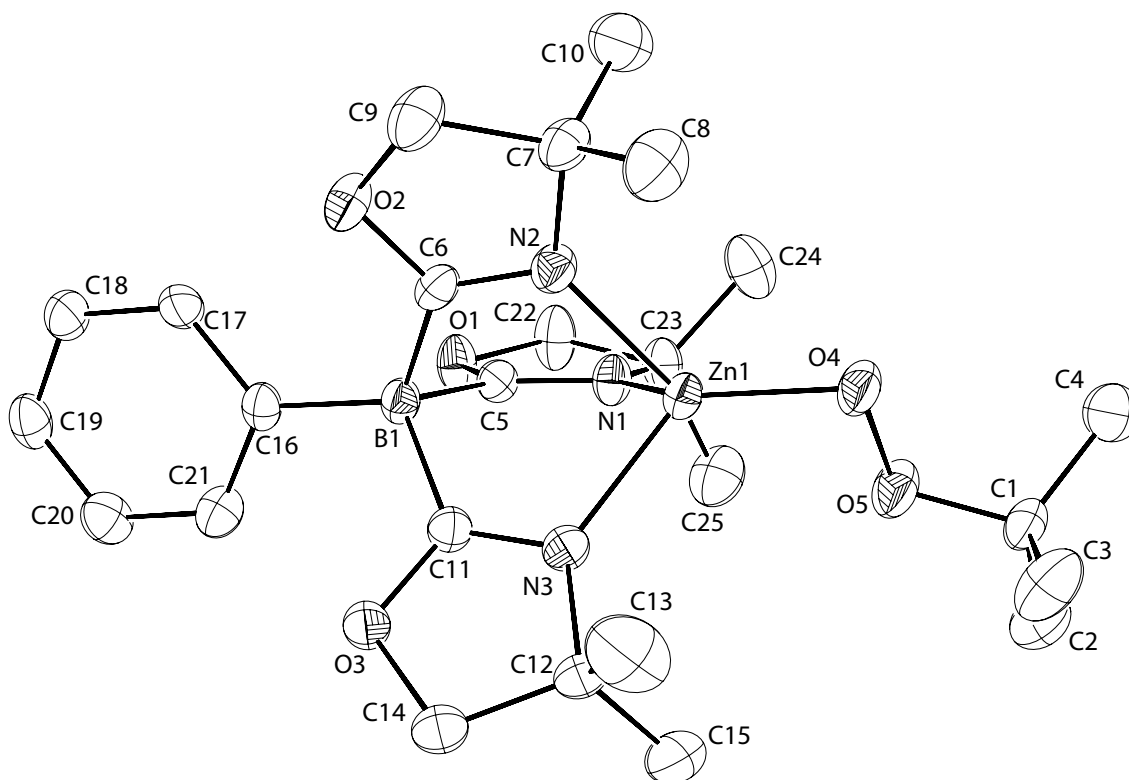


Figure S-20. ORTEP diagram of $To^M ZnOO(t-Bu)$ (**11**). Ellipsoids are drawn at 35% probability. Hydrogen atoms are not shown for clarity.

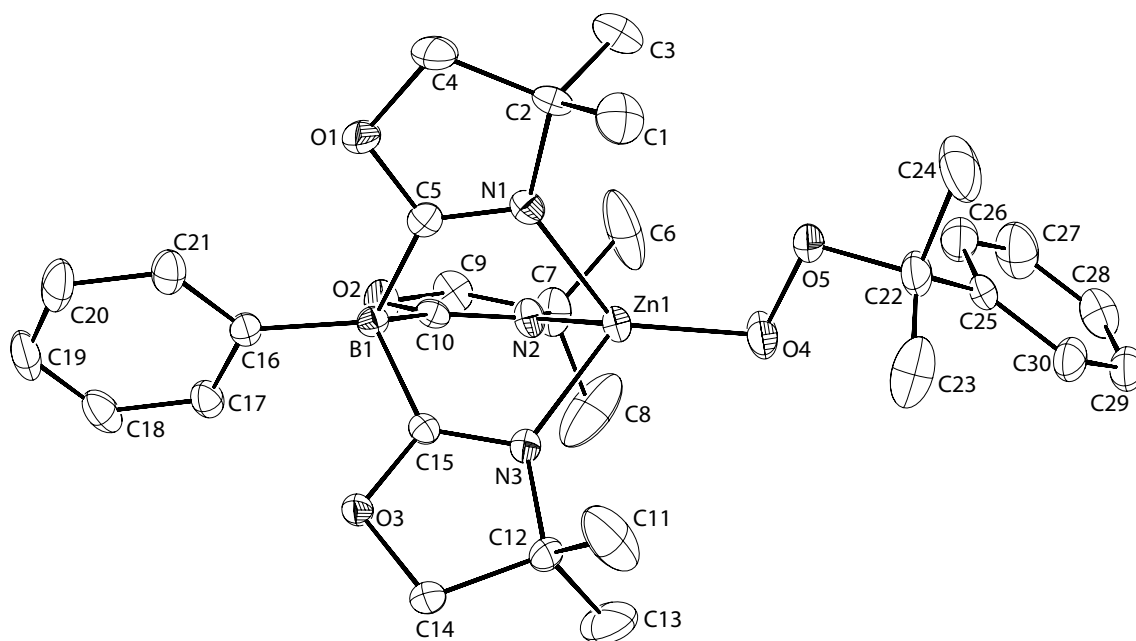


Figure S-21. ORTEP diagram of $\text{To}^{\text{M}}\text{ZnOOCMe}_2\text{Ph}$ (**12**). Ellipsoids are drawn at 35% probability. Hydrogen atoms are not shown for clarity.

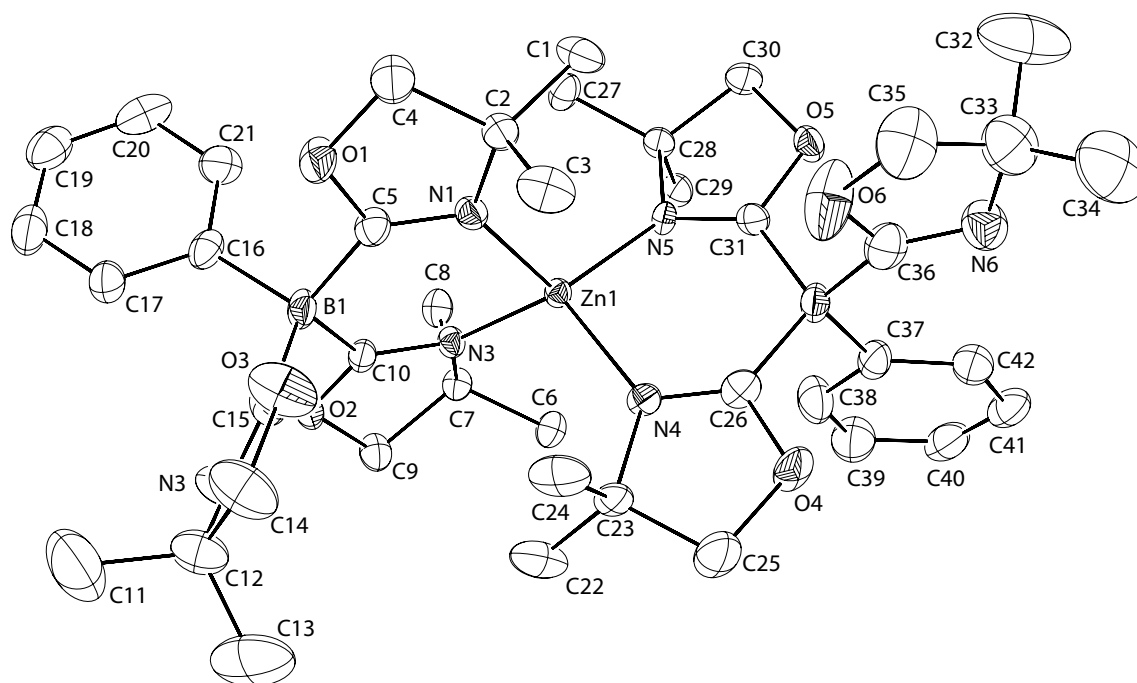


Figure S-22. ORTEP diagram of $(\text{To}^{\text{M}})_2\text{Zn}$ (**14**). Ellipsoids are drawn at 35% probability. Hydrogen atoms and two toluene solvent molecules are not shown for clarity.

Chapter 6: Divergent reaction pathways of tris(oxazolinyl)borato zinc and magnesium silyl compounds

Modified from a paper published in *Chemical Communications*[‡]

Debabrata Mukherjee,^a Nicole L. Lampland,^a KaKing Yan,^a James F. Dunne,^a Arkady Ellern,^a and Aaron D. Sadow^{*a}

Department of Chemistry, U.S. DOE Ames Laboratory, Iowa State University, Ames, IA

50011-3111

This work has been carried out in collaboration with other people in our lab.[❖]

Abstract.

Synthesis and reactivity of monomeric magnesium and zinc silyl compounds $To^M M-Si(SiHMe_2)_3$ and $To^M M-Si(SiMe_3)_3$ are described ($To^M =$ tris(4,4-dimethyl-2-oxazolinyl)phenylborate). The magnesium compounds react slowly with water and air, while the zinc compounds are inert. With CO_2 , $To^M Mg-Si(SiHMe_2)_3$ provides $To^M MgO_2CSi(SiHMe_2)_3$ through CO_2 insertion, whereas $To^M Zn-Si(SiHMe_2)_3$ affords $To^M ZnOCHO$.

❖ Other Author's contributions

Nicole L. Lampland: Synthesis and characterization of $HO_2CSi(SiHMe_2)_3$; Independent synthesis and characterization of $To^M MO_2CSi(SiHMe_2)_3$ using $HO_2CSi(SiHMe_2)_3$, DOSY-NMR experiments and several other NMR experiments including thermal stability check and reactions with CO_2 , moisture, methanol, and HCl etc. Mechanistic study for the transformation of $To^M ZnSi(SiHMe_2)_3$ to $To^M ZnOCHO$ from the reaction with CO_2 .

Kaking Yan: First person in our group to synthesize the silyl ligands, $\text{KSi}(\text{SiHMe}_2)_3$ and $\text{KSi}(\text{SiMe}_3)_3$.

James F. Dunne: First person in our group to synthesize the magnesium starting materials, $\text{To}^{\text{M}}\text{MgBr}$ and $\text{To}^{\text{M}}\text{MgMe}$, used in this study. Also, the first person to observe the formation of $\text{To}^{\text{M}}\text{MgOMe}$ species in NMR-scale reaction between $\text{To}^{\text{M}}\text{MgMe}$ and MeOH.

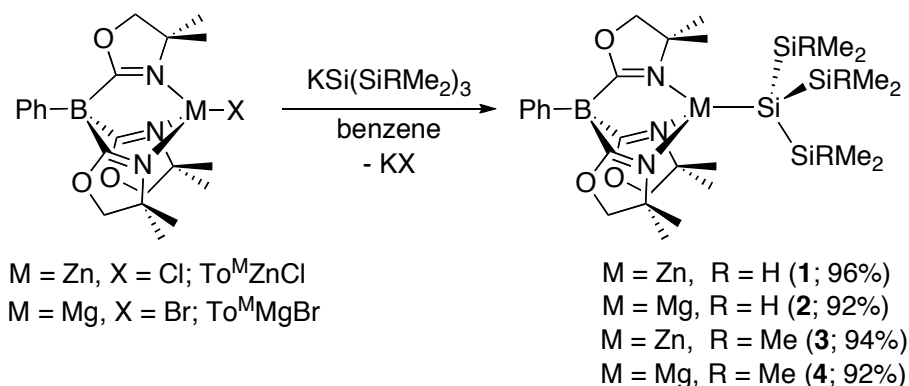
Introduction.

Zinc and magnesium alkyls are among the earliest and most frequently used organometallic compounds, whereas related metal silyls have received less attention. Magnesium and zinc-catalyzed hydrosilylations¹ and dehydrogenative silylations² involve mixtures of organosilanes and these main group organometallics. However, metal silyl species are generally not postulated intermediates in most proposed catalytic cycles for such transformations, and studies of main-group metal silyl compounds have mostly focused on structural characterization and applications in transmetalation.^{3,4} Less is known about their reactivity in steps that might be involved in catalysis. Metal silyl compounds, supported by tris(oxazolanyl)borate ancillaries employed in our catalytic investigations, may provide further insight into catalysis, possible side reactions, and the fundamental reactivity of these compounds.

Results and Discussion.

The targeted silyl complexes $\text{To}^{\text{M}}\text{ZnSi}(\text{SiHMe}_2)_3$ (**1**), $\text{To}^{\text{M}}\text{MgSi}(\text{SiHMe}_2)_3$ (**2**), $\text{To}^{\text{M}}\text{ZnSi}(\text{SiMe}_3)_3$ (**3**) and $\text{To}^{\text{M}}\text{MgSi}(\text{SiMe}_3)_3$ (**4**) (To^{M} = tris(4,4-dimethyl-2-oxazolanyl)phenylborate) are efficiently prepared by salt metathesis reactions. $\text{To}^{\text{M}}\text{ZnCl}^5$ or $\text{To}^{\text{M}}\text{MgBr}$ react with the appropriate potassium silyl reagent, $\text{KSi}(\text{SiHMe}_2)_3$ or $\text{KSi}(\text{SiMe}_3)_3$,⁶

in benzene at ambient temperature (Scheme 1).



Scheme 1. Synthesis of Zinc silyls and Magnesium silyls

Compounds **1**, **2** and **4** are formed quantitatively within 30 min at ambient temperature, whereas the preparation of compound **3** requires longer time (2 h). One set of oxazoline resonances was observed in the ¹H NMR spectra for compounds **1–4** (as well as all the To^MMX compounds reported here). This pattern is consistent with time-averaged C_{3v}-symmetry for the complexes and suggests tridentate coordination of To^M. Downfield SiH chemical shifts of **1** (4.64 ppm) and **2** (4.71 ppm), high silicon–hydrogen coupling constants (¹J_{SiH} = 172.2 and 169.7 Hz respectively), and infrared bands assigned to the ν_{SiH} of **1** (2064 cm⁻¹) and **2** (2064 cm⁻¹) are consistent with terminal, 2-center-2-electron bonded Si–H moieties. In addition, the infrared spectra provide support for tridentate To^M coordination by the single ν_{CN} band for each compound (**1** and **3**: 1591 cm⁻¹; **2** and **4**: 1582 cm⁻¹).

Single crystal X-ray analyses of **1** (Fig. 1) and **3** further support the spectroscopically assigned structures.^{7,8} Terminal β-SiH's in **1** are located in the difference Fourier map, but

the $\text{Si}(\text{SiHMe}_2)_3$ is disordered. In the model, the three SiHMe_2 groups are oriented with the SiH's pointing away from the zinc center and are related by pseudo- C_3 rotations.

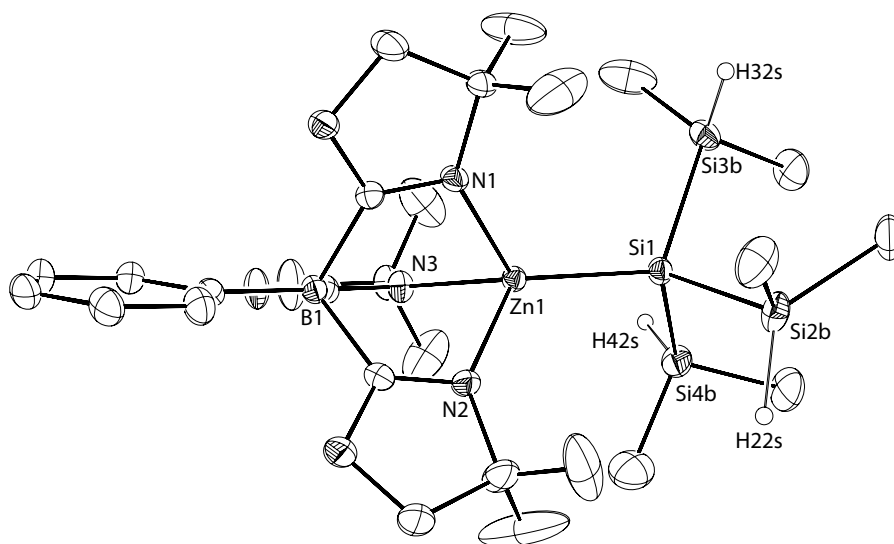


Fig. 1 ORTEP diagram of $\text{To}^{\text{M}}\text{ZnSi}(\text{SiHMe}_2)_3$ (**1**) with ellipsoids plotted at 35% probability. One of the $\text{Si}(\text{SiHMe}_2)_3$ positions and the hydrogen atoms on To^{M} and Me groups are not illustrated for clarity.

The Zn1–Si1 interatomic distance is slightly shorter in **1** (2.4028(5) Å) than in **3** (2.427(1) Å), and these distances are on the long side compared to other zinc silyls. For example, the Zn–Si distances in $\text{Zn}(\text{Si}(\text{SiMe}_3)_2)_2$,⁴ $((\text{Me}_3\text{Si})_3\text{SiZnCl}(\text{thf}))_2$,⁹ and $(\text{Ph}(\text{Me}_3\text{Si})_2\text{SiZnCl}(\text{thf}))_2$ are similar (2.35 ± 0.01 Å).⁹ Sterically hindered groups give longer Zn–Si distances; for example, the distances in $\text{Zn}(\text{Si}(\text{SiMe}_3)_2\text{Si}(\text{SiMe}_3)_3)_2$ are $\sim 2.405 \pm 0.002$ Å.¹⁰

Metal silyls **1–4** are thermally resilient, and starting materials are recovered after heating toluene- d_8 solutions in sealed NMR tubes at 170 °C for 24 h. Furthermore, the zinc compounds **1** and **3** are inert to reaction with O_2 at pressures up to 100 psi and temperatures up to 120 °C for 24 h, under a 450 W Hg lamp at ambient temperature, or in the presence of

AIBN at 60 °C. For comparison, $\text{To}^{\text{M}}\text{ZnH}$ and $\text{To}^{\text{M}}\text{ZnMe}$ also are inert to O_2 , whereas $\text{To}^{\text{M}}\text{ZnR}$ compounds react with O_2 following the trend ($\text{R} = \text{Et} < n\text{-C}_3\text{H}_7 < i\text{-C}_3\text{H}_7 < t\text{-Bu}$) to form isolable alkylperoxyzinc species.¹¹ These data suggest that, despite their steric bulk, the resistance of **1** and **3** to oxidation may result from electronic effects associated with the To^{M} ligand. For comparison, $\text{Zn}(\text{Si}(\text{SiMe}_3)_3)_2$ and $\text{Zn}(\text{Si}(\text{SiMe}_3)_3)_2\text{TMEDA}$ are air sensitive (the TMEDA adduct reacts slowly in air).⁴

Magnesium silyls **2** and **4** react slowly with 1 atm of O_2 at ambient temperature over 24 and 36 h forming mixtures of unidentified species. Under similar reaction conditions, $\text{To}^{\text{M}}\text{MgMe}$ and O_2 form $(\text{To}^{\text{M}}\text{Mg}(\mu\text{-OMe}))_2$ (**5**) within 5 min.. Compound **5** is crystallographically characterized as a dimer containing tri-dentate tris(oxazolonyl)borate and bridging methoxide ligands (Fig. 2), centered on a two-fold axis.¹² The ^1H NMR spectrum is consistent with pseudo- C_{3v} symmetry.

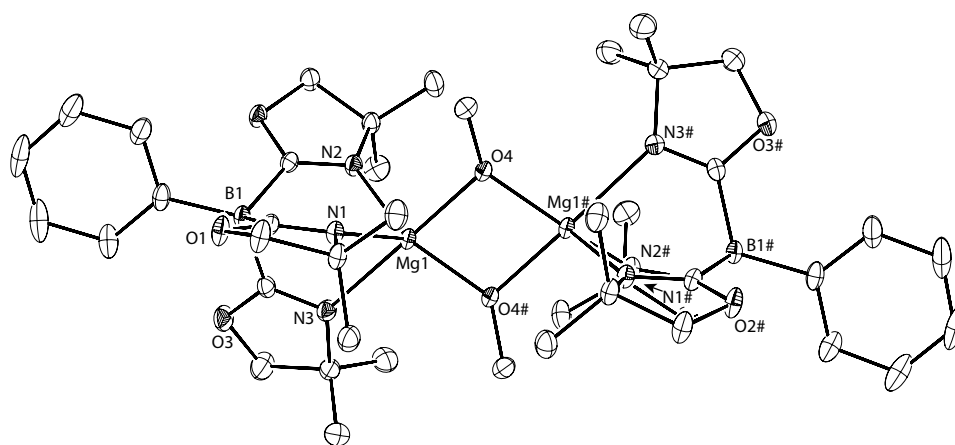
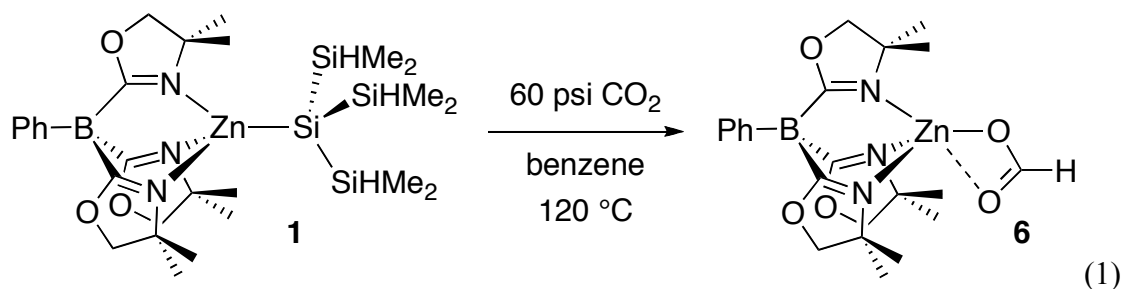


Fig. 2 ORTEP diagram of $(\text{To}^{\text{M}}\text{MgOMe})_2$ (**5**) with ellipsoids plotted at 35% probability. Symmetry-related atoms are labelled with #. Hydrogen atoms and two benzene molecules are not plotted for clarity.

Surprisingly, zinc silyls **1** and **3** are also inert to water and methanol. Only starting materials are detected after attempted thermolysis of **1** or **3**, benzene-*d*₆, and excess water at 80 °C for 12 h. **1** and **3** are insoluble in pure water, and the ¹H NMR spectra of the solids recovered from water and redissolved in benzene-*d*₆ contain only signals assigned to the zinc silyls. Similarly, **1** and **3** are insoluble in methanol at room temperature. A suspension of **1** partly dissolves in methanol-*d*₄ after heating at 60 °C for 4 h. The ¹H NMR spectrum of the resulting solution contained silyl and oxazoline resonances for **1** that are distinct from HSi(SiHMe₂)₃ and To^MZnOMe. Additionally, the ¹H NMR spectrum (acquired in benzene-*d*₆) of the solid recovered from methanol contained only signals assigned to **1**. This inert nature **5** contrasts the reactions of To^MZnR (R = H, alkyl, phenyl) and H₂O that provide a trimeric hydroxide (To^MZnOH)₃.¹¹ Addition of 12 M HCl to a benzene-*d*₆ solution of **1**, however, produces HSi(SiHMe₂)₃. The magnesium silyls **2** and **4** are hydrolytically sensitive, forming hydrosilanes HSi(SiHMe₂)₃ and HSi(SiMe₃)₃ 10 upon treatment with water. Compounds **2** and **4** slowly react with methanol (**2**: 4 h, r.t.; **4**: 5 h, r.t.) to provide **5**. Note that To^MMgMe and methanol provide **5** quantitatively after 5 min in benzene. Interestingly, **1** and CO₂ (60 psi) react at 120 °C to form the zinc formate To^MZnOCHO (**6**) (t_{1/2} = 18 h, eqn (1)). The ¹H NMR spectrum of **6** contained a downfield singlet resonance attributed to the ZnOCHO (8.76 ppm); a similar signal was reported for Tp^{tBu}ZnOCHO (Tp^{tBu} = tris(3-*tert*-butyl-pyrazolyl)borate) (8.91 ppm).¹³ A peak at 169 ppm in the ¹³C{¹H} NMR spectrum of **6** was assigned to the formate carbon.



The identity of compound **6** is further supported by its independent preparation from $\text{To}^{\text{M}}\text{ZnH}$ and CO_2 (1 atm) in benzene at ambient temperature. Two new bands in the solid-state infrared spectrum of **6** at 1629 and 1307 cm^{-1} are assigned to the $\nu_{\text{CO}(\text{asym})}$ and $\nu_{\text{CO}(\text{sym})}$ of the $[\text{Zn}]\text{OCHO}$ moiety; the $\Delta\nu_{\text{CO}}$ of 322 cm^{-1} suggests monodentate formate coordination.¹⁴ For comparison, the assigned bands for $\text{Tp}^{\text{tBu}}\text{ZnOCHO}$ are 1655 and 1290 cm^{-1} ($\Delta\nu_{\text{CO}} = 365\text{ cm}^{-1}$), and the bands for TptmZnOCHO are 1621 and 1317 cm^{-1} ($\Delta\nu_{\text{CO}} = 304\text{ cm}^{-1}$, $\text{Tptm} = \text{tris}(2\text{-pyridylthio})\text{methane}$).¹⁵

An X-ray structure determination provides additional characterization of **6** (Fig. 3).¹⁶ The zinc–oxygen distances associated with the formate moiety are inequivalent (Zn1–O4 , $1.909(1)$; Zn1–O5 , 2.792 \AA). The first distance is equal to the sum of covalent radii of Zn–O (1.9 \AA),¹⁷ and the latter distance is slightly shorter than the sum of van der Waal radii (2.91 \AA). For comparison, the Zn–O distance in monomeric $\text{To}^{\text{M}}\text{ZnO}^{\text{tBu}}$ is $1.835(1)\text{ \AA}$,⁵ whereas the distance in TptmZnOCHO is $2.036(1)\text{ \AA}$.¹⁵

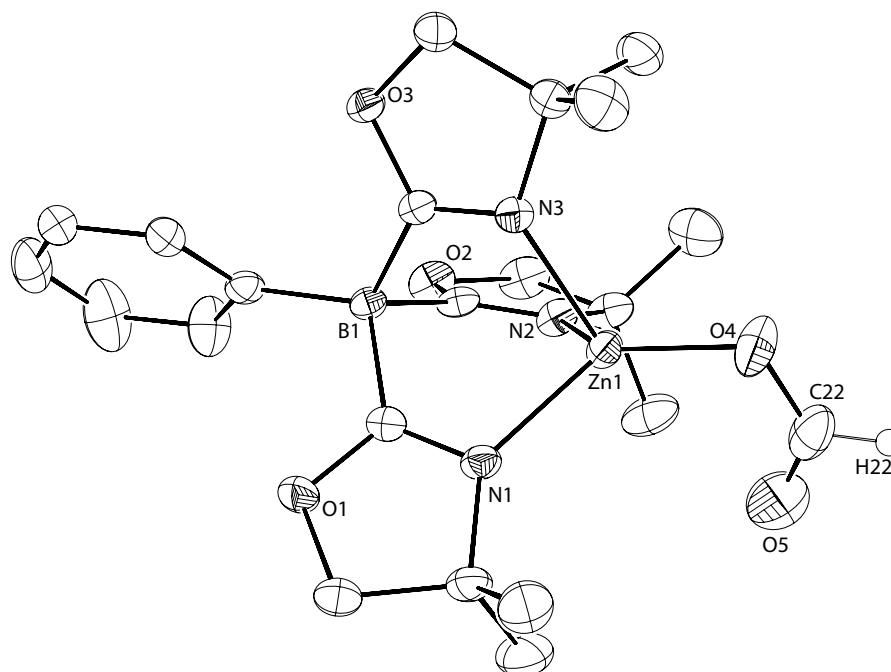
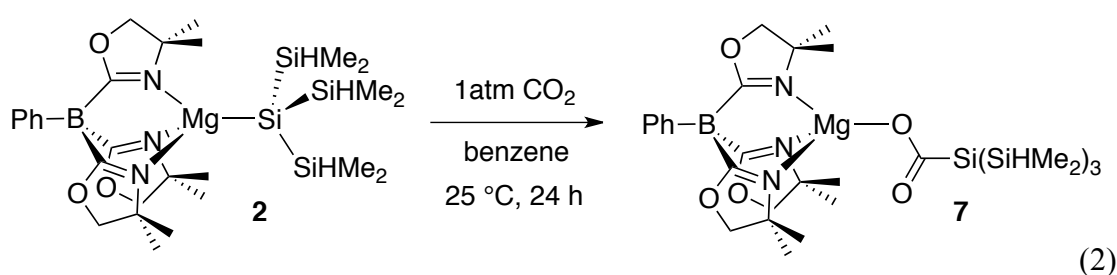


Fig. 3 ORTEP diagram of $To^M ZnOCHO$ (**6**), with ellipsoids plotted at 35% probability. Only the formate hydrogen atom is illustrated.

Interestingly, reactions of CO_2 with isostructural **1** and **2** provide dissimilar products. CO_2 (1 atm) reacts with **2** at ambient temperature in benzene to give $To^M MgO_2CSi(SiHMe_2)_3$ (**7**) quantitatively over 24 h (eqn (2)).



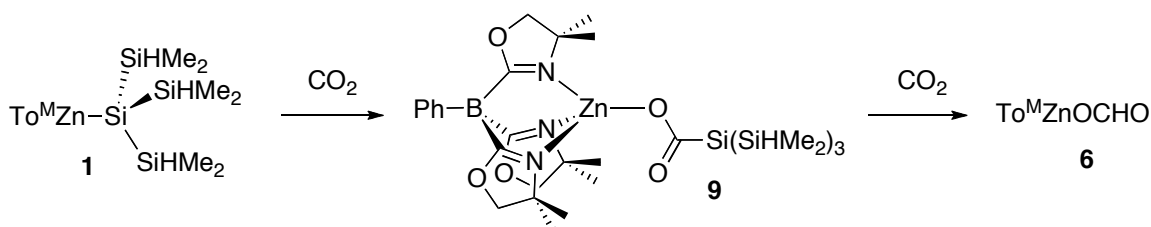
Higher temperature and greater CO_2 pressure increase the reaction rate. For example, complete conversion of **2** to **7** is achieved in 45 min at $100\text{ }^\circ\text{C}$ with 70 psi of CO_2 . A $^{13}\text{C}\{^1\text{H}\}$

NMR resonance at 202.61 ppm is assigned to the silanecarboxylate $\text{MgOC(O)Si(SiHMe}_2)_3$. This value is similar to those of other metal silanecarboxylates, such as monomeric $\text{Mo(=NAryl)(=CHCMe}_2\text{Ph)\{O}_2\text{CSi(SiMe}_3)_3\}_2$ (211.4 ppm, Aryl = 2,6- $\text{C}_6(i\text{-C}_3\text{H}_7)_2\text{H}_3$)¹⁸ and $(\text{Cp}_2\text{Sc}\{\mu\text{-O}_2\text{CSi(SiMe}_3)_3\})_2$ (200.81 ppm).¹⁹ Unfortunately, X-ray diffraction experiments on **7** were unsuccessful, and the IR bands associated with silanecarboxylate were not assigned. Compound **7** was characterized as a monomeric species by DOSY experiments that reveal similar diffusion constants of monomeric **2** ($6.95 \times 10^{-10} \text{ m}^2 \text{ s}^{-1}$) and **7** ($6.85 \times 10^{-10} \text{ m}^2 \text{ s}^{-1}$) (See Experimental section).

Compound **7** is thermally robust, and the starting material is unchanged after a benzene- d_6 solution is heated at 120 °C for 12 h. During the conversion of **2** to **7**, signals assigned to those two compounds are the only ones observed in the ^1H NMR spectra of reaction mixtures. In contrast, $\text{Cp}_2\text{Zr}(\eta^2\text{-SiMe}_2\text{N}^t\text{Bu})$ and CO_2 react to give the decarbonylated product $[\text{Cp}_2\text{Zr}(\mu\text{-O-}\kappa^2\text{-O,N-O-SiMe}_2\text{N}^t\text{Bu})]_2$ and CO .²⁰ The dimeric silanecarboxylate $(\text{Cp}_2\text{Sc}\{\mu\text{-O}_2\text{CSi(SiMe}_3)_3\})_2$ is unchanged after 60 h at 95 °C.¹⁹ However, a side-product, postulated to be $\text{Cp}_2\text{ScOSi(SiMe}_3)_3$, is formed during the reaction of $\text{Cp}_2\text{ScSi(SiMe}_3)_3$ THF and CO_2 . This species may form from $\text{Cp}_2\text{ScO}_2\text{CSi(SiMe}_3)_3$ prior to dimerization.

Additional evidence for Si–C bond formation is provided by the reaction of **7** and MeOH, which gives compound **5** and $\text{HO}_2\text{CSi(SiHMe}_2)_3$ (**8**). Compounds **7** and **8** are characterized by their independent preparation: **8** is synthesized by adapting a literature procedure for $\text{HO}_2\text{CSi(SiMe}_3)_3$.²¹ Compound **7** is independently prepared from $\text{To}^{\text{M}}\text{MgMe}$ and **8**. The identical spectroscopic properties of the two species support the assignment of **7** as a silanecarboxylate.

$\text{To}^{\text{M}}\text{ZnO}_2\text{CSi}(\text{SiHMe}_2)_3$ (**9**) is a possible intermediate in the formation of **6** from **2**. Therefore, the zinc silanecarboxylate $\text{To}^{\text{M}}\text{ZnO}_2\text{CSi}(\text{SiHMe}_2)_3$ was prepared from $\text{To}^{\text{M}}\text{ZnEt}$ and **8**. The $^{13}\text{C}\{^1\text{H}\}$ NMR spectrum of **9** contained a resonance at 193.38 ppm assigned to the carboxylate. The diffusion constant $6.43 \times 10^{-10} \text{ m}^2 \text{ s}^{-1}$ obtained from a DOSY experiment in benzene- d_6 indicated that **9** is monomeric in solution. Thermolysis of **9** at 120 °C for 12 h under a N_2 atmosphere returns starting material unchanged. However, thermal treatment of **9** under 60 psi of CO_2 at 120 °C affords the formate **6** ($t_{1/2} = 6 \text{ h}$). Thus, a plausible and kinetically competent pathway for the formation of **6** is shown in Scheme 2, although **9** is not detected in the reaction mixture and our current evidence does not rule out a one step pathway. We are currently investigating this transformation to better understand the route(s) to compound **6**.



Scheme 2 A possible pathway for the formation of $\text{To}^{\text{M}}\text{ZnOCHO}$ from **1** and CO_2 .

Conclusion.

Still, the dichotomic reactivity of isostructural zinc and magnesium silyls and silylcarboxylates toward carbon dioxide is intriguing. In addition, the reaction of zinc silylcarboxylate **9** with CO_2 provides a new fundamental step that could be applied in catalytic CO_2 conversions.

References.

- (1) B. Marciniec, *Hydrosilylation: A comprehensive Review on Recent Advances*, Springer, Berlin, 2009; H. Mimoun, J. Y. de Saint Laumer, L. Giannini, R. Scopelliti and C. Floriani, *J. Am. Chem. Soc.*, 1999, **121**, 6158–6166; V. M. Mastranzo, L. Quintero, C. Anaya de Parrodi, E. Juaristi and P. J. Walsh, *Tetrahedron*, 2004, **60**, 1781–1789; V. Bette, A. Mortreux, D. Savoia and J.-F. Carpentier, *Adv. Synth. Catal.*, 2005, **347**, 289–302; S. Gérard, Y. Pressel and O. Riant, *Tetrahedron: Asymmetry*, 2005, **16**, 1889–1891.
- (2) H. Mimoun, *J. Org. Chem.*, 1999, **64**, 2582–2589; D. Mukherjee, R. R. Thompson, A. Ellern and A. D. Sadow, *ACS Catal.*, 2011, 698–702; J. F. Dunne, S. R. Neal, J. Engelkemier, A. Ellern and A. D. Sadow, *J. Am. Chem. Soc.*, 2011, **133**, 16782–16785.
- (3) C. Marschner, *Organometallics*, 2006, **25**, 2110–2125.
- (4) J. Arnold, T. D. Tilley, A. L. Rheingold and S. J. Geib, *Inorg. Chem.*, 1987, **26**, 2106–2109.
- (5) D. Mukherjee, A. Ellern and A. D. Sadow, *J. Am. Chem. Soc.*, 2010, **132**, 7582–7583.
- (6) C. Marschner, *Eur. J. Inorg. Chem.*, 1998, 221–226.
- (7) Crystal data for $C_{27}H_{47}BN_3O_3Si_4Zn$ (**1**), $M = 650.22$, monoclinic, $P2_1/c$, $a = 9.4488(12) \text{ \AA}$, $b = 27.824(4) \text{ \AA}$, $c = 13.6110(18) \text{ \AA}$, $\beta = 93.087(2)^\circ$, $V = 3573.2(8) \text{ \AA}^3$, $T = 173(2) \text{ K}$, $Z = 4$, reflections: 38908 collected, 9895 independent ($R_{\text{int}} = 0.0609$), $R_1 = 0.0471$, $wR_2 = 0.1285$ ($I > 2\sigma(I)$).
- (8) Crystal data for $C_{30}H_{56}BN_3O_3Si_4Zn$ (**3**), $M = 695.32$, triclinic, $P1$, $a = 10.242(4) \text{ \AA}$, $b = 11.576(4) \text{ \AA}$, $c = 17.786 \text{ \AA}$, $\alpha = 92.073(6)^\circ$, $\beta = 106.240(6)^\circ$, $\gamma = 103.685(6)^\circ$, $V = 1955(1) \text{ \AA}^3$, $T = 173(2) \text{ K}$, $Z = 2$, reflections: 15694 collected, 6954 independent ($R_{\text{int}} = 0.0690$), $R_1 = 0.0468$, $wR_2 = 0.0783$ ($I > 2\sigma(I)$).
- (9) M. Nanjo, T. Oda and K. Mochida, *J. Organomet. Chem.*, 2003, **672**, 100–108.

- (10) W. Gaderbauer, I. Balatoni, H. Wagner, J. Baumgartner and C. Marschner, *Dalton Trans.*, 2010, **39**, 1598–1603.
- (11) D. Mukherjee, A. Ellern and A. D. Sadow, *J. Am. Chem. Soc.*, 2012, **134**, 13018–13026.
- (12) Crystal data for $C_{56}H_{76}B_2Mg_2N_6O_8$ (**5**), $M = 1031.47$, monoclinic, $C2/c$, $a = 9.500(2)$ Å, $b = 26.648(6)$ Å, $c = 22.844(5)$ Å, $\beta = 97.235(3)^\circ$, $V = 5753(2)$ Å³, $T = 173(2)$ K, $Z = 4$, reflections: 29698 collected, 7356 independent ($R_{int} = 0.0326$), $R_1 = 0.0403$, $wR_2 = 0.1001$ ($I > 2\sigma(I)$).
- (13) A. Looney, R. Han, I. B. Gorrell, M. Cornebise, K. Yoon, G. Parkin and A. L. Rheingold, *Organometallics*, 1995, **14**, 274–288.
- (14) G. B. Deacon and R. J. Phillips, *Coord. Chem. Rev.*, 1980, **33**, 227–250.
- (15) W. Sattler and G. Parkin, *J. Am. Chem. Soc.*, 2011, **133**, 45 9708–9711.
- (16) Crystal data for $C_{22}H_{30}BN_3O_5Zn$ (**6**), $M = 492.67$, monoclinic, $P2_1/c$, $a = 11.1030(5)$ Å, $b = 13.3614(5)$ Å, $c = 16.2115(7)$ Å, $\beta = 95.795(1)^\circ$, $V = 2392.7(2)$ Å³, $T = 173(2)$ K, $Z = 4$, reflections: 24027 collected, 5942 independent ($R_{int} = 0.0369$), $R_1 = 0.0307$, $wR_2 = 0.0699$ ($I > 2\sigma(I)$).
- (17) B. Cordero, V. Gomez, A. E. Platero-Prats, M. Reves, J. Echeverria, E. Cremades, F. Barragan and S. Alvarez, *Dalton Trans.*, 2008, 2832–2838.
- (18) R. R. Schrock, Z. J. Tonzetich, A. G. Lichtscheidl, P. Müller and F. J. Schattenmann, *Organometallics*, 2008, **27**, 3986–3995.
- (19) B. K. Campion, R. H. Heyn and T. D. Tilley, *Inorg. Chem.*, 1990, **29**, 4355–4356.
- (20) L. J. Procopio, P. J. Carroll and D. H. Berry, *Organometallics*, 1993, **12**, 3087–3093.
- (21) A. G. Brook and L. Yau, *J. Organomet. Chem.*, 1984, **271**, 9–14.

Experimental data

General Procedures. All reactions were performed under a dry argon atmosphere using standard Schlenk techniques or under a nitrogen atmosphere in a glovebox, unless otherwise indicated. Benzene, toluene, pentane, diethyl ether, and tetrahydrofuran were dried and deoxygenated using an IT PureSolv system. Benzene- d_6 was heated to reflux over Na/K alloy and vacuum-transferred. The starting materials (TMEDA)MgMeBr,¹ H[To^M],² To^MMgMe,³ To^MZnCl,⁴ Si(SiHMe₂)₄,⁵ and KSi(SiMe₃)₃⁶ were synthesized according to literature procedures. ¹H, ¹³C{¹H}, ²⁹Si and ¹¹B NMR spectra were collected on Agilent MR-400, Bruker DRX400 or AVIII 600 spectrometers. ¹¹B NMR spectra were referenced to an external BF₃OEt₂ standard. ²⁹Si NMR spectra were acquired with INEPT sequences and referenced to an external SiMe₄ standard. ¹⁵N chemical shifts were determined by ¹H-¹⁵N HMBC experiments on a Bruker AVII 600 spectrometer with a Bruker Z-gradient inverse TXI ¹H/¹³C/¹⁵N 5mm cryoprobe; ¹⁵N chemical shifts were originally referenced to an external liquid NH₃ standard and recalculated to the CH₃NO₂ chemical shift scale by adding -381.9 ppm. Elemental analyses were performed using a Perkin-Elmer 2400 Series II CHN/S by the Iowa State Chemical Instrumentation Facility. X-ray diffraction data was collected on a Bruker APEX II diffractometer.

Caution! High-pressure glass apparatuses must be handled with care. Thick-walled NMR tubes equipped with J. Young-style resealable Teflon valves (pressured to 100 psi with CO₂) were obtained from Wilmad-Labglass and attached to a high-pressure steel manifold through commercial Swagelock fittings. The pressurized NMR tubes were handled in protective

jackets.

To^MMgBr(THF)₂. H[To^M] (0.100 g, 4.25 mmol) and (TMEDA)MgMeBr (0.163 g, 4.25 mmol) were dissolved in THF and stirred for 30 min at ambient temperature. The volatile materials were evaporated, the residue was washed with pentane (3 × 5 mL), and the resulting white solid was dried under vacuum to provide To^MMgBr(THF)₂ (0.230 g, 0.365 mmol, 85.8%). Analytically pure To^MMgBr(THF)₂ and X-ray quality single crystals were obtained from a concentrated THF solution of To^MMgBr(THF)₂ at -30 °C. Additionally, the quantity of THF in the product can vary from zero to two equivalents; the data is given for a batch isolated with two equivalents of THF. ¹H NMR (400 MHz, benzene-*d*₆): δ 1.06 (s, 18 H, CNCMe₂CH₂O), 1.42 (t, ³J_{HH} = 6.6 Hz, 8 H, β-THF), 3.36 (s, 6 H, CNCMe₂CH₂O), 3.58 (t, ³J_{HH} = 6.6 Hz, 8 H, α-THF), 7.36 (t, ³J_{HH} = 7.2 Hz, 1 H, *para*-C₆H₅), 7.53 (t, ³J_{HH} = 7.2 Hz, 2 H, *meta*-C₆H₅), 8.23 (d, ³J_{HH} = 7.2 Hz, 2 H, *ortho*-C₆H₅). ¹³C {¹H} NMR (benzene-*d*₆, 175 MHz): δ 26.15 (β-THF), 28.44 (CNCMe₂CH₂O), 65.64 (CNCMe₂CH₂O), 68.17 (α-THF), 80.80 (CNCMe₂CH₂O), 126.54 (*para*-C₆H₅), 127.32 (*meta*-C₆H₅), 136.32 (*ortho*-C₆H₅), 142.84 (br, *ipso*-C₆H₅), 191.30 (br, CNCMe₂CH₂O). ¹¹B NMR (128 MHz, benzene-*d*₆): δ -18.2. ¹⁵N NMR: δ -160.9. IR (KBr, cm⁻¹): 3050 (m), 2972 (s), 2873 (m), 1599 (s, ν_{CN}), 1492 (w), 1462 (s), 1433 (m), 1389 (m), 1371 (s), 1354 (m), 1303 (m), 1273 (s), 1253 (m), 1197 (s), 1155 (s), 1047 (s), 995 (s), 966 (s), 939 (m), 890 (m), 843 (m), 822 (w), 777 (w), 708 (m), 695 (s), 685 (w), 666 (w), 649 (w). Anal. Calcd. for C₂₉H₄₅BBrMgN₃O₅: C, 55.23; H, 7.19; N, 6.66. Found: C, 54.75; H, 6.70; N, 6.58. Mp: 251-253 °C.

KSi(SiHMe₂)₃. Si(SiHMe₂)₄ (6.00 g, 0.027 mol) and KO^tBu (3.95 g, 0.027 mol) were dissolved in benzene (25 mL). The solution was allowed to stir for 30 min, and the product

precipitated as a white solid during this time. The solid was isolated by filtration, washed with pentane, and recrystallized from toluene at $-30\text{ }^{\circ}\text{C}$ to give a white crystalline solid (5.99 g, 0.024 mol, 90.7%). ^1H NMR (benzene- d_6 , 600 MHz): δ 0.559 (d, 18 H, $^3J_{\text{HH}} = 4.5$ Hz, SiHMe_2), 4.22 (sept, 3 H, $^3J_{\text{HH}} = 4.5$ Hz, $^1J_{\text{SiH}} = 151.8$ Hz, SiHMe_2). $^{13}\text{C}\{^1\text{H}\}$ NMR (benzene- d_6 , 150 MHz): δ 2.47 (SiHMe_2). ^{29}Si (benzene- d_6 , 119.3 MHz) δ -23.8 (SiHMe_2), -202.3 ($\text{Si}(\text{SiHMe}_2)_3$). IR (KBr, cm^{-1}): 2959 (s), 2894 (s), 2020 (s, ν_{SiH}), 1419 (m), 1242 (s), 1041 (s), 872 (s), 766 (m), 685 (m), 645 (m). Anal. Calcd. for $\text{C}_6\text{H}_{21}\text{KSi}_4$: C, 29.45; H, 8.65. Found C, 29.20; H, 8.51. Mp 123-125 $^{\circ}\text{C}$.

To^MZnSi(SiHMe₂)₃ (1). To^MZnCl (0.235 g, 0.486 mmol) and KSi(SiHMe₂)₃ (0.119 g, 0.486 mmol) were dissolved in benzene, and the reaction mixture was stirred for 30 min. The reaction mixture was filtered to remove KCl, the filtrate was evaporated, and the resulting solid residue was washed with pentane and dried under vacuum to afford To^MZnSi(SiHMe₂)₃ (0.303 g, 0.464 mmol, 95.5%) as an analytically pure white solid. X-ray quality single crystals were grown by slow pentane diffusion into a concentrated toluene solution of To^MZnSi(SiHMe₂)₃ at $-30\text{ }^{\circ}\text{C}$. ^1H NMR (400 MHz, benzene- d_6): δ 0.57 (d $^3J_{\text{HH}} = 4.4$ Hz, 18 H, SiHMe_2), 1.14 (s, 18 H, $\text{CNCMe}_2\text{CH}_2\text{O}$), 3.45 (s, 6 H, $\text{CNCMe}_2\text{CH}_2\text{O}$), 4.64 (sept, $^3J_{\text{HH}} = 4.4$ Hz, 3 H, SiHMe_2), 7.35 (t, $^3J_{\text{HH}} = 7.2$ Hz, 1 H, *para*- C_6H_5), 7.53 (t, $^3J_{\text{HH}} = 7.6$ Hz, 2 H, *meta*- C_6H_5), 8.31 (d, $^3J_{\text{HH}} = 7.2$ Hz, 2 H, *ortho*- C_6H_5). $^{13}\text{C}\{^1\text{H}\}$ NMR (175 MHz, benzene- d_6): δ 0.16 (SiHMe_2), 28.76 ($\text{CNCMe}_2\text{CH}_2\text{O}$), 66.08 ($\text{CNCMe}_2\text{CH}_2\text{O}$), 81.06 ($\text{CNCMe}_2\text{CH}_2\text{O}$), 126.37 (*para*- C_6H_5), 127.30 (*meta*- C_6H_5), 136.46 (*ortho*- C_6H_5), 142.30 (br, *ipso*- C_6H_5), 190.18 (br, $\text{CNCMe}_2\text{CH}_2\text{O}$). ^{11}B NMR (128 MHz, benzene- d_6): δ -18.5 . ^{29}Si NMR (120 MHz, benzene- d_6): δ -28.3 ($^1J_{\text{SiH}} = 172.2$ Hz, $\text{Si}(\text{SiHMe}_2)_3$), -171.3

(*Si*(*SiHMe*₂)₃). ¹⁵N NMR (59.2 MHz, benzene-*d*₆): δ -157.4. IR (KBr, cm⁻¹): 3079 (w), 2967 (s), 2897 (m), 2064 (s, ν_{SiH}), 1591 (s, ν_{CN}), 1495 (w), 1462 (m), 1431 (w), 1387 (m), 1368 (m), 1276 (s), 1241 (s), 1195 (s), 1158 (s), 961 (s), 867 (s), 747 (m), 703 (s). Anal. Calcd. for C₂₇H₅₀BSi₄N₃O₃Zn: C, 49.64; H, 7.71; N, 6.43. Found: C, 49.21; H, 7.58; N, 6.37. Mp: 208-210 °C.

To^MMgSi(*SiHMe*₂)₃ (2). To^MMgBr(THF)₂ (0.706 g, 1.12 mmol) and KSi(*SiHMe*₂)₃ (0.275 g, 1.12 mmol) were dissolved in benzene (12 mL) and stirred for 30 min at ambient temperature. The reaction mixture was filtered, and evaporation of the filtrate gave a white solid. The solid was washed with pentane (3 × 5 mL) and dried under vacuum providing crystalline, analytically pure To^MMgSi(*SiHMe*₂)₃ (0.630 g, 1.03 mmol, 91.5%). X-ray quality single crystals were obtained from a concentrated toluene solution cooled to -30 °C. ¹H NMR (600 MHz, benzene-*d*₆): δ 0.61 (d, ³J_{HH} = 4.2 Hz, 18 H, *SiHMe*₂), 1.13 (s, 18 H, CNCMe₂CH₂O), 3.38 (s, 6 H, CNCMe₂CH₂O), 4.71 (sept, ³J_{HH} = 4.2 Hz, 3 H, *SiHMe*₂), 7.36 (t, ³J_{HH} = 7.2 Hz, 1 H, *para*-C₆H₅), 7.53 (t, ³J_{HH} = 7.6 Hz, 2 H, *meta*-C₆H₅), 8.26 (d, ³J_{HH} = 7.2 Hz, 2 H, *ortho*-C₆H₅). ¹³C{¹H} NMR (175 MHz, benzene-*d*₆): δ 0.76 (*SiHMe*₂), 28.89 (CNCMe₂CH₂O), 65.91 (CNCMe₂CH₂O), 80.65 (CNCMe₂CH₂O), 126.42 (*para*-C₆H₅), 127.27 (*meta*-C₆H₅), 136.41 (*ortho*-C₆H₅), 142.30 (br, *ipso*-C₆H₅), 192.83 (br, CNCMe₂CH₂O). ¹¹B NMR (128 MHz, benzene-*d*₆): δ -18.2. ²⁹Si NMR (120 MHz, benzene-*d*₆): δ -27.2 (¹J_{SiH} = 169.7 Hz, *Si*(*SiHMe*₂)₃), -186.8 (*Si*(*SiHMe*₂)₃). ¹⁵N NMR (59.2 MHz, benzene-*d*₆): δ -161.9. IR (KBr, cm⁻¹): 3078 (w), 3048 (w), 2966 (s), 2054 (s, ν_{SiH}), 1582 (s, ν_{CN}), 1495 (w), 1463 (m), 1432 (w), 1387 (w), 1369 (m), 1352 (m), 1274 (s), 1246 (m), 1194 (s), 1160 (m), 963 (s), 894 (s), 861 (s), 832 (s), 747 (m), mmol, 95.5%) as an analytically pure white solid. X-ray quality

single crystals were grown by slow pentane diffusion into a concentrated toluene solution of $\text{To}^{\text{M}}\text{ZnSi}(\text{SiHMe}_2)_3$ at $-30\text{ }^\circ\text{C}$. ^1H NMR (400 MHz, benzene- d_6): δ 0.57 (d, $^3J_{\text{HH}} = 4.4$ Hz, 18 H, SiHMe_2), 1.14 (s, 18 H, $\text{CNCMe}_2\text{CH}_2\text{O}$), 3.45 (s, 6 H, $\text{CNCMe}_2\text{CH}_2\text{O}$), 4.64 (sept, $^3J_{\text{HH}} = 4.4$ Hz, 3 H, SiHMe_2), 7.35 (t, $^3J_{\text{HH}} = 7.2$ Hz, 1 H, *para*- C_6H_5), 7.53 (t, $^3J_{\text{HH}} = 7.6$ Hz, 2 H, *meta*- C_6H_5), 8.31 (d, $^3J_{\text{HH}} = 7.2$ Hz, 2 H, *ortho*- C_6H_5). $^{13}\text{C}\{^1\text{H}\}$ NMR (175 MHz, benzene- d_6): δ 0.16 (SiHMe_2), 28.76 ($\text{CNCMe}_2\text{CH}_2\text{O}$), 66.08 ($\text{CNCMe}_2\text{CH}_2\text{O}$), 81.06 ($\text{CNCMe}_2\text{CH}_2\text{O}$), 126.37 (*para*- C_6H_5), 127.30 (*meta*- C_6H_5), 136.46 (*ortho*- C_6H_5), 142.30 (br, *ipso*- C_6H_5), 190.18 (br, $\text{CNCMe}_2\text{CH}_2\text{O}$). ^{11}B NMR (128 MHz, benzene- d_6): δ -18.5 . ^{29}Si NMR (120 MHz, benzene- d_6): δ -28.3 ($^1J_{\text{SiH}} = 172.2$ Hz, $\text{Si}(\text{SiHMe}_2)_3$), -171.3 ($\text{Si}(\text{SiHMe}_2)_3$). ^{15}N NMR (59.2 MHz, benzene- d_6): δ -157.4 . IR (KBr, cm^{-1}): 3079 (w), 2967 (s), 2897 (m), 2064 (s, ν_{SiH}), 1591 (s, ν_{CN}), 1495 (w), 1462 (m), 1431 (w), 1387 (m), 1368 (m), 1276 (s), 1241 (s), 1195 (s), 1158 (s), 961 (s), 867 (s), 747 (m), 703 (s). Anal. Calcd. for $\text{C}_{27}\text{H}_{50}\text{BSi}_4\text{N}_3\text{O}_3\text{Zn}$: C, 49.64; H, 7.71; N, 6.43. Found: C, 49.21; H, 7.58; N, 6.37. Mp: 208-210 $^\circ\text{C}$.

$\text{To}^{\text{M}}\text{MgSi}(\text{SiHMe}_2)_3$ (2). $\text{To}^{\text{M}}\text{MgBr}(\text{THF})_2$ (0.706 g, 1.12 mmol) and $\text{KSi}(\text{SiHMe}_2)_3$ (0.275 g, 1.12 mmol) were dissolved in benzene (12 mL) and stirred for 30 min at ambient temperature. The reaction mixture was filtered, and evaporation of the filtrate gave a white solid. The solid was washed with pentane (3×5 mL) and dried under vacuum providing crystalline, analytically pure $\text{To}^{\text{M}}\text{MgSi}(\text{SiHMe}_2)_3$ (0.630 g, 1.03 mmol, 91.5%). X-ray quality single crystals were obtained from a concentrated toluene solution cooled to $-30\text{ }^\circ\text{C}$. ^1H NMR (600 MHz, benzene- d_6): δ 0.61 (d, $^3J_{\text{HH}} = 4.2$ Hz, 18 H, SiHMe_2), 1.13 (s, 18 H, $\text{CNCMe}_2\text{CH}_2\text{O}$), 3.38 (s, 6 H, $\text{CNCMe}_2\text{CH}_2\text{O}$), 4.71 (sept, $^3J_{\text{HH}} = 4.2$ Hz, 3 H, SiHMe_2), 7.36 (t, $^3J_{\text{HH}} = 7.2$ Hz,

1 H, *para*-C₆H₅), 7.53 (t, ³J_{HH} = 7.6 Hz, 2 H, *meta*-C₆H₅), 8.26 (d, ³J_{HH} = 7.2 Hz, 2 H, *ortho*-C₆H₅). ¹³C{¹H} NMR (175 MHz, benzene-*d*₆): δ 0.76 (SiHMe₂), 28.89 (CNCMe₂CH₂O), 65.91 (CNCMe₂CH₂O), 80.65 (CNCMe₂CH₂O), 126.42 (*para*-C₆H₅), 127.27 (*meta*-C₆H₅), 136.41 (*ortho*-C₆H₅), 142.30 (br, *ipso*-C₆H₅), 192.83 (br, CNCMe₂CH₂O). ¹¹B NMR (128 MHz, benzene-*d*₆): δ -18.2. ²⁹Si NMR (120 MHz, benzene-*d*₆): δ -27.2 (¹J_{SiH} = 169.7 Hz, Si(SiHMe₂)₃), -186.8 (Si(SiHMe₂)₃). ¹⁵N NMR (59.2 MHz, benzene-*d*₆): δ -161.9. IR (KBr, cm⁻¹): 3078 (w), 3048 (w), 2966 (s), 2054 (s, ν_{SiH}), 1582 (s, ν_{CN}), 1495 (w), 1463 (m), 1432 (w), 1387 (w), 1369 (m), 1352 (m), 1274 (s), 1246 (m), 1194 (s), 1160 (m), 963 (s), 894 (s), 861 (s), 832 (s), 747 (m), 703 (m), 689 (m), 670 (m), 650 (m), 639 (m). Anal. Calcd. for C₂₇H₅₀BN₃O₃Si₄Mg: C, 52.98; H, 8.23; N, 6.86. Found: C, 53.14; H, 8.35; N, 6.91. Mp: 201-203 °C.

(To^MMgOMe)₂ (5). A benzene solution of To^MMgMe (0.300 g, 0.712 mmol) was exposed to O₂ (1 atm) for 5 minutes in a 100 mL Schlenk flask. The flask was sealed and then allowed to stand for 1 h at room temperature to form crystals. White, X-ray quality crystals were isolated by cannula filtration. The crystals were washed with pentane (3 × 5 mL) and dried under vacuum providing analytically pure To^MMgOMe (0.225 g, 0.514 mmol, 72.2%). ¹H NMR (400 MHz, benzene-*d*₆): δ 1.16 (s, 18 H, CNCMe₂CH₂O), 3.54 (s, 6 H, CNCMe₂CH₂O), 3.57 (s, 3 H, OMe), 7.29 (t, ³J_{HH} = 7.2 Hz, 1 H, *para*-C₆H₅), 7.49 (t, ³J_{HH} = 7.2 Hz, 2 H, *meta*-C₆H₅), 8.20 (d, ³J_{HH} = 7.2 Hz, 2 H, *ortho*-C₆H₅). ¹³C{¹H} NMR (175 MHz, benzene-*d*₆): δ 28.71 (CNCMe₂CH₂O), 52.51 (OMe), 66.68 (CNCMe₂CH₂O), 79.10 (CNCMe₂CH₂O), 125.96 (*para*-C₆H₅), 127.47 (*meta*-C₆H₅), 135.29 (*ortho*-C₆H₅), 151.90 (br, *ipso*-C₆H₅), 189.99 (br, CNCMe₂CH₂O). ¹¹B NMR (128 MHz, benzene-*d*₆): δ -17.6. ¹⁵N

NMR (71 MHz, benzene- d_6): δ -154.9. IR (KBr, cm^{-1}): 3047 (w), 2965 (s), 2884 (s), 1595 (s, ν_{CN}), 1496 (w), 1465 (m), 1434 (w), 1383 (w), 1365 (m), 1349 (m), 1267 (s), 1198 (s), 1153 (s), 1024 (w), 966 (s), 934 (w), 892 (w), 837 (w), 810 (w), 748 (w), 702 (s), 658 (s), 638 (s). Anal. Calcd. for $\text{C}_{22}\text{H}_{32}\text{BN}_3\text{O}_4\text{Mg}$: C, 60.38; H, 7.37; N, 9.60. Found: C, 59.95; H, 6.95; N, 9.77. Mp 275-280 °C (dec).

To^MZnOCHO (6). A 100 mL sealable reaction flask with a Teflon valve was charged with To^MZnH (0.450 g, 1.00 mmol) dissolved in benzene (15 mL). The solution was degassed, the flask was cooled to -78 °C, and excess, dry CO₂ was condensed into the flask. The reaction was allowed to warm to room temperature, and the resulting mixture was stirred for 30 min. The volatile materials were evaporated, and the white residue was washed with pentane (3 × 5 mL) and subsequently dried under vacuum to provide analytically pure To^MZnOCHO as a white powder. X-ray quality single crystals were grown from a concentrated toluene solution of To^MZnOCHO at -35 °C (0.463 g, 0.940, 93.7%). ¹H NMR (600 MHz, benzene- d_6): δ 1.13 (s, 18 H, $\text{CNCMe}_2\text{CH}_2\text{O}$), 3.46 (s, 6 H, $\text{CNCMe}_2\text{CH}_2\text{O}$), 7.37 (m, $^3J_{\text{HH}} = 7.2$ Hz, 1 H, *para*-C₆H₅), 7.55 (m, $^3J_{\text{HH}} = 7.2$ Hz, 2 H, *meta*-C₆H₅), 8.31 (d, $^3J_{\text{HH}} = 7.2$ Hz, 2 H, *ortho*-C₆H₅), 8.76 (s, 1 H, OCHO). ¹³C{¹H} NMR (175 MHz, benzene- d_6): δ 27.95 ($\text{CNCMe}_2\text{CH}_2\text{O}$), 65.84 ($\text{CNCMe}_2\text{CH}_2\text{O}$), 81.36 ($\text{CNCMe}_2\text{CH}_2\text{O}$), 126.54 (*para*-C₆H₅), 127.37 (*meta*-C₆H₅), 136.37 (*ortho*-C₆H₅), 140.90 (br, *ipso*-C₆H₅), 169.18 (ZnOCHO), 189.80 (br, $\text{CNCMe}_2\text{CH}_2\text{O}$). ¹¹B NMR (128 MHz, benzene- d_6): δ -18.1. ¹⁵N NMR (59.2 MHz, benzene- d_6): δ -160.3. IR (KBr, cm^{-1}): 3072 (w), 2965 (s), 2923 (w), 1629 (s, ν_{CO}), 1595 (s, ν_{CN}), 1461 (m), 1423 (m), 1389 (m), 1370 (m), 1351 (m), 1307 (s, ν_{CO}), 1273 (s), 1197 (s), 1163 (m), 1124 (m), 1033 (w), 1019 (m), 996 (m), 957 (s), 946 (s), 893 (m), 871 (m), 844 (w), 819

(m). Anal. Calcd. For $C_{22}H_{30}BZnN_3O_5$: C, 53.63; H, 6.14; N, 8.53. Found C, 53.91; H, 6.19; N, 8.49. Mp 207-213 °C.

To^MMgO₂CSi(SiHMe₂)₃ (7). A 15 mL benzene solution of To^MMgSi(SiHMe₂)₃ (0.230 g, 0.376 mmol) was degassed and stirred under CO₂ (1 atm) for 24 h at ambient temperature. The volatile components were evaporated, and the white residue was washed with pentane (3 × 5 mL). Vacuum drying provided analytically pure To^MMgO₂CSi(SiHMe₂)₃ (0.226 g, 0.344 mmol, 91.5%). ¹H NMR (600 MHz, benzene-*d*₆): δ 0.48 (d, ³J_{HH} = 4.4 Hz, 18 H, SiHMe₂), 1.16 (s, 18 H, CNCMe₂CH₂O), 3.46 (s, 6 H, CNCMe₂CH₂O), 4.45 (sept, ³J_{HH} = 4.4 Hz, 3 H, SiHMe₂) 7.37 (t, ³J_{HH} = 7.2 Hz, 1 H, *para*-C₆H₅), 7.55 (t, ³J_{HH} = 7.8 Hz, 2 H, *meta*-C₆H₅), 8.36 (d, ³J_{HH} = 7.2 Hz, 2 H, *ortho*-C₆H₅). ¹³C{¹H} NMR (175 MHz, benzene-*d*₆): δ -3.65 (SiHMe₂), 28.20 (CNCMe₂CH₂O), 65.87 (CNCMe₂CH₂O), 80.63 (CNCMe₂CH₂O), 126.16 (*para*-C₆H₅), 127.16 (*meta*-C₆H₅), 136.57 (*ortho*-C₆H₅), 191.65 (br, CNCMe₂CH₂O), 202.61 (MgO₂CSi). ¹¹B NMR (128 MHz, benzene-*d*₆): δ -18.1. ²⁹Si NMR (120 MHz, benzene-*d*₆): δ -35.51 (d, ¹J_{SiH} = 169.7 Hz, SiHMe₂), -86.34 (Si(SiHMe₂)₃). ¹⁵N NMR (59.2 MHz, benzene-*d*₆): δ -157.4. IR (KBr, cm⁻¹): 3076 (w), 3046 (w), 2965 (s), 2928 (w), 2897 (w), 2101 (s, ν_{SiH}), 1593 (s, ν_{CN}), 1463 (s), 1389 (w), 1366 (s), 1272 (s), 1248 (s), 1195 (s), 1161 (m), 963 (s), 888 (s), 859 (s), 838 (s), 705 (m), 672 (m), 639 (w), 619 (w), 514 (m). Anal. Calcd. for C₂₈H₅₀BSi₄N₃O₅Mg: C, 51.25; H, 7.68; N, 6.40. Found: C, 51.25; H, 7.39; N, 6.46. Mp: 190-193 °C.

HO₂CSi(SiHMe₂)₃ (8). Tetrakis(dimethylsilyl)silane (2.00 g, 7.56 mmol) was dissolved in THF (20 mL). Methylolithium (7.08 mL, 11.3 mmol, 1.6 M in ether) was added. The reaction was stirred at room temperature for 3 days, and then the mixture was poured into a slurry of

dry ice in ether. After excess CO₂ had evaporated, the reaction mixture was washed with 2% HCl (3 × 50 mL), and the ether layer was collected and dried over Na₂SO₄. The ether was evaporated to give a colorless oil (0.697 g, 2.78 mmol, 36.9%). ¹H NMR (benzene-*d*₆, 600 MHz): δ 0.297 (br, 18 H, SiHMe₂), 4.27 (sept, 3 H, ³J_{HH} = 4.5 Hz, SiHMe₂), 11.67 (br, 1 H, HO₂CSi). ¹³C{¹H} NMR (benzene-*d*₆, 175 MHz): δ 195.22 (HO₂CSi), 1.76 (SiHMe₂). ²⁹Si (benzene-*d*₆, 120 MHz) δ -26.1 (d, ¹J_{SiH} = 180.6 Hz, SiHMe₂), -85.2 (Si(SiHMe₂)₃). High Resolution MS Calcd. For C₇H₂₂O₂Si₄: (M⁺-1), 249.0619. Found: *m/z*, 249.0974 (M⁺-1).

To^MZnO₂CSi(SiHMe₂)₃ (9). To^MZnEt (0.035 g, 0.073 mmol) and HO₂CSi(SiHMe₂)₃ (0.018 g, 0.073 mmol) were dissolved in benzene and stirred for 30 min. Evaporation of the volatile components under reduced pressure provided a white solid, which was washed with pentane (3 × 5 mL) and dried under vacuum to obtain analytically pure To^MZnO₂CSi(SiHMe₂)₃ (0.047 g, 0.067 mmol, 92.3%). ¹H NMR (400 MHz, benzene-*d*₆): δ 0.51 (d, ³J_{HH} = 4.3 Hz, 18 H, SiHMe₂), 1.18 (s, 18 H, CNCMe₂CH₂O), 3.48 (s, 6 H, CNCMe₂CH₂O), 4.46 (sept, ³J_{HH} = 4.3 Hz, 3 H, SiHMe₂), 7.35 (t, ³J_{HH} = 7.6 Hz, 1 H, *para*-C₆H₅), 7.53 (t, ³J_{HH} = 7.4 Hz, 2 H, *meta*-C₆H₅), 8.31 (d, ³J_{HH} = 7.2 Hz, 2 H, *ortho*-C₆H₅). ¹³C{¹H} NMR (175 MHz, benzene-*d*₆): δ -3.75 (SiHMe₂), 28.00 (CNCMe₂CH₂O), 65.90 (CNCMe₂CH₂O), 81.30 (CNCMe₂CH₂O), 126.41 (*para*-C₆H₅), 127.30 (*meta*-C₆H₅), 136.42 (*ortho*-C₆H₅), 141.72 (br, *ipso*-C₆H₅), 190.19 (br, CNCMe₂CH₂O), 193.38 (ZnO₂CSi). ¹¹B NMR (128 MHz, benzene-*d*₆): δ -18.3. ²⁹Si NMR (120 MHz, benzene-*d*₆): δ -36.36 (d, ¹J_{SiH} = 169.7 Hz, ZnOC(O)Si(SiHMe₂)₃), -87.38 (s, ZnOC(O)Si(SiHMe₂)₃). ¹⁵N NMR (61 MHz, benzene-*d*₆): δ -158.0. IR (KBr, cm⁻¹): 3077 (w), 3049 (w), 2963 (s), 2928 (w), 2898 (w), 2103 (s, ν_{SiH}), 1598 (s, ν_{CN}), 1510 (m), 1464 (m), 1368 (m), 1352 (m), 1261 (s), 1196 (m), 961 (m), 907 (m),

838 (s), 813 (s), 777 (w), 704 (m), 687 (m), 639 (m), 624 (w). Anal. Calcd. for $C_{28}H_{50}BSi_4N_3O_5Zn$: C, 48.23; H, 7.23; N, 6.03. Found: C, 47.81; H, 7.38; N, 5.69. Mp: 218-220 °C.

Procedures for DOSY (Diffusion-Ordered Spectroscopy) experiment. All the measurements were performed on a Bruker DRX400 spectrometer using a DOSY stimulated spin-echo pulse program with bipolar gradients.⁷ Accurately known concentrations of the species in question, $To^M MgSi(SiHMe_2)_3$ (**2**), $To^M MgO_2CSi(SiHMe_2)_3$ (**7**), and $To^M ZnO_2CSi(SiHMe_2)_3$ (**9**) were determined by integration of resonances corresponding to species of interest and integration of a tetrakis(trimethylsilyl)silane standard of accurately known concentration. The temperature in the NMR probe was preset to 296 K, and the probe was maintained at a constant temperature for each experiment. The delay time in between pulses was set to 5 s in order to ensure the spins are fully relaxed to their ground states. During the experiments, a series of 1D 1H NMR spectra were acquired at increasing gradient strength. The signal intensity decay was fit by non-linear least squares regression analysis to Equation 1 to obtain the diffusion coefficient D (Figure S-1, S-2, and S-3),⁷

$$\ln\left(\frac{I}{I_0}\right) = -(\gamma\delta)^2 G^2 \left(\Delta - \frac{\delta}{3}\right) D \quad (1)$$

where I is the observed intensity, D is the diffusion coefficient, γ is the gyromagnetic ratio of the nucleus, δ is the length of the gradient pulse, and Δ is the diffusion time. These experiments were performed on $To^M MgSi(SiHMe_2)_3$ ($6.945 \times 10^{-10} \text{ m}^2/\text{s}$), $To^M MgO_2CSi(SiHMe_2)_3$ ($6.849 \times 10^{-10} \text{ m}^2/\text{s}$), $To^M ZnO_2CSi(SiHMe_2)_3$ ($6.429 \times 10^{-10} \text{ m}^2/\text{s}$), and To^M_2Mg ($6.00 \times 10^{-10} \text{ m}^2/\text{s}$). From this trend, we conclude that the silane carboxylate

compounds are monomeric, as we would expect diffusion constants $< 6 \times 10^{-10} \text{ m}^2/\text{s}$ for dimeric compounds.

Figure S-1. Plot of intensity versus gradient strength that was used to determine the diffusion coefficient ($6.945 \times 10^{-10} \text{ m}^2/\text{s}$) for $\text{To}^{\text{M}}\text{MgSi}(\text{SiHMe}_2)_3$ (**2**).

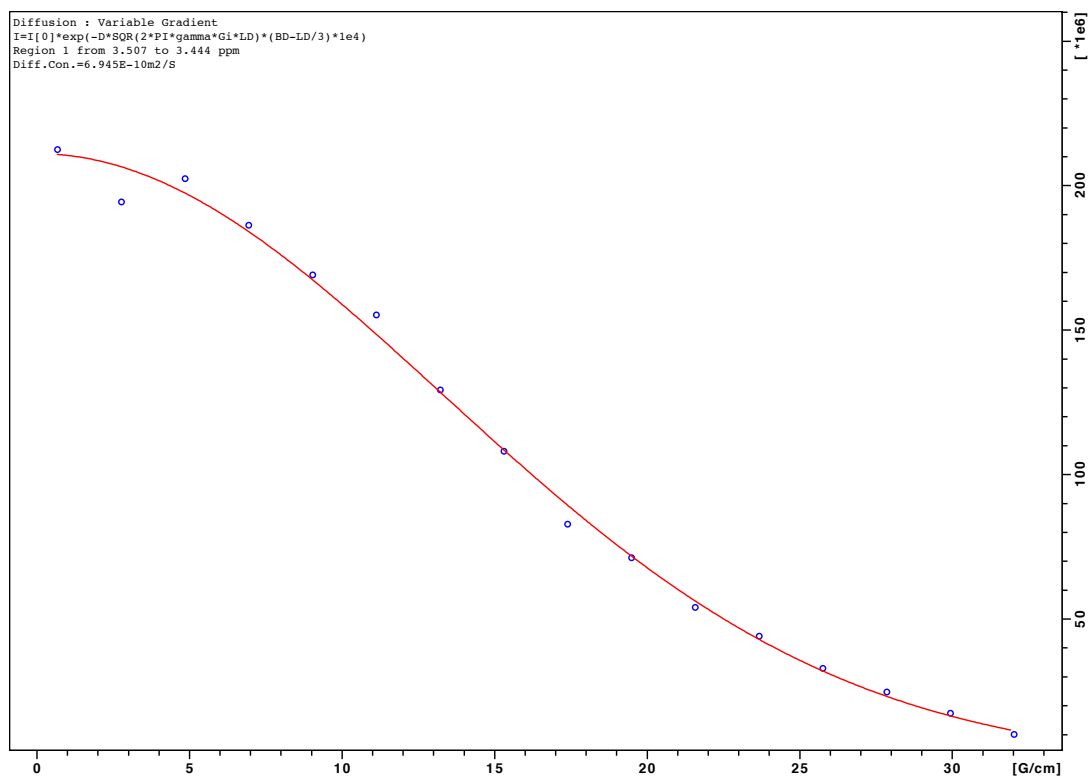


Figure S-2. Plot of intensity versus gradient strength that was used to determine the diffusion coefficient ($6.849 \times 10^{-10} \text{ m}^2/\text{s}$) for $\text{To}^{\text{M}}\text{MgO}_2\text{CSi}(\text{SiHMe}_2)_3$ (7).

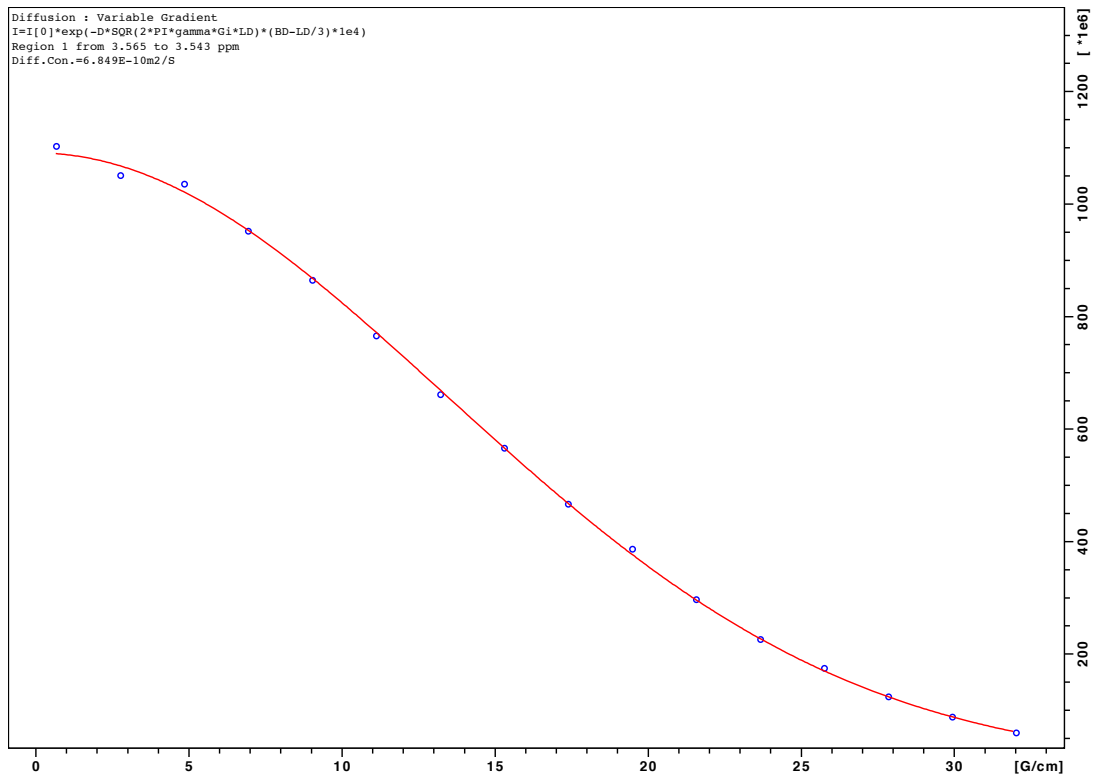
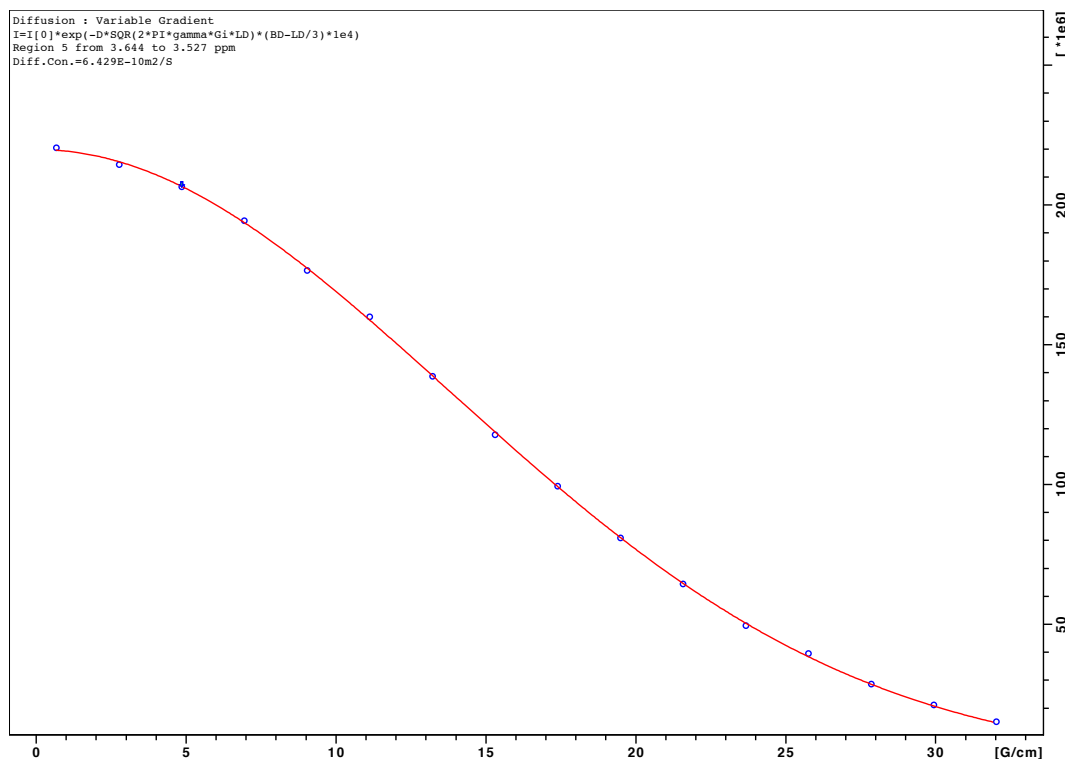


Figure S-3. Plot of intensity versus gradient strength that was used to determine the diffusion coefficient ($6.429 \times 10^{-10} \text{ m}^2/\text{s}$) for $\text{To}^{\text{M}}\text{ZnO}_2\text{CSi}(\text{SiHMe}_2)_3$ (**9**).



References.

- (1) R. I. Yousef, B. Walfort, T. Ruffer, C. Wagner, H. Schmidt, R. Herzog and D. Steinborn, *J. Organomet. Chem.*, 2005, **690**, 1178-1191.
- (2) J. F. Dunne, J. Su, A. Ellern and A. D. Sadow, *Organometallics*, 2008, **27**, 2399-2401.
- (3) J. F. Dunne, D. B. Fulton, A. Ellern and A. D. Sadow, *J. Am. Chem. Soc.*, 2010, **132**, 17680-17683.
- (4) D. Mukherjee, A. Ellern and A. D. Sadow, *J. Am. Chem. Soc.*, 2010, **132**, 7582-7583.
- (5) J. B. Lambert, J. L. Pflug and J. M. Denari, *Organometallics*, 1996, **15**, 615-625.

(6) C. Marschner, *Eur. J. Inorg. Chem.*, 1998, **1998**, 221-226.

(a) P. S. Pregosin, E. Martinez-Viviente and P. G. A. Kumar, *Dalton Trans.*, 2003, 4007-4014. (b) M. Valentini, P. S. Pregosin and H. Ruegger, *Organometallics*, 2000, **19**, 2551-2555.

Chapter 7: Coordinatively Saturated Tris(oxazolinyl)borato Zinc Hydride-Catalyzed Carbonyl hydrosilylation and hydroboration.

Contains results from a manuscript to be submitted for publication

Debabrata Mukherjee, Arkady Ellern and Aaron D. Sadow

Abstract.

The air-stable four-coordinate zinc compound $To^M ZnH$ (**1**, To^M = tris(4,4-dimethyl-2-oxazolinyl)phenylborate) catalyzes hydrosilylation and hydroboration of aldehydes and ketones. The catalytic hydrosilylation of PhCHO with PhSiH₃ and PhMeSiH₂ selectively (~95%) provide PhSiH(OCH₂Ph)₂ and PhMeHSi(OCH₂Ph) respectively. However, reduction with a tertiary organosilane BnMe₂SiH is possible under similar catalytic condition. Catalytic reduction with pinacolborane as the hydride source is found to be a more efficient protocol compared to hydrosilylation. A hydride insertion mechanism for the catalytic hydrosilylation of PhCHO with BnMe₂SiH is proposed that also involves an inhibition effect from PhCHO. This substrate inhibition is explained based on the observed adduct formation between the zinc alkoxide ($To^M ZnOCH_2Ph$) and free PhCHO.

Introduction.

Alcohols are important building blocks for pharmaceuticals, agrochemicals, polymers, in natural product syntheses, auxiliaries, and ligand synthesis.¹ Reduction of carbonyl functional groups is a convenient route to access to alcohols. Extensive use of stoichiometric reductions with metal hydrides such as NaBH₄, LiAlH₄ has been reported but with limitations like poor selectivity, inappropriate reaction conditions, moisture sensitivity of LiAlH₄ and

difficulty in handling, and cost of large scale production. However, some decades ago, the application of transition metal catalysts for hydrosilylation and hydrogenation of carbonyl functionalities was developed as a useful and versatile alternative. Although in present situation, catalytic hydrogenation and transfer hydrogenation are the most developed routes to alcohols, catalytic hydrosilylation is still a desirable choice because of mild reaction conditions and simplicity. To date, numerous highly active catalysts comprising of a wide range of metals ranging from transition (Ti,² Re,³ W,⁴ Mo,⁵ Cu,⁶ Fe,⁷ Ni,⁸ Ir,⁹ Rh,¹⁰ Ru¹¹ etc.) to main group metals (Ca,¹² Al,¹³ Zn¹⁴) for hydrosilylation of carbonyl compounds have been developed. Compared to the costly and toxic heavy metals such as rhodium, ruthenium, or iridium, less-expensive metals, such as titanium, zinc, copper, and iron, are finding more attentions in this regard. A hydride insertion mechanism, as shown in fig.1, is commonly proposed in several metal-based catalytic systems including Zn.^{2,6,8,14} However, isolation of specific catalytic intermediates to get an insight of the mechanism is only rarely attempted.

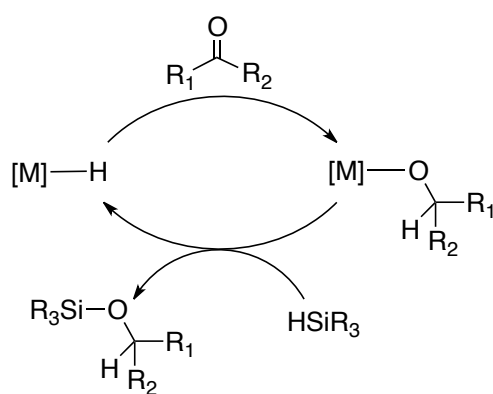


Fig. 1 commonly proposed hydride insertion mechanism for catalytic hydrosilylation.

Additionally, a few transition metal catalyzed hydrosilylations have been suggested to not go through the insertion/ σ -bond metathesis mechanism despite having positive evidences

for those individual steps.^{3,11,15} Our previous study on molecular $To^M ZnH$ catalyzed dehydrogenative coupling between alcohols (ROH) and silanes ($HSiR'_3$) showed that the zinc alkoxides ($To^M ZnOR$) are intermediates in the catalysis which transfer the $-OR$ group to silicon at the turnover limiting metathesis step.^{16,17} Our further exploration of the chemistry of $To^M ZnH$ (**1**) showed that zinc alkoxides ($To^M ZnOR$) are also accessible from **1** via carbonyl insertion into the $Zn-H$ bond. This insertion step, in combination with the methathesis with $Si-H$ moiety, provides an ideal opportunity to test the catalytic activity of **1** in hydrosilylation of carbonyls. The inertness of **1** towards air¹⁸ would make this system even more attractive and the concept of isolating intermediates and probing the mechanism using detailed kinetics experiments would facilitate in gaining an in-depth insight of this important organic transformation.

Results and Discussions.

We started with testing the product selectivity of primary ($PhSiH_3$) and secondary ($PhMeSiH_2$) silanes using $PhCHO$ as the aldehyde substrate in presence of 5 mol% of **1** in benzene- d_6 . Irrespective of the $PhCHO$: silane ratio, $PhSiH_3$ and $PhMeSiH_2$ selectively provided $PhSiH(OCH_2Ph)_2$ and $PhMeSiH(OCH_2Ph)$ respectively as shown in eqn.1 (~ 95% in both cases). The results are summarized in table 1.

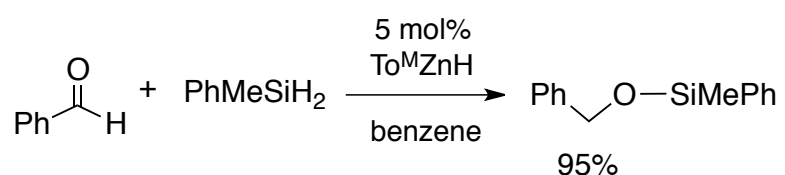
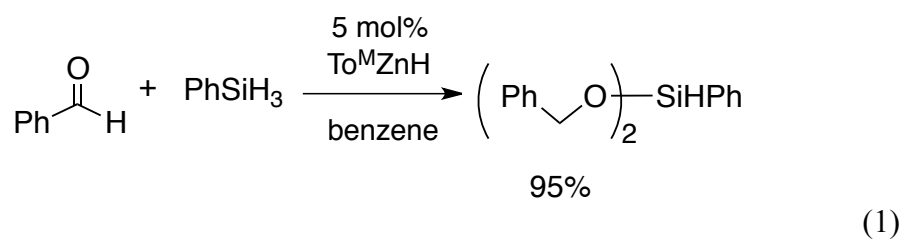
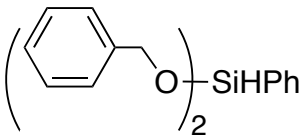
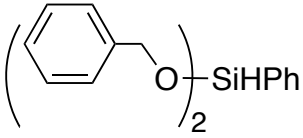
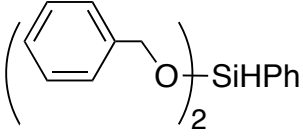
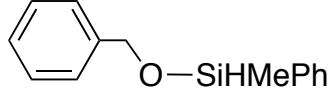
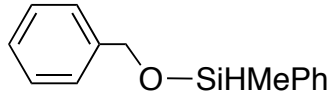


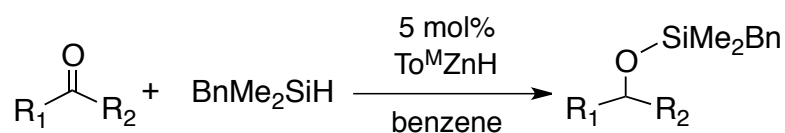
Table 1. Micromolar-scale reactions of PhSiH₃ and PhMeSiH₂ with PhCHO using 5 mol% of **1**.

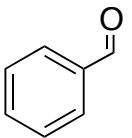
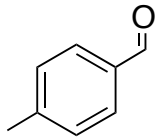
Entry	Silanes (equiv.)	temperature	time	Products	NMR yield%
1	PhSiH ₃ (1)	60 °C	36 h		>99%
2	PhSiH ₃ (2)	60 °C	36 h		>99%
3	PhSiH ₃ (3)	60 °C	24 h		>99%
4	PhMeSiH ₂ (1)	80 °C	4 h		>99%
5	PhMeSiH ₂ (2)	80 °C	3 h		>99%

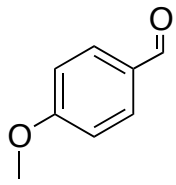
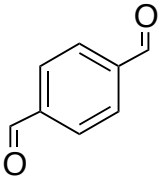
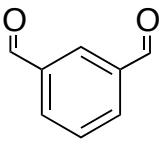
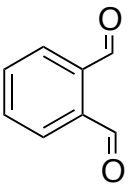
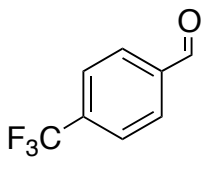
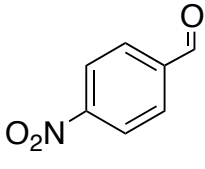
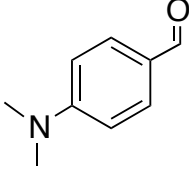
As expected, PhSiH₃ reacted at milder condition compared to PhMeSiH₂ due to steric reason. This result indicates that tertiary silanes should be unreactive as the hydride source in this system.

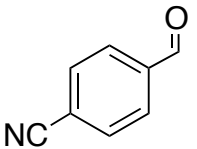
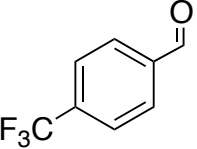
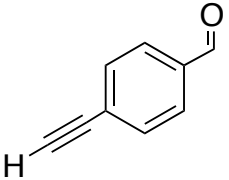
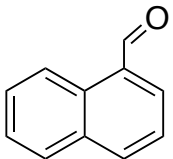
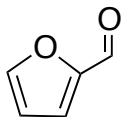
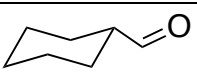
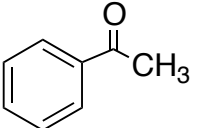
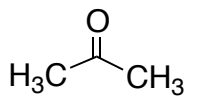
However, BnMe₂SiH, despite being a tertiary silane, proved to be an efficient hydride source and complete hydrosilylation was achieved under similar condition and catalyst loading providing BnMe₂SiOCH₂Ph. This is quite intriguing and we have also previously observed in our dehydrocoupling study that under similar condition and catalyst loading; BnMe₂SiH reacted faster than PhMeSiH₂ with smaller alcohols like MeOH, EOH and *i*-PrOH. Nonetheless, we chose BnMe₂SiH as the silane of interest to avoid multiple product formation and tested the scope of this system. The results are summarized in table 2.

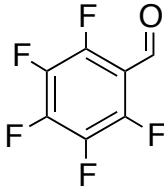
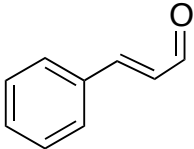
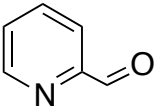
Table 2. Micromolar-scale hydrosilylation of carbonyls with BnMe₂SiH using 5 mol% of **1**.



Entry	Substrates	Temperature	Time	Conversion (%)	Isolated yield (%)
1		80 °C	4 h	>99%	93%
2		80 °C	6 h	>99%	95%

3		80 °C	6 h	>99%	92%
4 ^a		80 °C	8 h	>99%	96%
5 ^a		80 °C	8 h	>99%	----
6 ^a		80 °C	3 h	>99%	----
7		80 °C	6 h	>99%	95%
8		80 °C	4 h	>99%	93%
9		80 °C	6 h	>99%	92%

10		80 °C 80 °C	6 h 2 h ^b	>99% >99%	93%
11		80 °C	3 h	>99%	95%
12		120 °C	12 h	---	---
13		80 °C	10 h	>99%	---
14		80 °C	6 h	>99%	93%
15		80 °C	4 h	>99%	97%
16		80 °C	16 h	>99%	93%
17		80 °C	16 h	>99%	96%

18		80 °C	6 h	20%	----
19		80 °C	18 h	>99%	93%
20		80 °C	6 h	>99%	----

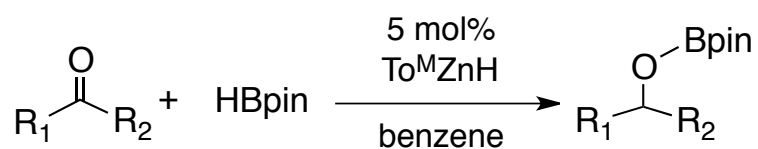
Percentage conversions were determined by measuring the concentration of the starting materials and products by comparison of corresponding integrated resonances to a known concentration of cyclooctane present in the reaction mixture.

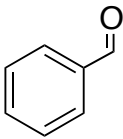
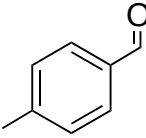
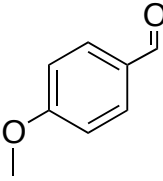
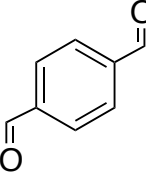
^a 2 equiv. of BnMe₂SiH were used. ^b 3 equiv. of BnMe₂SiH were used.

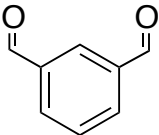
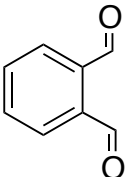
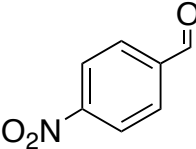
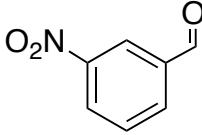
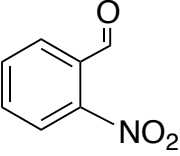
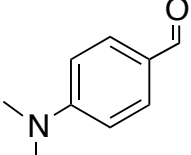
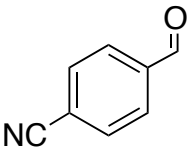
Functional group tolerance of this system was examined on different *para*-substituted benzaldehyde substrates. Satisfactory hydrosilylations were achieved for –Me, –OMe, –OH, –NO₂, –CN, –NMe₂, –OH, –CF₃, –F substituents. Two equivalents of BnMe₂SiH were used for di-carboxaldehydes (entry 4-6). No further reduction of –CN moiety was observed even in presence of three equivalents of BnMe₂SiH under the same catalytic condition (entry 10). (*p*-HCC)C₆H₄-CHO (entry 12) does not give any conversion, as the deactivation of catalyst **1** is evident in ¹H NMR due to protonation of the Zn–H by the acidic C–H alkynylic proton. Substrates like furfural (entry 14) and 2-pyridine carboxaldehyde (entry 20) also resulted into the corresponding hydrosilylation products in quantitative yield. Only 1,2-reduction was observed for α,β-unsaturated carbonyl moiety (entry 19). No enolization was observed for cyclohexylcarboxaldehyde, acetophenone, and acetone (entry 15-17).

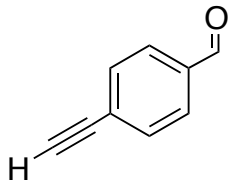
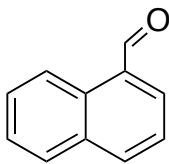
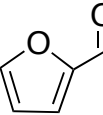

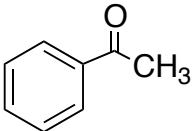
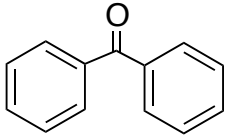
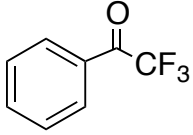
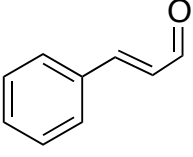
Hydroboration reduction instead of hydrosilylation using pinacol borane [HBpin] was also tested under similar catalytic conditions. Carbonyl substrates, previously used in the hydrosilylation study, were employed here as well and the results are listed in Table 3.

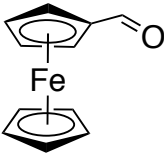
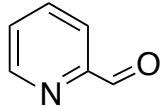
Table 3. Micromolar-scale hydroboration of carbonyls with HBpin using 5 mol% of **1**.



entry	Substrates	Temperature	Time	Conversion (%) ^a
1		25 °C	45 min	>99%
2		25 °C	1 h	>99%
3		25 °C	1.5 h	>99%
4		25 °C	1.5 h	>99%

5		25 °C	1.5 h	>99%
6		25 °C	45 min	>99%
7		25 °C	45 min	>99%
8		25 °C	1.5 h	>99%
9		25 °C	2 h	>99%
10		25 °C	2 h	>99%
11		25 °C	1 h	>99%

12		60 °C	1 h	----
15		25 °C	4 h	>99%
16		25 °C	1 h	>99%
17		25 °C	1 h	>99%
18		60 °C	3 h	>99%
19		60 °C	6 h	>99%
20		25 °C	2 h	>99%
22		25 °C	1 h	>99%

23		25 °C	3 h	>99%
25		25 °C	2 h	>99%

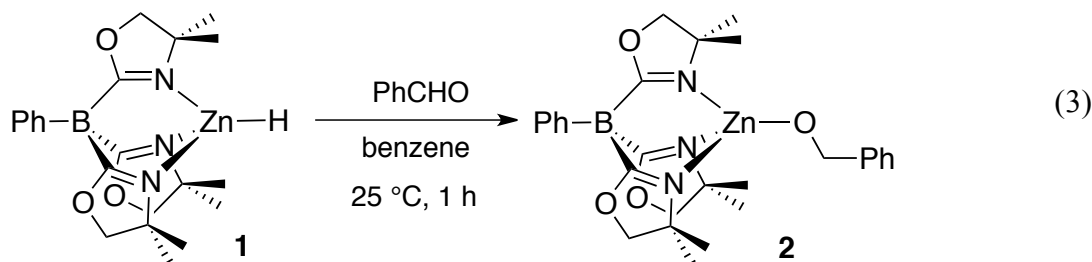
^a Percentage conversion was monitored using tetrakis(trimethylsilyl)silane as the internal standard.

Functional group tolerance remained the same. Ferrocenecarboxaldehyde substrate (entry 23) was also reduced under this catalytic condition. Surprisingly no substantial difference in overall reaction time was observed between aldehyde substrates with electron donating and withdrawing substituents. And again, no enolization or aldol condensation side reactions were observed in any case. The reaction conditions and the overall reaction time for completion indicate that under similar conditions, relative rate of hydroboration (with HBpin) is faster than the hydrosilylation (with BnSiHMe₂).

Mechanistic investigations.

Two tris(oxazoliny)borato zinc species were detected in the hydrosilylation reaction mixture of PhCHO and BnMe₂SiH. The ¹H NMR chemical shifts of the To^M (-CH₃) (1.12 ppm and 1.20 ppm) at 97.5 °C in toluene-*d*₈ solvent) indicate that the species are distinct from To^MZnH, and resonances for To^MZnH were not detected. Whereas, during the hydroboration catalysis of PhCHO or the other aldehyde substrates with HBpin, only the To^MZnH resonances were observed as the resting state of the catalyst. Therefore, we attempted to identify these intermediate species through stoichiometric experiments. Reaction of PhCHO

and $\text{To}^{\text{M}}\text{ZnH}$ in benzene at ambient temperature provides the zinc alkoxide $\text{To}^{\text{M}}\text{ZnOCH}_2\text{Ph}$ (**2**) in quantitative yield over 3 h (eq. 3).



^1H and $^{13}\text{C}\{^1\text{H}\}$ NMR spectroscopy of **2** in benzene- d_6 shows C_{3v} symmetric To^{M} resonances at ambient temperature. Whereas, a variable temperature NMR study in toluene- d_8 provided broad resonances for the To^{M} ligand and the CH_2Ph moiety. However, a single crystal X-ray diffraction study of **2** reveals a dimeric structure in the solid state. The two $-\text{OCH}_2\text{Ph}$ moieties are bridging between two zinc centers, each of which are coordinated to a $[\text{To}^{\text{M}}]$ ligand in κ^2 - fashion as depicted in the ORTEP figure. The interatomic Zn–O distance is 1.97(4) Å, slightly longer than the distance in monomeric $\text{To}^{\text{M}}\text{ZnO}^i\text{Bu}$ (1.85 Å).

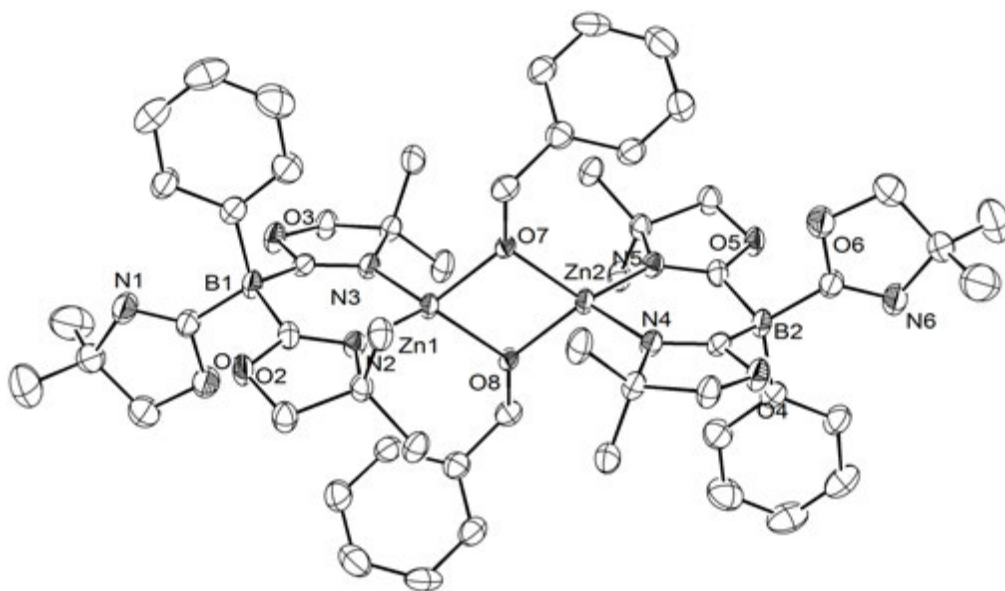
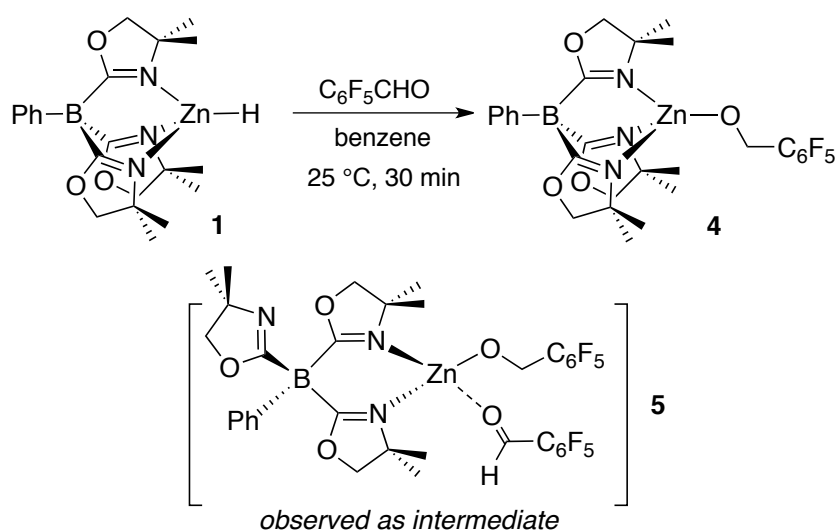


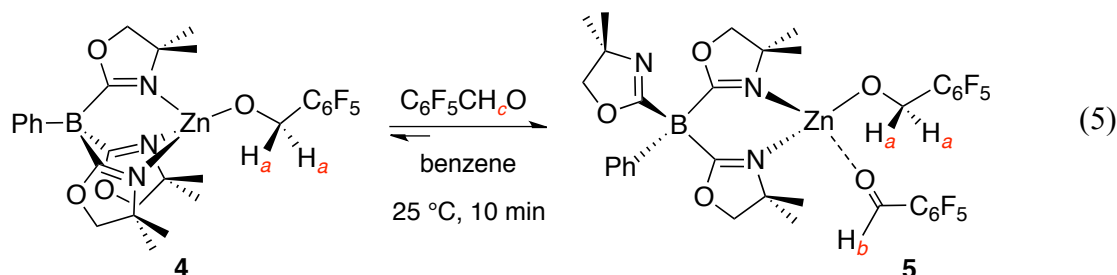
Figure 1. ORTEP diagram of $[(\kappa^2\text{-To}^{\text{M}})\text{ZnOCH}_2\text{Ph}]_2$ (**2**) drawn with ellipsoids at 50% probability. Hydrogen atoms are omitted for clarity.

^1H NMR spectra of **2** in toluene- d_8 acquired at 97.5 °C led to identify the major zinc species as the $\text{To}^{\text{M}}\text{ZnOCH}_2\text{Ph}$, present in the catalytic reaction mixture of PhCHO and BnMe_2SiH (see above). The minor zinc species (**3**) observed in the catalytic hydrosilylation reaction mixture contains broad resonances for tris(oxazolinyl)borate (C_{3v}) and a benzyloxy ligand. This minor species is also formed upon mixing **1** and PhCHO during the stoichiometric reaction and present throughout the reaction until all PhCHO is consumed. At the end **2** is the only species observed and isolated. However, excess PhCHO (10 equiv.) and $\text{To}^{\text{M}}\text{ZnH}$ give mixtures of **2** (major) and the second species (minor). Addition of PhCHO to isolated **2** also results in partial conversion to this species. Significant conversion of $\text{To}^{\text{M}}\text{ZnOCH}_2\text{Ph}$ occurs only at high [PhCHO] ($\sim > 13 \text{ M}$).

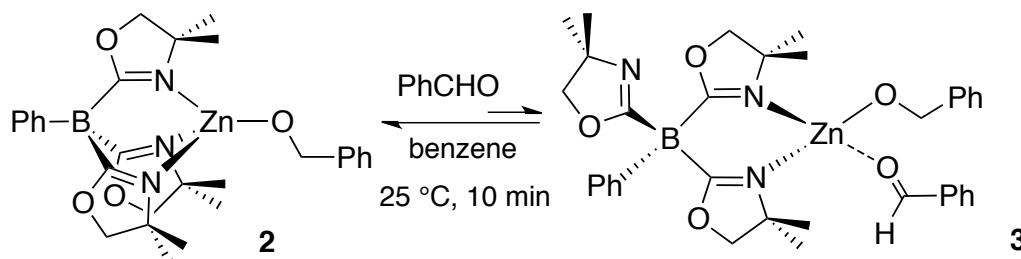
Similar treatment of $\text{C}_6\text{F}_5\text{CHO}$ and $\text{To}^{\text{M}}\text{ZnH}$ at ambient temperature also provides the corresponding alkoxide $\text{To}^{\text{M}}\text{ZnOCH}_2\text{C}_6\text{F}_5$ (**4**) within 1 h, and subsequently isolated. Again, the ^1H NMR spectrum, acquired during the reaction time course, showed the presence **4** and another zinc species associated with a local C_s -symmetric To^{M} ligand (**5**). Eventually, **4** is obtained as the sole zinc-containing species (eqn. 4).



Unlike the PhCHO, addition of only slightly more than 1 equiv. of C_6F_5CHO to **4** at ambient temperature provides **5** (eqn. 5) as the only zinc-containing species.

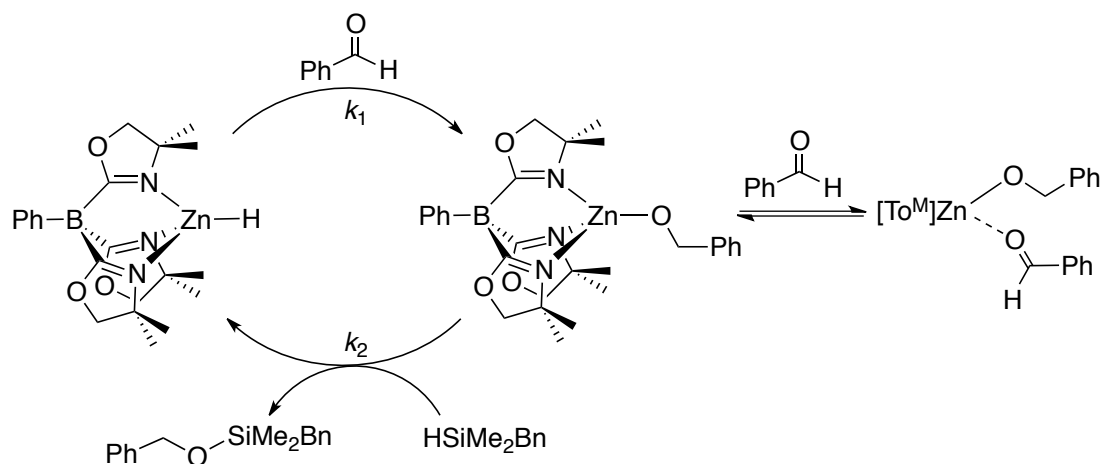


Species **5** possesses a lower symmetric (lower than C_{3v}) To^M ligand as indicated by the 1H NMR spectrum. A variable temperature NMR study of **5** in toluene- d_8 was conducted, and a locally C_s -symmetric splitting pattern for the To^M ligand stands out at low temperature range (273 K). An EXSY NMR study with **5** in benzene at ambient temperature shows cross peaks between H_a , H_b , and H_c set of protons, that establishes a dynamic β -H exchange process operative between the coordinated and free aldehyde and the zinc alkoxide moiety. This process is the MPV reduction/oppenauer oxidation through β -H transfer from a metal-alkoxide moiety to the electrophilic carbon of a coordinated aldehyde. Based on the similarity between C_6F_5CHO and PhCHO data, we assign the species **3** as the $To^M ZnOCH_2Ph(OCHPh)$. Species **3** is also in dynamic equilibrium with free PhCHO and **2** as shown below, confirmed by another EXSY experiment.



During catalytic hydrosilylation of PhCHO with BnMe₂SiH an inhibition effect from the PhCHO substrate on the overall reaction rate was noticed. This observation, in combination with the previous zinc alkoxide-aldehyde adduct formation, leads us to postulate the operative catalytic cycle as below (Fig. 2). PhCHO insertion into ToMZn–H results into the Zinc alkoxide, To^MZnOCH₂Ph **2**, which gets involved in a reversible exchange process, in presence of free aldehyde, with the adduct species **3**. Finally, the metathesis of Zn–OCH₂Ph with Si–H gives the turnover to generate **1** and product BnMe₂SiOCH₂Ph. Adduct **3** is presumably less reactive towards the silane metathesis step that would explain the effect of PhCHO inhibition.

Proposed cycle for To^MZnH-catalyzed Hydrosilylation of PhCHO with BnSiHMe₂.



This postulate is further supported by the fact that the hydrosilylation of C₆F₅CHO with BnMe₂SiH under similar catalytic condition resulted into only 20% conversion after 6 h at 80 °C. ¹H NMR spectrum acquired during the catalysis showed that resting state of the catalyst is solely the adduct species **5**. A detailed kinetics study for this whole reaction mechanism is underway.

Conclusion.

Thus we have established an exciting air-stable Zn catalytic system for hydrosilylation reduction of carbonyls. The real advantage of this system lies on the possibility of intermediate isolation and studying the reaction mechanism in details. Individual stoichiometric steps are also being probed to finally compare the overall catalysis with the combination of individual steps involved.

References.

1. (a) Lennon, I. C.; Ramsden, J. A.; *Org. Process Res. Dev.* **2005**, *9*, 110-112. (b) Hawkins, J. M.; Watson, T. J. N. *Angew. Chem. Int. Ed.* **2004**, *43*, 3224-3228. (c) Noyori, R.; Ohkuma, T. *Angew. Chem. Int. Ed.* **2001**, *40*, 40-73.
2. Yun, J.; Buchwald, S. L. *J. Am. Chem. Soc.* **1999**, *121*, 5640 – 5644.
3. Du, G.; Fanwick, P. E.; Abu-Omar, M. M. *J. Am. Chem. Soc.* **2007**, *129*, 5180-5187.
4. Dioumaev, V. K.; Bullock, R. M. *Nature*, **2003**, *424*, 530-532.
5. Peterson, E.; Khalimon, A. Y.; Simionescu, R.; Kuzmina, L. G.; Howard, J. A. K.; Nikonov, G. I. *J. Am. Chem. Soc.* **2009**, *131*, 908-909.
6. Lipshutz, B. H.; Noson, K.; Chrisman, W. *J. Am. Chem. Soc.* **2001**, *123*, 12917-12918.
7. Bart, S. C.; Lobkovsky, E.; Chirik, P. J. *J. Am. Chem. Soc.* **2004**, *126*, 13794-13807.
8. Chakraborty, S.; Krause, J. A.; Guan, H. *Organometallics* **2009**, *28*, 582-586.
9. Park, S.; Brookhart, M. *Organometallics* **2010**, *29*, 6057-6064.
10. César, V.; Gade, L.H.; Bellemin-Laponnaz, S. *Angew. Chem. Int. Ed.* **2004**, *43*, 1014-1017.
11. Zhu, G.; Terry, M.; Zhang, X. *J. Organomet. Chem.* **1997**, *547*, 97-10.
12. Spielmann, J.; Harder, S. *Eur. J. Inorg. Chem.* **2008**, 1480-1486.

13. Koller, J.; Bergman, R. G. *Organometallics* **2012**, *31*, 2530-2533.
14. Mimoun, H.; Laumer, J. Y.; Giannini, L.; Scopelliti, R.; Floriani, C. *J. Am. Chem. Soc.* **1999**, *121*, 6158-6166.
15. (a) Shirobokov, O. G.; Gorelsky, S. I.; Simionescu, R.; Kuzmina, L. G.; Nikonov, G. I. *Chem. Commun.* **2010**, *46*, 7831–7833. (b) Shirobokov, O. G.; Kuzmina, L. G.; Nikonov, G. I. *J. Am. Chem. Soc.* **2011**, *133*, 6487-6489.
16. D. Mukherjee, A. Ellern and A. D. Sadow, *J. Am. Chem. Soc.*, 2010, **132**, 7582–7583.
17. Mukherjee, D.; Thompson, R.; Ellern, A.; Sadow, A. D. *ACS Catal.* **2011**, *1*, 698-702.
18. Mukherjee, D.; Ellern A.; Sadow, A. D. *J. Am. Chem. Soc.* **2012**, *134*, 13018–13026.

Experimental data.

General Procedures. All reactions were performed under a dry argon atmosphere using standard Schlenk techniques or under nitrogen atmosphere in a glovebox, unless otherwise indicated. Water and oxygen were removed from benzene, toluene, pentane, diethyl ether, and tetrahydrofuran solvents using an IT PureSolv system. Benzene- d_6 was heated to reflux over Na/K alloy and vacuum-transferred. $To^M ZnH$ was synthesized according to the literature procedure. The aldehydes and ketones were purchased from Sigma-Aldrich and distilled and stored over dry molecular sieves inside the glove box. 1H , $^{13}C\{^1H\}$, ^{11}B , and ^{19}F NMR spectra were collected on a Varian MR400 spectrometer. ^{15}N chemical shifts were determined by 1H - ^{15}N HMBC experiments on a Bruker Avance II 700 spectrometer with a Bruker Z-gradient inverse TXI $^1H/^{13}C/^{15}N$ 5mm cryoprobe; ^{15}N chemical shifts were originally referenced to an external liquid NH_3 standard and recalculated to the CH_3NO_2 chemical shift scale by adding -381.9 ppm. Elemental analyses were performed using a

Perkin-Elmer 2400 Series II CHN/S by the Iowa State Chemical Instrumentation Facility. X-ray diffraction data was collected on a Bruker APEX II diffractometer.

To^MZnOCH₂Ph (2). 60 microliters of benzaldehyde (0.589 mmol) was added to a 12 mL benzene solution of To^MZnH (0.260 g, 0.580 mmol) and stirred for 4 h at ambient temperature. Volatiles were then removed under reduced pressure providing a white solid. It was then washed with pentane (3 × 5 mL) and further dried under vacuum to obtain 0.305 g (0.550 mmol, 93.4%) of To^MZnOCH₂Ph as a white powder. X-ray quality single crystals were grown from a concentrated toluene solution at – 35 °C. Analytically pure To^MZnOCH₂Ph was also obtained upon recrystallization from a concentrated toluene solution at – 30 °C.

¹H NMR (400 MHz, benzene-*d*₆): δ 1.07 (s, 18 H, CNCMe₂CH₂O), 3.46 (s, 6 H, CNCMe₂CH₂O), 5.57 (s, 2 H, ZnOCH₂C₆H₅), 7.15 (t, ³J_{HH} = 7.6 Hz, 1 H, *para*-ZnOCH₂C₆H₅), 7.24 (t, ³J_{HH} = 7.6 Hz, 2 H, *meta*-ZnOCH₂C₆H₅), 7.35 (t, ³J_{HH} = 7.2 Hz, 1 H, *para*-C₆H₅), 7.44 (t, ³J_{HH} = 7.2 Hz, 2 H, *meta*-C₆H₅), 7.77 (d, ³J_{HH} = 7.6 Hz, 2 H, *ortho*-ZnOCH₂C₆H₅), 8.15 (d, ³J_{HH} = 7.2 Hz, 2 H, *ortho*-C₆H₅). ¹³C{¹H} NMR (175 MHz, benzene-*d*₆): δ 27.47 (CNCMe₂CH₂O), 64.84 (CNCMe₂CH₂O), 70.52 (ZnOCH₂C₆H₅), 80.34 (CNCMe₂CH₂O), 125.39 (*para*-ZnOCH₂C₆H₅), 125.95 (*meta*-ZnOCH₂C₆H₅), 126.48 (*para*-C₆H₅), 127.02 (*meta*-C₆H₅), 133.87 (*ortho*-ZnOCH₂C₆H₅), 135.61 (*ortho*-C₆H₅), 141.70 (br, *ipso*-C₆H₅), 149.60 (*ipso*-ZnOCH₂C₆H₅), 189.84 (br, CNCMe₂CH₂O). ¹¹B NMR (128 MHz, benzene-*d*₆): δ –18.2. ¹⁵N NMR (59.2 MHz, benzene-*d*₆): δ –159.2. IR (KBr, cm⁻¹): 2967 (s), 2930 (m), 2873 (m), 1576 (s, ν_{CN}), 1491 (w), 1463 (m), 1432 (w), 1384 (w), 1369 (m), 1281 (s), 1255 (m), 1195 (s), 1037 (m), 1023 (m), 1004 (s), 969 (s), 899 (w), 845 (w), 751 (m),

704 (s). Anal. Calcd. for $C_{28}H_{36}BN_3O_4Zn$: C, 60.62; H, 6.54; N, 7.57. Found: C, 60.20; H, 6.49; N, 7.52. Mp: 215-220 °C (dec).

To^MZnOCH₂C₆F₅ (4). To^MZnOCH₂C₆F₅ was also synthesized following the similar procedure as described for **2**. Starting from 0.180 g (0.401 mmol) of To^MZnH and 50 microliters (0.405 mmol) of C₆F₅CHO, 0.234 g (0.363 mmol, 90.5%) of To^MZnOCH₂C₆F₅ was isolated. Analytically pure sample of **3** was obtained from recrystallizing a concentration toluene solution at – 30 °C.

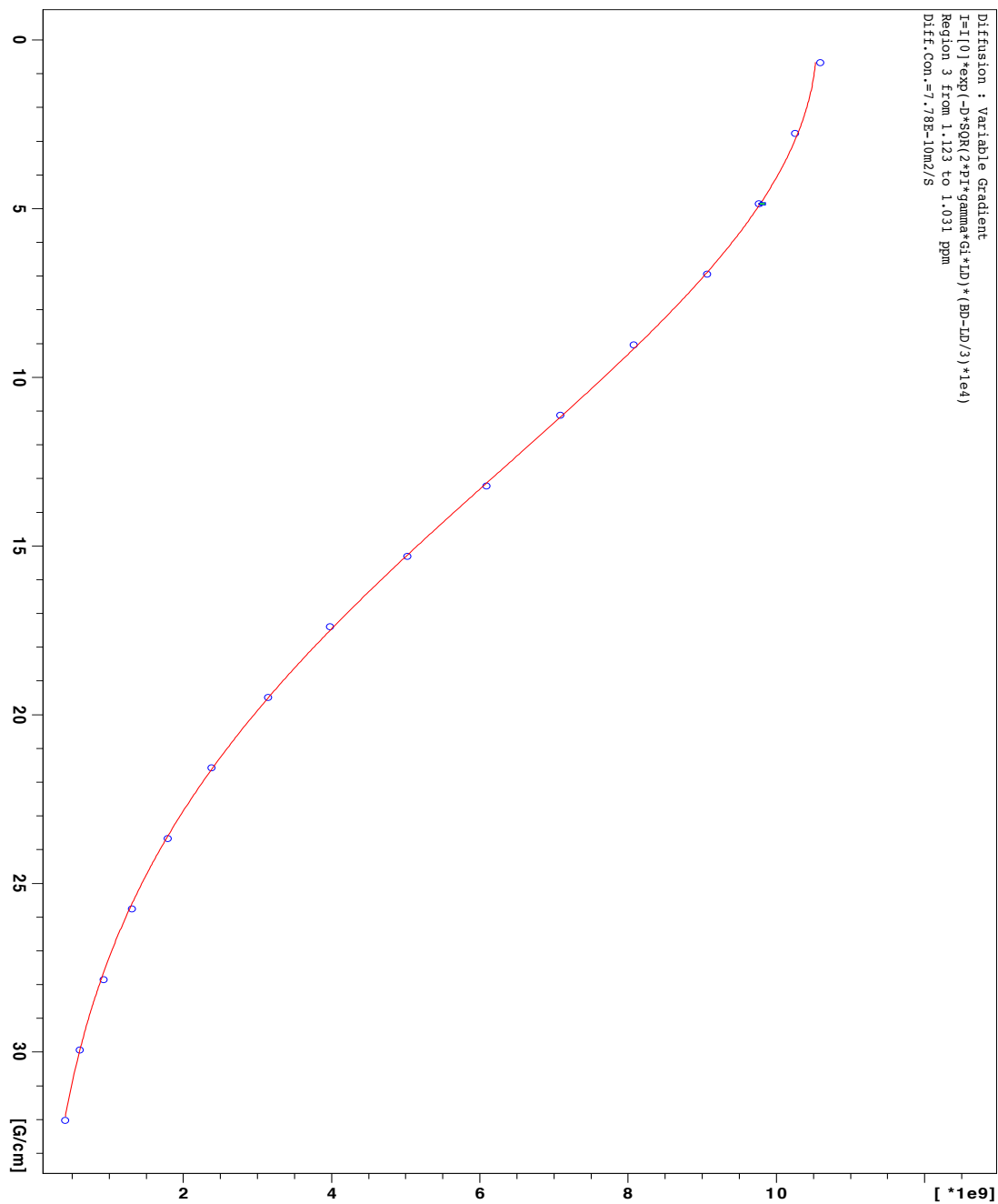
¹H NMR (400 MHz, benzene-*d*₆): δ 1.07 (s, 18 H, CNCMe₂CH₂O), 3.45 (s, 6 H, CNCMe₂CH₂O), 5.40 (s, 2 H, ZnOCH₂C₆H₅), 7.36 (t, ³J_{HH} = 7.6 Hz, 1 H, *para*-C₆H₅), 7.53 (t, ³J_{HH} = 7.6 Hz, 2 H, *meta*-C₆H₅), 8.26 (d, ³J_{HH} = 7.6 Hz, 2 H, *ortho*-C₆H₅). ¹³C{¹H} NMR (175 MHz, benzene-*d*₆): δ 28.18 (CNCMe₂CH₂O), 59.35 (ZnOCH₂C₆F₅), 65.47 (CNCMe₂CH₂O), 81.06 (CNCMe₂CH₂O), 126.56 (*para*-C₆H₅), 127.38 (*meta*-C₆H₅), 136.29 (*ortho*-C₆H₅), 137.37 (ZnOCH₂C₆F₅), 138.78 (ZnOCH₂C₆F₅), 139.21 (ZnOCH₂C₆F₅), 139.69 (ZnOCH₂C₆F₅), 141.17 (br, *ipso*-C₆H₅), 145.43 (ZnOCH₂C₆F₅), 146.81 (ZnOCH₂C₆F₅), 190.63 (br, CNCMe₂CH₂O). ¹¹B NMR (128 MHz, benzene-*d*₆): δ –18.0. ¹⁵N NMR (59.2 MHz, benzene-*d*₆): δ –159.7. ¹⁹F NMR (benzene-*d*₆, 376 MHz): δ –146.76 (*ortho*-ZnOCH₂C₆F₅), –159.64 (*para*-ZnOCH₂C₆F₅), –164.26 (*meta*-ZnOCH₂C₆F₅). IR (KBr, cm⁻¹): 3048 (w), 2969 (s), 2932 (w), 2901 (w), 2826 (w), 1652 (w, ν_{CN}), 1593 (s, ν_{CN}), 1499 (s, ν_{CF}), 1463 (s), 1388 (w), 1368 (m), 1276 (s), 1197 (s), 1166 (m), 1114 (m), 1086 (m), 1055 (m), 957 (s), 936 (s), 820 (w), 745 (w), 704 (s), 679 (w), 640 (w). Anal. Calcd. for $C_{28}H_{31}BN_3O_4F_5Zn$: C, 52.16; H, 4.85; N, 6.52. Found: C, 52.24; H, 4.86; N, 6.34. Mp: 238-242 °C (dec).

To^MZnOCH(C₆F₅)OCH₂C₆F₅ (5). A 5 mL toluene mixture containing 0.360 g (0.802 mmol) of To^MZnH and 0.2 mL (1.620 mmol) of C₆F₅CHO was kept at -30 °C for two weeks. X-ray quality single crystals of To^MZnOCH(C₆F₅)OCH₂C₆F₅ were deposited in the mean time which were then isolated by decanting the supernatant solution. Further drying the crystals under vacuum provided 0.205 g (0.244 mmol) of analytically pure To^MZnOCH(C₆F₅)OCH₂C₆F₅. ¹H NMR (600 MHz, toluene-*d*₈): δ 1.00 (s, 9 H, CNCMe₂CH₂O), 1.06 (s, 9 H, CNCMe₂CH₂O), 3.44 (s, 6 H, CNCMe₂CH₂O), 4.26 (d, ¹J_{HH} = 10.8 Hz, 1 H, ZnOCH₂C₆F₅(C₆F₅CHO)), 4.51 (d, ¹J_{HH} = 10.8 Hz, 1 H, ZnOCH₂C₆F₅(C₆F₅CHO)), 6.76 (s, 1 H, ZnOCH₂C₆F₅(C₆F₅CHO)), 7.29 (t, ³J_{HH} = 7.2 Hz, 1 H, *para*-C₆H₅), 7.44 (t, ³J_{HH} = 7.2 Hz, 2 H, *meta*-C₆H₅), 8.11 (d, ³J_{HH} = 7.2 Hz, 2 H, *ortho*-C₆H₅). ¹³C{¹H} NMR (175 MHz, benzene-*d*₆): δ 27.36 (CNCMe₂CH₂O), 27.77 (CNCMe₂CH₂O), 54.14 (ZnOCH₂C₆F₅(C₆F₅CHO)), 65.58 (CNCMe₂CH₂O), 81.13 (CNCMe₂CH₂O), 98.62 ((ZnOCH₂C₆F₅(C₆F₅CHO)), 112.75 (C₆F₅), 120.24 (C₆F₅), 126.55 (*para*-C₆H₅), 127.36 (*meta*-C₆H₅), 136.27 (*ortho*-C₆H₅), 137.28 (C₆F₅), 138.70 (C₆F₅), 140.20 (C₆F₅), 140.45 (br, *ipso*-C₆H₅), 140.87 (C₆F₅), 141.60 (C₆F₅), 142.28 (C₆F₅), 145.48 (C₆F₅), 146.90 (C₆F₅), 190.84 (br, CNCMe₂CH₂O). ¹¹B NMR (128 MHz, benzene-*d*₆): δ -18.3. ¹⁵N{¹H} NMR: δ -160.6. ¹⁹F NMR (benzene-*d*₆, 376 MHz): δ -143.24 (C₆F₅), -145.18 (C₆F₅), -155.20 (C₆F₅), -157.25 (C₆F₅), -163.13 (C₆F₅), -163.49 (C₆F₅). IR (KBr, cm⁻¹): 3080 (w), 3049 (w), 2973 (m), 2933 (m), 2905 (m), 1657 (w), 1650 (w), 1595 (s, ν_{CN}), 1522 (s), 1504 (s), 1464 (m), 1432 (w), 1390 (m), 1371 (m), 1356 (m), 1339 (w), 1298 (m), 1278 (m), 1253 (w), 1198 (s), 1168 (m), 1133 (m), 1110 (m), 1055 (m), 1038 (m), 1000 (s), 955 (s), 937 (s), 922 (m), 820 (m), 803 (m), 746 (m), 706 (m). Anal. Calcd. for C₃₅H₃₂BN₃O₅F₁₀Zn: C, 50.00; H, 3.84; N, 5.00. Found: C, 50.40; H, 3.99; N, 4.94. Mp: 165-170 °C (dec.)

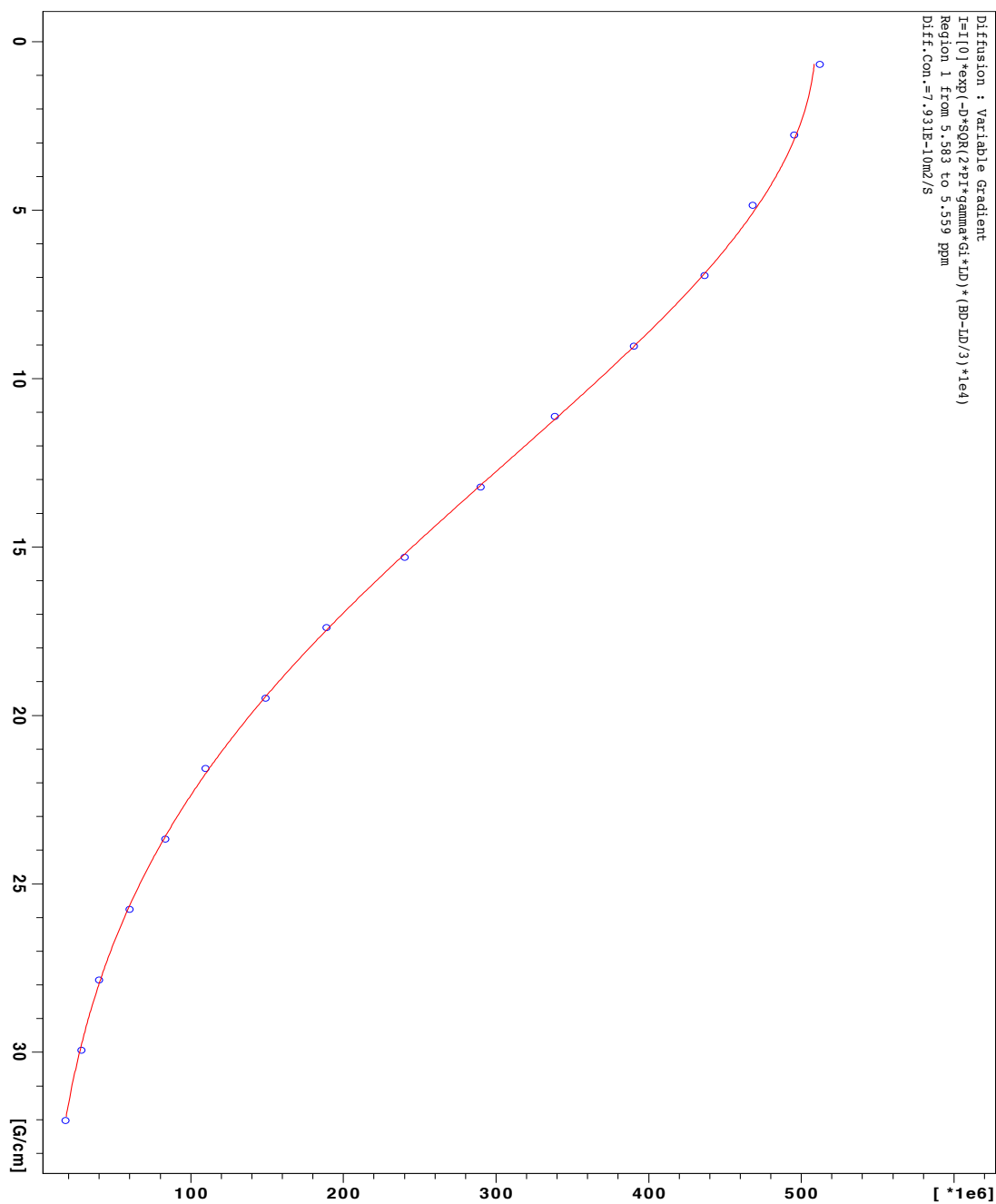
General procedure for gram-scale hydrosilylation reduction of carbonyls. Procedure for the hydrosilylation reduction of PhCHO using BnMe₂SiH is provided here as an example. Reductions of all the other substrates were achieved following similar procedure. A 5 mL toluene solution containing 0.5 mL (4.9 mmol) of PhCHO, 0.8 mL (5.1 mmol) of BnMe₂SiH, and 0.022 g (0.05 mmol) of To^MZnH was heated to reflux in a teflon sealed tube for 8 h. Upon cooling, the reaction mixture was added to 50 mL of 1 M aqueous NaOH solution and stirred for 2 h at ambient temperature. Subsequently, the product PhCH₂OH was extracted from the aqueous solution using diethyl ether (3×50 mL). Removal of diethyl ether using rotor vapor afforded 0.490 g (4.5 mmol, 91.8%) of PhCHO₂OH.

Procedures for DOSY (Diffusion-Ordered Spectroscopy) experiment. All the measurements were performed on a Bruker DRX400 spectrometer using a DOSY stimulated spin-echo pulse program with bipolar gradients. Accurately known concentrations of the species in question, To^MZnOCH₂Ph and To^MZnOCH₂C₆F₅(C₆F₅CHO) were determined by integration of the resonances corresponding to species of interest and integration of a tetrakis(trimethylsilane standard of accurately known concentration. The temperature in the NMR probe was preset to 298K, and the probe was maintained at a constant temperature for each experiment. The delay time in between pulses was set to 5 s in order to ensure the spins are fully relaxed to their ground states. During this experiments, a series of 1D ¹H NMR spectra were acquired at increasing gradient strength. The signal intensity decay was fit by non-linear least squares regression analysis to Equation 1 to obtain the diffusion coefficient D.

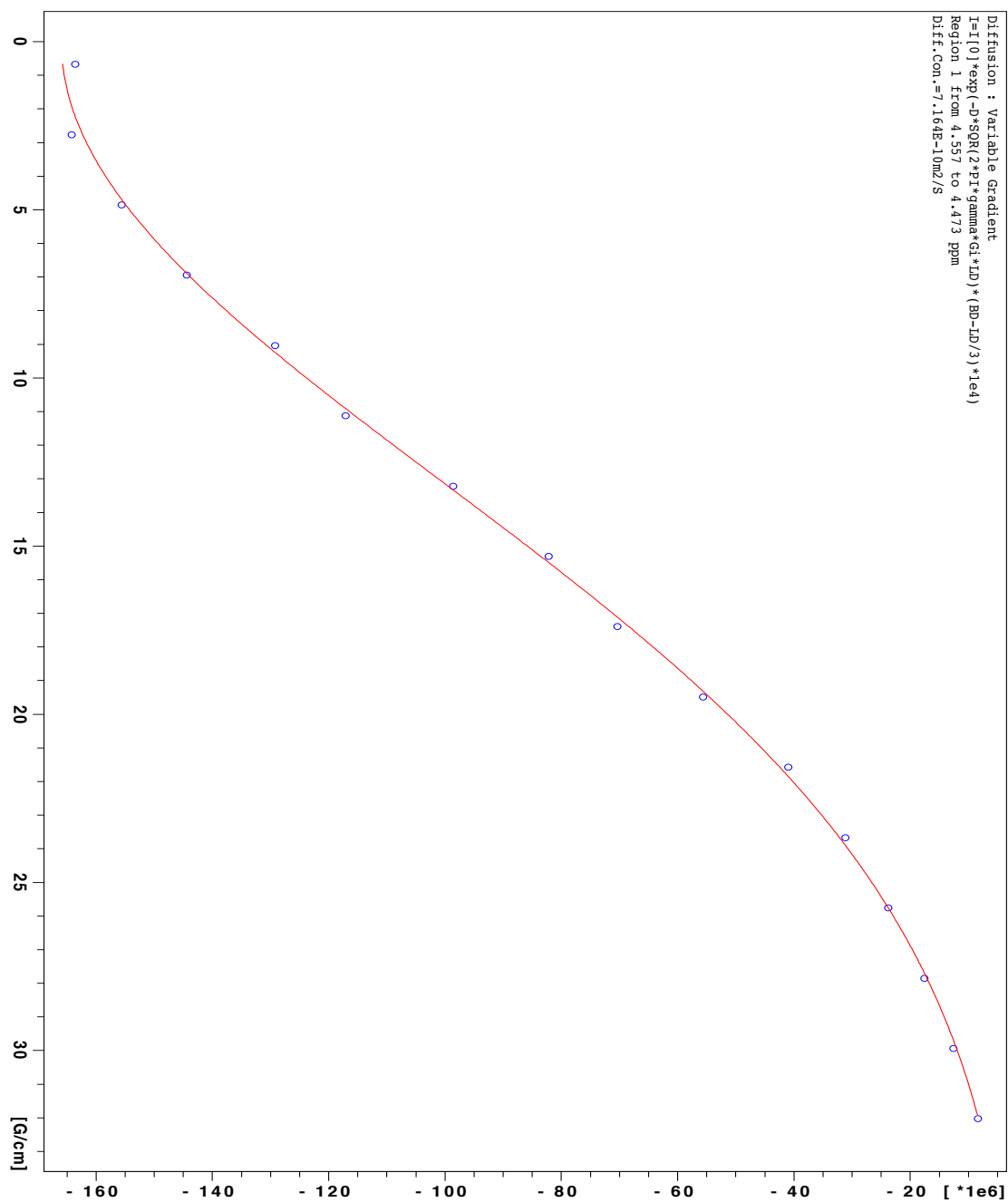
Plot of intensity vs. gradient strength that was used to determine the diffusion coefficient ($7.78 \times 10^{-10} \text{ m}^2/\text{s}$) for $\text{To}^{\text{M}}\text{ZnO}(3,5\text{-Me}_2\text{-C}_6\text{H}_3)$.



Plot of intensity vs. gradient strength that was used to determine the diffusion coefficient ($7.93 \times 10^{-10} \text{ m}^2/\text{s}$) for $\text{To}^{\text{M}}\text{ZnOCH}_2\text{Ph}$ (2).



Plot of intensity vs. gradient strength that was used to determine the diffusion coefficient ($7.16 \times 10^{-10} \text{ m}^2/\text{s}$) for $\text{To}^{\text{M}}\text{ZnOCH}_2\text{C}_6\text{F}_5(\text{OCHC}_6\text{F}_5)$ (5).



Chapter 8: $To^M MgMe$ is a multifunctional pre-catalyst for reductive hydroboration of carbonyls and esters as well for Tishchenko reaction and reversible trans esterification.

Contains results from a manuscript to be submitted for publication

Debabrata Mukherjee, Arkady Ellern and Aaron D. Sadow

Abstract.

Tris(oxazoliny)phenyl borato magnesium methyl is an active pre-catalyst for hydroboration of aldehydes, ketones, esters, and polyesters using HBpin as the hydride source. The same magnesium methyl complex also actively catalyzes the Tishchenko coupling of aldehydes to esters.

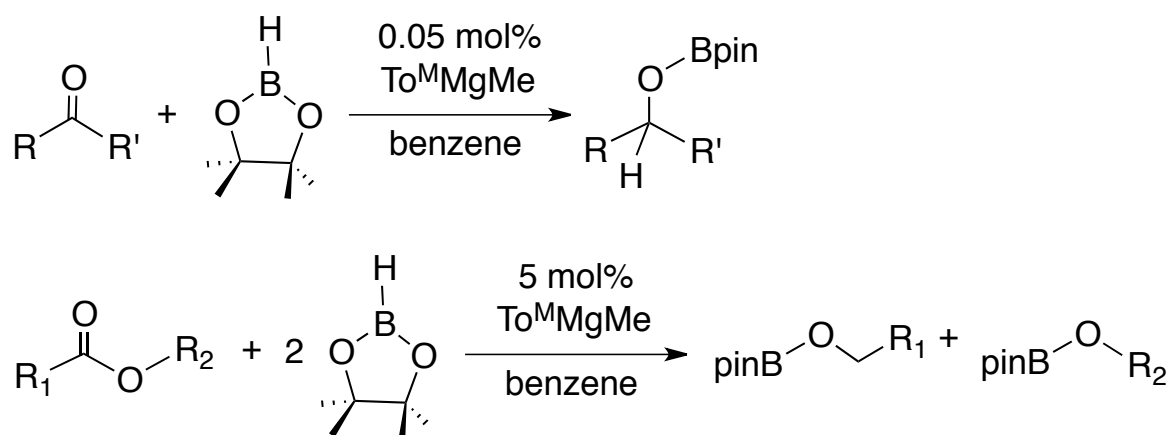
Introduction.

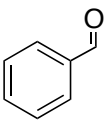
Although Grignard reagents are widely known for stoichiometric C-C bond formation reactions,¹ exploration of the potential catalytic activity of organometallic magnesium complexes in the context of carbonyl and ester reduction has begun only recently.^{2,-6} Inexpensive, non-toxic, and oxophilic nature of magnesium has made this metal system highly attractive. Recently we have reported that the $To^M MgMe$ [To^M = tris(4,4-dimethyl-2-oxazoliny)phenylborate] (**1**) is an active pre-catalyst for intramolecular hydroamination/cyclization of amino-olefins and dehydrocoupling Si-N bond formation reactions between amines and hydrosilanes.^{7,8} We continued to discover other potential use of **1** and here we report it's catalytic activity in hydroboration reduction of aldehydes, ketones, esters, imines, and amides as well as Tishchenko dimerization of aldehydes to esters. Hill and coworkers have recently reported a magnesium alkyl complex,

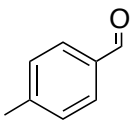
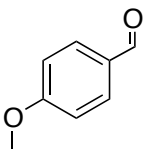
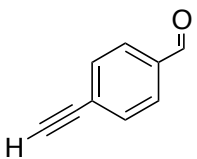
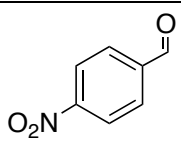
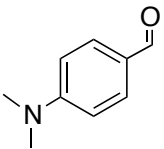
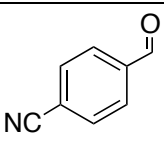
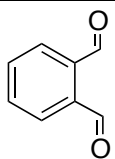
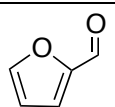
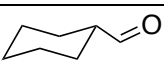
$[\text{CH}\{\text{C}(\text{Me})\text{NAr}\}_2\text{Mg}^n\text{Bu}$ [$\text{Ar} = 2,6\text{-}^i\text{Pr}_2\text{C}_6\text{H}_3$], as an active pre-catalyst for the hydroboration of carbonyl and pyridine derivatives.^{9,10} For ester to alcohol transformation, systems for catalytic hydrosilylation¹¹⁻¹⁵ and hydrogenation¹⁶ have been developed in order to avoid stoichiometric metal hydride reductions. Whereas examples of hydroboration reduction of esters are rare.¹⁰

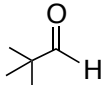
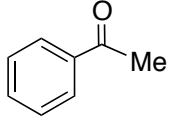
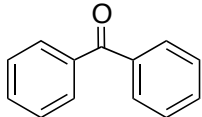
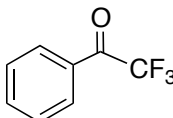
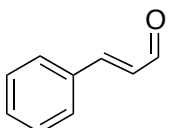
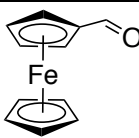
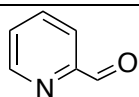
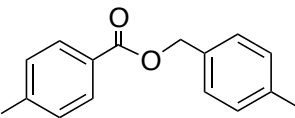
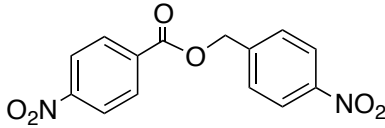
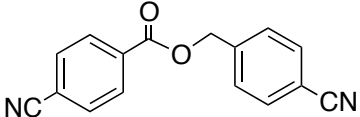
Results and Discussions.

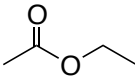
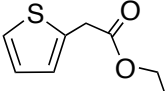
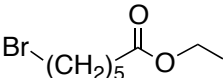
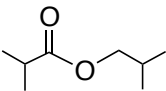
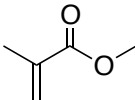
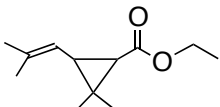
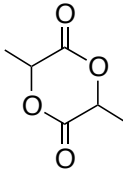
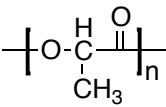
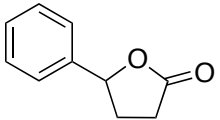
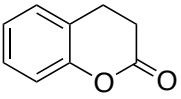
Inspired by Hill's report, we tested a wide range of aromatic and aliphatic aldehydes, ketones, esters, lactones, imines and amides for the hydroboration reactivity with HBpin using **1** as the pre-catalyst. Catalyst loading as low as 0.05 mol% readily afforded the borate ester products in quantitative yield at ambient temperature. The reactions were monitored by following ¹H and ¹¹B NMR spectroscopy.

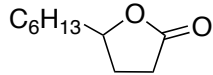
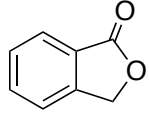
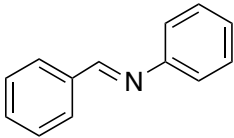
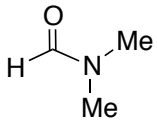


entry	Substrates	Temperature ^a	Time ^a	NMR yield (%)	Isolated yield (%) ^{b,c}
1		25 °C	15 min	>99%	96%

2		25 °C	45 min	>99%	93%
3		25 °C	15min	>99%	97%
4		60 °C	1 h	>99%	90%
5		25 °C	30 min	>99%	92%
6		25 °C	1 h	>99%	92%
7		25 °C	15 min	>99%	95%
8		25 °C	30 min	>99%	96%
9		25 °C	15 min	>99%	92%
10		25 °C	15 min	>99%	96%

11		25 °C	15 min	>99%	92%
12		60 °C	2 h	>99%	95%
13		60 °C	5 h	>99%	90%
14		60 °C	1 h	>99%	91%
15		25 °C	30 min	>99%	93%
16		60 °C	2 h	>99%	92%
17		25 °C	15 min	>99%	92%
18		25 °C	15 min	>99%	90%
19		25 °C	15 min	>99%	91%
20		25 °C	15 min	>99%	91%

21		25 °C	15 min	>99%	90%
22		25 °C	15 min	>99%	---
23		25 °C	15 min	>99%	---
24		25 °C	15 min	>99%	90%
25		25 °C	15 min	>99%	---
26		25 °C	15 min	>99%	---
27		25 °C	15 min	>99%	88%
28		25 °C	15 min	>99%	---
29		25 °C	15 min	>99%	---
30		25 °C	15 min	>99%	---

31		25 °C	15 min	>99%	---
32		25 °C	15 min	>99%	92%
33		25 °C	6 h	>99%	93%
34		25 °C	15 min	>99%	---

^a temperature and time are given for micromolar NMR-scale reactions. ^b Gram-scale reactions are conducted using 0.5 mol% catalyst loading. ^c products from some of the substrates were not isolated in gram-scale and hence the isolated yield is not reported.

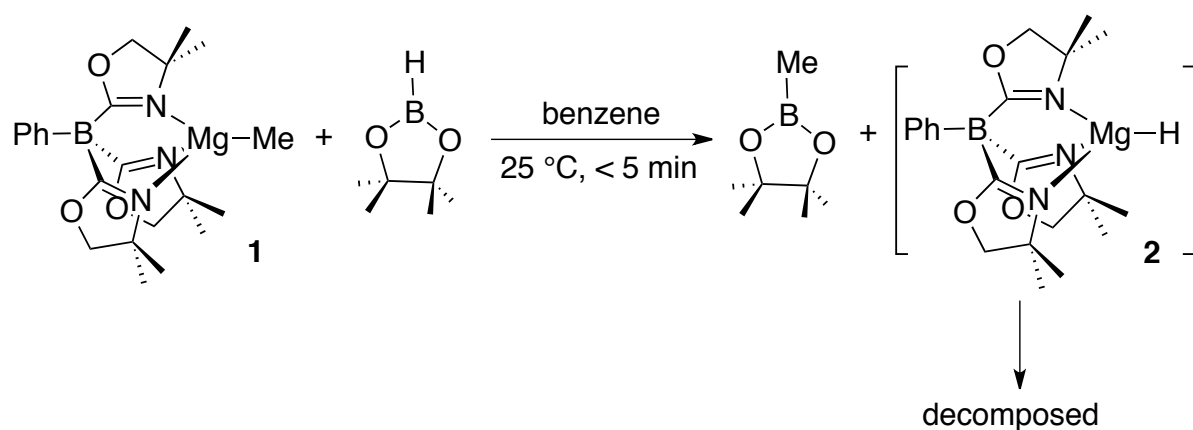
Para-substitued aromatic aldehydes with both electron-donating and -withdrawing groups undergo quantitative conversion within similar time scale under similar conditions (entry 1-7). Thus the facility of the catalysis is apparently controlled by steric properties of the substrates. For similar reason, the hydroboration of more sterically hindered ketonic substrates generally required higher catalyst loading or longer reaction time or elevated temperature (entry 12-14). *p*-cyano benzaldehyde (entry 7) is noteworthy since only the aldehyde moiety is reduced and the cyano-group remains untouched; even with 3 equiv. of HBpin and further heating at 60 °C. Similarly for pyridine-2-carboxaldehyde (entry 17) no dearomatization of the pyridine ring is observed. With α,β -unsaturated aldehyde (entry 15) only the 1,2-reduction is evident and the olefinic double bond remains intact even in presence of excess HBpin. Substrates like furfural and ferrocene-2-carboxaldehyde are also

successfully reduced quantitatively. Similar to Hill's β -diketiminato Mg system, no enolization or aldol condensation side reactions were observed in any case. Imines also undergo hydroboration under similar catalytic conditions. But the relative hydroboration rate is substantially slower than the aldehydes and ketones. Thus, the reduction of N-benzelidine aniline (entry 33) occurs at ambient temperature over a period of 6 h in presence of 5 mol % of **1**. Gram-scale hydroboration of the substrates (table 1) were successfully conducted using 0.5 mol% of **1**, thus establishing the practicability of this system. Hydrosilylation using PhSiH_3 instead hydroboration gives poor results in carbonyl reduction in this catalytic system. As for examples, hydrosilylation of PhC(O)CH_3 with PhSiH_3 using **1** as the pre-catalyst proceeds slowly only at elevated temperature (120 °C) and gives only partial conversion (40%, 20 h). Reduction of esters with two equivalents of HBpin is also successfully carried out using 0.5 mol% of catalyst loading and similar functional group tolerance is envisaged. Interestingly, monomeric *rac*-lactide and polymerized lactide (entry 10, 11) are also successfully hydroborated [*rac*-lactide polymerization was accomplished using $\text{To}^{\text{M}}\text{AlMe}_2$ catalyst.¹⁷ Buchwald's Ti-system for catalytic hydrosilylation of lactones performs partial reduction providing lactols with high selectivity over diols following work up.¹⁸ However, under our current catalytic condition diols are the only observed products.

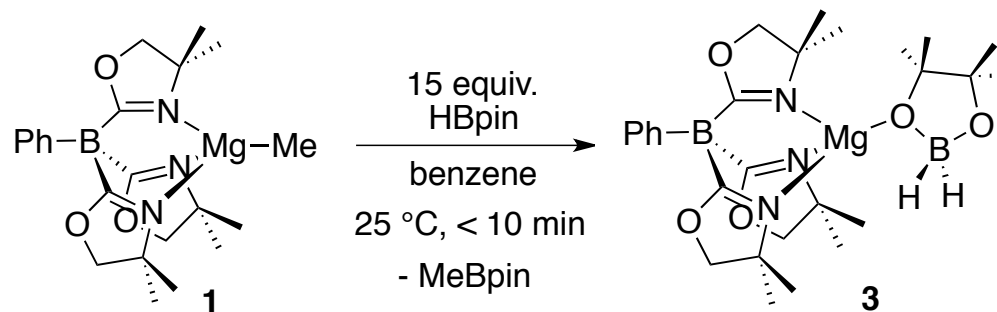
Ancillary To^{M} ligand provides unique support to isolate reactive intermediates, which in turn facilitates mechanism elucidation. We therefore set out to study the mechanism involved in the reductions using stoichiometric reactions and ^1H NMR kinetics, especially of esters since this is less explored compared to aldehydes and ketones. A possible catalytic cycle involving a crucial β -dealkoxylation step from a Ti-alkoxide intermediate has been proposed by Buchwald et. al.¹⁸ But a detailed mechanistic study on metal mediated catalytic

hydrosilylation or hydroboration reduction of esters to alcohols and convincing evidence in favor of the β -dealkoxylation step is missing in the literature. Similar to Buchwald's Ti-system of no rearrangement product is found in the reduction of a vinylcyclopropyl ester and thus a radical pathway for the ester reduction mechanism is unlikely here.

$\text{To}^{\text{M}}\text{MgMe}$ (**1**) readily reacts with HBpin in benzene- d_6 to generate methyl boronic acid pinacol ester (confirmed by a singlet resonance at 35 ppm in ^{11}B NMR spectrum) along with $\text{To}^{\text{M}}\text{MgH}$ (**2**), which subsequently undergoes rapid decomposition.



However, in presence of excess HBpin (15 equivalents), **2** is trapped as a borohydride species, $\text{To}^{\text{M}}\text{MgH}_2\text{B}(\text{pin})$ (**3**) (eqn. 1). Thus, the compound **3** is synthesized and isolated following a slow addition of a benzene solution of **1** to HBpin (15 equivalents) at ambient temperature.



Species **3** is pseudo- C_{3v} -symmetric in solution, as indicated by the equivalent oxazoline groups in ^1H and ^{13}C spectra. The ^1H NMR spectrum also contains a broad quartet at 4.19 ppm equivalent to 2 protons assigned to $\text{To}^{\text{M}}\text{MgH}_2\text{Bpin}$ and the 12 equivalent methyl protons of the pinacol unit appear as a broad singlet at 1.42 ppm. Although, the broad signal suggests fluxionality of the pinacol unit in solution at ambient temperature, the signal only sharpened below $0\text{ }^\circ\text{C}$. In the ^{11}B NMR spectrum, a characteristic triplet resonance at 3.44 ppm ($^1J_{\text{BH}} = 93.5\text{ Hz}$), assigned to the MgH_2Bpin boron, was observed along with the usual To^{M} borate resonance (-18.4 ppm). The solid-state IR spectrum of **3** showed a broad peak at 2309 cm^{-1} corresponding to ν_{BH} band. A single crystal X-ray diffraction study of **3** (fig. 1) revealed that the pinacol unit is coordinated to the Mg center through one of the two oxygen atoms. The only similar but not so well-defined structurally characterized example is the dimeric $[(\text{HC}\{(\text{Me})\text{CN}(2,6\text{-}^i\text{Pr}_2\text{C}_6\text{H}_3)\}_2\text{Mg})_2\text{-}\mu\text{-H-}\mu\text{-}\{\text{H}_2\text{Bpin}\}]$ complex, reported by Hill and coworkers,¹⁰ in which the Mg-centers are bridged by $\mu\text{-Mg-H-Mg}$ and O-B-O interactions.

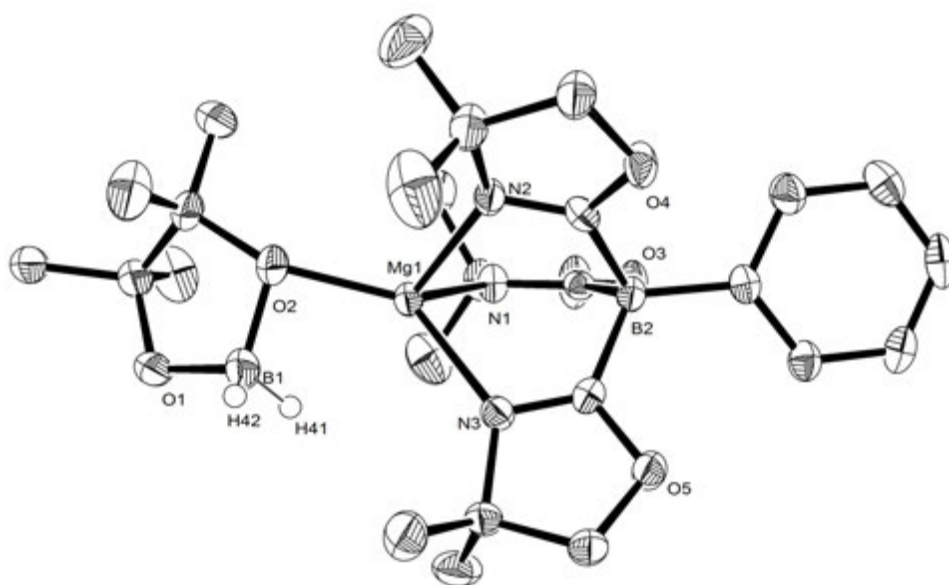
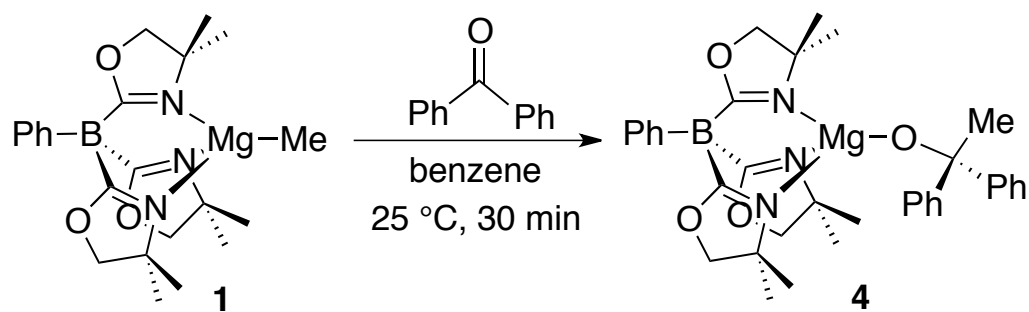


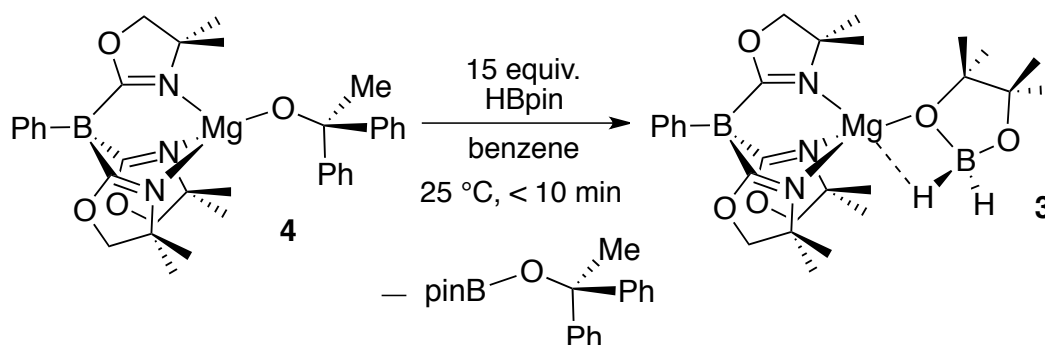
Fig. 1 ORTEP diagram of $\text{To}^{\text{M}}\text{MgH}_2\text{Bpin}$ (**3**) with ellipsoids plotted at 50% probability. Hydrogen atoms other than the -BH_2 moiety are not illustrated for clarity.

Apparently none of the two H_2B hydrides are pointing towards the Mg-center. However, one of the two Mg–H distances (2.300 Å and 2.913 Å) is shorter than the sum of the van der Waal radii of Mg and O (2.82 Å); and thus a secondary interaction between them cannot be over ruled. Species **3** is isolable and persistent at ambient temperature, as the concentration of **3** in a benzene- d_6 solution stored in Teflon-sealed NMR tube is maintained over 2 days. However, rapid decomposition to unidentified mixture of products occurs upon heating at 60 °C.

$To^M MgMe$ (**1**) and benzophenone readily provide $To^M MgOCMePh_2$ (**4**) in benzene at ambient temperature. Species **4** was isolated and fully characterized using spectroscopic, analytical, and X-ray diffraction techniques.



Similar to **1**, species **4** also possesses pseudo- C_{3v} symmetric To^M -coordination to the Mg center in solution and the $-CH_3$ singlet is now moved to 2.13 ppm from -0.65 ppm in **1** upon insertion. Monomeric nature of **4** is also maintained in solid state as confirmed by an X-ray crystal structure. The Mg–O interatomic distance, 1.829(4) Å, is shorter than the Mg–O distance in **3**. A subsequent reaction between **4** and HBpin produces $Ph_2MeCO-Bpin$ and **2**, which further undergoes rapid decomposition as mentioned above. Whereas adding excess HBpin (~ 15 equiv.) to a benzene- d_6 solution of **4** provides $Ph_2MeCO-Bpin$ and **3**.



The ester reduction mechanism is further investigated using ^1H NMR kinetics. Ethyl acetate (EtOAc) and HBpin were chosen as the substrates for this study. Under initial conditions of 0.30 M $[\text{EtOAc}]_{\text{ini}}$, 0.85 M $[\text{HBpin}]_{\text{ini}}$ with 6.6 mM - 25.2 mM $[\text{To}^{\text{M}}\text{MgMe}]$ (**1**) pre-catalyst in toluene- d_8 at 287 K (calibrated) plots of $[\text{EtOAc}]$ versus time follow a half-order decay over three half-lives (nonlinear least squares analysis of the integrated half-order rate law provides k_{obs} for a particular catalyst concentration. Several reactions were attempted with a range of concentrations of HBpin with constant $[\text{EtOAc}]_{\text{ini}}$ and $[\text{To}^{\text{M}}\text{MgMe}]$; k_{obs} does not change with $[\text{HBpin}]$ ranging from 0.85 M - 2.4 M. This lack of dependence on HBpin concentration confirms its zero-order contribution to the rate law with EtOAc as the limiting reagent. In contrast, a plot of k_{obs} vs. $[\text{To}^{\text{M}}\text{MgMe}]$ shows a linear correlation giving $k_{\text{obs}}' = 1.79 \times 10^{-2} \text{ mol}^{-1/2} \text{ sec}^{-1}$. Under these conditions the empirical rate law is:

$$-d[\text{EtOAc}]/dt = k_{\text{obs}}' [\text{To}^{\text{M}}\text{MgMe}] [\text{EtOAc}]^{1/2} [\text{HBpin}]^0$$

The half-order dependence on $[\text{EtOAc}]$ indicates that the C-O bond breakage (β -dealkoxylation) is relatively fast and the turnover-limiting step lies somewhere following it. Assuming that the insertion of the resulting CH_3CHO into the Mg-H moiety is really fast, the metathesis step between the $\text{To}^{\text{M}}\text{MgOEt}$ (**5**) and HBpin could be the slowest and hence turnover-limiting step. However, the fact that the empirical rate law is independent of

[HBpin] suggests a rapid adduct formation between $\text{To}^{\text{M}}\text{MgOEt}$ and HBpin, followed by a slow internal hydride transfer could be a possibility. In order to verify this and identify the true nature of the resting state of the Mg-species, the catalysis in toluene- d_8 was monitored at a lower temperature (267K) and with a relatively higher catalyst loading ($[\text{To}^{\text{M}}\text{MgMe}] = 54$ mM, $[\text{EtOAc}]_{\text{ini}} = 0.58$ M, $[\text{HBpin}]_{\text{ini}} = 1.18$ M). Lowering the temperature would essentially slow down the reaction and a higher [Mg] would help to identify the resting state. Under these conditions a new Mg-species was truly identified and spectroscopically characterized as $\text{To}^{\text{M}}\text{MgOEt}\cdot\text{HBpin}$ (**6**) adduct which is distinct from $\text{To}^{\text{M}}\text{MgMe}$, $\text{To}^{\text{M}}\text{MgH}_2\text{Bpin}$ and $\text{To}^{\text{M}}\text{MgOEt}$. The ^1H NMR of the reaction mixture contains two diastereotopic sets of six methyl protons (1.33 ppm and 1.36 ppm), identified as the HBpin coordinated to $\text{To}^{\text{M}}\text{MgOEt}$, which is different from free HBpin (0.99 ppm) or $\text{To}^{\text{M}}\text{MgH}_2\text{Bpin}$ (1.42 ppm). Similarly the triplet resonance (1.46 ppm) corresponding to the new MgOEt moiety is different from that of $\text{To}^{\text{M}}\text{MgOEt}$ (1.27 ppm) and free EtOAc. The ^{11}B NMR of this reaction mixture contains a broad resonance at 7.2 ppm assigned as the $\text{To}^{\text{M}}\text{MgOEt}\cdot\text{HBpin}$, which is again markedly different from that of $\text{To}^{\text{M}}\text{MgH}_2\text{Bpin}$ (3.4 ppm). Attempts to isolate this species or X-ray quality single crystals from the catalytic reaction mixtures at low temperatures failed. Thus we propose a catalytic cycle as shown in fig. 2 operative for the hydroboration reduction of ethyl acetate, where the resting state of the catalyst is an adduct $\text{To}^{\text{M}}\text{MgOEt}\cdot\text{HBpin}$ and the turnover-limiting step being the intramolecular metathesis.

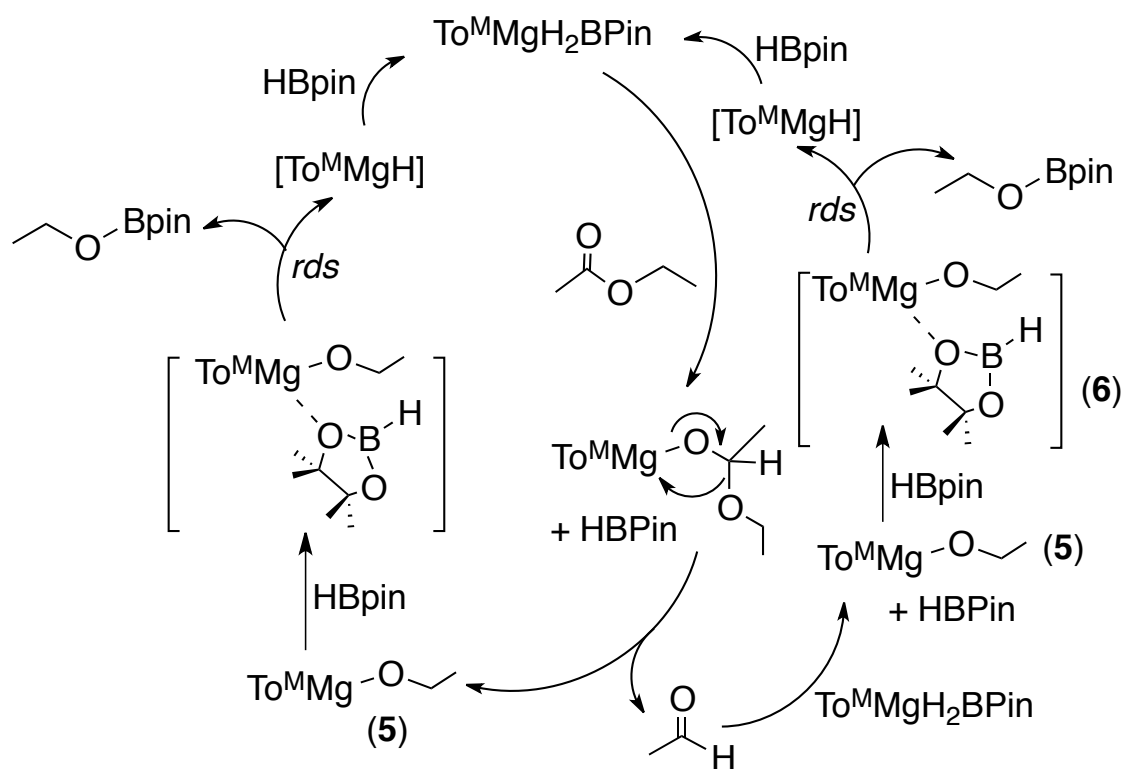
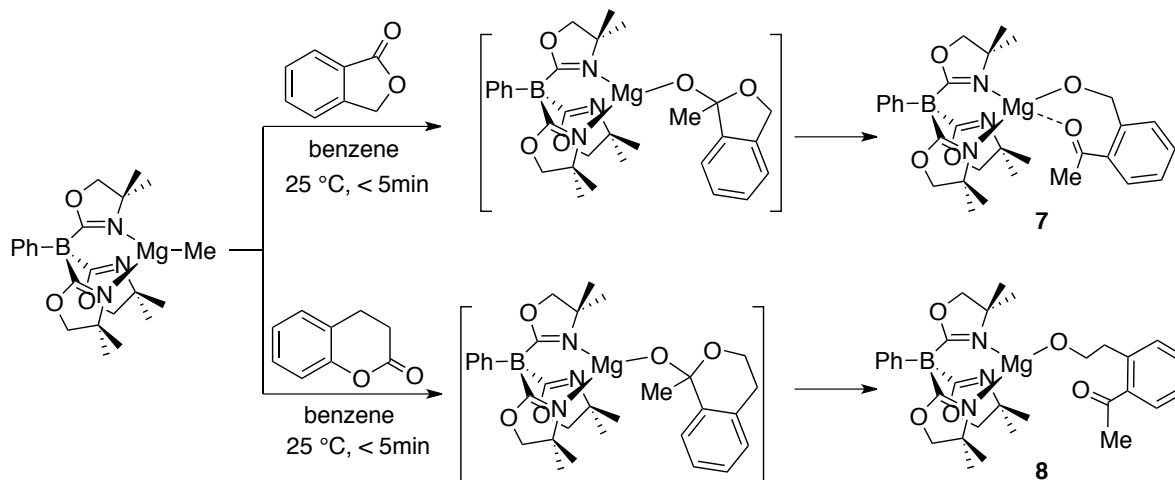


Fig. 2 proposed cycle for the hydroboration of EtOAc using HBpin and **1** as the pre-catalyst.

The proposed β -dealkoxylation step is further probed using stoichiometric reaction. Reaction between **1** and EtOAc in benzene- d_6 at ambient temperature readily provides a mixture $To^M MgOEt$ (**5**) and acetone. Formation of acetone was confirmed by comparing with a standard sample in benzene- d_6 , whereas compound **5** was precipitated out from the above solution mixture as X-ray quality single crystals. Although we were not able to identify the intermediate Mg alkoxide (**7**), formation of **5** and acetone strongly suggests a true β -dealkoxylation pathway. Compound **5** is a dimer in the form of $[(\kappa^2-To^M)Mg(\mu-OEt)]_2$, confirmed by its solid-state X-ray crystal structure. The Mg–O interatomic distance is 1.95 Å, similar to the Mg–O distance in **3** but longer than that in **4**, due to dimeric nature. Compound **5** is independently synthesized from **1** and EtOH and subsequently completely characterized.

Lactones are also used to identify the β -dealkoxylation step. Thus the stoichiometric reactions of **1** with phthalide and dihydrocoumarin provide the corresponding alkoxides **7** and **8** respectively, resulting from the Mg–Me insertion into C=O followed by rapid β -dealkoxylation.

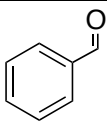
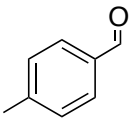


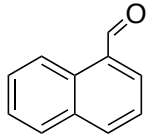
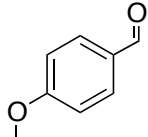
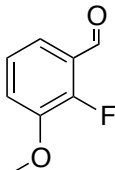
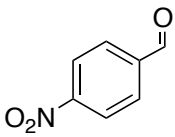
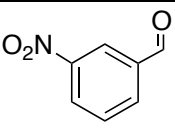
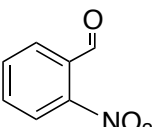
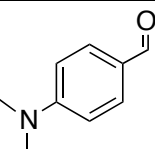
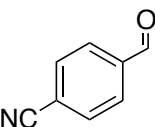
^{13}C NMR spectrum of **7** indicates that the ketone functional group is coordinated to the Mg-center as the chemical shift of the carbonyl carbon (123 ppm) is observed to be upfielded. Species **7** slowly precipitates out from solution as it forms; but its NMR (^1H , ^{13}C , ^{11}B , ^{15}N) spectroscopic characterization is successfully conducted. In species **8**, however, the ketone moiety is non-coordinating as evident from the ^{13}C chemical shift (214 ppm).

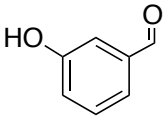
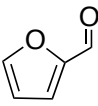
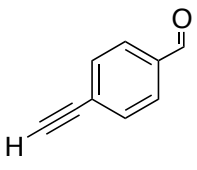
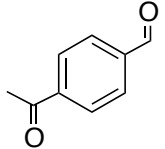
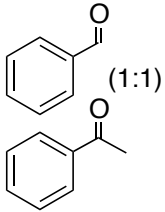

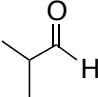
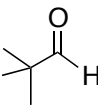
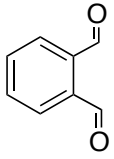
Interestingly, when the reaction time course of hydroboration of PhCHO was monitored, it turns out that the change in the order of substrate addition to the catalyst gives rise to different scenarios. Thus adding a benzene- d_6 solution mixture of PhCHO and HBpin (1:1) to another benzene- d_6 solution of $\text{To}^{\text{M}}\text{MgMe}$ (**1**) provides PhCH₂O-Bpin as the only product. Whereas, consecutive addition of PhCHO and HBpin to a benzene- d_6 solution of **1** initially gives a mixture of PhCH₂O-Bpin and benzyl benzoate [PhCO₂CH₂Ph] ester. The ester is eventually reduced as well to provide PhCH₂O-Bpin as the sole final product. Such

observation indicates that **1** could also be an active pre-catalyst for Tishchenko coupling of aldehydes.

Dimerization of aldehydes to analogous carboxylic esters, known as Tishchenko reaction, is a century old atom-economical process for the direct synthesis of organic esters. This reaction is quite appealing as the resulting esters have wide applications in medicine, food and perfume industries.¹⁹ Aluminium alkoxides²⁰ were initially the catalyst of choice for long time until recently a series of catalyst systems ranging from transition metals,²¹ lanthanides,²² actinides²³ to alkali (Na²⁴, K²⁵) and alkaline earth metals (Mg²⁶, Ca²⁷, Ba²⁸, Sr²⁹) in the past two decades are explored for the above transformation. Among the group 2 alkaline earth metals, use of isolable molecular magnesium catalysts for Tishchenko coupling is an attractive option due to the low cost, less toxicity and easy availability. Furthermore, with a suitable choice of supporting ancillary ligand reactive intermediates could be isolated which are important to probe the reaction mechanism. Thus, the catalytic activity of **1** was tested with a wide range of aromatic and aliphatic aldehydes with different functional groups.

Entry	Substrates	Temperature	Time	Conversion (%) ^a	Isolated yield (%)
1		25 °C	2 h	94%	88%
2		25 °C 60 °C	12 h 16 h	70% 94%	86%

3		25 °C	12 h	65%	84%
		60 °C	12 h	93%	
4		60 °C	2 h	~ 2%	---
5		120 °C	9 h	70%	---
6		25 °C	15min	12%	67%
		60 °C	30 h	85%	
7		25 °C	15min	20%	90%
		60 °C	5 h	98%	
8		25 °C	15min	17%	88%
		60 °C	21 h	93%	
9		80 °C	12 h	~ 4%	---
10		25 °C	15 min	58%	90%
		60 °C	12 h	98%	

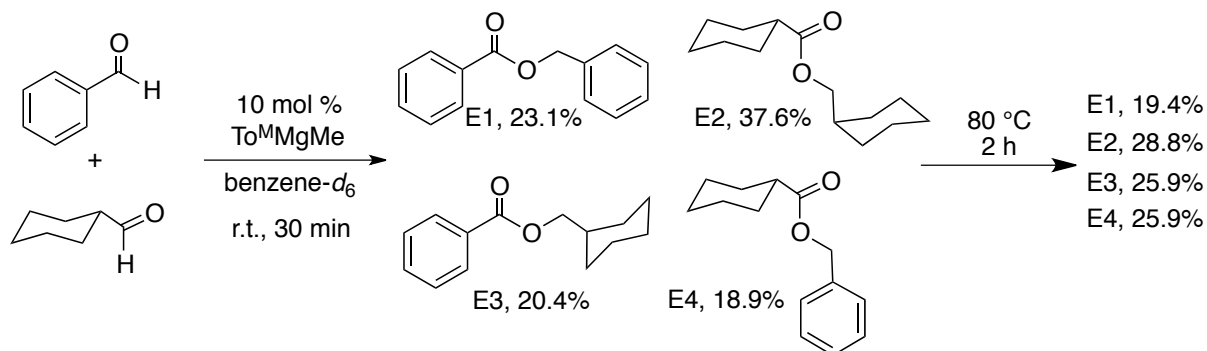
11		120 °C	2 h	---	---
12		120 °C	28 h	9%	---
13		25 °C 60 °C	2 h 45 h	25% 97%	90%
14		120 °C	2 h	---	---
15		60 °C	12 h	----	---
16		25 °C	15 min	>99%	94%
17		25 °C	15 min	>99%	93%
18		80 °C	12 h	98%	88%
19 ^b		25 °C	15 min	>99%	95%

^a Percentage conversion is monitored in micromolar NMR-scale reactions. ^b Phthaldialdehyde gives cyclic phthalide ester.

Surprisingly, p-acetyl benzaldehyde (entry 14) remains unreacted under the above catalytic condition even at elevated temperature (120 °C). Similarly when a 1:1 mixture of benzaldehyde and acetophenone (entry 15) is treated under the similar catalytic condition only starting materials are recovered even after heating at 60 °C for 12 h and PhCO₂CH₂Ph or a crossed-Tischenko product are not detected in ¹H NMR. As evident from the table above, a lot of aldehyde substrates undergo relatively rapid conversion into substantial amount of products at the initial stage of the reaction at ambient temperature. However they eventually slow down and further conversion requires elevated temperature and prolonged reaction time. Given the fact that there is no sign of catalyst decomposition as evident from the ¹H NMR of the reaction mixture (intensity of To^M-CH₃ and To^M-CH₂ resonance remains unaffected), we speculated that either **1** catalyzed Tishchenko coupling of aldehydes is reversible or there is substrate or product inhibition. Coles *et. al.* also reported similar kind of scenario in their guanidinato-Mg system, but from their report the reason behind the catalysis inhibition was not clear.^{26a} We further observed that keeping [substrate] the same, increasing the catalyst loading increases the amount of product formation at ambient temperature. This is against the suspected reversibility since the aldehyde ↔ ester equilibrium should not be affected by the [catalyst]. Furthermore, when a catalytic reaction was performed with a substrate mixture of PhCHO and CyCHO in 1:1 ratio using 10 mol% of **1** as the pre-catalyst, a mixture of four esters, namely PhCO₂CH₂Ph (**E1**, 23.1%), CyCO₂CH₂Cy (**E2**, 37.6%), PhCO₂CH₂Cy (**E3**, 20.4%), and CyCO₂CH₂Ph (**E4**, 18.9%) was initially observed after 15 min at ambient temperature. Subsequent heating of the solution mixture at 80 °C for 2 h redistributed the

relative amount of the products as **E1** (19.4 %), **E2** (28.8 %), **E3** (25.9 %), **E4** (25.9 %).

Further heating for another 6 h did not result into a significant change.



This experiment indicates that the catalyst species can participate in a reversible trans-esterification. Such trans-esterification can also rationalize the observed product inhibition during the catalytic Tishchenko coupling of aldehydes. Increase in [product] during the reaction time course eventually takes the catalyst away from the productive cycle and involves in a reversible trans-esterification. Similarly $\text{To}^{\text{M}}\text{MgOEt}$ (**5**) reacts with $\text{CycCO}_2\text{CH}_2\text{Cyc}$ ester to give partial conversion into $\text{To}^{\text{M}}\text{MgOCH}_2\text{Cyc}$ and CycCO_2Et . In most catalysis involving metal alkoxides a common mechanism has been proposed that involves an aldehyde insertion into the metal alkoxide followed by β -H abstraction by another aldehyde molecule as shown in Fig.3.

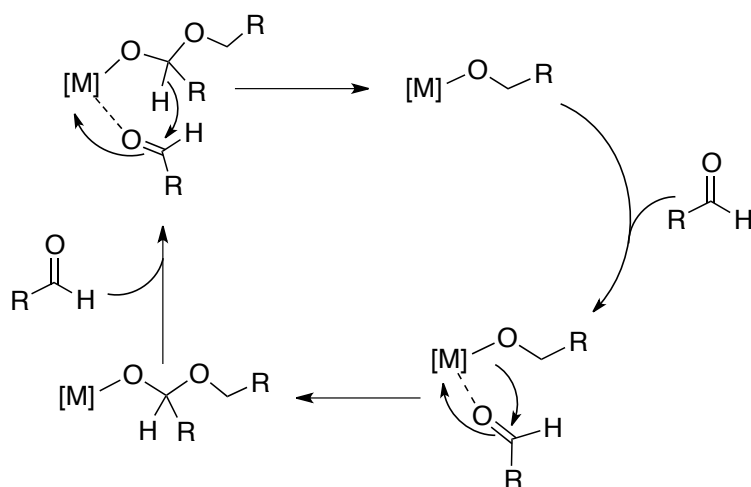
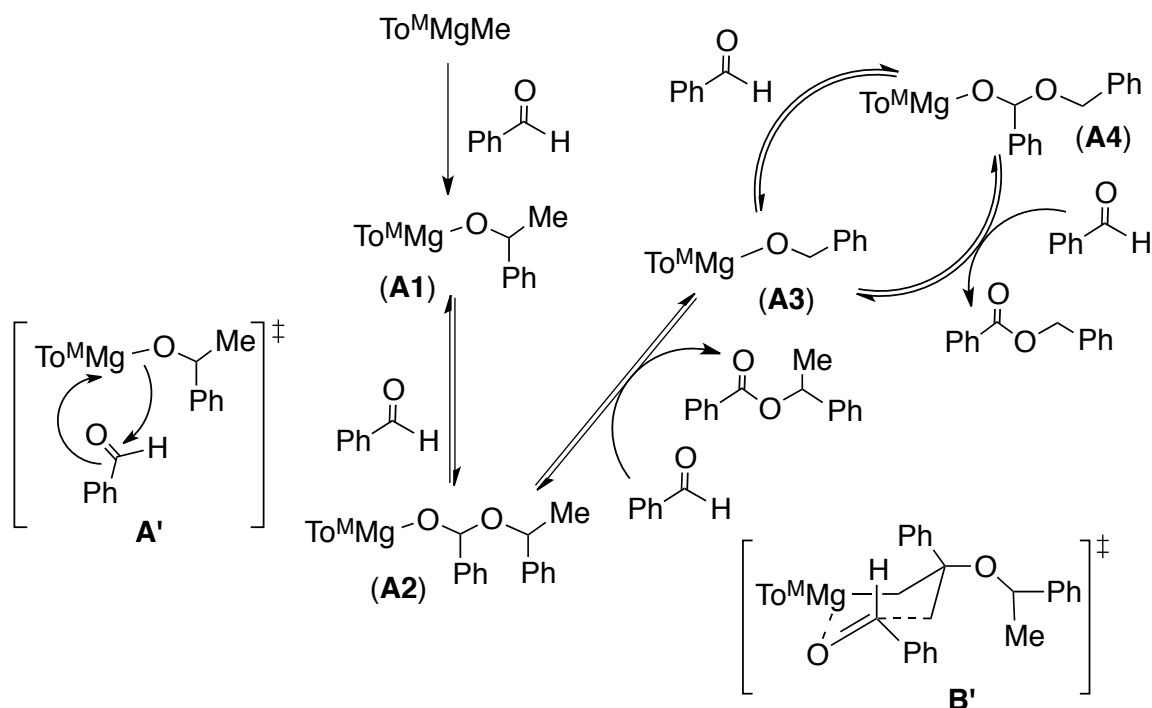


Fig. 3 catalytic cycle commonly proposed for Tishchenko coupling of aldehydes.

We propose a similar but slightly modified catalytic cycle as shown below for the overall Tishchenko coupling of PhCHO, which incorporates the reversible trans-esterification of the product ester. Insertion reaction between pre-catalyst **1** and PhCHO gives alkoxide **A1**. A reversible insertion of another molecule of PhCHO into the Mg-O bond provides the alkoxide **A2** (transition state **A''**). Finally a third molecule of PhCHO abstracts a β -H from the alkoxide **A2** following a six membered transition state (**B''**) to give the ester PhCO₂CHMePh and alkoxide **A3**. Alkoxide **A3** is the resting state of the catalyst, which then dimerizes two PhCHO molecules following insertion (**A''**) and subsequently β -H abstraction (**B''**) steps.



This aldehyde insertion into Mg-alkoxide mechanism is further supported by the fact that X-ray quality single crystals of dimeric $[(\kappa^2\text{-To}^{\text{M}})\text{MgO}^i\text{Bu}]_2$ were obtained from the reaction mixture of isobutyraldehyde (entry 17) catalysis.

Conclusion.

Thus we have established a new multi-purpose magnesium catalyst to perform several important organic transformations. We are currently looking into the mechanistic details of these reactions.

References.

- (1) (a) Jastrzebski, J. T. B. H.; Boersma, J.; Van Koten, G. *The Chemistry of Organomagnesium Compounds*; Rappoport, Z., Ed.; Wiley: Hoboken, 2008; Vol. 1, p. 2-4. (b)

Hanusa, T.P. *Comprehensive Organometallic Chemistry III*; Crabtree, R.H.; Mingos, M.D.P., Ed.; Elsevier: Oxford, 2006; Vol. 2, p.66-152.

(2) (a) Chisholm, M. H.; Huffman, J. C.; Phomphrai, K. *J. Chem. Soc., Dalton Trans.* **2001**, *6*, 222-224. (b) Chisholm, M. H.; Gallucci, J.; Phomphrai, K. *Inorg. Chem.* **2002**, *41*, 2785-2794. (c) Chisholm, M. H.; Phomphrai, K. *Inorg. Chimica Acta* **2003**, *350*, 121-125.

(3) (a) Crimmin, M. R.; Casely, I. J.; Hill, M. S. *J. Am. Chem. Soc.* **2005**, *127*, 2042-2043. (b) Barrett, A. G. M.; Crimmin, M. R.; Hill, M. S.; Kociok-Kohn, G.; Lachs, J. R.; Procopiou, P. A. *Dalton Trans.* **2008**, 1292-1294. (c) Crimmin, M. R.; Arrowsmith, M.; Barrett, A. G. M.; Casely, I. J.; Hill, M. S.; Procopiou, P. A. *J. Am. Chem. Soc.* **2009**, *131*, 9670-9685.

(4) (a) Bailey, P. J.; Dick, C. M. E.; Fabre, S.; Parsons, S. *J. Chem. Soc., Dalton Trans.* **2000**, 655-1661. (b) Datta, S.; Roesky, P.W. *Organometallics* **2007**, *26*, 4392-4394.

(5) (a) Buch, F.; Brettar, J.; Harder, S. *Angew. Chem. Int. Ed.* **2006**, *45*, 2741-2745. (b) Buch, F.; Harder, S. *Z. Naturforsch* **2008**, *63b*, 169-177.

(6) Crimmin, M. R.; Barrett, A. G. M.; Hill, M. S.; Hitchcock, P. B.; Procopiou, P. A. *Organometallics* **2007**, *26*, 2953-2956.

(7) Dunne, J. F.; Fulton, B.; Ellern, A.; Sadow, A. D. *J. Am. Chem. Soc.* **2010**, *132*, 17680-17683.

(8) Dunne, J. F.; Neal, S. R.; Engelkeimer, J. Ellern, A.; Sadow, A. D. *J. Am. Chem. Soc.* **2011**, *133*, 16782-16785.

(9) Arrowsmith, M.; Hadlington, T. J.; Hill, M. S.; Kociok-Köhn, G. *Chem. Commun.* **2012**, *48*, 4567-4569.

(10) Arrowsmith, M.; Hill, M. S.; Hadlington, T. J.; Kociok-Köhn, G.; Weetman, C. *Organometallics* **2011**, *30*, 5556-5559.

(11) (a) Berk, S. C.; Kreutzer, K.; Buchwald, S. L. *J. Am. Chem. Soc.* **1991**, *113*, 5093-5095.

(b) Berk, S. C.; Buchwald, S. L. *J. Org. Chem.* **1992**, *57*, 3751-3753. (c) Reding, M. T.; Buchwald, S. L. *J. Org. Chem.* **1995**, *60*, 7884-7890. (d) Barr, K. J.; Berk, S. C.; *J. Org. Chem.* **1994**, *59*, 4323-4326. (e) Sato, F.; Jinbo, T.; Sato, M. *Tetrahedron Lett.* **1980**, *21*, 2175-2178.

(12) Mimoun, H.; *J. Org. Chem.* **1999**, *64*, 2582-2589.

(13) Mao, Z.; Gregg, B.T.; Cutler, A. R. *J. Am. Chem. Soc.* **1995**, *117*, 10139-10140.

- (14) (a) Matsubara, K.; Iura, T.; Maki, T.; Nagashima, H. *J. Org. Chem.* **2002**, *67*, 4985-4988. (b) Park, S.; Brookhart, M. *Organometallics* **2010**, *29*, 6057-6064.
- (15) Das, S.; Möller, K.; Junge, K.; Beller, M. *Chem. Eur. J.* **2011**, *17*, 7414-7417.
- (16) (a) Zhang, J.; Leitus, G.; Ben-David, Y.; Milstein, D. *Angew. Chem. Int. Ed.* **2006**, *45*, 1113-1115. (b) Zhang, J.; Balaraman, E.; Leitus, G.; Milstein, D. *Organometallics* **2011**, *30*, 5716-5724.
- (17) Dunne, J. F.; Manna, K.; Wiench, J. W.; Ellern, A.; Pruski, M.; Sadow, A. D. *Dalton Trans.*, 2010, **39**, 641-653.
- (18) (a) Verdaguer, X.; Berk, S. C.; Buchwald, S. L. *J. Am. Chem. Soc.* **1995**, *117*, 12641-12642. (b) Verdaguer, X.; Hansen, M. C.; Berk, S. C.; Buchwald, S. L. *J. Org. Chem.* **1997**, *62*, 8522-8528.
- (19) Seki, T.; Nakajo, T.; Onaka, M. *Chem. Lett.* **2006**, *35*, 824-829.
- (20) Tschischenko, W. *Chem. Zentralbl.* **1906**, *77*, 1309.
- (21) (a) Morita, K.; Nishiyama, Y.; Ishii, Y. *Organometallics* **1993**, *12*, 3748-3752. (b) Horino, H. Ito, T.; Yamamoto, A. *Chemistry letters*, **1978**, 17-20. (c) Simon, M.; Darses, S. *Adv. Synth. Catal.* **2010**, *352*, 305-308. (d) Barrio, P.; Esteruelas, M. A.; Oñate, E. *Organometallics* **2004**, *23*, 1340-1348. (e) Tejel, C.; Ciriano, M. A.; Passarelli, V. *Chem. Eur. J.* **2011**, *17*, 91-95. (f) Oshima, K.; Ohmura, T.; Suginome, M. *J. Am. Chem. Soc.* **2012**, *134*, 3699-3702. (g) MingLun, P.; YingMing, Y.; Yong, Z.; Qi, S. *Chinese Science Bulletin*. **2008**, *53*, 1978-1982. (h) Suzuki, T.; Yamada, T.; Matsuo, T.; Watanabe, K.; Katoh, T. *Synlett*. **2005**, *9*, 1450-1452. (i) Ohishi, T.; Shiotani, Y.; Yamashita, M. *Organometallics* **1994**, *13*, 4641-4642.
- (22) (a) Onozawa, S.; Sakakura, T.; Tanaka, M.; Shiro, M. *Tetrahedron* **1996**, *52*, 4291-4302. (b) Berberich, H.; Roesky, P. W. *Angew. Chem. Int. Ed.* **1998**, *37*, 1569-1571. (c) Bürgstein, M. R.; Berberich, H.; Roesky, P. W. *Chem. Eur. J.* **2001**, *7*, 3078-3085. (d) Zuyls, A.; Roesky, P. W. Deacon, G. B.; Konstas, K.; Junk, P. C. *Eur. J. Org. Chem.* **2008**, 693-697. (e) Hsu, J.; Fang, J. *J. Org. Chem.* **2001**, *66*, 8573-8584.
- (23) (a) Andrea, T.; Barnea, E.; Eisen, M. S. *J. Am. Chem. Soc.* **2008**, *130*, 2454-2455. (b) Sharma, M.; Andrea, T.; Brookes, N. J.; Yates, B. F.; Eisen, M. S. *J. Am. Chem. Soc.* **2011**, *133*, 1341-1356.

- (24) (a) Werner, T.; Koch, J. *Eur. J. Org. Chem.* **2010**, 6904-6907. (b) Waddell, D. C.; Mack, J. *Green Chem.* **2009**, *11*, 79-82. (c) Query, I. P.; Squier, Larson, E. M.; Isley, N. A.; Clark, T. B. *J. Org. Chem.* **2011**, *76*, 6452-6456.
- (25) Bideau, F. L.; Coradin, T.; Gourier, D.; Hénique, J.; Samuel, E. *Tetrahedron Lett.* **2000**, *41*, 5215-5218.
- (26) (a) Day, B. M.; Mansfield, N. E.; Coles, M. P.; Hitchcock, P. B. *Chem. Commun.* **2011**, 47, 4995-4997. (b) Day, B. M.; Knoweldena, W.; Coles, M. P. *Dalton Trans.* **2012**, *41*, 10930-10933. (c) Cronin, L.; Manoni, F.; O' Connor, C. J.; Connon, S. J. *Angew. Chem. Int. Ed.* **2010**, *49*, 3045-3048. (d) O' Connor, C. J.; Manoni, F.; Curran, S. P.; Connon, S. J. *New J. Chem.* **2011**, *35*, 551-553.
- (27) (a) Crimmin, M. R.; Barrett, A. G. M.; Hill, M. S.; Procopiou, P. A. *Org. Lett.* **2007**, *9*, 331-333. (b) Seki, T.; Hattori, H. *Chem. Commun.* **2001**, 2510-2511. (c) Seki, T.; Akutsu, K.; Hattori, H. *Chem. Commun.* **2001**, 1000-1001.

Experimental Data

General Procedures. All reactions were performed under a dry argon atmosphere using standard Schlenk techniques or under a nitrogen atmosphere in a glovebox, unless otherwise indicated. Benzene, toluene, pentane, diethyl ether, and tetrahydrofuran were dried and deoxygenated using an IT PureSolv system. Benzene- d_6 was heated to reflux over Na/K alloy and vacuum-transferred. $\text{To}^{\text{M}}\text{MgMe}$ (**1**) was synthesized according to the literature procedure. Carbonyl and ester substrates were purchased from Sigma-Aldrich and stored under N_2 atmosphere inside glovebox. Liquid substrates were distilled over CaH_2 and stored over molecular sieves prior use. HBpin, also purchased from Sigma-Aldrich, was stored at -30°C inside the glovebox and used as it is. ^1H , $^{13}\text{C}\{^1\text{H}\}$, and ^{11}B NMR spectra were collected on a Bruker AVII 600 or a DRX 400 spectrometer. ^{15}N chemical shifts were determined by ^1H -

^{15}N HMBC experiments on a Bruker AVII 600 spectrometer with a Bruker Z-gradient inverse TXI $^1\text{H}/^{13}\text{C}/^{15}\text{N}$ 5mm cryoprobe; ^{15}N chemical shifts were originally referenced to an external liquid NH_3 standard and recalculated to the CH_3NO_2 chemical shift scale by adding -381.9 ppm. Elemental analyses were performed using a Perkin-Elmer 2400 Series II CHN/S by the Iowa State Chemical Instrumentation Facility. X-ray diffraction data was collected on a Bruker APEX II diffractometer.

To^MMgH₂Bpin. To a 10 mL benzene solution of HBpin (1.3 mL, 8.959 mmol) 2 mL benzene solution of To^MMgMe (0.250 g, 0.593 mmol) was added drop wise with occasional stirring at ambient temperature and subsequently filtered. Evaporation of the volatile materials under reduced pressure resulted into a white solid, which was then washed with pentane (3×5 mL) and subsequently dried under vacuum to provide analytically pure To^MMgH₂Bpin (0.248 g, 0.463 mmol, 78.1%) as white powder. X-ray quality single crystals were grown from a slow pentane diffusion into a concentrated toluene solution of To^MMgH₂Bpin at -35 °C. ^1H NMR (600 MHz, benzene-*d*₆): δ 1.15 (s, 18 H, $\text{CNCMe}_2\text{CH}_2\text{O}$), 1.42 (br, s, 12 H, $\text{Me}_2\text{COBOCMe}_2$) 3.38 (s, 6 H, $\text{CNCMe}_2\text{CH}_2\text{O}$), 4.19 (br, q, 2 H, MgH_2B), 7.36 (t, $^3J_{\text{HH}} = 7.2$ Hz, 1 H, *para*- C_6H_5), 7.54 (t, $^3J_{\text{HH}} = 7.2$ Hz, 2 H, *meta*- C_6H_5), 8.26 (d, $^3J_{\text{HH}} = 7.8$ Hz, 2 H, *ortho*- C_6H_5). $^{13}\text{C}\{^1\text{H}\}$ NMR (175 HMz, benzene-*d*₆): δ 25.27 ($\text{Me}_2\text{COBOCMe}_2$), 28.38 ($\text{CNCMe}_2\text{CH}_2\text{O}$), 66.40 ($\text{CNCMe}_2\text{CH}_2\text{O}$), 80.94 ($\text{CNCMe}_2\text{CH}_2\text{O}$), 83.48 ($\text{Me}_2\text{COBOCMe}_2$), 126.24 (*para*- C_6H_5), 127.16 (*meta*- C_6H_5), 136.47 (*ortho*- C_6H_5), 142.41 (br, *ipso*- C_6H_5), 192.49 (br, $\text{CNCMe}_2\text{CH}_2\text{O}$). ^{11}B NMR (128 MHz, benzene-*d*₆): δ -18.4 (*B* of To^M), 3.4 (t, $^1J_{\text{BH}} = 93.5$ Hz MgH_2B). $^{15}\text{N}\{^1\text{H}\}$ NMR: δ -161.1. IR (KBr, cm^{-1}): 3041 (w), 2971 (s), 2930 (m), 2309 (br, ν_{BH}), 1581 (s, ν_{CN}), 1463 (br, m), 1367

(m), 1272 (s), 1195 (s), 1157 (s), 1034 (w), 961 (s), 894 (w), 850 (w), 813 (w), 750 (w), 706 (m), 679 (m), 661 (w), 638 (m), 580 (w). Anal. Calcd. for $C_{27}H_{43}B_2N_3O_5Mg$: C, 60.55; H, 8.09; N, 7.85. Found: C, 60.18; H, 7.89; N, 7.77. Mp: 50-60 °C (dec.)

To^MMgOCMePh₂. A 10 mL benzene solution of To^MMgMe (0.310 g, 0.735 mmol) and benzophenone (0.134 g, 0.735 mmol) was stirred for 1 h at ambient temperature. Volatiles were then removed under reduced pressure to obtain a white solid. Washing the white solid with pentane (3 × 5 mL) and further drying under vacuum afforded 0.362 g of analytically pure To^MMgOCMePh₂ (0.668 mmol, 90.9%). X-ray quality single crystals were obtained from a concentrated toluene solution of To^MMgOCMePh₂ at -35 °C. ¹H NMR (600 MHz, benzene-*d*₆): δ 0.99 (s, 18 H, CNCMe₂CH₂O), 2.13 (s, 3 H, MgOCMePh₂) 3.38 (s, 6 H, CNCMe₂CH₂O), 7.12 (t, ³J_{HH} = 7.2 Hz, 2 H, *para*-MgOCMe(C₆H₅)₂), 7.28 (t, ³J_{HH} = 7.2 Hz, 2 H, *meta*-MgOCMe(C₆H₅)₂), 7.35 (t, ³J_{HH} = 7.2 Hz, 1 H, *para*-C₆H₅), 7.53 (t, ³J_{HH} = 7.2 Hz, 2 H, *meta*-C₆H₅), 7.84 (d, ³J_{HH} = 7.2 Hz, 2 H, *ortho*-MgOCMe(C₆H₅)₂), 8.27 (d, ³J_{HH} = 7.2 Hz, 2 H, *ortho*-C₆H₅). ¹³C{¹H} NMR (175 MHz, benzene-*d*₆): δ 28.33 (CNCMe₂CH₂O), 36.41 (MgOCMe(C₆H₅)₂), 65.65 (CNCMe₂CH₂O), 75.74 (MgOCMePh₂), 80.58 (CNCMe₂CH₂O), 125.79 (*para*-MgOCMe(C₆H₅)₂), 126.32 (*para*-C₆H₅), 127.11 (*ortho*-MgOCMe(C₆H₅)₂), 127.22 (*meta*-C₆H₅), 128.11 (*meta*-MgOCMe(C₆H₅)₂), 136.43 (*ortho*-C₆H₅), 141.70 (br, *ipso*-C₆H₅), 156.86 (*ipso*-MgOCMe(C₆H₅)₂), 191.16 (br, CNCMe₂CH₂O). ¹¹B NMR (128 MHz, benzene-*d*₆): δ -18.3. ¹⁵N{¹H} NMR: δ -158.1. IR (KBr, cm⁻¹): 3078 (m), 3056 (m), 2967 (s), 2925 (m), 2869 (m), 2275 (w), 2122 (w), 1953 (w), 1889 (w), 1821 (w), 1586 (s, ν_{CN}), 1486 (m), 1462 (m), 1446 (m), 1387 (m), 1367 (m), 1355 (m), 1275 (s), 1195 (s), 1162 (s), 1067 (m), 1027 (m), 961 (s), 896 (w), 843 (m), 820 (m), 781 (m), 749 (m),

706 (s), 678 (m), 660 (m), 643 (m), 621 (m), 575 (m), 549 (m). Anal. Calcd. for $C_{23}H_{34}BN_3O_4Mg$: C, 61.16; H, 7.59; N, 9.30. Found: C, 60.88; H, 7.79; N, 9.45. Mp: 168-172 °C

To^MMgOEt. To a 10 mL benzene solution of To^MMgMe (0.387 g, 0.918 mmol), 5.5 microliter of EtOH (0.942 mmol) was added and subsequently stirred for 1 h. Evaporation of the volatile materials under reduced pressure resulted into a white solid, which was then washed with pentane (3 × 5 mL) and subsequently dried under vacuum to provide 0.350 g (0.775 mmol, 84.4 %) of analytically pure To^MMgOEt as a white power. X-ray quality single crystals were obtained in NMR tube when this reaction was carried out in NMR-scale at ambient temperature. ¹H NMR (600 MHz, benzene-*d*₆): δ 1.21 (s, 18 H, CNCMe₂CH₂O), 1.27 (t, ³J_{HH} = 7.2 Hz, 3 H, MgOCH₂CH₃), 3.54 (s, 6 H, CNCMe₂CH₂O), 3.81 (q, ³J_{HH} = 7.2 Hz, 2 H, MgOCH₂CH₃), 7.25 (t, ³J_{HH} = 7.2 Hz, 1 H, *para*-C₆H₅), 7.46 (t, ³J_{HH} = 7.2 Hz, 2 H, *meta*-C₆H₅), 8.08 (d, ³J_{HH} = 7.2 Hz, 2 H, *ortho*-C₆H₅). ¹³C {¹H} NMR (175 MHz, benzene-*d*₆): δ 22.14 (MgOCH₂CH₃), 29.06 (CNCMe₂CH₂O), 58.54 (MgOCH₂CH₃), 66.71 (CNCMe₂CH₂O), 78.61 (CNCMe₂CH₂O), 125.98 (*para*-C₆H₅), 127.70 (*meta*-C₆H₅), 134.56 (*ortho*-C₆H₅), 147.12 (br, *ipso*-C₆H₅), 187.94 (br, CNCMe₂CH₂O). ¹¹B NMR (128 MHz, benzene-*d*₆): δ -17.4. ¹⁵N {¹H} NMR: δ -157.1. IR (KBr, cm⁻¹): 3038 (w), 2966 (s), 2931 (m), 2868 (m), 1628 (m, ν_{CN}), 1594 (s, ν_{CN}), 1568 (s, ν_{CN}), 1463 (m), 1431 (w), 1386 (m), 1369 (m), 1281 (m), 1198 (s), 1154 (s), 1118 (s), 1066 (m), 1003 (s), 969 (s), 930 (w), 896 (m), 880 (w), 842 (w), 810 (w), 764 (w), 753 (w), 713 (m), 702 (m), 655 (m), 638 (w), 618 (w), 595 (w), 560 (m). Anal. Calcd. for $C_{23}H_{34}BN_3O_4Mg$: C, 61.16; H, 7.59; N, 9.30. Found: C, 60.88; H, 7.79; N, 9.45. Mp: 225-230 °C (dec.)

To^MMgOEt(HBpin). This species has been synthesized in situ by adding a mixture of 40 microliters of EtOAc (0.407 mmol) and 120 microliters of HBpin (0.827 mmol) to a toluene-*d*₈ solution of To^MMgMe (0.016 g, 0.038 mmol), precooled at – 78 °C and subsequently warming up the solution mixture to – 10°C. Spectroscopic characterizations were carried out at 267 K. ¹H NMR (400 MHz, toluene-*d*₈): δ 1.14 (s, 18 H, CNCMe₂CH₂O), 1.33 (s, 6 H, Me₂COBOCMe₂), 1.36 (s, 6 H, Me₂COBOCMe₂), 1.46 (t, ³J_{HH} = 7.2 Hz, 3 H, MgOCH₂CH₃), 3.39 (s, 6 H, CNCMe₂CH₂O), 3.80 (q, ³J_{HH} = 7.2 Hz, 2 H, MgOCH₂CH₃), 7.29 (t, ³J_{HH} = 7.2 Hz, 1 H, *para*-C₆H₅), 7.45 (t, ³J_{HH} = 7.2 Hz, 2 H, *meta*-C₆H₅), 8.09 (d, ³J_{HH} = 7.2 Hz, 2 H, *ortho*-C₆H₅). ¹³C{¹H} NMR (175 HMz, toluene-*d*₈): δ 17.48 (MgOCH₂CH₃), 25.05 (Me₂COBOCMe₂), 26.26 (Me₂COBOCMe₂), 27.64 (CNCMe₂CH₂O), 58.87 (MgOCH₂CH₃), 65.96 (CNCMe₂CH₂O), 79.40 (CNCMe₂CH₂O), 79.55 (Me₂COBOCMe₂), 125.14 (*para*-C₆H₅), 126.22 (*meta*-C₆H₅), 135.39 (*ortho*-C₆H₅), 143.47 (br, *ipso*-C₆H₅), 190.73 (br, CNCMe₂CH₂O). ¹¹B NMR (128 MHz, benzene-*d*₆): δ –18.2 (*B* of To^M), 7.2 (br, HBpin). ¹⁵N{¹H} NMR: δ –158.8.

To^MZnOCH(C₆F₅)OCH₂C₆F₅. A 5 mL toluene mixture containing 0.360 g (0.802 mmol) of To^MZnH and 0.2 mL (1.620 mmol) of C₆F₅CHO was kept at –30 °C for two weeks. X-ray quality single crystals of To^MZnOCH(C₆F₅)OCH₂C₆F₅ were deposited in the mean time which were then isolated by decanting the supernatant solution. Further drying the crystals under vacuum provided 0.205 g (0.244 mmol) of analytically pure To^MZnOCH(C₆F₅)OCH₂C₆F₅. ¹H NMR (600 MHz, toluene-*d*₈): δ 1.00 (s, 9 H, CNCMe₂CH₂O), 1.06 (s, 9 H, CNCMe₂CH₂O), 3.44 (s, 6 H, CNCMe₂CH₂O), 4.26 (d, ¹J_{HH} =

10.8 Hz, 1 H, $\text{ZnOCH}_2\text{C}_6\text{F}_5(\text{C}_6\text{F}_5\text{CHO})$), 4.51 (d, $^1J_{\text{HH}} = 10.8$ Hz, 1 H, $\text{ZnOCH}_2\text{C}_6\text{F}_5(\text{C}_6\text{F}_5\text{CHO})$), 6.76 (s, 1 H, $\text{ZnOCH}_2\text{C}_6\text{F}_5(\text{C}_6\text{F}_5\text{CHO})$), 7.29 (t, $^3J_{\text{HH}} = 7.2$ Hz, 1 H, *para*- C_6H_5), 7.44 (t, $^3J_{\text{HH}} = 7.2$ Hz, 2 H, *meta*- C_6H_5), 8.11 (d, $^3J_{\text{HH}} = 7.2$ Hz, 2 H, *ortho*- C_6H_5). $^{13}\text{C}\{^1\text{H}\}$ NMR (175 MHz, benzene- d_6): δ 27.36 ($\text{CNCMe}_2\text{CH}_2\text{O}$), 27.77 ($\text{CNCMe}_2\text{CH}_2\text{O}$), 54.14 ($\text{ZnOCH}_2\text{C}_6\text{F}_5(\text{C}_6\text{F}_5\text{CHO})$), 65.58 ($\text{CNCMe}_2\text{CH}_2\text{O}$), 81.13 ($\text{CNCMe}_2\text{CH}_2\text{O}$), 98.62 ($\text{ZnOCH}_2\text{C}_6\text{F}_5(\text{C}_6\text{F}_5\text{CHO})$), 112.75 (C_6F_5), 120.24 (C_6F_5), 126.55 (*para*- C_6H_5), 127.36 (*meta*- C_6H_5), 136.27 (*ortho*- C_6H_5), 137.28 (C_6F_5), 138.70 (C_6F_5), 140.20 (C_6F_5), 140.45 (br, *ipso*- C_6H_5), 140.87 (C_6F_5), 141.60 (C_6F_5), 142.28 (C_6F_5), 145.48 (C_6F_5), 146.90 (C_6F_5), 190.84 (br, $\text{CNCMe}_2\text{CH}_2\text{O}$). ^{11}B NMR (128 MHz, benzene- d_6): δ -18.3. $^{15}\text{N}\{^1\text{H}\}$ NMR: δ -160.6. ^{19}F NMR (benzene- d_6 , 376 MHz): δ -143.24 (C_6F_5), -145.18 (C_6F_5), -155.20 (C_6F_5), -157.25 (C_6F_5), -163.13 (C_6F_5), -163.49 (C_6F_5). IR (KBr, cm^{-1}): 3080 (w), 3049 (w), 2973 (m), 2933 (m), 2905 (m), 1657 (w), 1650 (w), 1595 (s, ν_{CN}), 1522 (s), 1504 (s), 1464 (m), 1432 (w), 1390 (m), 1371 (m), 1356 (m), 1339 (w), 1298 (m), 1278 (m), 1253 (w), 1198 (s), 1168 (m), 1133 (m), 1110 (m), 1055 (m), 1038 (m), 1000 (s), 955 (s), 937 (s), 922 (m), 820 (m), 803 (m), 746 (m), 706 (m). Anal. Calcd. for $\text{C}_{35}\text{H}_{32}\text{BN}_3\text{O}_5\text{F}_{10}\text{Zn}$: C, 50.00; H, 3.84; N, 5.00. Found: C, 50.40; H, 3.99; N, 4.94. Mp: 165-170 °C (dec.)

To^MMgOCH₂[(*o*-COCH₃)C₆H₄]. A 10 mL toluene solution of mixture of To^MMgMe (0.315 g, 0.747 mmol) and phthalide (0.332 g, 2.241 mmol) was stirred for 10 minutes and subsequently stored in -30 °C freezer for 12 h. A yellowish white solid precipitated over time, which was then isolated via decantation of the top solution. The solid was washed with pentane (3 × 5 mL) and further dried under vacuum to provide 0.253 g (0.455 mmol, 60.9 %) of analytically pure To^MMgOCH₂[(*o*-COCH₃)C₆H₄] as a yellowish white power. ^1H NMR

(600 MHz, toluene- d_8): δ 1.07 (s, 18 H, CNCMe₂CH₂O), 1.93 (s, 3 H, MgOCH₂[(*o*-COCH₃)C₆H₄]), 3.45 (s, 6 H, CNCMe₂CH₂O), 4.82 (s, 2 H, MgOCH₂[(*o*-C)CH₃)C₆H₄]), 6.86 (d, ³J_{HH} = 7.2 Hz, 1 H, MgOCH₂Ar'), 7.07 (t, ³J_{HH} = 7.2 Hz, 1 H, MgOCH₂Ar'), 7.13 (t, ³J_{HH} = 7.2 Hz, 1 H, MgOCH₂Ar'), 7.36 (t, ³J_{HH} = 7.2 Hz, 1 H, *para*-C₆H₅), 7.54 (t, ³J_{HH} = 7.2 Hz, 2 H, *meta*-C₆H₅), 7.59 (d, ³J_{HH} = 7.2 Hz, 1 H, MgOCH₂Ar'), 8.33 (d, ³J_{HH} = 7.2 Hz, 2 H, *ortho*-C₆H₅). ¹³C{¹H} NMR (175 MHz, benzene- d_6): δ 27.45 (CNCMe₂CH₂O), 31.31 (MgOCH₂[(*o*-COCH₃)C₆H₄]), 65.55 (CNCMe₂CH₂O), 66.41 ((MgOCH₂[(*o*-COCH₃)C₆H₄]), 79.36 (CNCMe₂CH₂O), 113.25 (MgOAr'), 121.11 (MgOAr'), 122.77 (MgOCH₂[(*o*-COCH₃)C₆H₄]), 125.28 (MgOAr'), 126.66 (*para*-C₆H₅), 127.71 (*meta*-C₆H₅), 128.33 (MgOAr'), 130.90 (MgOAr'), 136.44 (*ortho*-C₆H₅), 141.66 (br, *ipso*-C₆H₅), 162.56 (MgOCH₂Ar'), 191.56 (br, CNCMe₂CH₂O). ¹¹B NMR (128 MHz, toluene- d_8): δ -17.1. ¹⁵N{¹H} NMR: δ -158.5. IR (KBr, cm⁻¹): 2969 (m), 2928 (m), 2911 (m), 2886 (m), 2862 (m), 2832 (w), 1765 (m), 1747 (m), 1719 (w), 1662 (s), 1618 (s, ν_{CN}), 1596 (s, ν_{CN}), 1584 (s, ν_{CN}), 1490 (s), 1462 (s), 1431 (m), 1381 (w), 1365 (s), 1314 (w), 1296 (m), 1275 (m), 1200 (s), 1158 (m), 1143 (m), 1088 (w), 1069 (w), 1024 (m), 1000 (w), 976 (w), 908 (m), 893 (s), 880 (w), 842 (s), 808 (w), 769 (s), 709 (s). Anal. Calcd. for C₃₀H₃₈BN₃O₅Mg: C, 64.83; H, 6.89; N, 7.56. Found: C, 65.15; H, 6.44; N, 7.48. Mp: 176-182 °C (dec.)

To^MMgO[(*o*-CH₂CH₂COCH₃)C₆H₄]. A 10 mL toluene solution of mixture of To^MMgMe (0.350 g, 0.830 mmol) and dihydrocoumarin (0.195 g, 1.316 mmol) was stirred for 10 minutes. Immediate removal of the volatiles under reduced pressure provided a white solid. The solid was then washed with pentane (3 × 5 mL) and further dried under vacuum to afford 0.338 g (0.593 mmol, 71.4 %) of analytically pure To^MMgO[(*o*-CH₂CH₂COCH₃)C₆H₄] as a

white power. ^1H NMR (600 MHz, toluene- d_8): δ 1.11 (s, 18 H, $\text{CNCMe}_2\text{CH}_2\text{O}$), 1.38 (s, 3 H, $\text{MgO}[(o\text{-CH}_2\text{CH}_2\text{COCH}_3)\text{C}_6\text{H}_4]$), 2.40 (t, $^3J_{\text{HH}} = 6$ Hz, 2 H, $\text{MgO}[(o\text{-CH}_2\text{CH}_2\text{COCH}_3)\text{C}_6\text{H}_4]$), 2.86 (t, $^3J_{\text{HH}} = 6$ Hz, 2 H, $\text{MgO}[(o\text{-CH}_2\text{CH}_2\text{COCH}_3)\text{C}_6\text{H}_4]$), 3.49 (s, 6 H, $\text{CNCMe}_2\text{CH}_2\text{O}$), 6.79 (t, $^3J_{\text{HH}} = 7.2$ Hz, 1 H, MgOAr'), 7.04 (d, $^3J_{\text{HH}} = 7.2$ Hz, 1 H, MgOAr'), 7.11 (d, $^3J_{\text{HH}} = 7.2$ Hz, 1 H, MgOAr'), 7.30 (t, $^3J_{\text{HH}} = 7.2$ Hz, 1 H, MgOAr'), 7.38 (t, $^3J_{\text{HH}} = 7.2$ Hz, 1 H, *para*- C_6H_5), 7.58 (t, $^3J_{\text{HH}} = 7.2$ Hz, 2 H, *meta*- C_6H_5), 8.41 (d, $^3J_{\text{HH}} = 7.2$ Hz, 2 H, *ortho*- C_6H_5).

$^{13}\text{C}\{^1\text{H}\}$ NMR (175 MHz, toluene- d_8): δ 23.52 ($\text{MgO}[(o\text{-CH}_2\text{CH}_2\text{COCH}_3)\text{C}_6\text{H}_4]$), 27.80 ($\text{CNCMe}_2\text{CH}_2\text{O}$), 30.60 ($\text{MgO}[(o\text{-CH}_2\text{CH}_2\text{COCH}_3)\text{C}_6\text{H}_4]$), 46.71 ($\text{MgO}[(o\text{-CH}_2\text{CH}_2\text{COCH}_3)\text{C}_6\text{H}_4]$), 65.28 ($\text{CNCMe}_2\text{CH}_2\text{O}$), 79.98 ($\text{CNCMe}_2\text{CH}_2\text{O}$), 114.21 (MgOAr'), 120.65 (MgOAr'), 126.16 (MgOAr'), 126.94 (*para*- C_6H_5), 127.72 (*meta*- C_6H_5), 128.11 (MgOAr'), 129.97 (MgOAr'), 136.25 (*ortho*- C_6H_5), 141.30 (br, *ipso*- C_6H_5), 163.81 (MgOAr'), 191.07 (br, $\text{CNCMe}_2\text{CH}_2\text{O}$), 214.26 ($\text{MgO}[(o\text{-CH}_2\text{CH}_2\text{COCH}_3)\text{C}_6\text{H}_4]$).

^{11}B NMR (128 MHz, benzene- d_6): δ -18.1. $^{15}\text{N}\{^1\text{H}\}$ NMR: δ -157.8. IR (KBr, cm^{-1}): 3070 (w), 3046 (m), 2966 (s), 2933 (m), 2884 (m), 1773 (w), 1750 (w), 1709 (m), 1651 (w), 1590 (s, ν_{CN}), 1573 (s, ν_{CN}), 1489 (s), 1458 (s), 1433 (m), 1371 (m), 1351 (m), 1332 (w), 1312 (w), 1272 (s), 1250 (s), 1231 (w), 1195 (s), 1140 (s), 1107 (m), 1075 (m), 1003 (s), 967 (s), 931 (w), 914 (m), 893 (m), 880 (w), 820 (m), 833 (m), 760 (m), 709 (m). Anal. Calcd. for $\text{C}_{31}\text{H}_{40}\text{BN}_3\text{O}_5\text{Mg}$: C, 65.35; H, 7.08; N, 7.37. Found: C, 64.99; H, 6.74; N, 7.44. Mp: 125-132 °C (dec.)

General description of gram-scale hydroboration of carbonyls. A mixture of 1.5 mL of acetophenone and 1.9 mL of HBpin was added to a 10 mL benzene solution of 5 mg of **1**.

The reaction mixture was then taken into a Teflon-sealable storage flask and stirred at 60 °C

for 6 h. The reaction was quenched with 1 M aqueous NaOH solution and the reduced alcohol was extracted with diethyl ether.

General description of gram-scale Tishchenko coupling of aldehydes. A mixture of 1.5 mL of acetophenone and 1.9 mL of HBpin was added to a 10 mL benzene solution of 5 mg of **1**. The reaction mixture was then taken into a Teflon-sealable storage flask and stirred at 60 °C for 6 h. The reaction was quenched with 1 M aqueous NaOH solution and the reduced alcohol was extracted with diethyl ether.

General description of gram-scale hydroboration of esters. A mixture of 1.5 mL of acetophenone and 1.9 mL of HBpin was added to a 10 mL benzene solution of 5 mg of **1**. The reaction mixture was then taken into a Teflon-sealable storage flask and stirred at 60 °C for 6 h. The reaction was quenched with 1 M aqueous NaOH solution and the reduced alcohol was extracted with diethyl ether.

General Procedure for kinetic measurements. All kinetics measurements were conducted by monitoring the reaction with ^1H NMR spectroscopy using a Bruker DRX-400 spectrometer. The NMR probe was pre-set to desired temperature before each set of experiments and calibrated using 100% CD_3OD (for temperatures below 300K). The substrate to product conversion was monitored by taking a single-scan ^1H NMR spectrum at preset intervals. Concentration of the $\text{To}^{\text{M}}\text{MgMe}$ pre-catalyst was determined prior the addition of substrate mixture in each case and the same concentration value is used as the $[\text{Mg}]_{\text{tot}}$ during plotting. Change in $[\text{HBpin}]$ was not monitored with time as the corresponding resonance partially overlaps with that of EtOBpin and EtOAc. Therefore all the kinetic experiments were carried out under the pseudo 1st order condition with respect to $[\text{HBpin}]$

and the initial concentration values ($[\text{HBpin}]_{\text{int}}$) were used in plotting. Concentration of every species of interest was determined by comparison of corresponding integrated resonances to a known concentration of tetrakis(trimethylsilyl)silane dissolved in toluene- d_8 .

General description of ^1H NMR kinetic experiments for the catalytic hydroboration of EtOAc using HBpin and $\text{To}^{\text{M}}\text{MgMe}$ (1) as the pre-catalyst. A 10 mL of toluene- d_8 stock solution containing known concentrations of tetrakis(trimethylsilyl)silane (6 mM, as an internal standard) was prepared. The samples were prepared by adding a measured volume (0.64 mL) of this solution to pre-weighed $\text{To}^{\text{M}}\text{MgMe}$ (1) giving $[\text{Mg}]_{\text{tot}}$ ranging from 6.6 mM to 25.2 mM. Individual sample was placed in a septa-capped NMR tube and cooled to -78 °C. A substrate mixture containing 0.22 mL of EtOAc and 0.96 mL of HBpin was prepared and 120 microliters of this mixture was added to the sample through the septa using a microliter syringe. The hole was sealed with silicone grease. The sample was placed in the NMR spectrometer probe, preset and calibrated to 287 K. Single-scan spectra were acquired automatically at preset time intervals. The concentrations of EtOAc and EtOBpin were determined by comparison of corresponding integrated resonances to the known concentration of the internal standard (TMSS). The reactions were followed over three half-lives of the time course.

Determination of rate dependence on $[\text{EtOAc}]$ under the condition of $[\text{EtOAc}]_{\text{int}} = 0.30$ M and $[\text{HBpin}]_{\text{int}} = 0.85$ M. Plots of $[\text{EtOAc}]$ vs. time follow a half-order decay. The half-order rate constants (k_{obs}) for each $[\text{Mg}]_{\text{tot}}$ were obtained by a nonweighted linear least-squares fit of the data to the integrated half-order rate law:

$$2 ([\text{EtOAc}]_0^{1/2} - [\text{EtOAc}]_t^{1/2}) = k_{\text{obs}} t$$

Determination of rate dependence on [HBpin] under the condition of [EtOAc]_{int} = 0.30 M and [HBpin]_{int} = 0.85 M. k_{obs} values are equivalent within error at [HBpin] ranging from 0.85 M to 2.4 M while keeping [Mg]_{tot} indifferent. This shows a zero-order [HBpin] dependence on the overall rate law.

Determination of rate dependence on [Mg]_{tot} under the condition of [EtOAc]_{int} = 0.30 M and [HBpin]_{int} = 0.85 M. An observed linear correlation between [Mg]_{tot} and the corresponding k_{obs} indicates a first-order [Mg]_{tot} dependence on overall catalytic rate law. The overall three-half order rate constant (k') value was obtained from the nonweighted linear least-square fit on the plot of k_{obs} vs. [Mg]_{tot}.

Thus the rate law for the overall catalysis is written as follows:

$$-d[\text{EtOAc}]/dt = k' [\text{EtOAc}]^{1/2} [\text{Mg}]_{\text{tot}}^1 [\text{HBpin}]^0$$

Chapter 9. Conclusion

The development of zinc and magnesium catalysts remains an important area of research within the field of organometallic chemistry. The non-toxic and environmentally benign nature of these metals makes them superior than more harmful metals. Moreover, the cheap abundance compared to other rare metals makes them highly desirable for practical purposes. This work also highlights the importance of the choice of ancillary ligands in order to control, manipulate and fine-tune the reactivity and selectivity of catalyst systems. We have shown that the unique steric properties of tris(oxazolanyl)borate ligands enable isolation of several reactive intermediates including alkyl, silyl, alkoxide, amide, hydride, alkyl peroxides etc. that are important in the context of catalysis and mechanistic explorations. Thus the remarkable thermal stability of $To^M ZnOOR$ ($R = Et, n\text{-}Pr, i\text{-}Pr, t\text{-}Bu$) compounds ($> 120\text{ }^\circ\text{C}$) is one of the main-highlights of this thesis. Despite the robustness, these compounds are not completely inert and demonstrate several interesting reactivity. Furthermore, lack of redox activity of zinc and magnesium makes these studies less complicated. These studies need to be continued along the line of catalysis and mechanistic studies. Enantioselective transformations could also be accomplished using the chiral tris(oxazoilyl)phenylborate ligands, which are accessible from enantio-pure amino acids. Products resulted from $To^M MgMe$ mediated ester hydroboration are completely different from the hydroboration of amides, under similar catalytic condition. Esters undergo C–O bond cleavage to produce alkoxy boranes, whereas, amides undergo C=O bond reduction resulting amines and B–O–B linkage. Such reactivity difference is quite intriguing and requires additional mechanistic study in details.